

Coordination Polymerization of Polar Vinyl Monomers by Single-Site Metal Catalysts

Eugene Y.-X. Chen*

Department of Chemistry, Colorado State University, Fort Collins, Colorado 80523-1872

Received January 19, 2009

Contents

1. Introduction	5157	5.2. Vinyl Ketones	5196
1.1. Background	5157	6. Copolymerization	5197
1.2. Terminology	5158	6.1. Polar–Nonpolar Block Copolymers	5197
1.2.1. Initiator vs Catalyst	5158	6.2. Polar–Nonpolar Random Copolymers	5199
1.2.2. Single-Site vs Multisite Catalyst	5159	6.3. Polar–Polar Copolymers	5204
1.2.3. Polymerization vs Polymer Characteristics	5159	7. Ion-Pairing Polymerization	5206
1.2.4. Stereospecific vs Stereoselective Polymerization	5160	8. Summary and Outlook	5208
1.2.5. Coordination–Insertion vs Coordination–Addition Polymerization	5160	9. Acknowledgments	5208
1.3. Scope of Review	5161	10. References	5208
2. Methacrylate Polymerization	5161		
2.1. Lanthanide Complexes	5161	1. Introduction	
2.1.1. Nonbridged Lanthanocenes	5161	1.1. Background	
2.1.2. <i>ansa</i> -Lanthanocenes	5164		
2.1.3. Half-Lanthanocenes	5166		
2.1.4. Non-lanthanocenes	5166		
2.2. Group 4 Metallocenes	5170		
2.2.1. Nonbridged Catalysts	5170		
2.2.2. <i>ansa</i> -C _{2v} -Ligated Catalysts	5173		
2.2.3. <i>ansa</i> -C ₂ -Ligated Catalysts	5173		
2.2.4. <i>ansa</i> -C ₁ -Ligated Catalysts	5176		
2.2.5. <i>ansa</i> -C _s -Ligated Catalysts	5177		
2.2.6. Constrained Geometry Catalysts	5178		
2.2.7. Half-Metallocene Catalysts	5180		
2.2.8. Supported Catalysts	5180		
2.3. Other Metallocene Catalysts	5180		
2.4. Nonmetallocene Catalysts	5181		
2.4.1. Group 1 and 2 Catalysts	5181		
2.4.2. Group 13 Catalysts	5183		
2.4.3. Group 14 Catalysts	5186		
2.4.4. Transition-Metal Catalysts	5187		
3. Acrylate Polymerization	5188		
3.1. Lanthanocenes	5188		
3.2. Group 4 Metallocenes	5189		
3.3. Nonmetallocenes	5190		
4. Acrylamide and Methacrylamide Polymerization	5191		
4.1. Acrylamides	5191		
4.2. Methacrylamides	5192		
4.3. Asymmetric Polymerization	5193		
5. Acrylonitrile and Vinyl Ketone Polymerization	5196		
5.1. Acrylonitrile	5196		

* To whom correspondence should be addressed. E-mail: eugene.chen@colostate.edu.

A prolific coupling of polymer science with organometallic chemistry has recently yielded phenomenal scientific and commercial successes in the production of revolutionary polyolefin materials by (co)polymerization of *nonpolar* α -olefins using single-site catalysts (SSCs) such as metallocenes and related discrete nonmetallocene metal complexes.^{1–13} These remarkable successes and ever growing interest in this field have also produced a large number of special journal issues and books^{1–13} as well as comprehensive reviews on α -olefin polymerization catalyzed by group 4 metallocenes,^{14–27} nonmetallocenes,^{28–30} late-transition-metal complexes,^{31,32} lanthanide complexes,^{33–36} and mixed transition-metal complexes,^{37–40} on cocatalysts,^{41–43} as well as on living alkene polymerization^{44–47} and functionalization of polyolefins^{48–51} by such catalysts. There has been a paradigm shift, however, on the utilization of these electron-deficient, highly active metallocene and related single-site metal catalysts for the polymerization of heteroatom (e.g., N, O) functionalized, *polar* vinyl monomers, such as (meth)acrylates and (meth)acrylamides, as well as copolymerization of such polar vinyl monomers with nonpolar olefins. For early metal systems, this shift is typically accompanied by a switch of the polymerization mechanism: from migratory insertion polymerization of α -olefins to coordinative-anionic addition (or coordination–addition, *vide infra*) polymerization of polar vinyl monomers.^{52–54} One-directional mechanistic crossover from coordination–insertion polymerization of olefins to coordination–addition polymerization of polar monomers (i.e., one-way block copolymerization) has been achieved with lanthanocenes⁵⁵ and group 4 catalysts.^{56,57} However, the mechanistic mismatch, along with their high oxophilicity, presents an unmet challenge for direct random copolymerization of olefins with polar vinyl monomers using such early metal catalysts, unless appropriate strategies, such as *steric shielding or electronic protecting of the functional groups* of the polar monomers, are employed.⁵⁸ Hence, from a



Eugene Chen is a Professor of Chemistry at Colorado State University (CSU). He attended Shangrao Teachers College, Nankai University, and University of Massachusetts at Amherst, where he earned a Ph.D. in 1995 with Profs. J. C. W. Chien and the late M. D. Rausch. After a postdoctoral stint at Northwestern University with Prof. T. J. Marks, he joined The Dow Chemical Company in late 1997, where he was promoted from Sr. Research Chemist to Project Leader. He moved to CSU in August 2000, where he went through the ranks of Assistant, Associate, and Full Professors. His research has lain at the interfaces of polymer and organometallic chemistry as well as inorganic and materials chemistry, while his current research interests include polymerization catalysis (polar monomers and biorenewable feedstocks), renewable energy (nonfood biomass conversion and polymer solar photoconversion systems), and materials synthesis (organic/inorganic nanocomposite materials and hybrid polymers).

nonpolar–polar vinyl copolymerization perspective, copolymerizations catalyzed by functionality-tolerant late-metal complexes have enjoyed much more notable successes in direct copolymerization of α -olefins with *unprotected* polar vinyl monomers.^{31,58–61} This latest development of late-metal catalyzed copolymerization holds great future promise, due to its ability to incorporate a wide range of polar vinyl monomers at controllable levels into polyolefins having diverse topologies and thus to deliver new classes of copolymers unattainable by other means of polymerization, such as radical polymerization, a commercial process exclusively employed in the copolymerization of ethylene with polar vinyl monomers.

On the other hand, early metal-catalyzed homopolymerization of polar vinyl monomers has been highly successful.^{46,52,53,62} Four decades ago, conventional Ziegler–Natta-type catalysts, including $\text{TiCl}_4/\text{AlR}_3$ ^{63,64} and $\text{Cp}_2\text{TiCl}_2/\text{AlEt}_3$,⁶⁵ were already employed for syndiospecific polymerization of methyl methacrylate (MMA) at low temperatures (-28 to -78 °C) and for copolymerization of MMA with acrylonitrile (AN) at high temperatures (40 – 80 °C), respectively, despite the fact that active species, polymerization mechanism, and degree of polymerization control were unknown. Ballard and van Lienden reported in 1972 the use of metal tetrabenzyl complexes, such as $\text{Zr}(\text{CH}_2\text{Ph})_4$, to polymerize MMA in toluene via a postulated coordinative anionic polymerization.⁶⁶ The rate of polymerization was significantly enhanced upon exposure to light at wavelengths between 450 and 600 nm; at wavelengths below 450 nm the polymerization was dominated by a radical process due to photolysis of $\text{Zr}(\text{CH}_2\text{Ph})_4$. In 1988, Farnham and Hertler⁶⁷ disclosed in a U.S. patent that discrete chloro-metallocene enolates, $\text{Cp}_2\text{MCl}[\text{OC}(\text{OMe})=\text{CMe}_2]$ ($\text{Cp} = \eta^5\text{-cyclopentadienyl}$; $\text{M} = \text{Ti, Zr, Hf}$), were active for polymerization of MMA; however, the activity and polymer yield of this system were very low (e.g., at ambient temperature in THF for 18 h, only

20% yield was achieved for the chloro-zirconocene enolate in a low $[\text{MMA}]/[\text{Zr}]$ ratio of 20), and the poly(methyl methacrylate) (PMMA) produced had low molecular weight (MW) with broad (polydispersity index, $\text{PDI} > 2$) or bimodal MW distributions (MWDs). Two subsequent, independent *JACS Communications* reported in 1992 marked the beginning of the controlled/living polymerization of acrylic monomers using *discrete metallocene complexes*: these are seminal works of Yasuda and co-workers⁶⁸ involving neutral, single-component lanthanocenes, such as dimeric samarocene hydride $[\text{Cp}^*_2\text{SmH}]_2$ ($\text{Cp}^* = \eta^5\text{-C}_5\text{Me}_5$), as living MMA polymerization catalysts and Collins and Ward⁶⁹ involving a two-component group 4 metallocene system, consisting of cationic zirconocenium complex $[\text{Cp}_2\text{ZrMe}(\text{THF})]^+[\text{BPh}_4]^-$ as catalyst and neutral zirconocene dimethyl Cp_2ZrMe_2 as initiator, for high-conversion polymerization of MMA to high MW PMMA with relatively narrow MWDs ($\text{PDI} = 1.2\text{--}1.4$).

Significant advances have been achieved in the coordination polymerization of polar vinyl monomers by discrete lanthanide and early and late metal catalysts for the past 16 years, especially in the area of stereochemical control of polymerization, producing a large body of publications on this important topic. Additionally, major advances in the coordination copolymerization of polar vinyl monomers with nonpolar olefins by late metal catalysts have been made since two *Chemical Reviews* articles published in 2000 by Boffa and Novak⁵⁸ and by Ittel, Johnson, and Brookhart.³¹ Hence, the above-mentioned major progress in the field of coordination polymerization of polar vinyl monomers by single-site metal catalysts calls for a need for a comprehensive review of this field, which is the effort of this article.

1.2. Terminology

1.2.1. Initiator vs Catalyst

The most common terminology used in polymerization science is perhaps “initiator” or “catalyst”. In a broad sense, all polymerization processes are “catalytic”, by definition, because multiple equivalents of the monomer (substrate) are consumed per initiating molecule to form polymer chains consisting of covalently bonded monomer repeat units. In practice, such an initiating molecule is termed either “initiator” or “catalyst”, depending on whether the reagent produces one or more than one polymer chain. The term “initiator” is explicit in free radical, cationic, and anionic polymerizations, but in *metal-mediated coordination* polymerizations the use of “initiator” or “catalyst” is much more relaxed in the literature because a metal complex often serves as *both* initiator (by having a nucleophilic initiating ligand) and catalyst (by activating the enchaining monomer via metal–monomer complexation/coordination). Where “catalyst” is used in this review, it emphasizes the *catalyzed monomer enchainment*. Thus, it is a catalyst when emphasizing the fundamental catalytic event of monomer enchainment (i.e., the propagation catalysis cycle), but it is not a “true” catalyst if the catalytic production of polymer chains is concerned. On the other hand, *catalytic polymerization* explicitly defines a polymerization that exhibits turnover numbers (TONs) for both monomer consumption and polymer chain production. This type of polymerization is typically achieved by catalyzed internal chain-transfer processes (e.g., β -H elimination) or by addition of an external chain-transfer reagent (CTR). For instance, living polymerization is not a catalytic polymerization per se (i.e., only one polymer chain produced per

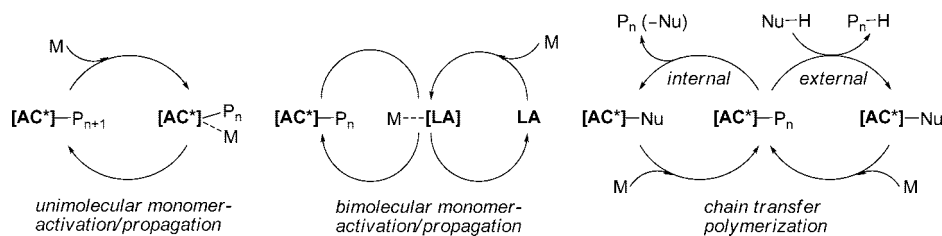


Figure 1. Catalytic cycles in three major types of catalyzed polymerization processes: $[AC^*]$ = active center; P_n = growing polymer chain; M = monomer; LA = Lewis acid; Nu = nucleophile.

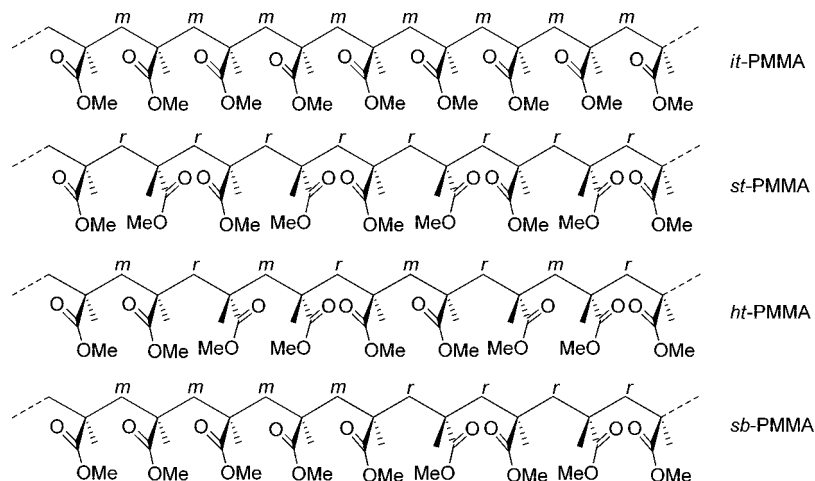


Figure 2. Tactic PMMA stereomicrostructures.

initiating molecule), unless a suitable CTR is added to promote efficient chain-transfer processes. Catalytic polymerization exhibits economical advantages over noncatalytic processes and thus is significant in industry. In principle, a polymerization having an initiator efficiency (I^*) value of >100 means more than one polymer chain is produced per initiating molecule. In short, “catalytic” elements are readily identifiable in the metal-mediated polymerization processes, as shown in Figure 1, which illustrates “catalytic” events in the three major types of catalyzed polymerization processes, including catalyzed monomer enchainment (unimolecular and bimolecular) as well as catalytic production of polymer chains—chain transfer (internal and external) polymerization.

1.2.2. Single-Site vs Multisite Catalyst

The term SSC was coined to differentiate discrete homogeneous molecular catalysts, such as metallocenes or related discrete organometallic complexes, from typically multisite heterogeneous catalysts. It is worthwhile to note that one should not take the term SSC literally to refer to a catalyst with only one active site or center, because metallocene-type catalysts can have more than one site (e.g., C_2 -, C_s -, and C_1 -ligated group 4 metallocene catalysts possess two homotopic, enantiotopic, and diastereotopic coordination sites, respectively) and can even involve more than one center (e.g., polynuclear catalysts). The term SSC more precisely defines the catalyst with *only one type of catalytically active species*. A multisite catalyst system, which contains more than one type of catalytically active species, typically produces a polymer exhibiting a multimodal MWD in a gel permeation chromatograph (GPC) trace, unless all active species possess very similar catalytic properties or there exhibits rapid exchange among those active species.

1.2.3. Polymerization vs Polymer Characteristics

In each polymerization catalyst or initiator system reviewed herein, *five* most important characteristics of polymerization and the resulting polymers are described, where possible, in terms of (a) reaction condition, (b) polymerization activity, (c) polymer tacticity, (d) stereocontrol mechanism, and (e) polymerization control. A given polymerization system reported in the literature may report all or just one to some of the above characteristics described therein.

First, reaction conditions include polymerization temperature (T_p), medium (solvent), or pressure where gaseous monomers are involved. *Second*, polymerization activity is converted (if not reported) by the reviewer to turnover frequency [TOF: mole of substrate (monomer) consumed per mole of catalyst (initiator) per hour] for meaningful comparisons among the systems reviewed. Polymerization systems with TOF (h^{-1}) of <10 , >10 , >100 , >1000 , and $>10,000$ are arbitrarily characterized as exhibiting *low*, *modest*, *high*, *very high*, and *exceedingly high* activities, respectively.

Third, polymer tacticity is revealed by the resulting polymer stereomicrostructure (stereoregularity), which is shown by stereogenic center sequence distributions. Figure 2 depicts tactic PMMA, as an example, to show the stereogenic center sequence distributions *mmmmmmmm*, *rrrrrrrr*, *mrmmrrmr*, and *mmmmrrrr*, corresponding to isotactic (*it*), syndiotactic (*st*), heterotactic (*ht*), and *it-block-st* stereoblock (*sb*) stereomicrostructures, respectively. A polymer is classified as atactic (*at*), *it*- or *st*-biased (rich) atactic, tactic, or highly tactic according to the level of its triad distributions; hence, polymers with $mr \sim 50$, mm (rr) = 55–69, mm (rr) = 70–89, and mm (rr) ≥ 90 are arbitrarily termed *at*, *it* (*st*)-rich *at*, *it* (*st*), and highly *it* (*st*) polymers, respectively. The degree of stereoregularity of a polymer determines its thermal properties, such as melting-

transition temperature (T_m) and glass-transition temperature (T_g); stereoregular (e.g., *it* and *st*) polymers are semicrystalline materials, thus usually exhibiting both T_m and T_g , whereas their *at*, amorphous counterpart shows only T_g . Highly crystalline polymers may show only T_m . In general, the physical and mechanical properties of the polymers having stereogenic centers in the repeating units depend largely on their stereochemistry.⁷⁰ Stereoregular polymers are typically crystalline materials as compared to their amorphous (*at*) counterparts, and crystallinity leads to superior materials properties, such as enhanced solvent resistance, high modulus, as well as excellent impact strength and fatigue resistance.

Fourth, the mechanism of stereocontrol⁷¹ for a given system is characterized by either an enantiomeric-site control mechanism—that is, the chirality of the active propagating center dictates the stereochemistry of monomer enchainment so that the stereoerror (*rr* triads in isospecific polymerization or *mm* triads in syndiospecific polymerization) is corrected on the next monomer addition—or a chain-end control mechanism—that is, the stereogenic center of the last enchainment monomer unit dictates the stereochemistry of further monomer enchainment so that the stereoerror (*r* dyads in isospecific polymerization or *m* dyads in syndiospecific polymerization) is propagated.

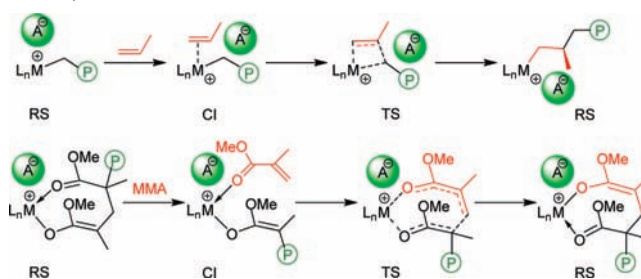
Fifth, the degree of polymerization control is reflected by polymer MW (number average M_n or weight average M_w), MWD (M_w/M_n), and initiator (catalyst) efficiency, $I^* = M_n(\text{calcd})/M_n(\text{exptl})$, where $M_n(\text{calcd}) = \text{MW}(\text{monomer}) \times [\text{monomer}]_0/[\text{initiator}(\text{catalyst})]_0 \times \text{conversion \%} + \text{MW}(\text{end groups})$. A controlled polymerization demonstrates its capacity for controlling MW, architecture, or function. On the other hand, living polymerizations provide the maximum degree of control for polymer synthesis; accordingly, a living polymerization is much more rigorously tested, and a set of experimental criteria⁷² must be met before claiming a living polymerization system.

1.2.4. Stereospecific vs Stereoselective Polymerization

According to the definitions recommended by IUPAC, *stereospecific* polymerization is the polymerization in which a tactic polymer is formed,⁷³ while *stereoselective* polymerization is the polymerization in which a polymer is formed from a mixture of stereoisomeric monomer molecules by preferential incorporation of one stereoisomeric species.⁷⁴ Accordingly, polymerization of prochiral monomers such as propylene and methacrylates yielding isotactic or syndiotactic polymers is termed stereospecific polymerization, which is the widely used terminology in the polymer literature when describing such polymerizations. However, polymerization in which stereoisomerism present in the monomer is merely retained in the polymer is not regarded as stereospecific polymerization. Thus, polymerization of chiral monomers (e.g., D-propylene oxide and L-lactide) with retention of configuration and polymerization of racemic lactides to isotactic polymer is commonly regarded as stereoselective polymerization. A common misconception here is that a polymerization is named stereospecific polymerization only when it is 100% or nearly 100% stereoselective.

It should be noted here that these IUPAC polymerization definitions are different than the definitions for stereospecificity and stereoselectivity of fundamental reactions. If one strictly applies the definitions for stereospecific and stereoselective reactions to polymerizations, then polymerizations

Scheme 1. Elementary Steps: Migratory Insertion vs Conjugate Addition (RS = Resting State, CI = Coordination Intermediate, TS = Transition State, L_n = Supporting Ligand, M = Metal, A = Anion, and P = Growing Polymer Chain)



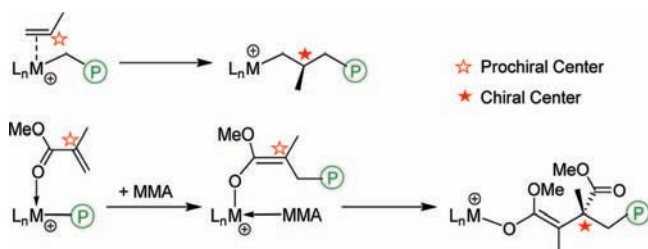
that yield tactic polymers from prochiral vinyl monomers would be termed stereoselective polymerizations⁷⁵ because they result in the preferential formation of one stereoisomer over another with the starting materials absent of different configurations. As a result, some polymer literature uses the term stereoselective (isoselective or syndiospecific) polymerization to describe a polymerization reaction yielding a tactic (isotactic or syndiotactic) polymer. This review attempts to adopt the above-described IUPAC definitions for stereospecific and stereoselective polymerization, but it occasionally uses them interchangeably by keeping the terms consistent with those adopted in the cited paper.

1.2.5. Coordination–Insertion vs Coordination–Addition Polymerization

In this review coordination polymerization of polar vinyl monomers by single-site metal catalysts will include two major types of coordination polymerization: migratory insertion (i.e., *coordination–insertion*) and conjugate addition (*coordination–addition*). Metal-catalyzed coordination–insertion polymerization of nonpolar or polar α -olefins and metal-mediated coordination–addition polymerization of polar vinyl monomers are two fundamentally different polymerization processes (Scheme 1). Regarding the elementary steps of the polymerization, the catalyst resting state (RS) for the former polymerization is the contact or solvent-separated ion pair. Displacement of the weakly coordinated anion by an olefin molecule forms the coordination intermediate (CI), which is followed by the formation of the four-membered-ring transition state (TS), completion of migratory insertion, and regeneration of the catalyst in its RS (Scheme 1, where propylene is used as an example). On the other hand, the catalyst RS for the coordination–addition polymerization of polar vinyl monomers such as MMA is the 8-membered-ring chelate. Ring-opening of the chelate by the incoming monomer gives the catalyst–monomer complex (i.e., CI). Intramolecular conjugate addition proceeds with an eight-membered-ring TS before completion of monomer addition and regeneration of the catalyst RS (Scheme 1).^{46,52,53,62,76,77}

Regarding the stereoselection events, the selection is made between the enantiofaces of the prochiral monomer in α -olefin polymerization, and the chirality of the monomer unit is determined once enchainment (Scheme 2). In sharp contrast, in MMA polymerization, the selection is made between the enantiofaces of the prochiral growing chain (not the monomer), and the chirality is determined one step later (i.e., after an additional monomer enchainment).^{76,77}

Scheme 2. Stereoselection Events: Enantiofaces of Prochiral Monomer vs Prochiral Chain End



1.3. Scope of Review

This review covers polymerization of polar vinyl monomers mediated by single-site metal catalysts including discrete metallocene and nonmetallocene metal complexes; it focuses on the *coordination*-type of polymerization (*vide supra*). Many reviews have covered general topics on polymerization of polar vinyl monomers,⁷⁸ including radical polymerization mediated by metal complexes^{79–81} as well as classical cationic and anionic polymerizations^{82–86} involving metal species. Radical and ionic types of polymerization are not discussed in this review; however, relevant coordinative-anionic polymerization systems that are considered as early examples or precedents, albeit being multisite in nature, for the development of advanced single-site catalysts, are included.

Polar vinyl monomers covered in this review are limited to those technologically important ones incorporating hard-base (*O*, *N*) functional groups, including *methacrylates*, *acrylates*, *acrylamides*, *methacrylamides*, *vinyl ketones*, and *acrylonitrile*. The copolymerization section deals with three types of polar vinyl copolymers, one of which is dedicated to polar–nonpolar vinyl *random copolymers* (section 6.2) and discusses the reports appearing after the two 2000 *Chemical Reviews* reviews on copolymerization of olefins and polar vinyl monomers by Boffa and Novak⁸⁸ and by Ittel, Johnson, and Brookhart.³¹ Catalysts discussed in this review are centered on *single-site* metallocene and nonmetallocene complexes, a large majority of which belong to discrete group 3, 4, and 10 metal complexes. To assist the reader in categorizing metal–ligand combinations in metal complexes supported by non-Cp-based ligands (i.e., nonmetallocene complexes), a simple ligand classification system is used for ligands of hapticity ≥ 2 to directly indicate the *identity*, *number*, and *formal charge* of the metal-attached ligand atoms; for example, a tridentate bis(amido) nitrogen-donor ligand, where the neutral donor nitrogen atom is placed approximately at the central position between the two anionic amido functionalities, is conveniently represented as $[N^-, N, N^-]$. Except for the few examples included, patents and meeting proceedings are not reviewed.

2. Methacrylate Polymerization

2.1. Lanthanide Complexes

2.1.1. Nonbridged Lanthanocenes

Yasuda and co-workers discovered that neutral *trivalent* samarocenes, such as dimeric samarocene hydride $[\text{Cp}^*_2\text{SmH}]_2$ (**1**), function as both initiator (to effect chain initiation and growth via conjugate addition) and catalyst (to activate monomer via monomer coordination to the highly Lewis acidic Sm center) in the polymerization of MMA.⁶⁸

Chain initiation occurs via a two-step process involving nucleophilic attack of the Sm hydride to the coordinated (activated) MMA, followed by conjugate addition of the resulting ester enolate to a second MMA coordinated to Sm, giving rise to the eight-membered-chelate propagating species **2**⁸⁷ (Scheme 3). The structure of the initiated, cyclic propagating species **2** has been simulated and confirmed by the X-ray crystal structure of the complex independently synthesized from the reaction of $[\text{Cp}^*_2\text{SmH}]_2$ with 2 equiv of MMA (per Sm center). Propagation proceeds via repeated intramolecular conjugate Michael additions through the Sm enolate–monomer complex (active species) to the eight-membered-ring intermediate (i.e., catalyst resting state **3**) cycle (Scheme 3).

The polymerization by **1** exhibits living characteristics from T_p as low as $-95\text{ }^\circ\text{C}$ to T_p as high as $40\text{ }^\circ\text{C}$, thereby producing PMMA with controlled MW (determined by the $[\text{MMA}]_0/[\text{Sm}]_0$ ratio) and narrow MWD (PDI = 1.02–1.05, Table 1), as well as well-defined block copolymers of MMA with other alkyl methacrylates.⁸⁷ PMMA with M_n as high as 5.6×10^5 can be synthesized. At low T_p of $-95\text{ }^\circ\text{C}$, the activity is modest (0.1 mol % catalyst, 60 h, 82% monomer conversion for a TOF of $\sim 14\text{ h}^{-1}$), as is the initiator efficiency ($I^* = 44\%$); however, the PMMA produced is highly syndiotactic (95.3% *rr*). When the polymerization is carried out at $25\text{ }^\circ\text{C}$, both TOF (500 h^{-1}) and I^* (88%) values increase drastically, but the PMMA syndiotacticity drops significantly to 79.9% *rr*.

Methyl lanthanocenes, $\text{Cp}^*_2\text{LnMe}(\text{THF})$ ($\text{Ln} = \text{Sm}, \text{Y}, \text{Yb}, \text{Lu}$), and AlMe_3 complexes of lanthanocenes, $\text{Cp}^*_2\text{Ln}(\mu\text{-Me})_2\text{AlMe}_2$ ($\text{Ln} = \text{Y}, \text{Yb}, \text{Lu}$), behave in a fashion similar to that of $[\text{Cp}^*_2\text{SmH}]_2$ toward MMA polymerization, with the polymerization activity increasing with an increase in ionic radii of the Ln metal ($\text{Sm} > \text{Y} > \text{Yb} > \text{Lu}$) within the series.^{36,87} Yasuda and co-workers also supported $\text{Cp}^*_2\text{SmMe}(\text{THF})$ onto AlMe_3 -pretreated mesoporous MCM-41 silicates of various pore sizes and found that the complex adsorbed on the silicates with large pore sizes ($\geq 29\text{ \AA}$) afforded *st*-PMMA at $0\text{ }^\circ\text{C}$ in toluene with a higher syndiotacticity (86% *rr*) and MW ($M_n > 1.4 \times 10^5$, PDI ~ 1.5), as compared with the PMMA (82% *rr*) produced by the homogeneous system.^{88,89}

Other methacrylates can also be polymerized in the well-controlled manner, and as anticipated on steric grounds, the apparent rate of polymerization at $0\text{ }^\circ\text{C}$ decreases with an increase in the steric bulk of the R group of methacrylates $\text{CH}_2=\text{CH}(\text{Me})\text{COOR}$: TOF (h^{-1}) = 500, 490, 450, and 125, for R = Me, Et, *i*Pr, and *t*Bu, respectively.⁸⁷ Interestingly, contrary to an expectation based on the chain-end control mechanism, the syndiotacticity of the polymethacrylates obtained at $0\text{ }^\circ\text{C}$ is highest for smaller alkyl groups: *rr*% = 82.4, 80.9, 77.3, and 78.2, for R = Me, Et, *i*Pr, and *t*Bu, respectively.⁸⁷ Replacing the H or Me ligand of the above samarocene catalysts by BH_4 , namely $\text{Cp}^*_2\text{Sm}(\text{BH}_4)(\text{THF})$, gives an ill-controlled, much less active catalyst, which gives only syndio-rich PMMA (54% *rr*) at $25\text{ }^\circ\text{C}$ in toluene (TOF = 110 h^{-1}) with a much broader MWD (PDI = 2.4) and a very low I^* of only 5.9%.⁹⁰

The MMA polymerization by lanthanocenes is typically carried out in toluene, but polar solvents including THF and Et_2O can also be used in the case of $\text{Cp}^*_2\text{SmMe}(\text{THF})$ and $\text{Cp}^*_2\text{YbMe}(\text{Et}_2\text{O})$ without noticeably altering the polymerization results, including PMMA syndiotacticity, M_n , and MWD.⁸⁷ This observation is noteworthy because this is *in*

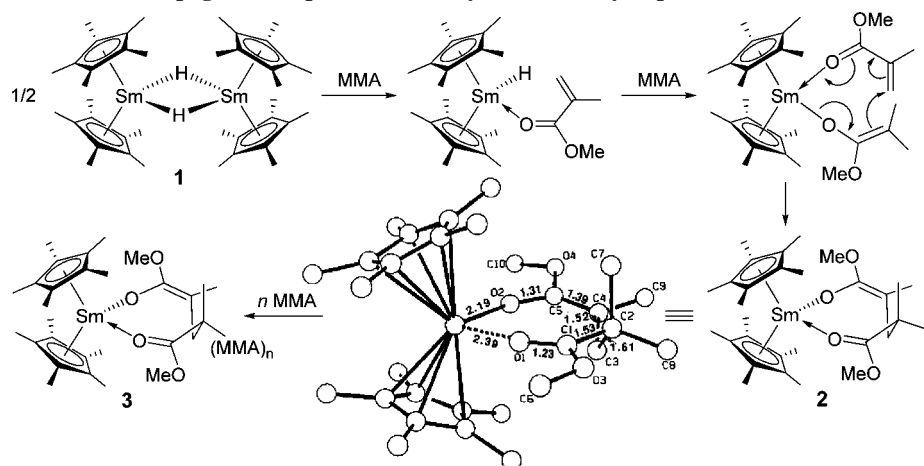
Scheme 3. Chain Initiation and Propagation Steps in MMA Polymerization by $[\text{Cp}^*_2\text{SmH}]_2$ (1)

Table 1. Characteristics of the MMA Polymerization by 1 in Toluene

T_p (°C)	TOF (h^{-1})	M_n (kD)	PDI	I^* (%)	rr (%)
-95	13.7	187	1.05	44	95.3
-78	26.9	82.0	1.04	59	93.1
0	500	58.0	1.02	86	82.4
25	500	57.0	1.02	88	79.9
40	500	55.0	1.03	91	77.3

sharp contrast to classic anionic polymerization of MMA initiated by organometallic lithium reagents, where solvents play a critical role in determining the tacticity of PMMA produced, especially at low temperatures, due to competition between counterion coordination to chain-end (penultimate ester group) and monomer vs solvation.⁹¹ Thus, polar coordinating solvents (e.g., THF, DME) strongly solvate the counterion, prohibiting it from exerting an influence on monomer enchainment because it is largely unassociated with the propagating enolate chain end when approaching the monomer, thereby favoring syndiotactic placement for steric reasons, whereas nonpolar solvents (e.g., toluene) typically favor isotactic placement through a rigid propagating chain model involving monomer precoordination to the counterion which is associated with the propagating chain end and additionally coordinated to the penultimate ester group. *Uniquely*, the current coordination polymerization system by neutral lanthanocenes involves *no counteranions*, and as such, the influence of solvent is limited to the effect on the polymerization rates as donor solvent molecules compete with monomer molecules for coordination to the highly electrophilic metal center. However, donor solvents should also impact polymerization stereochemistry in the case of chiral lanthanocene catalysts possessing two nonhomotopic lateral coordination sites, even without counterions involved, as such solvents can exert an influence on catalyst site-isomerization processes (section 2.1.2).

Trimethylsilyl-substituted lanthanocene methyl complexes, $[(\text{Me}_3\text{SiC}_5\text{H}_4)_2\text{SmMe}]_2$ (**4**), $\{[(\text{Me}_3\text{Si})_2\text{C}_5\text{H}_3]_2\text{SmMe}\}_2$ (**5**), and $\{[(\text{Me}_3\text{Si})_2\text{C}_5\text{H}_3]_2\text{NdMe}\}_2$ (**6**),⁹² also initiate living polymerization of MMA at -78 °C with even higher TOFs than $[\text{Cp}^*_2\text{SmH}]_2$, but the PMMA syndiotacticity is lower (86–90% rr , Table 2) as compared to 93% rr of the PMMA produced by $[\text{Cp}^*_2\text{SmH}]_2$ at -78 °C. Furthermore, these mono- and bis(silyl)-substituted lanthanocenes are nonliving at 25 °C, producing PMMA with considerably broader MWDs (PDI = 1.31–1.82) and also lower syndiotacticity

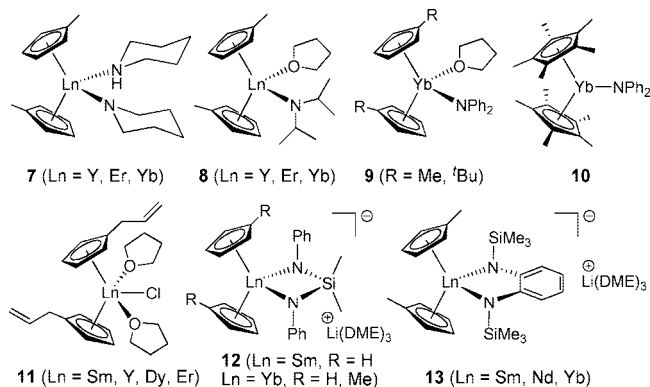
Table 2. Characteristics of the MMA Polymerization by Silyl-Substituted Lanthanocenes⁹²

complex	T_p (°C)	TOF (h^{-1})	M_n (kD)	PDI	I^* (%)	rr (%)
4	-78	500	75	1.05	67	86
4	25	790	51	1.82	77	73
5	-78	500	69	1.05	72	87
5	25	410	67	1.43	31	73
6	-78	175	88	1.05	20	90
6	25	455	45	1.31	101	72

(72–73% rr) than the PMMA (1.02 PDI and 80% rr) produced by $[\text{Cp}^*_2\text{SmH}]_2$ at 25 °C.

Lanthanocenes incorporating *amido* initiating ligands, **7** ($\text{Ln} = \text{Yb}, \text{Er}, \text{Y}$),⁹³ polymerize MMA to *st*-PMMA with MWDs ranging from low 1.11 to high 3.74, depending on metal and T_p , but with comparable polymerization activity and polymer tacticity with those by most commonly employed hydrido or hydrocarbyl initiating ligands. The observed activity order in this series, $\text{Yb} > \text{Er} > \text{Y}$, is in reverse order of ionic radii and thus completely different from the order observed for the lanthanocene hydrido or hydrocarbyl complexes. However, the MMA polymerization activity of analogous diisopropylamido lanthanocenes **8** ($\text{Ln} = \text{Yb}, \text{Er}, \text{Y}$) increases with an increase of ionic radii of the lanthanide (i.e., $\text{Y} > \text{Er} > \text{Yb}$).⁹⁴ Lanthanocene amides were also utilized to polymerize (dimethylamino)ethyl methacrylate (in toluene, -78 to 40 °C) to high MW ($M_n > 10^5$) polymers.⁹⁵ The polymer produced by **8** $\{(\text{Me}_3\text{C}_5\text{H}_4)_2\text{YbN}(\text{Pr})_2(\text{THF})\}$ at -78 °C is highly syndiotactic (92.8% rr), while the syndiotacticity drops considerably to 78% rr at 0 °C. Closely related monoalkyl-substituted ytterbocene diphenylamido complexes, $(\text{RC}_5\text{H}_4)_2\text{YbN}(\text{Ph})_2(\text{THF})$ (**9**), exhibit high MMA polymerization activity (up to 250 h^{-1} TOF) at 0 °C, producing PMMA with $M_n = 2.53 \times 10^5$, 1.33×10^5 and PDI = 1.67, 1.26, for $\text{R} = \text{Me}, \text{tBu}$, respectively.⁹⁶ Interestingly, the pentamethyl-substituted derivative **10** showed no activity at all.

Even lanthanocene *chloride* complexes, such as $(\text{CH}_2=\text{CHCH}_2\text{C}_5\text{H}_4)_2\text{LnCl}(\text{THF})_2$ (**11**, $\text{Ln} = \text{Y}, \text{Sm}, \text{Dy}, \text{Er}$), were found to be active for MMA polymerization at 40 °C;



however, the activity is low, with the yttrocene being the most active (7 h^{-1} TOF), and the polymerization is also uncontrolled.⁹⁷ Likewise, $\text{Cp}_2\text{YCl}(\text{THF})$ in combination with 1000 equiv of Et_2Zn showed low MMA polymerization activity at 0°C , producing *at*-PMMA with a broad MWD of 4.78.⁹⁸ Alkyl⁹⁹ or thienyl¹⁰⁰ substituted lanthanocene chloride complexes can also be activated with 10–20 equiv of AlEt_3 or NaH to a highly active system (with TOF reaching 800 h^{-1} for the NaH -activated system) for MMA polymerization, producing *at*-PMMA with broad (>2) or bimodal MWDs. Anionic lanthanocene complexes supported by the Me_2Si -bridged diamide ligand, $\{[\text{Me}_2\text{Si}(\text{NPh})_2]\text{-LnCp}'_2\}[\text{Li}(\text{DME})_3]$ (**12**, $\text{Cp}' = \text{Cp}$, $\text{Ln} = \text{Sm}$, Yb ; $\text{Cp}' = \text{MeCp}$, $\text{Ln} = \text{Yb}$), also promote nonliving MMA polymerization in THF at 30°C , producing syndio-rich *at*-PMMA with PDI ranging from 1.54 to 1.85.¹⁰¹ The calculated initiator efficiencies were between 100 and 200%, suggesting an involvement of either chain transfer reactions or more than one initiating ligand per Ln center. Within this series, the yttrocene complex $\{[\text{Me}_2\text{Si}(\text{NPh})_2]\text{YbCp}_2\}[\text{Li}(\text{DME})_3]$ exhibits the highest activity, with TOF reaching 360 h^{-1} . Closely related anionic lanthanocenes supported by the 1,2-phenylene bridged diamide ligand, $\{[o\text{-(Me}_3\text{SiN)}_2\text{C}_6\text{H}_4]\text{Ln}(\text{MeCp})_2\}[\text{Li}(\text{DME})_3]$ (**13**, $\text{Ln} = \text{Sm}$, Yb , Nd), exhibit similar polymerization characteristics for the MMA polymerization in THF at 30°C .¹⁰²

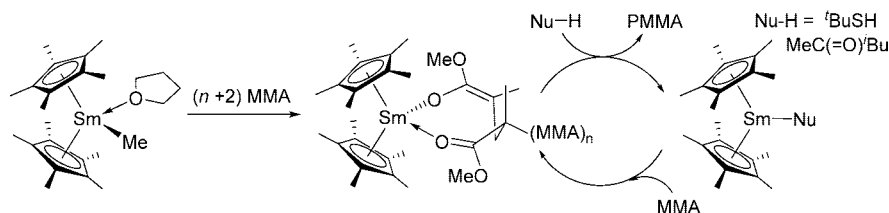
Catalytic chain transfer is a highly efficient approach to control the MW of the polymers produced by free-radical polymerization.¹⁰³ To render a catalytic production of polymer chains in the coordination–addition polymerization catalyzed by metal complexes, a suitable CTR added externally must effectively cleave the growing polymer chain from the active center, and the resulting new species containing part of the CTR moiety (typically in its deprotonated form) must efficiently reinitiate the polymerization. A typical, systematic procedure to examine if a reagent of choice is an appropriate CTR for a given polymerization process or not is as follows. The *first* step is to investigate the reaction of this reagent with the resting intermediate of polymerization, where possible to identify (if not possible, one may alternatively use the starting initiating species), to make sure the reagent can effectively cleave the active center–polymer bond. The *second* step is to evaluate the polymerization behavior of the independently prepared active center containing the nucleophilic part of the reagent (e.g., the deprotonated form) to make sure such species can effectively reinitiate the polymerization and have compatible polymerization kinetics. The *third* step is to study the polymerization in the presence of a varied amount of CTR (i.e., change of the $[\text{CTR}]/[\text{initiator}]$ ratio) and analyze the resulting polymer MW. A well-behaved chain transfer

polymerization with only one-type of mechanism being operative should give rise to a linear relationship between $1/M_n$ and $[\text{CTR}]$ (i.e., an inverse relationship).

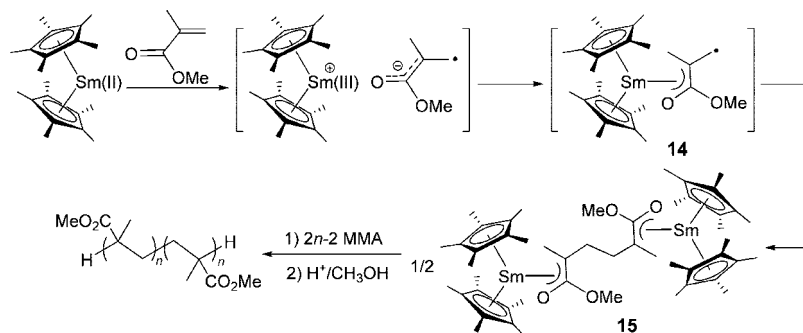
The above-described catalytic chain transfer strategy has been applied to the MMA polymerization by $\text{Cp}^*_2\text{SmMe}(\text{THF})$. Addition of organic acids such as alkyl thios and enolizable ketones as CTRs was found to transform the living MMA polymerization by $\text{Cp}^*_2\text{SmMe}(\text{THF})$ to a chain transfer polymerization for the catalytic production of PMMA.¹⁰⁴ Specifically, *tert*-butyl thiol and methylisobutylketone were among the most effective CTRs for this polymerization, as both can effectively cleave the Sm –PMMA bond derived from the MMA polymerization initiated by $\text{Cp}^*_2\text{SmMe}(\text{THF})$ and the resulting Sm thiolate and ketone enolate reinitiate the polymerization (Scheme 4). However, the effectiveness for the catalytic polymer production by this system is limited ($\text{TON} = 5$) even with a $[\text{CTR}]/[\text{Sm}]$ ratio as high as 29.¹⁰⁴

An early study by Yasuda and co-workers revealed that addition of trialkylaluminum (AlR_3) compounds to *divalent* ytterbocene $\text{Cp}^*_2\text{Yb}(\text{THF})_2$ leads to formation of adducts $\text{Cp}^*_2\text{Yb}\cdot\text{AlR}_3(\text{THF})$ in which one alkyl group bridges two metal centers.¹⁰⁵ Such adducts comprise both transition metal and main group moieties, the hallmark of a homogeneous Ziegler–Natta catalyst. Indeed, the adduct $\text{Cp}^*_2\text{Yb}\cdot\text{AlEt}_3(\text{THF})$ exhibits high activity for MMA polymerization, producing *st*-PMMA (76% *rr*) at 25°C . Investigation into the stoichiometric reaction of the adduct with MMA showed, however, the formation of a complex mixture containing at least four kinds of species.⁵⁵ Subsequently, Yasuda and co-workers discovered that AlR_3 -free *divalent lanthanocenes*, such as $\text{Cp}^*_2\text{Yb}(\text{THF})_2$, $\text{Cp}^*_2\text{Sm}(\text{THF})_2$, and $(\text{Ind})_2\text{Yb}(\text{THF})_2$, promote living polymerization of methacrylates. *Interestingly*, the I^* values, which were calculated based on a monometallic model, were low ($I^* < 30\%$) for such divalent lanthanocenes,⁸⁷ thus greatly inflating the observed MW. Later on, Boffa and Novak¹⁰⁶ revealed that the true active propagating species in the MMA polymerization starting with divalent lanthanocenes, such as Cp^*_2Sm and $\text{Cp}^*_2\text{Sm}(\text{THF})_2$, are *bimetallic trivalent* samarocenes derived from a redox–then–radical–coupling process (Scheme 5). Specifically, chain initiation involves one-electron transfer from the $\text{Sm}(\text{II})$ center to MMA, forming a MMA radical anion and a $\text{Sm}(\text{III})$ cation which combine to $\text{Sm}(\text{III})$ -enolate complex radicals **14**; the radicals **14** subsequently couple in a tail-to-tail fashion to generate bimetallic $\text{Sm}(\text{III})$ -enolate complex **15**, which acts as a bifunctional diinitiator for living polymerization of (meth)acrylates. This mechanism satisfactorily explains the typically observed low I^* values based on the monometallic model; as two Sm centers are now linked as a diinitiator, the PMMA produced has a MW twice that calculated based on the monometallic polymerization model, as does the calculated I^* value. Using preformed bimetallic $\text{Sm}(\text{III})$ initiators $\text{Cp}^*_2\text{Sm}-\text{R}-\text{SmCp}^*_2$ (e.g., bis-allyl bimetallic complexes), PMMA and poly(ϵ -caprolactone) with discrete functionalities at the center of the backbone (“link-functionalized” polymers¹⁰⁷) have been synthesized.¹⁰⁸

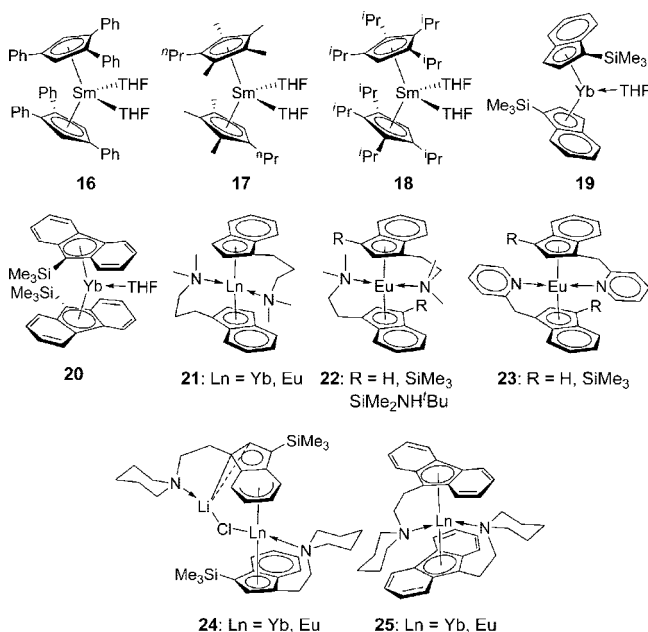
A strong influence of Cp-substituents in $\text{Cp}'_2\text{Sm}(\text{THF})_2$ complexes on the MMA polymerization activity and syndioselectivity—(Cp^{Ph_3})₂ $\text{Sm}(\text{THF})_2$ (**16**, 21 h^{-1} TOF, 1.5 PDI, 78% *rr*), ($\text{Cp}^{\text{Pr}^i\text{Me}_4}$)₂ $\text{Sm}(\text{THF})_2$ (**17**, 7.7 h^{-1} TOF, 2.4 PDI, 88% *rr*), and (Cp^{Pr^t})₂ $\text{Sm}(\text{THF})_2$ (**18**, 1.9 h^{-1} TOF, 6.1 PDI, 68% *rr*)—is exhibited under identical polymerization conditions (0°C , 0.2 mol % Sm , toluene, 24 h).¹⁰⁹ A

Scheme 4. Chain Transfer Polymerization of MMA by Cp*₂SmMe(THF)

Scheme 5. Chain Initiation and Propagation Steps in MMA Polymerization by Divalent Samarocenes



syndiotacticity of 88% *rr* by the *n*-propyltetramethyl-substituted Cp samarocene **17** at 0 °C is noticeably higher than 82.4% *rr* of the PMMA produced by [Cp*₂SmH]₂ at the same *T_p*,⁸⁷ but the activity (7.7 h⁻¹ TOF) is substantially lower than that of [Cp*₂SmH]₂ (500 h⁻¹ TOF). Additionally, the MWDs of the PMMA produced by these complexes are relatively broad (PDI = 1.5–6.1).¹⁰⁹ Divalent ytterbocenes bearing trimethylsilyl-substituted indenyl (Ind) or fluorenyl (Flu) ligands, (1-SiMe₃Ind)₂Yb(THF) (**19**) and (9-SiMe₃Flu)₂Yb(THF) (**20**), catalyze the polymerization of MMA in toluene to different stereomicrostructures (*st*, *it*, or *st-b-it* multiblock) depending on *T_p*, which was attributed to their conformational sensitivity to polymerization conditions.¹¹⁰ Complexation of divalent ytterbocenes with alane AlH₃ further enhances MMA polymerization activity, achieving highly syndiotactic PMMA (93% *rr*, 1.74 PDI, 84% *I*^{*}) with Cp*₂Yb•AlH₃(NEt₃) at -40 °C.¹¹¹

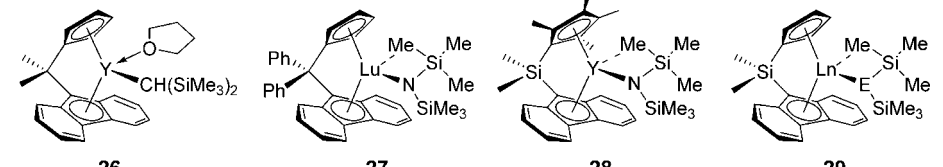


Divalent lanthanocenes (Yb, Eu) supported by indenyl ligands functionalized with *N*-containing side arm substituents,

including (dimethylamino)propyl (**21**), ethyl (**22**),¹¹² 2- (and 3)-pyridylmethyl (**23**),¹¹³ and piperidineethyl (**24**)¹¹⁴ groups, exhibit *exceptionally high activity* for nonliving MMA polymerization at low temperatures, with the highest TOF approaching 171,000 h⁻¹ in THF at -60 °C for **24** (Eu).¹¹⁴ However, unlike the MMA polymerization catalyzed by trivalent unbridged lanthanocene complexes, solvents play a critical role in determining the tacticity of the PMMA produced by these divalent lanthanocenes at low temperatures: polar solvents such as THF and DME typically favor syndiotactic placement, affording syndio-rich *at*-PMMA, whereas nonpolar solvents such as toluene favor isotactic placement, producing iso-rich *at*-PMMA. The PMMAs produced have PDI values in the range of 1.3 to 2.5. Unexpectedly, homoleptic trivalent lanthanocenes (Sm and Nd) bearing the three piperidineethyl-functionalized indenyl ligands all η⁵-π-bonded to Ln (Sm, Nd), that is without σ-bonded initiating groups, are also highly active for MMA polymerization.¹¹⁴ Analogous divalent lanthanocenes **25** (Yb, Eu) supported by a fluorenyl ligand functionalized with the *N*-piperidineethyl group also show exceptionally high activity for MMA polymerization, especially at low temperatures, with the highest TOF approaching 54,600 h⁻¹ in THF at -60 °C for the Eu complex, producing syndio-rich PMMA (47% *rr*) with *M_n* = 9.31 × 10⁴, PDI = 1.16, and *I*^{*} = 49% (based on the unimetallic model).¹¹⁵ In general, the polymerization activity decreases with an increase in *T_p*, and again, the polymerization in THF produces syndio-rich *at*-PMMA (up to 67% *rr* at -60 °C by the Yb complex), while the polymerization in toluene gives iso-rich *at*-PMMA (up to 67% *mm* at -60 °C by the Eu complex). The activity and tacticity trend as a function of Ln, *T_p*, and solvent is the same for the analogous complexes functionalized with the tetrahydro-2-*H*-pyranyl group.

2.1.2. *ansa*-Lanthanocenes

The characteristics of the MMA polymerization by C₅-ligated *ansa*-lanthanocenes have been investigated using a series of *ansa*-lanthanocene hydrocarbyls or amides incorporating *ansa*-Cp-9-Flu ligands, including Me₂C< bridged ytrocene **26** in toluene,¹¹⁶ Ph₂C< bridged lutocene **27** in

Table 3. Characteristics of the MMA Polymerization by C_s -Ligated *ansa*-Lanthanocenes^a


complex	T_p (°C)	TOF (h ⁻¹)	M_n (kD)	PDI	I^* (%)	rr (%)	ref
26	20	375	271	1.80	14	60	116
27	0	12	24.0	2.27	10	59	117
28	25	1.3	91.3	1.39	3.2	58 (<i>mm</i>)	118
29	20	160–200	<i>n.a.</i>	<i>n.a.</i>	<i>n.a.</i>	60–61	119, 120
29	–95	160–200	<i>n.a.</i>	<i>n.a.</i>	<i>n.a.</i>	80–83	119, 120

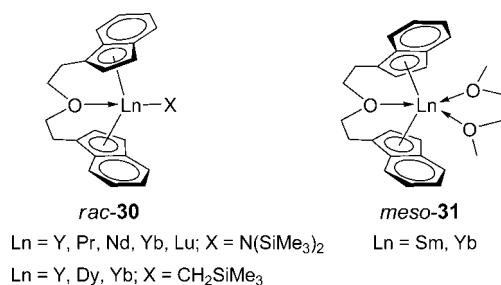
Ln = Dy, Er; E = N, CH

^a *n.a.* = data not available.

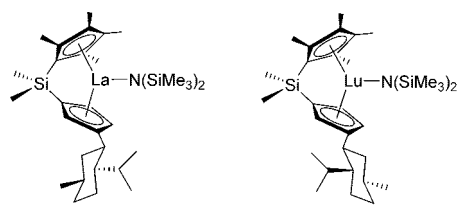
toluene,¹¹⁷ and Me₂Si< bridged yttrocene **28** in toluene,¹¹⁸ as well as Me₂Si< bridged dysprosio- and erbocenes **29** in toluene or THF.^{119,120} When compared to the unbridged, C_{2v} -ligated Cp*₂LnR(THF)-type catalysts, these C_s -ligated *ansa*-lanthanocene catalysts are *less* active and syndiospecific (~60% *rr* at 20 °C or ~82% *rr* at –95 °C), and their catalyzed MMA polymerizations are also *uncontrolled* and give very *low* initiator efficiencies (I^* = 3 to 14%, Table 3). Methyl triad distributions of the PMMA prepared by these C_s -ligated *ansa*-lanthanocenes are characteristic of *chain-end control*. The Me₂Si< bridged yttrocene **28** even produced iso-rich PMMA (58% *mm* at 25 °C, 56% *mm* at 0 °C) in toluene despite its C_s -ligation. The syndiotacticity of the PMMA produced by di-*tert*-butyl-substituted fluorenyl-Cp *ansa*-yttrocene Me₂C(Cp)(2,7-*t*Bu₂-Flu)YCH(SiMe₃)₂ was reported to be 78–79% *rr*, but no polymerization conditions were given.¹²¹

ansa-C₂-symmetric lanthanocene amides and hydrocarbyls, *rac*-[O(CH₂CH₂-Ind)₂]LnX (**30**, X = N(SiMe₃)₂, Ln = Nd, Y, Yb, Lu; X = CH₂SiMe₃, Ln = Dy, Y, Yb), polymerize MMA to iso-rich (in toluene) or syndio-rich (in THF or DME) PMMA.¹²² The resulting PMMA tacticity is also strongly influenced by polymerization temperature; the reversal of the iso-rich tacticity at low T_p to the syndio-rich one at high T_p in THF or DME was rationalized with *rac/meso* interconversion of the active center. The order of the polymerization activity in this lanthanide series is in agreement with the decreasing order of ionic radii.¹²² Divalent *ansa*-lanthanocenes have also been examined for MMA polymerization. Specifically, *meso*-[O(CH₂CH₂-Ind)₂]Ln• (DME) **31**, Ln = Sm, Yb) *ansa*-lanthanocenes polymerize MMA at –78 or 0 °C in toluene, THF, or DME, to syndio-rich *at*-PMMA (40–61% *rr*) with broad MWDs (PDI = 2.69–3.60).¹²³ Nonbridged analogues, [1-(MeOCH₂CH₂-Ind)₂]Ln, showed higher activity without altering much polymer tacticity and MWD. Me₂Si< bridged neodymocene chloride Me₂Si(SiMe₃Cp)₂NdCl (as a *rac/meso* mixture) was activated with ^{*n*}BuMgCl to an active catalyst for MMA polymerization at 40 °C in toluene, reaching a TOF of 125 h⁻¹ and affording also syndio-rich PMMA (67.5% *rr*, 1.65 PDI).¹²⁴ As unbridged chlorolanthanocenes, *ansa*-lanthanocene chloride complexes O(C₂H₄C₅H₃)₂LnCl (Ln = Y, Nd, Sm) can directly initiate MMA polymerization (TOF up to 40 h⁻¹), typically in bulk at high temperature (80 °C), affording syndio-rich, high MW PMMA (PDI = 1.8).¹²⁵

Marks and co-workers reported that bridged chiral C₁-symmetric lanthanocene catalyst **32** bearing the (+)-neo-

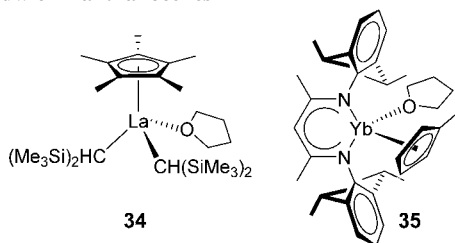


menthyl chiral auxiliary (Figure 3) produces highly *isotactic* PMMA (94% *mm*) in toluene at –35 °C.¹²⁶ However, this catalyst exhibits low activity (TOF = 3 h⁻¹) and efficiency (I^* = 37%) as well as produces PMMA with a broad MWD (PDI = 6.7) at this temperature. The activity was enhanced at T_p = 25 °C, but the isotacticity dropped significantly to 75% *mm*. In sharp contrast, C₁-symmetric lanthanocene complex **33** bearing the (–)-menthyl chiral auxiliary affords *syndiotactic* PMMA (73% *rr*) at ambient temperature, albeit very low activity (TOF = 6 h⁻¹) and efficiency (I^* = 2.3%). Analysis of the resulting PMMA stereomicrostructures indicated neither pure enantiomeric-site nor chain-end control is operative in this system. Accordingly, the observed sharply different stereoselectivity of these two C₁-symmetric lanthanocene complexes was rationalized on the basis of competing conjugate addition and enolate isomerization pathways.¹²⁶ Specifically, because MMA can in principle coordinate to the asymmetric Ln center at either of the two diastereotopic lateral sites, the isoselectivity was proposed to arise as a result of isomerization of the enolate intermediate at a rate faster than propagation to one laterally dissymmetric site of the complex (i.e., MMA addition to the same site).



cat	T_p	TOF (h ⁻¹)	M_n (kD)	PDI	I^* (%)	<i>mm</i> (<i>rr</i>)
32	–35	3	134	6.7	37	94
32	25	15	38	4.1	38	75
33	25	6	521	3.2	2.3	(73)

Figure 3. Structures of Two Chiral C₁-Symmetric Lanthanocene Catalysts and Their MMA Polymerization Characteristics

Table 4. Characteristics of the MMA Polymerization by Half-Sandwich Lanthanocenes

complex	T_p (°C)	TOF (h^{-1})	M_n (kD)	PDI	I^* (%)	rr (%)	ref
34	-78	3	157	1.11	4.2	91	127
34	0	100	46.1	1.18	22	80	127
34	25	200	43.2	1.23	23	74	127
35	-20	740	60.9	3.15	61	22	131

On the other hand, syndioselectivity is a result of faster conjugate addition of the propagating enolate to the monomer relative to the enolate isomerization (i.e., alternate MMA addition to both sites). However, Yasuda offered an alternative explanation for the reversed stereoselectivity in these two complexes, suggesting that the menthyl complex **33** produces *st*-PMMA via a cyclic eight-membered-ring intermediate (i.e., much like the Cp^*_2SmR), whereas the neomenthyl complex **32** produces *it*-PMMA via a noncyclic intermediate.³³

2.1.3. Half-Lanthanocenes

Half-sandwich lanthanocene complex $\text{Cp}^*\text{La}[\text{CH}(\text{SiMe}_3)_2]_2$ - (THF) (**34**) polymerizes MMA to highly syndiotactic (91% *rr*), high M_n (1.57×10^5), and narrow MWD (1.11) PMMA at -78 °C but with extremely low activity (3 h^{-1} TOF) and I^* ($\sim 4\%$).¹²⁷ With an increase of T_p to 0 and 25 °C, the activity was drastically increased to 100 h^{-1} and 200 h^{-1} TOF, but the syndiotacticity was dropped to 80% *rr* and 74% *rr*, respectively, which was also coupled with broader MWDs (Table 4). The mechanism of the polymerization was proposed to proceed with a coordination–addition pathway, identical to that proposed for trivalent lanthanocenes.

Rare earth metal complexes incorporating linked Cp-amido ligands are active for polymerization of both nonpolar vinyl monomers such as ethylene and styrene and polar vinyl monomers such as acrylates and acrylonitrile (see sections 3.1 and 5.1).¹²⁸ Bridged fluorenyl-amido yttrium complex $[\eta^3\text{-}\eta^1\text{-}(3,6\text{-}^t\text{Bu}_2\text{C}_{13}\text{H}_6)\text{SiMe}_2(\text{BuN})]\text{YCH}_2\text{SiMe}_3(\text{THF})_2$ showed low MMA polymerization activity (TOF $< 1 \text{ h}^{-1}$) in toluene at 25 or 50 °C, producing iso-rich *at*-PMMA (42% *mm*, 29% *rr*, 25 °C); however, an ionic lanthanum salt containing the linked 3,6-di-*tert*-butyl-substituted fluorenyl-amido ligand, $\{[\eta^3\text{-}\eta^1\text{-}(3,6\text{-}^t\text{Bu}_2\text{C}_{13}\text{H}_6)\text{SiMe}_2(\text{BuN})]_2\text{La}\}[\text{Li}(\text{THF})_4]$, exhibited modest activity toward MMA polymerization ($T_p = 50$ °C, TOF = 27 h^{-1} , $I^* = 54\%$, *mr* = 40%, $M_n = 6.0 \times 10^4$, PDI = 3.6).¹²⁹ Boron-bridged indenyl-carboranyl neodymium complex $[\eta^5\text{-}\sigma\text{-}^i\text{Pr}_2\text{NB}(\text{C}_9\text{H}_6)(\text{C}_2\text{B}_{10}\text{H}_{10})]\text{NdN}(\text{SiHMe}_2)_2$ - $(\text{THF})_2$ also showed modest MMA polymerization activity (TOF = 13 h^{-1}) in toluene at 25 °C, producing syndio-rich PMMA (69% *rr*).¹³⁰ On the other hand, divalent ytterbium complex **35** supported by methyl-substituted Cp and a β -diketiminato ligand is highly active for MMA polymerization at -20 °C, with TOF reaching 741 h^{-1} .¹³¹ The PMMA produced exhibits a broad MWD (PDI = 3.15) and is essentially atactic (*mr* = 47%); the calculated I^* value based on a monometallic model is 61%, seemingly inconsistent with the one-electron transfer initiator mechanism leading

to a trivalent diinitiator for this complex. Related half-sandwich trivalent samarium bromide incorporating the β -diketiminato ligand has good activity (up to 126 h^{-1} TOF) at 0 °C in toluene, producing iso-rich *at*-PMMA (63% *mm*, PDI = 1.37).¹³²

2.1.4. Non-lanthanocenes

Research in the development of discrete nonmetallocene catalysts for polymerization of polar vinyl monomers is intimately coupled with the growing interest in the use of such catalysts for olefin polymerization where intense efforts have been made to develop non-Cp-based catalyst systems that can function comparably with, or even better than, the Cp-based metallocene systems. In the early stage of this development, such efforts were made often to address patent issues, not solely scientifically driven. Additionally, most nonmetallocene systems utilize bulky ancillary ligands to simulate Cp-based ligand functions (electronics, sterics, and symmetry) and to render the formation of isolable discrete complexes.

Lanthanide hydrocarbyl complexes, including $\text{Sm}(\text{CH}_2\text{-SiMe}_3)_3(\text{THF})_2$, $\text{Y}(\text{CH}_2\text{SiMe}_3)_3(\text{THF})_2$, and $\text{Sm}[\text{CH}(\text{SiMe}_3)_2]_3$, produce in general iso-rich to atactic PMMA in toluene or syndio-rich PMMA in THF.¹³³ Both the activity and degree of control over polymerization by these nonlanthanocene complexes are much lower, as compared with the polymerization by the prototype lanthanocene $\text{Cp}^*_2\text{SmMe}(\text{THF})$. Homoleptic lanthanum silylamide $\text{La}[\text{N}(\text{SiMe}_3)_2]_3$ gives atactic PMMA (48% *mr*) in toluene at 23 °C,¹³⁴ interestingly, when grafted onto nonporous silica, this complex afforded *it*-MMA, with the isotacticity being a function of silica calcining temperature: 92% *mm* at 250 °C, 86% *mm* at 500 °C, and 77% *mm* at 700 °C. This phenomenon was accounted for by the different distributions of mono- and bis-grafted surface lanthanide silylamide species, controlled by adjustment of the silica support dehydroxylation temperature.¹³⁴ The PMMAs produced by the supported catalysts actually exhibit narrower MWDs (PDI = 1.90–2.43) than the parent homogeneous catalyst $\text{La}[\text{N}(\text{SiMe}_3)_2]_3$ (PDI = 3.01). On the other hand, lanthanocene silylamide–LiCl salts, $[(\text{Me}_3\text{Si})_2\text{N}]_3\text{Ln}(\mu\text{-Cl})\text{Li}(\text{THF})_3$ ($\text{Ln} = \text{Sm}, \text{Nd}, \text{Eu}$), afford syndio-rich PMMA in THF or DME (56–66% *rr*) at 0 °C, with the Nd complex being the most active in THF (TOF = 222 h^{-1}).¹³⁵ An amido yttrium metalate, $[\text{Na}(12\text{-crown-4})_2][\text{Y}\{\text{N}(\text{SiMe}_3)_2\}_3(\text{OSiMe}_3)]$, was also found to be active for MMA polymerization, leading to high MW PMMA ($M_n = 1.4 \times 10^6$, PDI = 1.34) but with exceedingly low I^* ($< 1\%$) and modest activity at 0 °C in chlorobenzene (TOF = 14 h^{-1}).¹³⁶

Arnold and co-workers discovered that highly isotactic PMMA (97.8% *mm*) can be produced by bis(pyrrolylaldiminato)samarium hydrocarbyl complex **36** in toluene at 0 °C.¹³⁷ This complex displays molecular C_1 symmetry with the two pyrrolylaldiminato ligands adopting an approximate C_2 arrangement, and its activity rivals those of unbridged parent lanthanocenes $\text{Cp}^*_2\text{LnR}(\text{THF})$ or $[\text{Cp}^*_2\text{SmH}]_2$. Most remarkably, the high level of stereocontrol is maintained at ambient (23 °C, 94.9% *mm*) and higher (40 °C, 93.8% *mm*; 65 °C, 91.3% *mm*) temperatures, although chain transfer became evident at 40 °C, as adjudged by an I^* value of 153% (Table 5). The methyl triad tests of the PMMA produced by **36** indicate that the polymerization conforms to neither pure site control nor chain-end control, while less stereoselective but more active analogous yttrium complex **37** seems to

Table 5. Characteristics of the Isospecific MMA Polymerization by Trivalent Non-lanthanocenes^a

complex	T_p (°C)	TOF (h ⁻¹)	M_n (kD)	PDI	I^* (%)	<i>mm</i>	ref
36	0	250	160	1.40	62.5	97.8	137
36	23	250	106	1.63	70.8	94.9	137
36	40	500	32.7	1.48	153	93.8	137
37	0	500	9.20	1.46	1087	84.9	137
37	23	500	14.9	1.72	671	81.9	137
38	25	<i>n.a.</i>	778	1.26	<i>n.a.</i>	88	140
39	25	>82	476	1.48	10	52	141
40	25	>82	295	4.38	17	77	141

^a *n.a.* = data not available.

Table 6. Characteristics of the Syndiospecific MMA Polymerization by Trivalent Non-lanthanocenes^a

complex	T_p (°C)	TOF (h ⁻¹)	M_n (kD)	PDI	I^* (%)	<i>rr</i> (%)	ref
42	-78	250	111	1.91	45	67.8	143
42	0	147	908	1.83	32	67.4	143
43	-78	250	983	1.63	50	74.1	143
43	0	116	833	1.78	28	71.0	143
44	0	95	25.9	2.66	37	<i>n.a.</i>	144
45	-78	19	25.2	2.58	22	80.5	146
45	0	46	28.8	1.87	44	60.9	146
46	-78	703	99.6	1.46	141	80	147

^a *n.a.* = data not available.

conform to a pure site-control mechanism. There exists substantial chain transfer in the MMA polymerization by yttrium complex **37**, as shown by the I^* values of 671–1087%. Inspection of the stoichiometric reaction of **36** with MMA and the PDI values (≥ 1.40) of the PMMA produced suggest slower initiation with respect to chain propagation.

On the other hand, yttrium, samarium, and ytterbium complexes supported by the closely related, 1,1'-binaphthyl-bridged bis(pyrrolylaldiminato) ligand exhibit very low activity toward MMA polymerization (0.4–0.6 h⁻¹ TOF) at RT in toluene, affording syndio-rich *at*-PMMA (51%–60% *rr*),¹³⁸ replacing one of the pyrrolylaldiminato linkages with a hydroxyl somewhat enhanced the activity (up to ~12 h⁻¹ TOF at -20 °C) without improving the syndiotacticity.¹³⁹ Racemic, *trans*-1,2-diaminocyclohexane-bridged bis(iminophosphonamido)yttrium complex **38** also catalyzes isospecific MMA polymerization, producing PMMA with isotacticity up to 88% *mm* at 23 °C in toluene.¹⁴⁰ Introduction of a less bulky amide ligand, -N(SiMe₂H)₂, lowers the PMMA isotacticity to 73% *mm*. A control run using Y[N(CH₂-SiHMe₂)₂]₃(THF)₃, under otherwise identical conditions, gave *st*-PMMA (70% *rr*), confirming the significant influence of the current iminophosphonamide ligand system exerted on the stereospecificity of the MMA polymerization. A yttrium

hydrocarbyl complex supported by the chelating ferrocene-diamide ligand, {[3,4-Ph₂C₅H₂(NPh)₂Fe]YCH₂SiMe₃(THF)₂ (**39**), showed modest activity (up to 82 h⁻¹ TOF) for the MMA polymerization at 25 °C in toluene, producing, however, iso-rich *at*-PMMA (52% *mm*).¹⁴¹ The analogues lutetium complex **40** elevates the isotacticity to 77% *mm* but also broadens the MWD significantly (from 1.48 by **39** to 4.38 by **40**). Both Y and Lu complexes supported by the same ligand, but without the phenyl substituents on the Cp ring, afforded PMMA with lower isotacticity and bimodal MWDs. Yttrium hydrocarbyl complex **41** supported by a 1,2-azaborolyl ligand was found to be highly active (up to 2300 h⁻¹ TOF) for MMA polymerization at -20 °C in toluene, producing, however, syndio-rich PMMA (62.6% *rr*).¹⁴² The MW is high (M_n up to 3.52×10^5 and PDI = 1.43), but I^* is low (22%); additionally, the resulting polymers exhibit bimodal MWDs (high MW shoulders), which was postulated as a result of O₂-mediated coupling of two polymer chains.

Bis(quanidinato)lanthanide amido complexes **42** and **43** are active catalysts for MMA polymerization at T_p below 0 °C in toluene.¹⁴³ Both Y and Nd amido complexes exhibit high activity at -78 °C (250 h⁻¹ TOF), producing syndio-rich PMMA (67% to 74% *rr*) with relatively broad MWDs (1.6 to 1.9 PDI) and low initiator I^* (28% to 50%, Table 6). When T_p was elevated to 0 °C, the polymerization activity

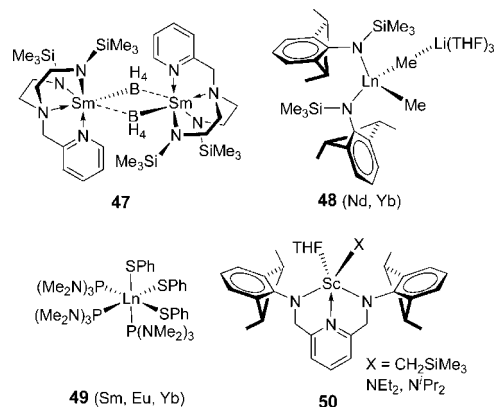
Table 7. Characteristics of the MMA Polymerization by Divalent Non-lanthanocenes

complex	T_p (°C)	TOF (h^{-1})	M_n (kD)	PDI	I^* (%)	mm (%)	ref
51	-78	50	510	1.10	20	97	133
51	0	49	153	1.20	64	78	133
52	0	5	13.6	4.65	18	45	152
52	-78	100	53.4 (25.6)	1.02 (1.02)		73	152
53	-78	54	2600(187)	2.45 (2.18)		78	152
54	-20	638	39.9	2.94	80	15(59 <i>rr</i>)	131
55	-50	13	85.0	1.12	11	1.0 (85 <i>rr</i>)	153
55	-70	7.3	34.9	1.13	15	0.4 (88 <i>rr</i>)	153
56	-25	9.4	18.6	1.79	35	40(33 <i>rr</i>)	153

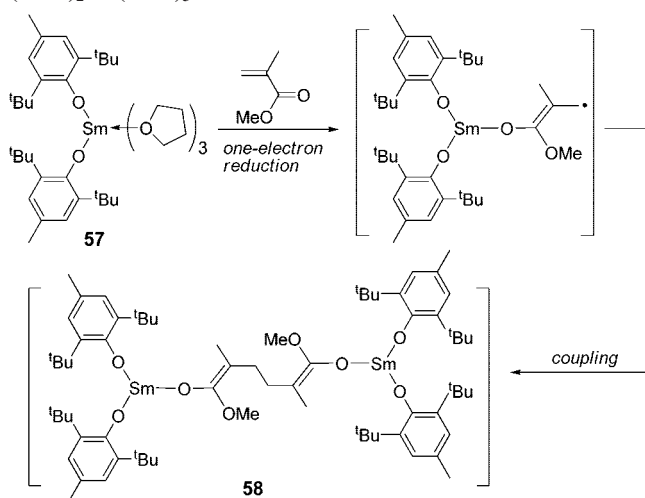
dropped by one-half for both complexes while the polymer tacticity remained the same. The MMA polymerization behavior of lanthanide borohydride complexes of the guanidinate ligand, $[(\text{SiMe}_3)_2\text{NC}(\text{NCy})_2]\text{Ln}(\text{BH}_4)_2(\text{THF})_2$ ($\text{Ln} = \text{Yb}, \text{Er}$), has also been examined.¹⁴⁴ The Er complex (**44**) is more active than the analogous Yb complex (95 h^{-1} vs 82 h^{-1} TOF) at 0°C , although both are less active than bis(quanidinato)lanthanide amido complexes **42** and **43**. On the other hand, the mono(quanidinato)lanthanide borohydride complexes are active at high T_p (up to 45°C), although the activity decrease with an increase of T_p . The PMMAs produced have relatively broad MWDs with typical PDI > 2. Closely related anionic bis(quanidinate) lanthanide borohydride complexes, $[(\text{SiMe}_3)_2\text{NC}(\text{NCy})_2]_2\text{Ln}(\text{BH}_4)_2\text{Li}(\text{THF})_2$ ($\text{Ln} = \text{Nd}, \text{Sm}, \text{Yb}$), were also found to be active in MMA polymerization, producing iso-rich PMMA (51% *mm*) at 21°C in toluene.¹⁴⁵ Chloroytterbium(III) amide **45**, incorporating the β -diketiminato ligand, exhibits only modest activity (up to 46 h^{-1} TOF) from 0 to 60°C in toluene, producing syndio-rich PMMA (40% to 61% *rr*) with broad MWDs ranging from 1.85 to 2.92.¹⁴⁶ The syndiotacticity reached 80.5% *rr* at -78°C . Chloro- and diphenylamido lanthanide(III) complex **46** bearing both rigid $[\text{CH}(\text{PPh}_2\text{NSiMe}_3)_2]^-$ and flexible $[(\text{Ph}_2\text{P})\text{N}]^-$ P,N-ligands in the same molecule are also active for MMA polymerization, with the La complex having the highest activity (up to 703 h^{-1} TOF) at -78°C in toluene and cocatalyzed with an addition of 8 equiv of AlMe_3 .¹⁴⁷ The PMMA produced under these conditions is syndiotactic (80% *rr*) and its $M_n = 9.96 \times 10^5$ and PDI = 1.46; an I^* of 141% suggests either multiple initiating ligands involved or the presence of chain transfer processes.

Samarium borohydride complex **47** supported by the diamide-diamine ligands $(2\text{-C}_5\text{H}_4\text{N})\text{CH}_2\text{N}(\text{CH}_2\text{CH}_2\text{NR})_2$ ($\text{R} = \text{SiMe}_3$ or mesityl) was reported to serve as a single-site catalyst for MMA polymerization in toluene/THF (10/1) in a wide temperature range, yielding syndio-biased PMMA with a relatively narrow MWD (~ 1.2 PDI).¹⁴⁸ At $T_p = -78^\circ\text{C}$, the syndiotacticity of the resulting PMMA is the highest (64.5% *rr*), but the activity is the lowest (20 h^{-1} TOF); raising T_p to 25°C enhances the activity (67 h^{-1} TOF) but decreases the syndiotacticity (35% *rr*). The activity of bis(arylamido)lanthanide methyl complexes **48** at -78°C is higher (up to 79 h^{-1} TOF), while the syndiotacticity is more or less the same (65.3% *rr*).¹⁴⁹ Lanthanoid(III) thiolate

complexes, such as $\text{Ln}(\text{SPh})_3[(\text{Me}_2\text{N})_3\text{P}]_3$ (**49**; $\text{Ln} = \text{Sm}, \text{Eu}, \text{Yb}$), also yielded *st*-PMMA (1.41 PDI) in THF (up to 82% *rr* at 0°C with the Sm catalyst).¹⁵⁰ The polymerization activity is low (24% yield for 24 h in a $[\text{MMA}]/[\text{Sm}]$ ratio of 50, i.e., $\text{TOF} = 0.5 \text{ h}^{-1}$), but it can be enhanced by ~ 3 -fold with addition of 3 equiv of $\text{MeAl}(\text{BHT})_2$ relative to Sm. Lanthanide hydrocarbyl and amido complexes **50** supported by chelating pyridine-diamide ligands showed modest activity (up to 10 h^{-1} TOF for the Sc complexes) at 40°C in toluene, leading to syndio-rich *at*-PMMA (44–50% *mr*, 50–42% *rr*, 1.28–1.60 PDI).¹⁵¹ In contrast, the corresponding complexes of the larger metal centers (Lu and Y) showed only negligible activity, giving PMMA of very broad MWDs (>17.5).



Yasuda et al. reported that divalent ytterbium homoleptic hydrocarbyl complex $\text{Yb}[\text{C}(\text{Me}_3\text{Si})_3]_2$ (**51**) is modestly active for MMA polymerization (50 h^{-1} TOF) but produces highly isotactic PMMA (97% *mm*) with high MW ($M_n = 5.10 \times 10^5$) and a narrow MWD ($M_w/M_n = 1.1$) at -78°C in toluene.¹³³ The PMMA isotacticity is substantially reduced to a low level of 78% *mm* when T_p is elevated to 0°C , but the I^* value calculated based on a monometallic model is more than tripled (from 20% to 64%, Table 7). Highly isotactic (98% *mm*) poly(2-(dimethylaminoethyl methacrylate)) was also synthesized at -78°C using **51**. The authors attributed the formation of *it*-PMMA to enantiomorphic-site control and to the conjugate addition chain growth not involving an eight-membered-ring intermediate.¹³³ However, it is not clear where the chirality at metal in complex **51** stems from for the postulated noncyclic intermediate mech-

Scheme 6. Chain Initiation Step in MMA Polymerization by (BHT)₂Sm(THF)₃


anism. Furthermore, as in the classic, non-site-controlled anionic polymerization of MMA initiated by organometallic lithium reagents, solvents play a critical role in determining the tacticity of the PMMA produced, especially at low temperatures: polar coordinating solvents (e.g., THF, DME) favor syndiotactic placement, whereas nonpolar solvents (e.g., toluene) typically favor isotactic placement (section 2.1.1). Accordingly, replacing toluene with THF under otherwise identical conditions, *st*-PMMA (87% *rr*) is resulted with this ytterbium complex.¹³³ On the other hand, divalent ytterbium complex **52** supported by the 1,5-diazapentadienyl ligand (aza-allyl type ligand) was found to be highly active toward MMA polymerization (100 h⁻¹ TOF) at *T_p* of -78 °C in toluene, producing isotactic (72.5% *mm*) PMMA with a bimodal MWD, although both low and high MW fractions have a very narrow MWD (1.02 PDI).¹⁵² Bridged bis(allyl)-type ytterbium complex **53** exhibits lower activity and is uncontrolled in MMA polymerization even at -78 °C.

Divalent ytterbium complex **54** supported by the BHT (BHT = 2,6-*t*Bu₂-4-Me-C₆H₂O) and the β-diketiminato ligand is highly active for MMA polymerization at -20 °C,

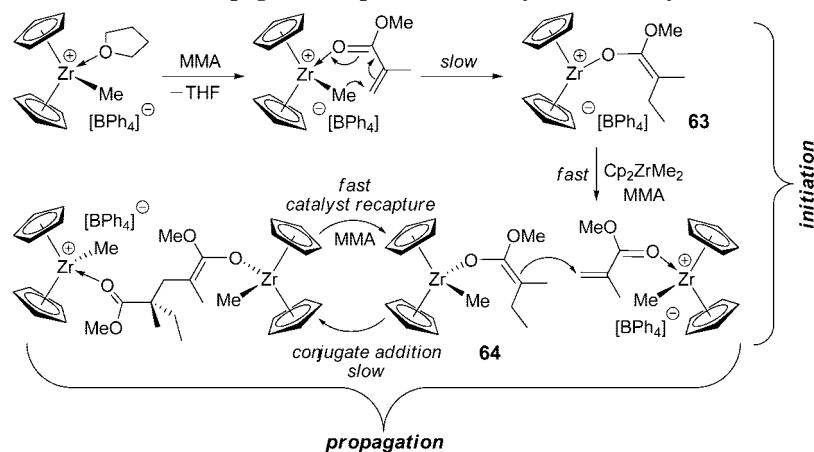
with the TOF reaching 638 h⁻¹.¹³¹ The PMMA (*M_n* = 3.99 × 10⁴) produced in toluene is syndio-rich (*rr* = 59%) and exhibits a broad MWD (PDI = 2.94). Interestingly, the calculated *I** value based on a unimetallic model is 80%, which seems inconsistent with the proposed one-electron transfer initiator mechanism leading to a trivalent diinitiator for this Yb(II) complex. Divalent samarium complexes incorporating the boratabenzene ligand, (C₅H₅BXPh₂)-Sm(THF)₂ (**55**, X = N), afford *st*-PMMA (84.8% *rr*) at -50 °C in toluene with modest activity (13 h⁻¹ TOF).¹⁵³ The *I** values, based on the unimetallic model, were low (11–15%; in the case of a bimetallic model, the values would be doubled). Interestingly, when X is changed from N to P (**56**), iso-rich *at*-PMMA (39.9% *mm*) was produced instead at -25 °C in toluene (9.4 h⁻¹ TOF).

Living polymerization of methacrylates was effected by SmI₂ (in the presence of catalytic amounts of SmI₃) as a diinitiator; the initiation and propagation mechanism was proposed to be similar to that described for the divalent lanthanocene [Cp*₂Sm]-initiated MMA polymerization (section 2.1.1).¹⁵⁴ A divalent nonmetallocene samarium complex supported by the bulky phenoxy ligand, (BHT)₂Sm(THF)₃ (**57**), was reported to polymerize MMA to *st*-PMMA.¹⁵⁵ A subsequent study indicates this complex promotes living polymerization of MMA in toluene at -78 °C (TOF = 200 h⁻¹, *M_n* = 4.30 × 10⁴, PDI = 1.08, *rr* = 90%);¹⁵⁶ negligible activity was observed for polymerizations carried out at >0 °C. The active propagating species was proposed to be bimetallic Sm(III) enolate **58** (Scheme 6), derived from the same redox and radical coupling initiation pathway, as already demonstrated for Cp*₂Sm(THF)₂ (cf. Scheme 5).¹⁰⁶ The added Lewis acid cocatalyst MeAl(BHT)₂ significantly modulates the tacticity of the resulting PMMA. Thus, as the [Al]/[Sm] ratio increases from 0 to 5, the *rr* % content decreases from 90 to 20% and the *mm* % content increases from 1 to 60%, while the heterotactic *mr* % content remains nearly constant. This phenomenon was explained by a scenario where syndiospecific and isospecific sites coexist on the propagating chain ends in which the isospecific propagation is effected by coordination of the aluminum

Table 8. Characteristics of the MMA Polymerization by Allyl Lanthanide(II) Complexes

complex	solvent	<i>T_p</i> (°C)	TOF (h ⁻¹)	<i>M_n</i> (kD)	PDI	<i>I*</i> (%)	<i>mr</i> (%)	ref
59	toluene	0	5	13.6	4.65	18	45 (<i>mm</i>)	152
61	toluene	0	83,100	43.8	2.0	158	43	157
61	toluene	-78	460	78.8	3.2	127		157
61	THF	0	68,800	35.7	2.2	164		157
61	THF	-78	97,700	68.2	4.7	81		157
62	toluene	0	86,400	99.9	3.0	72	54	158
62	THF	0	970	101	1.94	24	55	159

Scheme 7. Chain Initiation and Bimetallic Propagation Steps in MMA Polymerization by the Two-Component System



phenoxide ligand to the Sm center or by the monomer coordination to the aluminum center. The PMMA obtained at $[Al]/[Sm] = 4$ exhibits a unique methyl triad distribution of $[mm]/[mr]/[rr] = 42/11/47$ and a T_m of 161 °C, suggesting the formation of a stereocomplex between syndiotactic and isotactic PMMAs.

Divalent samarium complex **59** incorporating the 1,3-bis(trimethylsilyl)allyl ligand exhibits low activity (5 h^{-1} TOF) and efficiency (18% I^*) at 0 °C, producing iso-rich PMMA (45% mm) with a broad MWD of 4.65 (Table 8).¹⁵² On the other hand, Bochmann and co-workers discovered that divalent samarium allyl potassium salt complex **61** $\{Sm[C_3H_3(SiMe_3)_2]_3[\mu-K(THF)_2]\}_2$ supported by the bulky allyl ligand shows *exceptionally high activity* for MMA polymerization at 0 °C in toluene, with TOF reaching 83,100 h^{-1} (at 69% MMA conversion), producing predominately atactic PMMA ($\sim 43\% \text{ } mr$).¹⁵⁷ As indicated by the $>100\%$ I^* value (158% even based on a monometallic model), either chain transfer or two initiating ligands per Sm center are operative. The polymerization is much slower at $-78 \text{ } ^\circ\text{C}$ (460 h^{-1}), but the reaction at this low temperature enabled a quantitative monomer conversion. At $T_p = 0 \text{ } ^\circ\text{C}$, little difference is shown between the polymerizations in toluene and in THF; however, at $-78 \text{ } ^\circ\text{C}$, the polymerization in THF led to a >200 -fold increase in activity, giving a TOF of 97,700 h^{-1} . Related *ansa*-dimethyl silylene-bis(allyl) lanthanide complexes supported by the $[Me_2Si(C_3H_3SiMe_3)_2]^{2-}$ ligand are also highly active catalysts for the production of *at*-PMMA, with TOF reaching as high as 86,400 h^{-1} at 0 °C in toluene for the yttrium complex **62**.¹⁵⁸ The polymerization by **62** at 0 °C in THF is ~ 90 times slower than that in toluene,¹⁵⁹ with a low monomer conversion and a high MW ($M_n = 1.01 \times 10^5$), the calculated initiator efficiency is low ($I^* = 24\%$, based on the unimetallic model). The anionic lanthanide allyl complexes $\{Ln[3-(\eta^3-C_3H_3-SiMe_3)_2SiMe_2]\}_2[Li(OEt_2)(THF)_3]$ are also highly active for MMA polymerization at 0 °C in THF (45,100 h^{-1} TOF), but producing iso-rich PMMA (41.7% mm) with a broad MWD (5.40 PDI).¹⁵⁹ Neutral divalent (**59**, Ln = Eu, Yb, Sm) or trivalent (**60**, Ln = Ce, Nd) lanthanide complexes bearing the bulky 1,3-bis(trimethylsilyl)allyl ligand afford *at*-PMMA in toluene and are much less active than their corresponding potassium salt complexes “[Ln(allyl)₃]K(THF)_{*n*}” derived from *in situ* mixing of the neutral bis(allyl) complex with $K[1,3-(SiMe_3)_2(\eta^3-C_3H_3)]$.¹⁶⁰ However, this *in situ* mixture exhibited a reduced activity by ~ 5 -fold as compared with the isolated salt complex **61** prepared by the

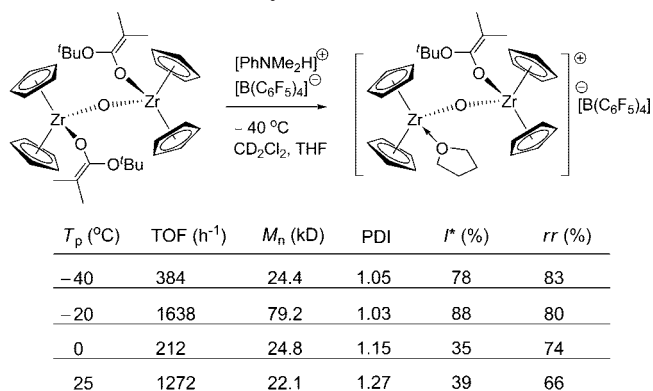
halide salt metathesis route.¹⁵⁷ More strikingly, the simple potassium salt $K[1,3-(SiMe_3)_2(\eta^3-C_3H_3)]$ alone shows exceedingly high activity at 0 °C in toluene with TOF = 92,500 h^{-1} , producing nearly perfect *at*-PMMA (54% mr) with high MW ($M_n = 1.10 \times 10^5$, PDI = 1.95) and high initiator efficiency ($I^* = 85\%$).¹⁶⁰

2.2. Group 4 Metallocenes

2.2.1. Nonbridged Catalysts

Collins and Ward initially employed a two-component system consisting of a cationic zirconocenium complex, $[Cp_2ZrMe(THF)]^+[BPh_4]^-$, as catalyst, and a zirconocene dimethyl complex, Cp_2ZrMe_2 , as initiator, to polymerize MMA to high MW, syndio-rich *at*-PMMA (80% r at 0 °C) by a chain-end control mechanism in a nonliving manner.⁶⁹ Subsequently, detailed kinetic (zero-order dependence in $[MMA]$) and mechanistic studies by Collins and co-workers revealed that slow initiation (with respect to propagation) involves the rate-limiting reaction of the cationic complex with MMA to generate cationic enolate species **63**, which, upon reaction with Cp_2ZrMe_2 , is subsequently converted to neutral zirconocene enolate **64** and the methyl zirconocene cation (Scheme 7).¹⁶¹ The mechanism of a propagation cycle consists of rate-limiting intermolecular Michael addition of the neutral enolate ligand to the MMA coordinated to (activated by) the methyl zirconocene cation (catalyst), followed by fast release of the catalyst by incoming MMA (Scheme 7).

Subsequent density functional theory (DFT) calculations by Sustmann et al. on three possible propagation mechanism scenarios¹⁶² and kinetic studies by Bandermann et al. using the similar system consisting of $Cp_2ZrMe_2 + [Ph_3C][B(C_6F_5)_4]$ (<1 equiv)¹⁶³ further support the proposed bimetallic propagation mechanism. This mechanistic insight brought about an efficient and living polymerization system at or below 0 °C by simply substituting the slow initiating Cp_2ZrMe_2 with the preformed neutral zirconocene enolate $Cp_2ZrMe[OC(O^tBu)=CMe_2]$; namely the $[Cp_2ZrMe(THF)]^+[BPh_4]^-/Cp_2ZrMe[OC(O^tBu)=CMe_2]$ pair.¹⁶¹ Further studies by the groups of Collins and Bandermann showed that neutral ester enolate $Cp_2ZrMe[OC(OR)=CMe_2]$ ($R = Me, ^tBu$) is inactive by itself, but its combination with the metallocenium cation Cp_2ZrMe^+ as catalyst is highly active and of living characteristics in a bimolecular MMA polymerization process.^{161,164} Other analogous catalyst/initiator

Scheme 8. Covalently Linked Bifunctional Initiator/Catalyst for Controlled MMA Polymerization


pairs, such as the $[Cp_2ZrCl]^+[B(C_6F_5)_4]^-/Cp_2ZrCl[OC(OMe)=CMe_2]$ pair derived from the proposed complex reaction sequence starting with $Cp_2ZrCl[OC(OMe)=CMe_2]$ and $[Ph_3C][B(C_6F_5)_4]$, have also been reported.¹⁶⁵

The initiator/catalyst components have been covalently linked via a robust μ -oxo linkage into a dinuclear enolate zirconocene complex (Scheme 8).¹⁶⁶ The corresponding cationic enolate complex, which consists of both the ester enolate initiator and the cationic zirconocene catalyst sites, can be generated upon treatment with $[PhNMe_2H][B(C_6F_5)_4]$, affording a highly active, controlled polymerization system producing *st*-PMMA ($\geq 80\%$ *rr*) with high I^* ($\geq 78\%$) and TOF ($>380 h^{-1}$) at $T_p \leq -20$ °C. On going from -40 to 25 °C, the syndiotacticity of the resulting PMMA decreases from 83% *rr* to 66% *rr*, a typical behavior for a chain-end control polymerization process.

Although nonbridged cationic zirconocenes based on the parent $[Cp_2Zr]^+$,^{161,167,168} $[(2-Ph-Ind)_2Zr]^+$,¹⁶⁹ or $[(Cp)(Flu)Zr]^+$ ¹⁷⁰ systems can also polymerize methacrylates via a *unimolecular* process involving intramolecular conjugate addition through cationic enolate intermediates, Collins¹⁶¹ and Chen¹⁶⁹ concluded that the *bimolecular* pathway using a neutral zirconocene/cationic zirconocene initiator/catalyst pair is considerably more efficient and competitive for nonbridged zirconocenes (Scheme 9¹⁶⁹). Two components (initiator and catalyst) promoting the bimolecular propagation can also be employed in the form of μ -methyl-bridged dinuclear zirconocenium complexes isolated by Marks¹⁷¹ and others.¹⁷² Owing to these competing processes available for the unbridged metallocene system, *caution should be exercised* when examining the polymerization characteristics of such a system, *especially when the catalyst is generated by in situ mixing of the catalyst precursor and activator*; the addition sequence of all reagents and monomers involved, relative amounts, and concentration can significantly alter polymerization results, determined by the relative contribution of unimolecular and bimolecular processes.

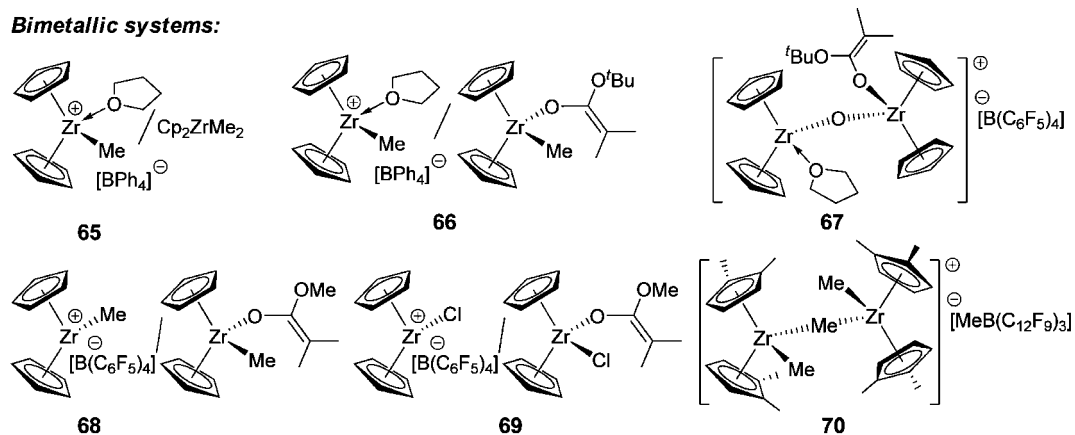
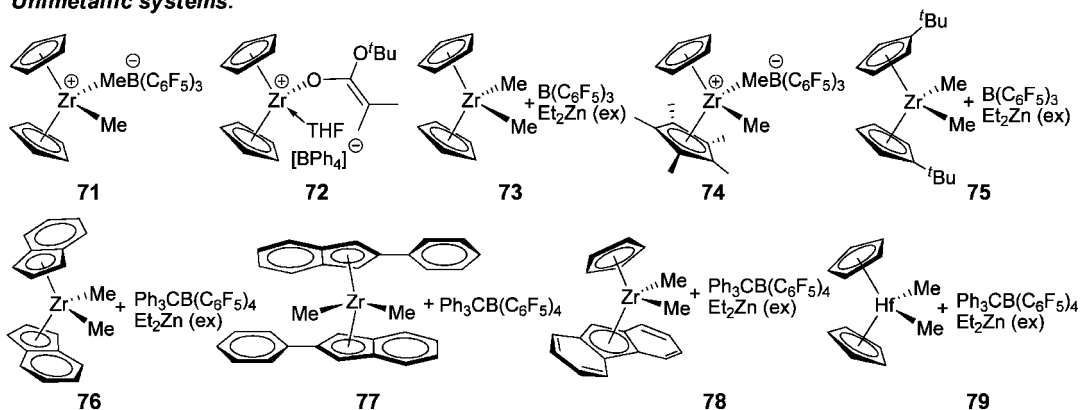
Soga et al. reported that a procedure involving addition of Cp_2ZrMe_2 to a toluene solution of MMA premixed with the activator $B(C_6F_5)_3$ or $[Ph_3C][B(C_6F_5)_4]$ was incapable of initiating MMA polymerization.¹⁷³ On the other hand, premixing MMA with a large excess of Et_2Zn (943 equiv per Zr) followed by additions of the activator and the metallocene yielded an active MMA polymerization system employing a high $[MMA]/[Zr]$ ratio of 3745 and a low Zr concentration of 0.227 mM, although the polymerization achieved only 64% yield at 0 °C (or 8% at 40 °C) in 24 h,

giving a TOF up to $100 h^{-1}$.¹⁷³ Likewise, no activity was observed for the MMA polymerization with Cp_2ZrCl_2 activated with MAO at 0 °C, but in the presence of excess Et_2Zn , the system again became active (TOF = $53 h^{-1}$), producing *at*-PMMA with a broad MWD (PDI = 10).¹⁷⁴ Dichlorozirconocene Cp_2ZrCl_2 (also Cp_2TiCl_2), combined with an anionic surfactant (sodium *n*-dodecyl sulfate) as emulsifier, has been reported to polymerize MMA (and styrene) in aqueous medium to high MW, syndio-rich *at*-PMMA (M_n up to 5.8×10^5 , PDI = 1.4, 50–60% *rr*) at 70–90 °C, through a claimed insertion mechanism.¹⁷⁵

The polymerization activity and polymer characteristics of the L_2ZrMe_2 ($L = Cp, ^tBuCp, Ind$)/ $B(C_6F_5)_3/Et_2Zn$ (excess) system were much improved later on through a better purification protocol, thereby leading to poly(alkyl methacrylate)s (alkyl = Me, *n*-butyl, *n*-hexyl, *n*-decyl, stearyl, and *sec*-butyl) with high MWs (M_n up to 7.5×10^5) and narrow MWDs (PDI = 1.09–1.20) as well as achieving $\geq 90\%$ yields.^{176,177} However, Gibson and co-workers reported that addition of MMA to a toluene solution of the preformed cationic complex $Cp_2ZrMe^+MeB(C_6F_5)_3^-$, derived from *in situ* mixing of Cp_2ZrMe_2 and $B(C_6F_5)_3$ (1–2% excess to ensure complete conversion of the dimethyl to the cationic species), is in fact highly active for MMA polymerization at 25 °C with TOF = $184 h^{-1}$ even without addition of any Et_2Zn ,¹⁷⁸ the PMMA produced is syndio-rich (67% *rr*) with PDI = 1.24, but I^* calculated based on the unimolecular propagation model is only $\sim 41\%$. It should be pointed out that the latter system employed a much higher catalyst concentration (16.2 mM) and a lower $[MMA]/[Zr]$ ratio of 200 than Soga's three-component system in the presence of excess Et_2Zn ($[Zr] = 0.227$ mM and $[MMA]/[Zr] = 3745$). Through its coordination with MMA, the role of Et_2Zn was suggested to protect the borane activator from being poisoned by the carbonyl group of the monomer,¹⁷⁸ besides its anticipated role as a scavenger, which is important, especially under very dilute catalyst conditions.

Application of the chain-transfer polymerization strategy to the MMA polymerization mediated by the unbridged group 4 metallocene system has been so far unsuccessful. For example, addition of 1–10 equiv of enolizable ketones to the MMA polymerization by $Cp_2ZrMe_2/B(C_6F_5)_3$ inhibited polymerization because the reaction between the zirconocene enolate reactive intermediate and ketones generates the inactive Zr-aldol product.¹⁶⁸ While this system can tolerate the presence of tBuSH and the resulting *tert*-butyl thiolate complex is still active for reinitiation of MMA polymerization, its poor initiation efficiency largely limited the effectiveness of tBuSH as a CTR in the MMA polymerization by the $Cp_2ZrMe_2/B(C_6F_5)_3$ system.

Unbridged titanocenes and hafnocenes have been examined to a much less extent for MMA polymerization. The $Cp_2TiMe_2/[Ph_3C][B(C_6F_5)_4]/Et_2Zn$ (excess) system was found to be inactive for MMA polymerization at 0 °C up to 24 h, and only marginal activity (TOF = $14 h^{-1}$) was observed for MMA polymerization upon replacing the titanocene with the hafnocene.¹⁷⁴ The PMMA produced by the hafnocene exhibits a lower syndiotacticity of 57% *rr* and a broader MWD of PDI = 2.03, as compared to 65%–67% *rr* and <1.38 PDI achieved by the zirconocene analogue. A patent lecture disclosed that titanocene mono-enolate or bis(enolate) complexes, such as $Cp_2TiCl[OC(OMe)=CMe_2]$ and $Cp_2Ti[OC(OMe)=CMe_2]_2$, upon activation with suitable activators, including $[PhNMe_2H][B(C_6F_5)_4]$, $AgN(SO_2CF_3)_2$,

Bimetallic systems:**Unimetallic systems:**

catalyst	T_p (°C)	TOF (h^{-1})	M_n (kD)	PDI	I^* (%)	rr (%)	ref.
65	0	190	149	1.32		80 (<i>r</i>)	69
66	0	1,320	14.1	1.05	78		161
67	-20	1,638	79.2	1.03	88	80	166
68	0	140	107	1.03	65		164
69	0		39.7	1.07	66		165
70	25	407				67	171
71	25	184	45.2	1.24	41	67	178
72	0	40	20.0	1.55	20		161
73	0	100	482	1.38	50	72	173
74	25	84	30.8	1.15	27	44	178
75	0	22	180	1.09	31	84 (<i>r</i>)	177
76	0	10	23.0	1.17	21	72	170
77	23	6	31.2	1.43	5	66	169
78	0	321	260	1.11	29	69	170
79	0	14	84.0	2.03	40	57	174

Figure 4. List of bimetallic and unimetallic MMA polymerization systems based on nonbridged group 4 metallocenes and their polymerization characteristics.

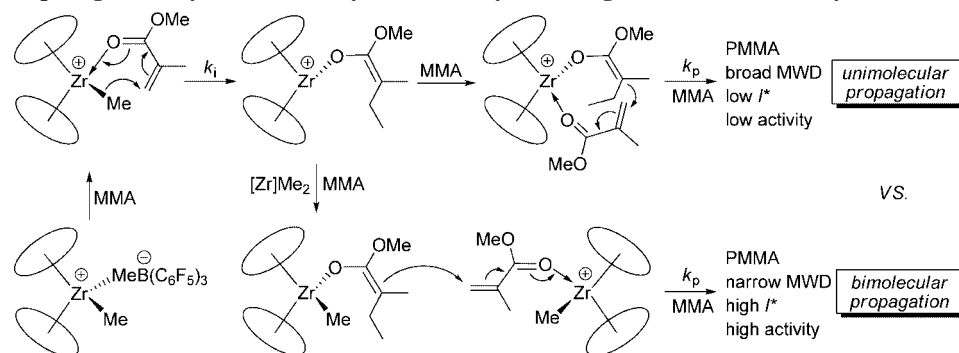
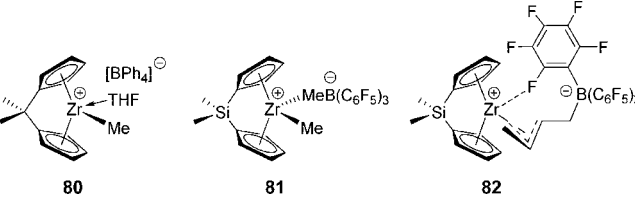
Scheme 9. Two Competing Pathways in MMA Polymerization by Nonbridged Metallocene Catalysts

Table 9. Characteristics of the MMA Polymerization by C_{2v} -Ligated *ansa*-Zirconocenes


catalyst	T_p (°C)	TOF (h^{-1})	M_n (kD)	PDI	I^* (%)	rr (%)	ref
80	-45	7	78.5	1.31	16	89	181
80	0	101	90.6	1.32	11	79	181
80	30	244	66.6	1.64	12	69	181
81	0	42 ^a	68.5	1.81		60	183
82	0	27 ^a	34.1	1.70		65	183

^a Percent monomer conversion per hour as the [MMA]/[Zr] ratio was not given in the reference.

and $B(C_6F_5)_3$, are found to be active for MMA polymerization.¹⁷⁹ However, the activity of this system was very low, and PMMA produced broad MWDs (PDI > 2). A chloro heterobimetallic metallocene of titanium and samarium, $Cl_2Ti(Cp)(C_5H_4)-CH_2CH_2-(C_5H_4)CpSmCl$, when used alone or in combination with $Al(tBu)_3$, produces syndio-rich PMMA (65% rr).¹⁸⁰

Figure 4 summarizes the MMA polymerization characteristics by nonbridged group 4 metallocenes, from which the following conclusions can be drawn: (1) Zr complexes are most reactive; (2) the bimolecular pathway is much more efficient and competitive than the unimolecular pathway; (3) the polymerization is chain-end controlled, and thus the syndiotacticity of the PMMA produced is largely affected by changing T_p rather than varying the ligand (i.e., a small tacticity modulation in a narrow window of 64% to 70% rr at ambient temperature); and (4) *the most reactive, efficient, and controlled polymerization system is the one consisting of a neutral metallocene ester enolate initiator and a cationic alkyl metallocene catalyst.*

2.2.2. *ansa*- C_{2v} -Ligated Catalysts

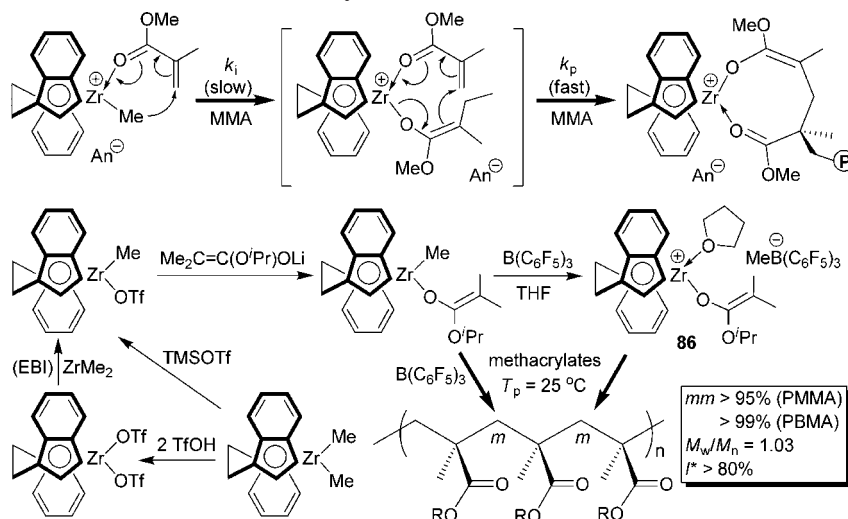
Höcker and co-workers reported that cation **80** derived from activation of C_{2v} -symmetric *ansa*-zirconocene $Me_2C(Cp)_2ZrMe_2$ with $[tBu_3NH][BPh_4]$ affords syndio-rich (69% rr at 30 °C) or syndiotactic (89% rr at -45 °C; Table 9) PMMA.¹⁸¹ The I^* values were low (<16%) at all T_p 's investigated, and as anticipated, the chain-end control mechanism is responsible for the syndiospecificity achieved by cation **80**. To explain why cation **80** is active for MMA polymerization while the unbridged analogue $[Cp_2ZrMe(THF)]^+[BPh_4]^-$ is inactive (when used alone for a monometallic pathway), the same group performed DFT calculations on stationary points along the reaction coordinate and showed that the initiation step involving transfer of the Zr bound methyl group to the MMA coordinated to Zr is endothermic for the unbridged cation $[Cp_2ZrMe(THF)]^+[BPh_4]^-$ but exothermic for the bridged cation **80** and, more importantly, the unbridged cation encounters higher activation energies along the reaction coordinate than the bridged cation **80**.¹⁸² This example highlights the *ansa*-effect in MMA polymerization: the metal center in the *ansa*-metallocene is more sterically accessible for approaching the growing enolate chain end to the coordinated monomer ready for intramolecular conjugate addition, thus promoting unimetallic propagation.

The MMA polymerization activity is further affected by the relative coordinating capacity of the counteranion. For example, $[Cp_2ZrMe(THF)]^+[BPh_4]^-$ is inactive¹⁸¹ while $Cp_2ZrMe^+MeB(C_6F_5)_3^-$ is active.¹⁷⁸ Erker and co-workers provided evidence for active involvement of anion in the polymerization activity and stereoselectivity while examining MMA polymerization characteristics using a series of alkyl-substituted dimethylsilyl-bridged bis(Cp) cationic complexes.¹⁸³ The parent Me_2Si -bridged C_{2v} -symmetric complex **81** affords syndio-rich PMMA (60% rr at 0 °C),¹⁸³ which is significantly lower than that produced by the Me_2C -bridged C_{2v} -symmetric complex **80** at the same T_p (79% rr at 0 °C).¹⁸¹ On the other hand, the zwitterionic catalyst **82** improved the syndiotacticity over **81** (65% rr vs 60% rr), at the expense of activity (Table 9).¹⁸³

2.2.3. *ansa*- C_2 -Ligated Catalysts

Highly isotactic PMMA ($mm > 94\%$) can be readily produced at *ambient temperature* with chiral *ansa*-zirconocene dimethyl complexes incorporating C_2 -symmetric ligands, *rac*-(EBI)ZrMe₂ [EBI = $C_2H_4(\eta^5\text{-indenyl})_2$] and *rac*-(SBI)ZrMe₂ [SBI = $Me_2Si(\eta^5\text{-indenyl})_2$], upon activation with suitable activators such as $B(C_6F_5)_3$ ¹⁷⁸ and $[Ph_3C][B(C_6F_5)_4]/Et_2Zn$ (excess)^{173,184} or with the isolated zirconocenium ion pairs.¹⁸⁵ The tetrahydroindenyl derivative *rac*-[$C_2H_4-(H_4Ind)_2$]ZrMe₂, once activated with $[tBu_3NH][BPh_4]$, affords also highly isotactic PMMA at 0 °C.¹⁸⁶ As can be seen from Figure 5, these methyl-based catalysts (**83**, **84**, and **85**) exhibit only modest to good activity (TOF = 20–200 h^{-1}), and importantly, they are ill-behaved and inefficient in MMA polymerization, thus giving rise to much higher measured M_n than the calculated M_n , low I^* of <50%, and relatively broad MWDs of >1.20.

Based on a hypothesis that the above-described undesirable characteristics of the MMA polymerization by the *alkyl-based* chiral catalyst are caused by slow initiation with the methyl ligand with respect to fast propagation with the more reactive ester enolate ligand (Scheme 10), Bolig and Chen synthesized a preformed cationic zirconocenium ester enolate catalyst, *rac*-(EBI)Zr⁺(THF)[OC(O'Pr)=CMe₂][MeB(C₆F₅)₃]⁻ (**86**, Figure 5).¹⁸⁷ The structure of **86** simulates the proposed active propagating species shown in Scheme 10, thus in essence bypassing the slow chain-initiation step, and therefore, it not only significantly enhances the polymerization activity (by ~20 fold), with TOF now reaching 3600 h^{-1} and a much higher I^* (by ~2 fold) of 80%, compared to the methyl-based catalyst, it also renders a living polymerization process, producing PMMA with controlled MW and a narrow MWD (PDI = 1.03, Figure 5). Accordingly, this catalyst polymerizes ≥ 400 equiv of MMA with quantitative monomer conversions in less than 10 min (vs hours with the methyl catalyst) at ambient temperature, producing PMMA with high isotacticity (95% mm). This polymerization is enantiomorphic-site controlled (as a methyl triad test using $2[rr]/[mr]$ gave 1.0) and of living nature with initiator efficiency, typically $\geq 80\%$. The MMA polymerization activity and initiator efficiency as well as the resulting polymer MWD and isotacticity with the isolated cationic ester enolate catalyst **86** are nearly identical to those of the polymerization with premixing the activator $B(C_6F_5)_3$ with MMA followed by addition of the neutral methyl ester enolate complex *rac*-(EBI)ZrMe[OC(O'Pr)=CMe₂] (Scheme 10); this latter convenient polymerization procedure employs directly the neutral ester enolate precursor (which is much easier to

Scheme 10. Slow Initiation and Fast Propagation Steps by the C₂-Ligated Chiral Zirconocenium Methyl Cation and Synthesis of Cationic Zirconocenium Ester Enolate **86 and Its Polymerization Characteristics**


handle than the corresponding cationic species) via in-reactor activation. Impressively, polymerization of *n*BMA by this catalyst system produces the corresponding polymer P(*n*-BMA) with quantitative isotacticity (*mm* > 99%), narrow MWD (PDI = 1.03), and high initiator efficiency (*I** = 95%).¹⁸⁷

Kinetic studies by Rodriguez and Chen have shown that the polymerization by **86** exhibits first-order dependence in concentrations of both the monomer and the active cationic enolate species.¹⁸⁸ The initiating ester end group ^tPrOC(=O)CMe₂-, derived from the initiating isopropyl isobutyrate group in complex **86**, and the termination chain-

	83	84	85	86
<i>T_p</i> (°C)	25	0	0	25
TOF (h ⁻¹)	198	62	20	3,600
<i>M_n</i> (kD)	48.7	320	11.4	75.5
PDI	1.20	1.32	1.71	1.03
<i>I</i> * (%)	40	46	41	80
<i>mm</i> (%)	95	94.4	86.8	95.3
ref.	178	184	184	187

Figure 5. Characteristics of the MMA Polymerization by C₂-Ligated Cationic *ansa*-Zirconocene Complexes

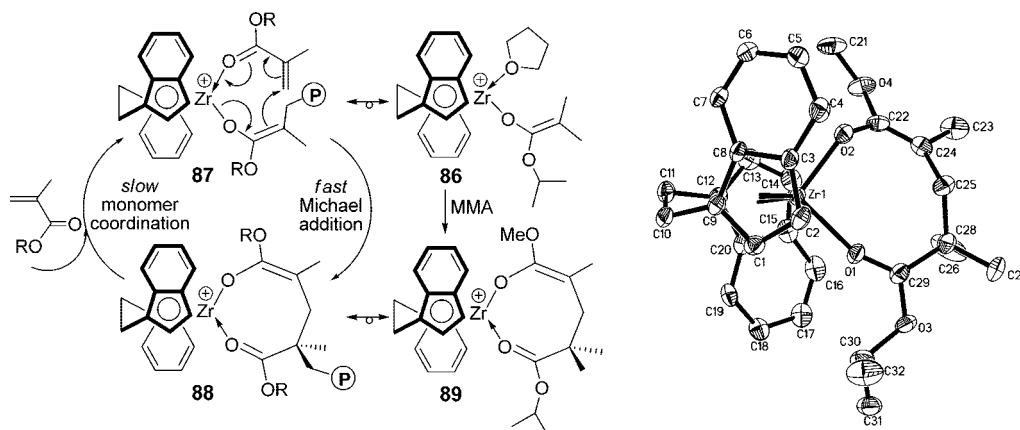


Figure 6. Mechanism of the propagation “catalysis” cycle, isolated model complexes **86** and **89** to simulate the structures of the catalyst–monomer complex and catalyst resting intermediate, respectively, and the X-ray structure of cation **89**. (Reprinted with permission from ref 189. Copyright 2006 American Chemical Society).

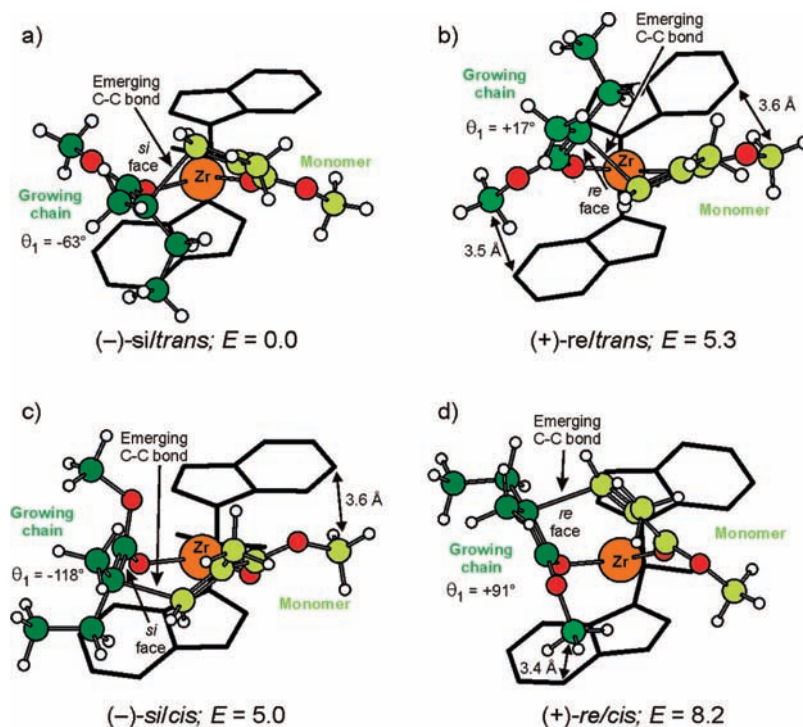


Figure 7. Four transition states for the conjugate addition step with the C_2 -symmetric rac - $Me_2C(Ind)_2Zr$ -based catalyst incorporating a (S,S)-coordinated bis(indenyl) ligand. Energies, relative to the most stable TS ($-$)- $si/trans$, are reported in kcal/mol. Reprinted with permission from ref 76. Copyright 2006 American Chemical Society.

end H, derived from the HCl-acidified methanol during the workup procedure, have been confirmed using MALDI-TOF mass spectroscopy. Their investigation has yielded several lines of evidence to support a *site-controlled, monometallic, coordination–addition mechanism* for the isospecific methacrylate polymerization by the preformed ester enolate cation **86**. In a propagation “catalysis” cycle depicted in Figure 6, the fast intramolecular Michael addition within the catalyst–monomer complex **87** produces the eight-membered-ring ester enolate chelate **88** as the resting intermediate, followed by the rate-limiting step of the associative displacement of the coordinated penultimate ester group by incoming methacrylate monomer (ring-opening of the chelate) to regenerate the active species **87**. The molecular structure of the resting intermediate was confirmed by the isolation and characterization of the single-monomer addition product **89**,¹⁸⁸ the cation of which was characterized by X-ray single-crystal diffraction analysis.¹⁸⁹

Cavallo and co-workers have shown that, through their DFT studies of the C_2 -symmetric rac - $Me_2C(Ind)_2Zr$ catalyst, the chiral catalyst induces a chiral orientation of the ester enolate growing chain which in turn selects its own enantioface for conjugate addition to MMA.⁷⁶ This stereocontrol mechanism is different from that for α -olefin polymerization, where the chirally orientated growing chain selects between the two enantiofaces of the prochiral monomer. Four transition states for the MMA polymerization by the catalyst center with a (S,S)-coordinated bisindenyl ligand were considered in this study (Figure 7). Calculations indicate that the ($-$)- $si/trans$ TS for attack of the si enantioface of the growing chain to MMA (Figure 7a) is the most favored, as a result of reduced steric stress in this geometry, since the methoxy groups of both the growing chain and MMA are oriented away from the indenyl groups of the metallocene. Considering two homotopic sites present in the C_2 -symmetric catalyst, the ΔE_{Stereo} of 5.3 kcal/mol ensures the selection of

the same enantioface of the enolate chain end for MMA addition when the addition takes place at either site, rationalizing the formation of highly isotactic ($\sim 95\%$ of mm at 25 °C) PMMA by C_2 -symmetric catalysts.

Chen and co-workers found that neutral methyl enolate complex rac -(EBI)ZrMe[OC(OⁱPr)=CMe₂] adds cleanly only 1 equiv of MMA, but triflate enolate complex rac -(EBI)Zr(OTf)[OC(OⁱPr)=CMe₂] can add either 1 equiv of MMA to form the single-MMA-addition product rac -(EBI)Zr(OTf)[OC(OMe)=C(Me)CH₂C(Me)₂C(OⁱPr)=O] (**90**) or multiple equivalents of MMA to form PMMA.¹⁹⁰ The MMA polymerization by **90** gives a very low TOF of $\sim 2\text{ h}^{-1}$ and a low I^* of 49%; thus, it is considerably slower and less efficient than the analogous cationic zirconocenium ester enolate species **86**. The PMMA produced has $M_n = 10,300$, PDI = 1.24, and a methyl triad distribution of $[mm] = 46.5\%$, $[mr] = 26.7\%$, $[rr] = 26.8\%$. Another C_2 -ligated chiral neutral group 4 metallocene complex that has been found to be active for MMA polymerization is a zirconocene complex incorporating the chelating isopropylidene-bridged Cp *o*-carboranyl ligand: rac -Zr(η^5 : η^1 -CpCMe₂CB₁₀H₁₀C)₂;¹⁹¹ this complex, however, polymerizes MMA in polar, coordinating THF (which typically retards or shuts down the coordination–addition polymerization of MMA by group 4 metallocene catalysts) and yields syndio-rich *at*-PMMA (65% rr) despite its C_2 symmetry. Furthermore, the I^* value based on the polymerization results for 24 h was calculated to be $\sim 510\%$, indicating considerable chain transfer processes.

Interestingly, pure *meso*-diastereomers, $meso$ -(EBI)ZrMe₂ and $meso$ -(SBI)ZrMe₂, upon activation with B(C₆F₅)₃, produce syndio-rich *at*-PMMA with bimodal MWDs.¹⁶⁹ The formation of bimodal polymers using these *meso*-diastereomers was attributed to the coexistence of two independent polymerization processes (i.e., unimetallic vs bimetallic). On the basis of the same reasoning, the diastereomeric mixtures

	91	92	93	94
T_p ($^{\circ}\text{C}$)	25	-20	25	23
TOF (h^{-1})	154	43	170	19,680
M_n (kD)	33.4	39.7	25.0	51.4
PDI	1.49	1.12	1.51	1.26
I^* (%)	46	32	68	64
mm (rr) (%)	81	89.7	54	(69)
ref.	178	192	178	195

Figure 8. Characteristics of the MMA Polymerization by C_1 -Ligated Cationic *ansa*-Zirconocene Complexes

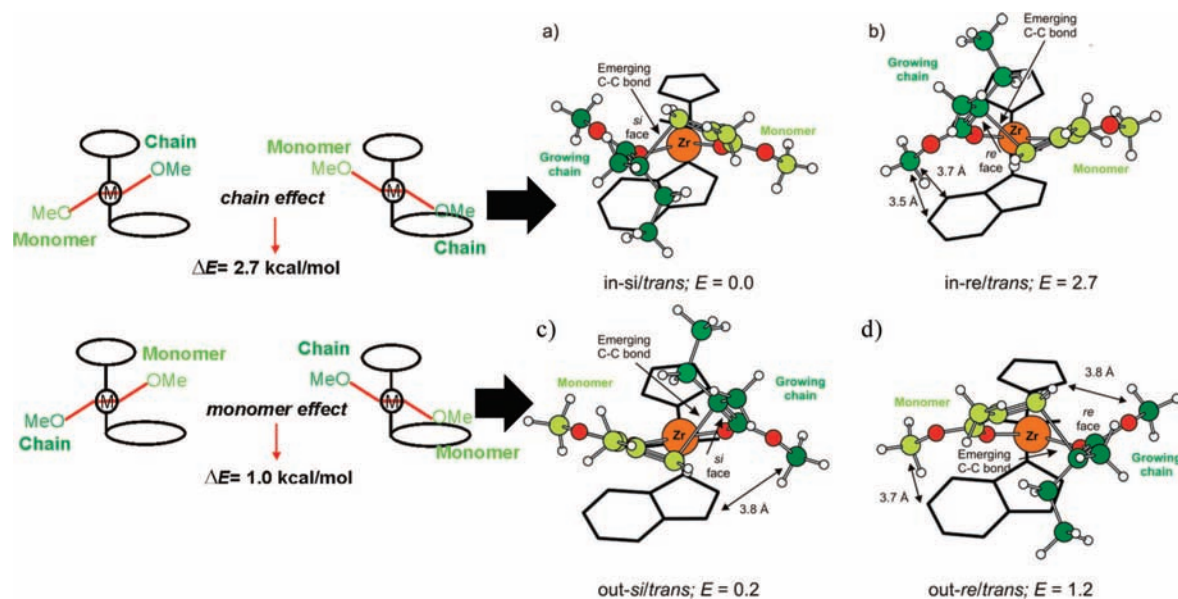


Figure 9. Steric interactions between the indenyl ligand and the methoxy group of the growing chain (chain effect) or MMA (monomer effect) involved in the TS for MMA-addition with the growing chain in the inward position (the hindered site, TS a and TS b) and with the growing chain in the outward position (the open site, TS c and TS d) of the C_1 -symmetric $\text{Me}_2\text{C}(\text{Cp})(\text{Ind})\text{Zr}$ catalyst with a (*S*)-coordinated indenyl ligand. Energies, relative to the most stable transition state *in-si/trans* (TSa), are reported in kcal/mol. Reprinted with permission from ref 77. Copyright 2008 American Chemical Society.

containing various percentages of the *meso*-diastereomer will also produce bimodal polymers, as was indeed observed.¹⁶⁹

2.2.4. *ansa*- C_1 -Ligated Catalysts

C_1 -Symmetric *ansa*-zirconocene $\text{Me}_2\text{C}(\text{Cp})(\text{Ind})\text{ZrMe}_2$ affords *it*-PMMA with a modest isotacticity of 81% *mm* at 25 $^{\circ}\text{C}$, through cation **91** derived from activation with $\text{B}(\text{C}_6\text{F}_5)_3$,¹⁷⁸ 84% *mm* at 20 $^{\circ}\text{C}$ or 90% *mm* at -20 $^{\circ}\text{C}$, through cation **92** derived from activation with $[\text{tBu}_3\text{NH}][\text{BPh}_4]/\text{THF}$ ¹⁹² (Figure 8). Gibson et al. found that introduction of a methyl group at the 2-position of the indenyl ring (i.e., cation **93**) significantly lowered the PMMA isotacticity to only 54% *mm*.¹⁷⁸ Höcker et al. performed pentad analysis of the *it*-PMMA produced by cation **92** and found the polymerization to be consistent with an enantiomeric-site control mechanism.¹⁸¹ The authors explained the formation of *it*-PMMA by a proposed unimetallic propagation mechanism that proceeds with stereoselective MMA addition taking place predominately on the same lateral coordination site of the metal center;¹⁸¹ this skipped addition mechanism, reminiscent of the isospecific propylene polymerization by

C_1 -symmetric metallocene catalysts, requires a fast catalyst site-epimerization following each monomer addition step. To further address the origin of isoselectivity of this C_1 -symmetric system, the same group performed *ab initio* calculations at the Hartree–Fock level on this system and concluded that the preferred geometry for the stereoselective MMA addition step is with the incoming MMA being coordinated to the more sterically hindered coordination site (i.e., the same side as the indenyl ring) and with the growing ester enolate chain being placed in the more open lateral coordination site.¹⁹³ Therefore, for subsequent monomer additions to occur in the same manner for the construction of the isotactic PMMA chain, this mechanism requires catalyst site-epimerization after each MMA addition step, which can be viewed as backside (relative to the leaving ester group) attack of the incoming monomer to ring-open the resting chelate.

On the other hand, DFT calculations by Cavallo and Caporaso offered a different account.⁷⁷ Specifically, the authors found that MMA addition is stereoselective when the growing enolate chain resides at *either* diastereotopic

	95 (R = Me, Cy, ⁱ Pr, ^t Bu)		96	97	
catalyst	T_p (°C)	conv (% h ⁻¹)	M_n (kD)	PDI	<i>mm</i> (%)
95, Me	0	47	51.6	2.17	41
95, Cy	0	36	27.6	2.32	64
95, ⁱ Pr	0	37	27.3	1.10	87
95, ^t Bu	0	53	22.7	1.19	83
96, Me	0	13	36.1	1.22	26
96, Cy	0	22	36.8	1.14	33
96, ⁱ Pr	0	29	21.8	1.10	36
96, ^t Bu	0	20	20.2	1.19	70
97	0	90	58.5	1.18	83

Figure 10. Characteristics of the MMA Polymerization by C_1 -Ligated Cationic *ansa*-Zirconocene Complexes.

coordination site of the catalyst, although stereoselectivity is higher when the growing chain is placed at the more hindered site ($\Delta E_{\text{stereo}} = 2.7$ kcal/mol), originated mainly from steric interactions between the methoxy group of the growing chain and the indenyl ligand (*strong chain effect*), than when it is at the more open site ($\Delta E_{\text{stereo}} = 1.0$ kcal/mol), originated mainly from steric interactions between the methoxy group of the incoming monomer and the indenyl ligand (*weak monomer effect*, Figure 9). In both cases the same enantioface of the enolate chain end is selected: for the catalyst center with the (*S*)-coordinated indenyl ligand, the *si* face of the enolate bond reacts preferentially with the coordinated monomer, which explains the isoselectivity of this polymerization system. Significantly, since there is no substantial energy difference (0.2 kcal/mol) between the most favored transition states of these two situations (Figure 9), there is no driving force for undergoing a catalyst site-epimerization following each monomer addition, and thus an almost regular chain-migratory mechanism, instead of the skipped addition mechanism described above, is consistent with the observed modest isotacticity (i.e., 81% *mm* at 25 °C) of the PMMA produced by this C_1 -symmetric system.

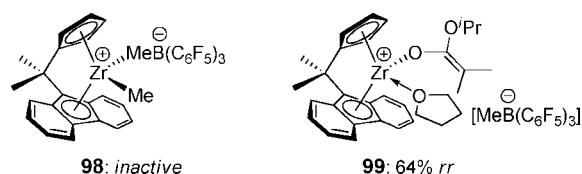
Surprisingly, Chen et al. found that C_1 -symmetric *ansa*-titanocene imido complex $\text{Me}_2\text{Si}(\eta^5\text{-Me}_4\text{C}_5)(\eta^2\text{-C}_9\text{H}_6)\text{Ti}(\text{=N}^t\text{Bu})(\text{THF})$ (**94**),¹⁹⁴ upon activation with $\text{Al}(\text{C}_6\text{F}_5)_3$, affords syndio-rich (69% *rr* at 23 °C) or syndiotactic (89% *rr* at -78 °C) PMMA and it exhibits no activity with the $\text{B}(\text{C}_6\text{F}_5)_3$ activation.¹⁹⁵ This **94**/ $\text{Al}(\text{C}_6\text{F}_5)_3$ system is extremely active, converting 400 equiv of MMA to PMMA in high conversions in 1 min, giving a TOF approaching 20,000 h⁻¹ (Figure 8). The *st*-PMMA production by the C_1 -symmetric *ansa*-titanocene imido complex **94** is due to a bimetallic propagation via the enolaluminate propagating species and the alane-activated monomer (cf. section 2.4.2).¹⁹⁵

Erker and co-workers examined both ligand and anion effects on the isotacticity of the PMMA produced by a series of alkyl-substituted, Me_2Si -bridged C_1 -ligated complexes **95** and **96**.¹⁸³ The cation (R = ^tBu) paired with more coordinating *N*-pyrrolyl-based borate anions is inactive for MMA polymerization. On the other hand, complex **95** paired with the $\text{MeB}(\text{C}_6\text{F}_5)_3^-$ anion exhibits good activity, and the isotacticity of the resulting PMMA increases from 41% *mm* to 87% *mm* on going from R = Me to ⁱPr, but a further increase of the steric bulk of the R group to ^tBu results in a slight drop in isotacticity (83% *mm*, Figure 10).¹⁸³ The (butadiene)zirconocene/ $\text{B}(\text{C}_6\text{F}_5)_3$ betaine system **96** exhibits only about half the activities as, and also much lower

isotacticity than, the alkyl cation system **95** with the same R group. Furthermore, the modulation of the isotacticity by the R groups in the betaine system is much less pronounced (except for ^tBu). However, the betaine system does not necessarily lead to lower stereocontrol in general. For example, catalyst **97** produces PMMA with similar tacticity to that by catalyst **91** paired with the $\text{MeB}(\text{C}_6\text{F}_5)_3^-$ anion. The observed substantial stereoselectivity difference between systems **95** and **96** with the same R group on the Cp ring but different anions was attributed to the involvement of the anion in the respective TS of the conjugate addition step in the system where the ion pairs are actual active species, therefore arguing a significant role of anion in stereocontrol of MMA addition.¹⁸³

2.2.5. *ansa*- C_s -Ligated Catalysts

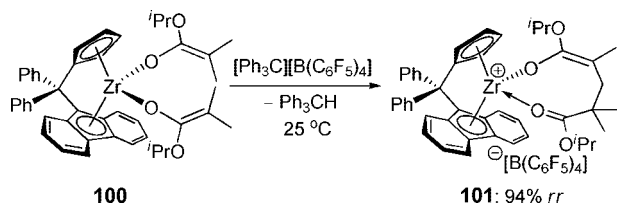
The C_s -ligated cationic zirconocene methyl complex $[\text{Me}_2\text{C}(\text{Cp})(\text{Flu})\text{ZrMe}]^+$ (**98**) is well-known for its ability to catalyze the syndiospecific polymerization of propylene.^{196–198} However, attempts to synthesize highly syndiotactic PMMA using C_s -symmetric $\text{Me}_2\text{C}(\text{Cp})(\text{Flu})\text{ZrMe}_2$, upon activation with various activators including $\text{B}(\text{C}_6\text{F}_5)_3$,¹⁷⁸ $\text{Ph}_3\text{CB}(\text{C}_6\text{F}_5)_4/\text{Et}_2\text{Zn}$ (excess),¹⁷³ and $\text{B}(\text{C}_{12}\text{F}_9)_3$,¹⁷¹ yielded no polymer formation. Although this inactivity issue was solved by using an ester enolate derivative, $\{\text{Me}_2\text{C}(\text{Cp})(\text{Flu})\text{Zr}(\text{THF})[\text{OC}(\text{O}^i\text{Pr})=\text{CMe}_2]\}^+$ (**99**),¹⁹⁰ which simulates the proposed active propagating species, the PMMA produced at ambient temperature is a syndio-rich *at*-polymer (64% *rr*, 32% *mr*, 4.0% *mm*) via an apparent chain-end control mechanism [as a methyl triad test using $4[\text{mm}][\text{rr}]/[\text{mr}]^2$ gave 1.0], rather than the expected site-controlled mechanism based on the propylene polymerization precedent.



Highly intriguingly, Ning and Chen discovered that $\text{Ph}_2\text{C}<$ bridged analogously C_s -ligated *ansa*-zirconocene bis(ester enolate) **100** (Scheme 11), upon activation with $[\text{Ph}_3\text{C}][\text{B}(\text{C}_6\text{F}_5)_4]$, produces highly syndiotactic PMMA (94% *rr*) at 25 °C via a predominately site-controlled mechanism.¹⁹⁹ The activation occurs via H^- abstraction from the methyl group of the enolate $[\text{OC}(\text{O}^i\text{Pr})=\text{CMe}_2]$ moiety by Ph_3C^+ forming Ph_3CH and the resulting isopropyl methacrylate coordinated to Zr, and subsequent nucleophilic addition of another enolate ligand to this activated methacrylate monomer gives the cationic eight-membered-ring chelate **101**, the active catalyst resting intermediate. Impressively, this high level of syndiotacticity remains even at T_p of 50 °C (93% *rr*).

Activation via methide abstraction by $\text{B}(\text{C}_6\text{F}_5)_3$ (as a THF adduct) converts instantaneously and quantitatively neutral mono(ester enolate) **102** to highly active cationic catalyst **103** (Figure 11) for MMA polymerization at 25 °C, with TOF reaching 1350 h⁻¹. Importantly, the PMMA produced by this catalyst exhibits a high syndiotacticity of 95% *rr*, T_g of 139 °C, and a relatively narrow MWD, ranging from 1.09 to 1.23 (Figure 11).¹⁹⁹ It is currently unclear why the profound differences in reactivity and stereoselectivity are observed between the $\text{Me}_2\text{C}<$ and $\text{Ph}_2\text{C}<$ bridged C_s -ligated

Scheme 11. Generation of Highly Syndiospecific *ansa*-Zirconocenium Ester Enolate Catalyst



ansa-zirconocene catalysts, although the authors tentatively attributed it to their different Thorpe–Ingold effects in terms of relative rates of ring-closing (Michael addition step) and ring-opening (monomer coordination step) as compared to the rate of MMA-assisted site-epimerization.

2.2.6. Constrained Geometry Catalysts

Half-sandwich metal complexes incorporating linked Cp-amido ligands^{200–204} are termed “constrained geometry catalysts” (CGCs), attributable to the phenomenal commercial successes in the production of revolutionary polyolefin materials via (co)polymerization of α -olefins using group 4 metal CGCs.^{205–208} The cationic CGC zirconocenium ester enolate complex, $\{(\text{CGC})\text{Zr}(\text{L})[\text{OC}(\text{O}^t\text{Bu})=\text{CMe}_2]\}^+[\text{B}(\text{Ar}_F)_4]^-$ [**105**, CGC = $\text{Me}_2\text{Si}(\eta^5\text{-(Me}_4\text{C}_5\text{)}^i\text{BuN})$, $\text{Ar}_F = 3,5\text{-(CF}_3)_2\text{C}_6\text{H}_3$, L = neutral donor ligand such as THF or isobutyrate, Figure 12] reported by Collins et al., exhibits low activity (TOF = 9.4 h^{-1}) and affords, unexpectedly (on the basis of its C_s ligation), highly isotactic PMMA (95.5% *mm*) via a site-control mechanism at low T_p (-60 and -40 °C) in a solvent mixture of toluene and CH_2Cl_2 .²⁰⁹ Further increasing T_p to -20 °C gave PMMA with a considerably lower isotacticity of 80.5% *mm*. Ambient temperature polymerization results were not reported, as this cationic (CGC)Zr complex is thermally unstable at $T \geq -20$ °C.

A key element in the proposed stereocontrol mechanism for the observed isospecificity of complex **105** is that stereoselective MMA addition occurs predominately at only

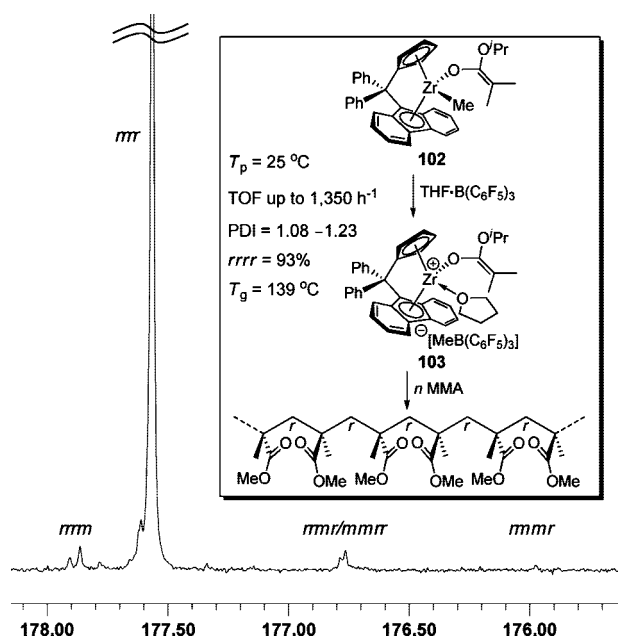
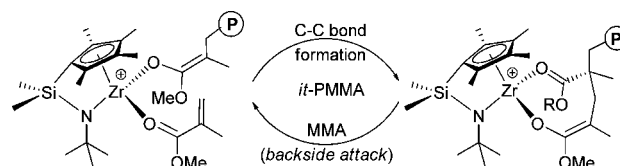


Figure 11. C_s -Ligated *ansa*-zirconocene catalysts for the synthesis of highly syndiotactic PMMA at RT. Reprinted with permission from ref 199. Copyright 2008 American Chemical Society.

	104 (inactive)	105	106	107
T_p (°C)		-40	23	23
TOF (h^{-1})		9.4	22	
M_n (kD)		20.1	23.6	27.1
PDI		1.18	1.09	1.12
I^* (%)		84	85	74
<i>rr</i> (<i>mm</i>) (%)		(95.5)	81.8	80
ref.	210	209	210	210

Figure 12. Characteristics of the MMA Polymerization by Group 4 CGC Complexes

Scheme 12. Stereoselective One-Site MMA Addition for *it*-PMMA Formation by (CGC)Zr Catalyst



one of the two enantiotopic lateral sites (i.e., MMA is coordinated to the same lateral Zr site for a site-retention mechanism, Scheme 12); this is possible provided that intramolecular 1,4-conjugate Michael addition within the catalyst–monomer complex is fast relative to racemization at Zr by exchange of free and bound MMA and that dissociation of the terminal ester group in the cyclic ester enolate resting intermediate is slow relative to associative displacement (backside attack) by MMA.²⁰⁹ Apparently, such conditions were met with the polymerization by the in situ-generated **105** in terms of a combination of the low T_p condition (≤ -40 °C) and the use of the oxonium acid activator $\text{H}(\text{OEt}_2)_2[\text{B}(\text{Ar}_F)_4]$ with concomitant delivery of coordinating ligands (diethyl ether and isobutyrate) for the resulting cation upon activation, thereby leading to the production of isotactic PMMA.

Unlike the isostructural, cationic (CGC)Zr alkyl complex (CGC)ZrMe⁺MeB(C₆F₅)₃⁻ (**104**), which is inactive for MMA polymerization at high or low temperatures, the cationic Ti alkyl complex (CGC)TiMe⁺MeB(C₆F₅)₃⁻ (**106**) effects living and syndiospecific polymerizations²¹⁰ of MMA²¹¹ and BMA at ambient temperature, reported by Chen and co-workers, or at higher temperatures (up to 100 °C),²¹² reported by Carpentier and co-workers, via an apparent chain-end control mechanism. The PMMA produced by **106** at ambient temperature exhibits syndiotacticity of 80–82% *rr* with controlled MW and narrow MWD (PDI = 1.09). The corresponding chiral cationic (CGC)Ti ester enolate complex, $\{(\text{CGC})\text{Ti}(\text{THF})[\text{OC}(\text{O}^i\text{Pr})=\text{CMe}_2]\}^+[\text{MeB}(\text{C}_6\text{F}_5)_3]^-$ (**107**, Figure 12), which simulates the structure of the active propagating species, behaves similarly to that of the (CGC)Ti alkyl complex,²¹⁰ producing syndiotactic PMMA (80% *rr*, 18% *mr*, 2.0% *mm*) at ambient temperature with predominately isolated *m* meso dyad stereocenters (...*rrrrmrrrr*...) and again pointing to the apparent chain-end control nature of the (CGC)Ti catalysts. Analysis of the stereomicrostructures at the pentad level reveals the *rrrm* to *rrmr* ratio to be approximately 1,²¹⁰ thus also consistent with a catalyst site-epimerization scheme in a site-control mechanism.

Further studies by Chen, Cavallo, and co-workers²¹³ showed that the MMA polymerization by complex **106**

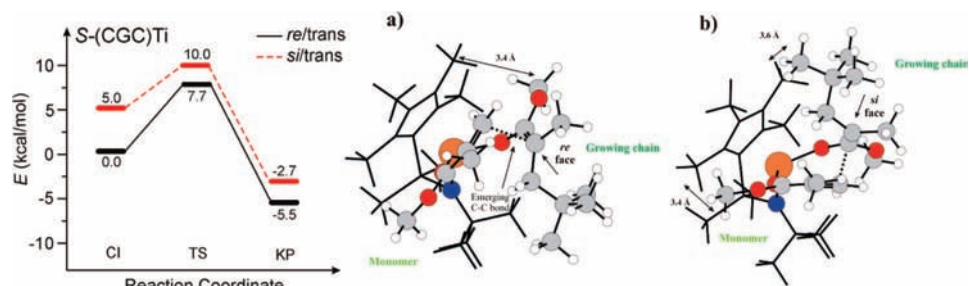


Figure 13. Energy diagrams for MMA addition to the *S*-metal center (energies in kcal/mol) and geometries of the two competing transition states of the (CGC)Ti system. Atoms depicted in spheres are Ti in orange, O in red, N in blue, C in gray, and H in white. Reprinted with permission from ref 213. Copyright 2008 American Chemical Society.

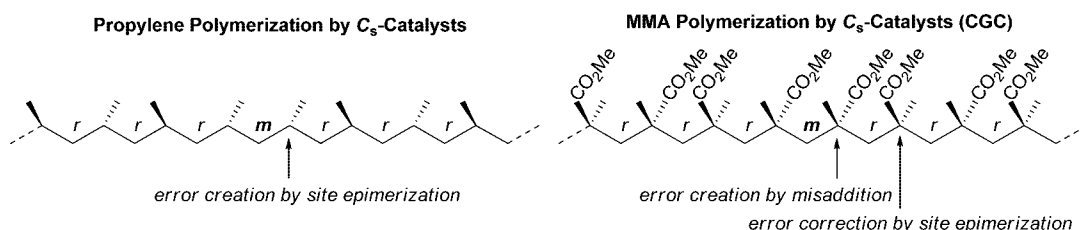
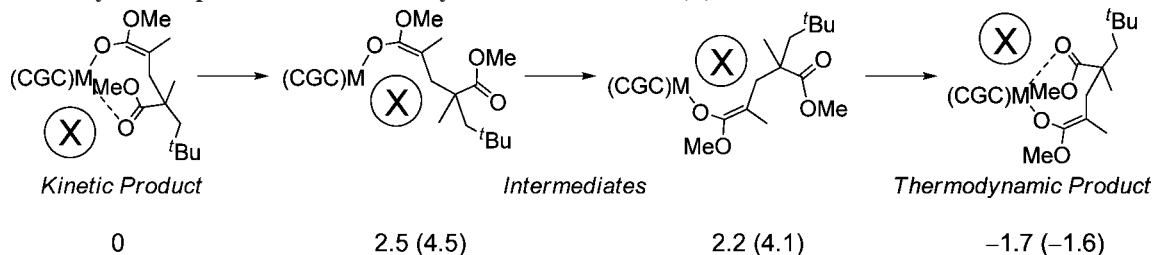


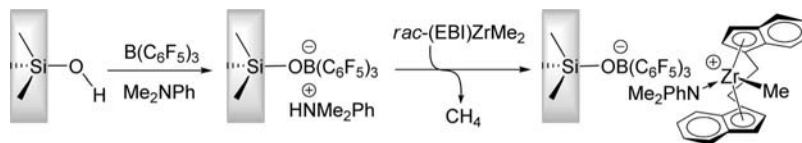
Figure 14. Comparison of isolated *m* dyad stereoregulation in the propylene and MMA polymerizations by C_s -ligated catalysts.

Scheme 13. Catalyst Site-Epimerization Assisted by the Monomer MMA (X) after a Stereomistake^a



^a Energies (kcal/mol) are reported in CH_2Cl_2 and toluene (numbers in parentheses).

Scheme 14. Preparation of Silica-Supported Chiral Zirconocenium Catalyst for MMA Polymerization



follows zero-order kinetics in [MMA], implying that, in a unimetallic propagation “catalysis” cycle, displacement of the coordinated ester group in the cyclic intermediate by the incoming monomer is fast relative to intramolecular conjugate MMA addition within the catalyst–monomer complex. This observation provides a kinetic basis for pathways leading to catalyst site-epimerization at Ti before MMA additions. There are exhibited negligible effects on the syndiotacticity of the polymerization by monomer and catalyst concentrations as well as ion-pairing strength varying with anion structure and solvent polarity. DFT calculations on CI, TS, and kinetic product (KP), focusing on the enantioselectivity of the MMA addition to an *S* chiral center, present a relative *trans* disposition of the methoxy groups of both the growing chain and the monomer (*cis* disposition has much higher energy) in the TS. As shown in Figure 13, the *re*-face of the enolate growing chain reacts preferentially in the case of an *S*-chirality at the metal, and there is a selection of the *re*-face of the chain even at the CI, although the enantioselectivity is determined by the energy difference at the TS with $\Delta E_{\text{Stereo}} = 2.3$ kcal/mol, indicating enantioselective MMA addition.

DFT calculations also provided theoretical support to the catalyst site-epimerization mechanism accounting for the formation of the predominately isolated *m* stereoregulation and indicated the driving force for an almost *regular site-epimerization reaction after a stereomistake* being in the higher energy (by 2.8 kcal/mol) of the 8-membered cycle formed after a stereomistake.²¹³ This MMA- or anion-assisted catalyst site-epimerization reaction converts the kinetic product after a stereomistake into a thermodynamically more stable resting state (Scheme 13). Owing to this site-epimerization reaction, the higher energy KP corresponding to a stereomistake (*S*-metal/*si*-chain) evolves into the *R*-metal/*si*-chain resting state that, by symmetry, is isoenergetic with the thermodynamic *S*-metal/*re*-chain product that is obtained from the favored TS. The MMA-assisted epimerization has a very smooth energy profile, since the two intermediates without a back-bonded C=O group are remarkably stabilized by a coordinated MMA molecule.²¹³

It is *fascinating* to point out here that, in the syndiospecific polymerization of propylene by C_s -ligated complexes, catalyst site-epimerization *generates* meso dyad stereoregulation (...rrrrmrrrr...), whereas, in the syndiospecific polymerization

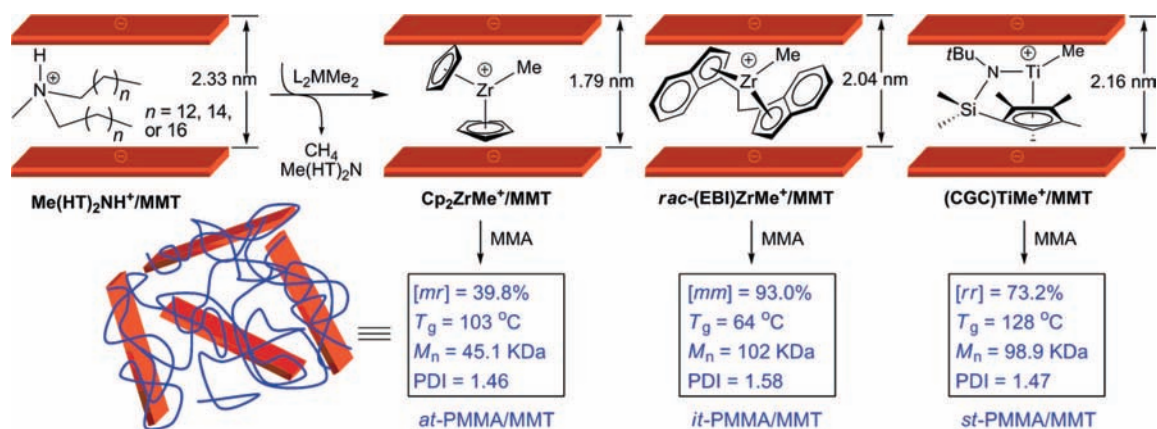


Figure 15. Exfoliated PMMA/silicate nanocomposites by the *in situ* polymerization approach. Reprinted with permission from ref 215. Copyright 2003 American Chemical Society.

of MMA by the (CGC)Ti complexes, catalyst site-epimerization *corrects* a stereomistake made in a previous enantiofacial misaddition (Figure 14).

2.2.7. Half-Metallocene Catalysts

Half-titanocene Cp^*TiMe_3 , upon activation with $B(C_6F_5)_3$, is moderately active ($TOF = 62\text{ h}^{-1}$) for MMA polymerization at ambient temperature, producing *st*-PMMA (74% *rr*) with $PDI = 1.37$.⁵³ Activating the same complex with $Al(C_6F_5)_3$ doubles the activity ($TOF = 120\text{ h}^{-1}$), also yielding syndio-rich PMMA ($PDI = 1.31$) but with a noticeably lower syndiotacticity of 69% *rr*.

2.2.8. Supported Catalysts

Heterogenization of the chiral rac -(EBI)ZrMe⁺ catalyst onto silica support was accomplished in a two-step process commonly employed in the preparation of supported metallocene catalysts for olefin polymerization:²¹⁴ formation of surface-bound borate anions paired with ammonium cations followed by protonolysis of rac -(EBI)ZrMe₂ to generate the supported metallocenium catalyst $[rac\text{-(EBI)-ZrMe}]^+[\equiv SiOB(C_6F_5)_3]^-$ (Scheme 14). The MMA polymerization by this supported catalyst led to the formation of PMMA with a high isotacticity (96% *mm*) as well as controlled MW [$M_n(\text{found}) = 4.49 \times 10^4$, $M_n(\text{calcd}) = 4.00 \times 10^4$, giving $I^* = 89\%$] and narrow MWD ($PDI = 1.10$).⁵³

Protonolysis of dimethyl metallocenes, including C_{2v} -symmetric Cp_2ZrMe_2 , C_2 -symmetric rac -(EBI)ZrMe₂, and C_s -symmetric (CGC)TiMe₂, with $Me(HT)_2NH^+/MMT$, a montmorillonite (MMT) clay modified by methyl bis(hydrogenated tallow alkyl) ammonium, produces the corresponding intergallery-anchored metallocene catalysts Cp_2ZrMe^+/MMT , rac -(EBI)ZrMe⁺/MMT, and (CGC)TiMe⁺/MMT, through elimination of methane and discharge of the resulting neutral amine (Figure 15).²¹⁵ Remarkably, these nanogallery-intercalated metallocene catalysts behave much like in solution—in terms of their ability to control the stereochemistry of MMA polymerization. Thus, metallocenium-intercalated silicates, Cp_2ZrMe^+/MMT , rac -(EBI)ZrMe⁺/MMT, and (CGC)TiMe⁺/MMT afford atactic (40% *mr*), isotactic (93% *mm*), and syndiotactic (72% *rr*), stereochemically controlled PMMA–exfoliated silicate nanocomposites, respectively. The exfoliated morphology of *it*-PMMA–silicate nanocomposite produced by rac -(EBI)ZrMe⁺/MMT has been further examined by powder X-ray diffraction (XRD) and confirmed by transmission electron microscopy (TEM),

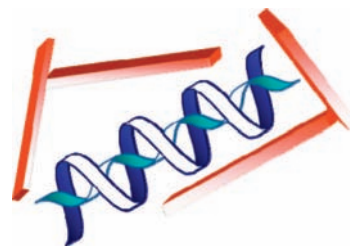


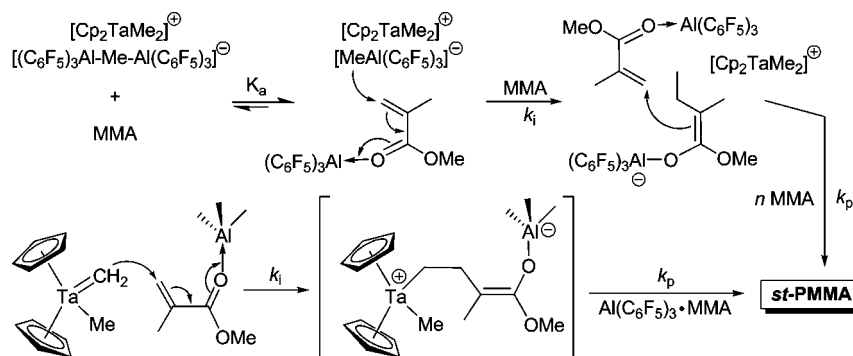
Figure 16. Schematic illustration of a supramolecular stereocomplex PMMA/exfoliated silicate nanocomposite.

where the low magnification image shows a homogeneous clay dispersion, whereas the high magnification image demonstrates exfoliation of the silicate nanoplatelets.²¹⁵

Chen et al. subsequently prepared double-stranded helical, supramolecular stereocomplex PMMA/silicate nanocomposites (Figure 16) by mixing dilute THF solutions of diastereomeric nanocomposites, *it*-PMMA/MMT and *st*-PMMA/MMT, in a 1:2 ratio, followed by reprecipitation or crystallization procedures.²¹⁶ The produced nanocomposite exhibits a predominantly exfoliated silicate morphology, as shown by XRD and by TEM, whereas the stereocomplex PMMA^{217–223} matrix is readily characterized by differential scanning calorimetry (DSC). Thus, the resulting crystalline stereocomplex PMMA matrix is resistant to boiling-THF or acetone extraction, and the stereocomplex nanocomposite exhibits a high T_m of 201 or 210 °C, depending on the preparation procedure, which is in sharp contrast to the diastereomeric (i.e., *it*- and *st*-) nanocomposite constituents, which can be extracted out with the same solvents and do not exhibit T_m on DSC. Furthermore, the resulting stereocomplex nanocomposite shows a one-step, narrow decomposition temperature window and a single, high maximum rate decomposition temperature of 377 °C.

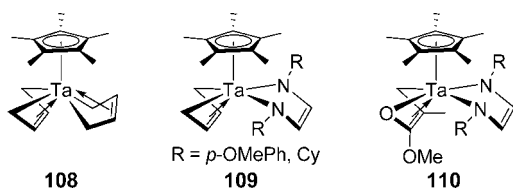
2.3. Other Metallocene Catalysts

Lindsell and co-workers reported in 1974 that calocene Cp_2Ca afforded highly syndiotactic PMMA (94% *rr*) at 0 °C in DME (at 8% monomer conversion after 12 h).²²⁴ However, a later study by Brittain et al. using the purified Cp_2Ca showed that the syndiotacticity is much lower (80% *rr*) under the same polymerization conditions.²²⁵ The Brittain group also employed the more soluble derivative Cp^*_2Ca for much enhanced activity, but this bulkier calocene gave PMMA with even lower syndiotacticity (57% *rr*) at 0 °C in DME; in THF or in toluene, the syndiotacticity dropped further down to 37% *rr* and 23% *rr*, respectively. Most

Scheme 15. Bimolecular Propagation Involving Enolaluminate Active Species in MMA Polymerization by Tantalocene/ $2\text{Al}(\text{C}_6\text{F}_5)_3$


recently, Steffens and Schumann investigated polymerization of MMA and copolymerization of MMA with other alkyl methacrylates using tetramethylcyclopentadienyl complexes $(\text{Me}_4\text{Cp})_2\text{Mg}$, $(\text{Me}_4\text{Cp})_2\text{Ca}(\text{THF})$, and $(\text{Me}_4\text{Cp})_2\text{Sr}(\text{THF})_2$ in toluene at various temperatures.²²⁶ In the presence of 7–20 equiv of Et_3Al (with respect to metal), all three metallocene complexes are active for MMA polymerization at $T_p \leq 0$ °C but exhibit essentially no activity at room temperature. The syndiotacticity is the highest (60% *rr*) for the Sr catalyst at -60 °C, which also shows the highest activity and degree of control of the polymerization within these three complexes. The role of Et_3Al was speculated to alkylate the divalent metallocene complex to form active species $[(\text{Me}_4\text{Cp})\text{M}-\text{Et}]$, in which the Et group was designated as the initiating group.

In contrast to a large number of group 4 metallocene complexes employed in the polymerization of polar vinyl monomers, application of group 5 metallocene and related complexes to such polymerizations is scarce. Mashima reported that half-tantalocene (Cp^*Ta) bis(η^4 -1,3-butadiene) complex **108** and $\text{Cp}^*\text{Ta}(\eta^2$ -1,4-diazabutadiene)(η^4 -1,3-butadiene) **109**, upon activation with 10 equiv of $\text{MeAl}(\text{BHT})_2$ (relative to Ta), polymerizes 100 equiv of MMA at 0 °C in 5–40 min, producing syndio-rich PMMA (68–73% *rr*, 1.4–2.3 PDI).^{227,228} Half-tantalocene **109** with R = Cy is most reactive, achieving a TOF of 1200 h^{-1} . Mashima and co-workers further reported living polymerization of MMA at -20 to -30 °C using half-tantalocene complexes **110** bearing MMA and 1,4-diaza-1,3-diene ligands, upon activation with 1 equiv of Me_3Al , also producing syndiotactic PMMA (71–78% *rr*).²²⁹



Chen et al. showed that cationic tantalocene complexes $[\text{Cp}_2\text{TaMe}_2]^+[\text{MeM}(\text{C}_6\text{F}_5)_3]^-$ (M = B, Al), $[\text{Cp}_2\text{TaMe}_2]^+[\text{B}(\text{C}_6\text{F}_5)_4]^-$,²³⁰ and $\text{Cp}_2\text{Ta}^+[\text{CH}_2\text{M}(\text{C}_6\text{F}_5)_3]^-$ (M = B, Al)²³¹ are inactive for MMA polymerization under various conditions; however, tantalocene trimethyl and alkylidene precursors Cp_2TaMe_3 and $\text{Cp}_2\text{Ta}(\text{=CH}_2)\text{Me}$, upon activation with 2 equiv of $\text{Al}(\text{C}_6\text{F}_5)_3$, become highly active in MMA polymerization. For example, the $\text{Cp}_2\text{Ta}(\text{=CH}_2)\text{Me}/2\text{Al}(\text{C}_6\text{F}_5)_3$ system in 1,2-dichlorobenzene at 25 °C reaches a high TOF of 800 h^{-1} and an I^* of 96%, producing PMMA with $M_n = 4.15 \times 10^4$, PDI = 1.65, and syndiotacticity =

72% *rr*.²³¹ The propagation was proposed to proceed via an aluminate (Al^-)/alane (Al) bimolecular process (Scheme 15).^{231,232} It is apparently general for such a bimetallic pathway involving the enolaluminate active species when combining an initiating molecule with 2 equiv of $\text{Al}(\text{C}_6\text{F}_5)_3$, extending to half-sandwich tantalocenes Cp^*TaMe_4 and $\text{Cp}^*\text{TaMe}_3(\text{OR})$,²³³ as well as alkyl main-group alkyl complexes.²³⁴

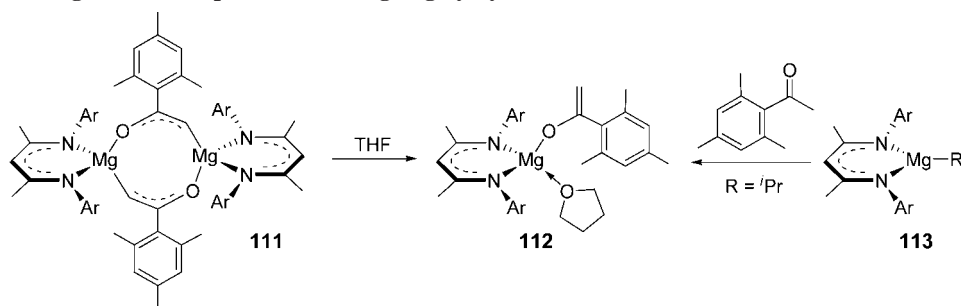
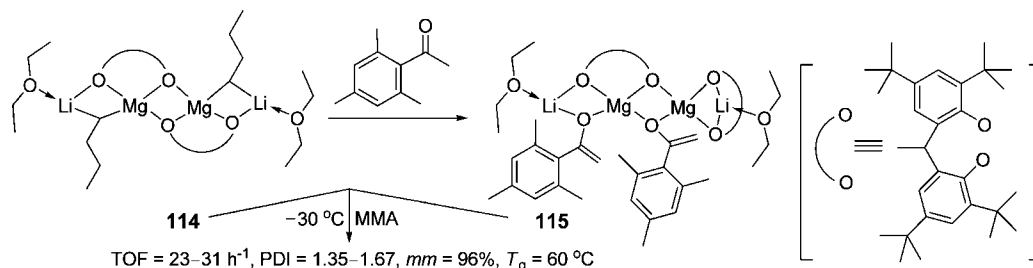
Polymerization of MMA by nickelocenes in combination with a large excess of MAO is reviewed in the section that immediately follows, in light of their common features with those of nonmetallocene group 10 metal systems in the presence of MAO (see section 2.4.4).

2.4. Nonmetallocene Catalysts

2.4.1. Group 1 and 2 Catalysts

Various lithium salts have been used to promote controlled polymerization of (meth)acrylates initiated by organolithium reagents.^{235,236} For example, the polymerization of *tert*-butyl acrylate by the $^t\text{BuLi}/5\text{LiCl}$ system in THF at -78 °C yielded the polymer with narrow MWD ($M_w/M_n = 1.20$), whereas, in the absence of LiCl, the polymer with broad, bimodal MWD ($M_w/M_n = 3.61$) was obtained.²³⁷ However, even in the presence of excess LiCl, increasing T_p from -78 to 0 °C brought about poor MW control and broadening of MWD from 1.20 to 1.63. Addition of LiCl influences the kinetics and mechanism of the MMA polymerization initiated with α -methylstyryllium in THF at -78 °C, producing PMMA with a narrow MWD ($M_w/M_n > 1.08$); addition of other lithium salts varying the size of counteranions, including LiF, LiBr, and LiBPh_4 , did not provide the same degree of control as the polymerization promoted by LiCl.²³⁸ However, other lithium salts such as LiClO_4 were found to enhance the livingness of the MMA polymerization in THF at -40 °C or in toluene/THF (9/1 v/v) at -78 °C.²³⁹ The LiClO_4 to initiator ratio has great influence on the degree of polymerization control. Likewise, lithium ester enolate initiators, when combined with 3–10 equiv of lithium *tert*-butoxide, also render controlled polymerization of methacrylates²⁴⁰ and acrylates²⁴¹ so that such systems can be used for the synthesis of (meth)acrylate di- and triblock copolymers at -60 °C in THF.²⁴²

Lithium silanolates were utilized to effect controlled and isospecific polymerization of MMA. Specifically, the system consisting of $^t\text{BuLi}$ and $^t\text{BuMe}_2\text{SiOLi}$ (which was formed *in situ* by the reaction of hexamethylcyclotrisiloxane + $^t\text{BuLi}$) in toluene at 0 °C led to high MW PMMA with a narrow MWD ($M_w/M_n < 1.20$) and high isotacticity (90%

Scheme 16. Discrete Magnesium Complexes Producing Highly Syndiotactic PMMA at $-30\text{ }^{\circ}\text{C}$ Scheme 17. Mixed Group 1 and 2 “Ate” Salts for Highly Isotactic PMMA at $-30\text{ }^{\circ}\text{C}$ 

mm).²⁴³ This system was also employed for the synthesis of isotactic random and block copolymers of alkyl methacrylates.²⁴⁴ Highly isotactic PMMA (99.5% *mm*, $M_w/M_n = 1.39$) was achieved using a combination of $\text{Me}_2\text{C}=\text{C}(\text{O}^i\text{Pr})\text{OLi}$ with 50 equiv of Me_3SiOLi in toluene at $-95\text{ }^{\circ}\text{C}$.²⁴⁵ The same polymerization yielded PMMA with an isotacticity of *mm* = 98.5% ($M_w/M_n = 1.23$) and 88.4% ($M_w/M_n = 1.09$) at $T_p = -78$ and $0\text{ }^{\circ}\text{C}$, respectively. For comparison, the isotacticity (*mm* = 73.4%) is much lower and the MWD ($M_w/M_n = 7.13$) is substantially broader for the MMA polymerization with the $\text{Me}_2\text{C}=\text{C}(\text{O}^i\text{Pr})\text{OLi}$ initiator alone (no lithium silanolate reagent) carried out in toluene at $-78\text{ }^{\circ}\text{C}$.

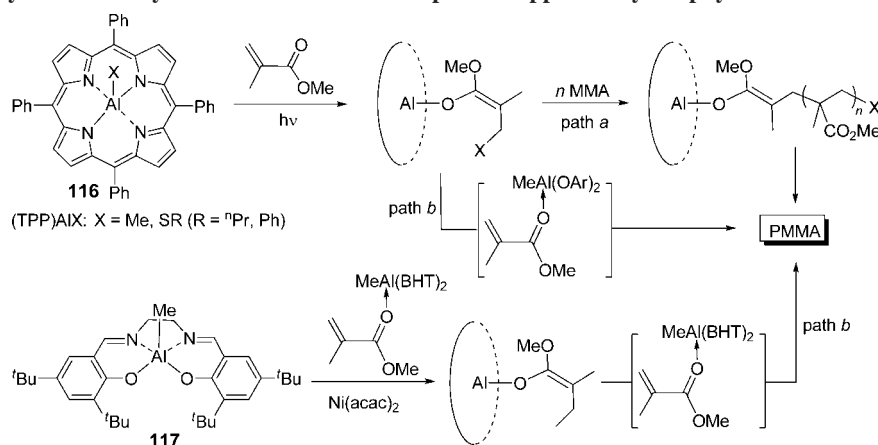
The simple potassium salt of the bulky allyl ligand, $\text{K}[\text{1,3}-(\text{SiMe}_3)_2(\eta^3\text{-C}_3\text{H}_5)]$, exhibits exceedingly high activity for MMA polymerization at $0\text{ }^{\circ}\text{C}$ in toluene with $\text{TOF} = 92,500\text{ h}^{-1}$, producing *at*-PMMA (54% *mr*) with high MW ($M_n = 1.10 \times 10^5$, $\text{PDI} = 1.95$) and high initiator efficiency ($I^* = 85\%$).¹⁶⁰ A mixed π -ferrocene- π -toluene complex of potassium tris(hexamethyldisilazide)magnesiate, $[\text{K}(\text{ferrocene})_2(\text{toluene})_2]^+[\text{Mg}[\text{N}(\text{SiMe}_3)_2]_3]^-$, yields PMMA of high MW ($M_n = 3.79 \times 10^5$, $\text{PDI} = 1.49$) in THF, with a low initiator efficiency of $I^* = 2.6\%$; however, the syndiotacticity is high (84% *rr*) considering the polymerization at RT.²⁴⁶ The study seems to indicate that the cation moiety, or more precisely ferrocene, has a major role in the observed high syndiotacticity of this system because control runs using $\text{KMg}[\text{N}(\text{SiMe}_3)_2]_3$ and $\text{KN}(\text{SiMe}_3)_2$ showed much reduced syndiotacticity of 44% *rr* and 31% *rr*, respectively.

Tanaka and co-workers utilized conventional Grignard reagents such as $^i\text{BuMgBr}$ in toluene at $-78\text{ }^{\circ}\text{C}$ ^{247,248} and $m\text{-(CH}_2=\text{CH)C}_6\text{H}_4\text{CH}_2\text{MgCl}$ in THF at $-110\text{ }^{\circ}\text{C}$ ²⁴⁹ for the synthesis of highly isotactic (97% *mm*) and highly syndiotactic (96.6% *rr*) PMMA, respectively. Identification of the active species in such systems was complicated by the dynamic Schlenk equilibrium process involving *aggregation*, *solvation*, and *ligand exchange*. Gibson and co-workers synthesized a discrete magnesium ketone enolate complex supported by the bulky *N,N*-diisopropylphenyl β -diketiminate ligand, $[\text{HC}(\text{C}(\text{Me})=\text{N}-2,6\text{-}^i\text{Pr}_2\text{C}_6\text{H}_3)_2\text{Mg}(\mu\text{-OC}(\text{=CH}_2)\text{-}2,4,6\text{-Me}_3\text{C}_6\text{H}_2)]_2$ (**111**, Scheme 16), which was found to rapidly polymerize MMA ($\text{TOF} > 2280\text{ h}^{-1}$) in a living

fashion at $-30\text{ }^{\circ}\text{C}$ in toluene or chloroform, leading to highly syndiotactic PMMA (92% *rr*) with a high T_g of $135\text{ }^{\circ}\text{C}$.²⁵⁰ As addition of donor ligands such as THF can break the dimer to form the monomeric Mg enolate complex **112** (Scheme 16), it can be envisioned that the MMA polymerization by the dimeric enolate complex proceeds via the monomeric enolate complex in the presence of MMA. The stereocontrol ability of this catalyst system relies on the steric bulk of the ligand rendered by the *N*-aryl groups; thus, changing from 2,6- $^i\text{Pr}_2\text{C}_6\text{H}_3$ to 2,6- $\text{Et}_2\text{C}_6\text{H}_3$ and 2,6- $\text{Me}_2\text{C}_6\text{H}_3$ *N*-aryl groups results in a substantial reduction of the syndiotacticity of the PMMA produced at $-30\text{ }^{\circ}\text{C}$ from 92% *rr* to 78% *rr* and 73% *rr*, respectively.⁵⁴ The magnesium alkyl, aryl, or amide complexes **113** ($\text{R} = \text{Me}$ (dimer), ^iPr , ^tBu , Ph , N^iPr_2) are also highly active catalysts for MMA polymerization, producing *st*-PMMA with $\sim 90\%$ *rr* at $-30\text{ }^{\circ}\text{C}$, with Me and ^tBu complexes being poorly controlled and the ^iPr complex exhibiting the best control over M_n ($I^* = 97\%$) and PDI (1.04).⁵⁴ Owing to the ligand-assisted, chain-end control nature of the polymerization by these discrete magnesium complexes, the syndiotacticity erodes drastically to only 75% *rr* for the polymerization carried out at ambient temperature ($23\text{ }^{\circ}\text{C}$).⁵⁴ Unpredictably, a magnesium isopropyl complex supported by the analogous bispyridyldiiminato $[\text{N}_2^-]$ ligand produces iso-rich *at*-PMMA (42% *mm*, 43% *mr*) at $-78\text{ }^{\circ}\text{C}$ in toluene with only a modest TOF of $\sim 22\text{ h}^{-1}$.²⁵¹

Intriguingly, highly isotactic PMMA (>95% *mm*) was produced in toluene at $-30\text{ }^{\circ}\text{C}$ by mixed bimetallic complexes (“ate” salts) linked by the bulky chelating diphenolate ligand, 2,2'-ethylidenebis(4,6-di-*tert*-butylphenoxy) (EDBP, Scheme 17): Mg-Li alkyl $[(\text{EDBP})\text{Mg}(\mu\text{-}^t\text{Bu})\text{Li}(\text{OEt}_2)]_2$ (**114**, 96.7% *mm*), Mg-Li enolate $\{(\text{EDBP})\text{Mg}[(\mu\text{-OC}(\text{Mes})\text{CH}_2)]\text{Li}(\text{OEt}_2)]_2$ (**115**, 96.1% *mm*), and Mg-Na alkyl $[(\text{EDBP})\text{Na}(\text{OEt}_2)\text{Mg}^i\text{Bu}]_2$ (95.4% *mm*).²⁵² The activities of these mixed group 1 and 2 complexes are modest with TOF ranging from 22 to 31 h^{-1} , and the PMMA produced exhibits relatively broad MWDs ($\text{PDI} = 1.35\text{--}1.67$). It remains to be seen where the isospecificity is originated from and how both heterobimetallic centers provide cooperativity in the initiation and propagation steps.

Scheme 18. MMA Polymerization by Discrete Aluminum Complexes Supported by Porphyrin and Schiff Base Ligands



2.4.2. Group 13 Catalysts

Inoue and co-workers²⁵³ discovered that the aluminum porphyrin complex (TPP)AlMe (TPP = tetraphenylporphyrinato, **116**, Scheme 18), upon irradiation with visible light, forms a living (or “immortal”) polymerization system.²⁵⁴ In the case of alkyl methacrylate polymerization, initiation involves the radiation-assisted formation of the aluminum-enolate bond, the active propagating species (path a, Scheme 18).²⁵⁵ This system has been employed for the successful synthesis of PMMA with controlled MW and narrow MWD as well as block copolymers of MMA with ⁿBu and ^tBu acrylates.²⁵⁶ The thiolate derivatives (TPP)AlSR can initiate the polymerization *without* irradiation.²⁵⁷ A potential drawback of this system is its long reaction time (12 h with a [MMA]/[Al] ratio of 100) and the discolorations to the polymer products by the intense chromophore carried by the porphyrin ligand.

The rates of the polymerization by the aluminum porphyrin complex (TPP)AlMe (**116**, X = Me) upon irradiation can be substantially accelerated by the use of sterically crowded organoaluminum Lewis acids, such as MeAl(BHT)₂ and MeAl(2,6-^tBu₂C₆H₃O)₂ (path b, Scheme 18).^{258,259} Thus, addition of 1–3 equiv (per initiating Al center) of such Lewis acids accelerates the polymerization of MMA with (TPP)AlMe by factors of *tens of thousands* with no detrimental effects on polymer yield or MWD. For example, addition of 3 equiv of MeAl(2,6-^tBu₂C₆H₃O)₂ to the MMA polymerization system by (TPP)AlMe that had been irradiated with a visible light source for 2.5 h at 35 °C converted quantitatively 200 equiv of MMA to PMMA with $M_n = 2.55 \times 10^4$ and PDI = 1.07 in only 3 s! Monomer activation, which facilitates nucleophilic attack of the initiating ligand at the Al center to the activated monomer, was proposed to be responsible for the observed drastic rate enhancement. Interestingly, in sharp contrast to the anionic polymerization initiated by lithium enolates or ^tBuLi, where boron Lewis acids such as B(C₆F₅)₃ completely halted MMA polymerization,¹⁸⁵ the (TPP)AlMe polymerization system is substantially accelerated by boranes such as BPh₃ and B(C₆F₅)₃.²⁶⁰

A system related to (TPP)AlMe is the methyl aluminum complex incorporating a tetradentate [O⁻,N,N,O⁻] Schiff base ligand (**117**, Scheme 18). When used alone, **117** is a poor initiator for MMA polymerization with low activity (TOF = 0.8 h⁻¹) and initiator efficiency ($I^* = 0.9\%$); when combined with the Lewis acid activator MeAl(BHT)₂, the two-component system improved activity (TOF = 9 h⁻¹) but not polymerization control.²⁶¹ However, Gibson and co-

workers found that addition of a nickel compound such as Ni(acac)₂ to the system containing **117** and MeAl(BHT)₂ generates the corresponding enolate propagating species via a proposed multistep Ni(acac)₂-catalyzed process.²⁶¹ Thus, the three-component system comprising **117** (1 equiv), Ni(acac)₂ (1 equiv), and MeAl(BHT)₂ (3 equiv) rapidly polymerizes 200 equiv of MMA at ambient temperature, achieving 92% monomer conversion within 2 min (TOF = 5520 h⁻¹). The PMMA produced at this temperature is controlled in MW (PDI = 1.17, $I^* = 81\%$) and syndio-rich (69% *rr*); lowering T_p to -20 °C improved syndiotacticity to 84% *rr*, benefiting this chain-end controlled polymerization. Control runs showed that the system without the Al complex **117** (i.e., 1 Ni(acac)₂ + 3 MeAl(BHT)₂) is even slightly more active (TOF = 5700 h⁻¹) and the syndiotacticity of the resulting PMMA is also slightly higher (72% *rr*); however, the difference is that the latter system without complex **117** is not controlled, producing PMMA with the much higher measured M_n than the calculated value ($I^* = 16\%$) and a broader MWD (PDI = 1.63).

Anionic active species derived from conventional initiators such as alkyllithium reagents and lithium ester enolates exist as aggregates, both in solid state and in solution. Such anionic active species alone cannot control the polymer MW and MWD due to the coexistence of various aggregated species that exhibit different reactivity and exchange comparably to, or more slowly than, the polymerization time scale.²⁶² Thus, they can be characterized as *multisite* anionic active species and produce polymers with ill-defined chain structures. Addition of a suitable organoaluminum Lewis acid to an anionically initiated polymerization system not only significantly enhances the conversion over polymerization, it also modulates the polymerization stereochemistry. This strategy was developed by Hatada et al.²⁶³ for the production of highly syndiotactic ($\geq 90\%$ *rr*) PMMA with a narrow MWD (PDI ≤ 1.19) using a ^tBuLi/R₃Al ($\leq 1/3$) combination in toluene at low temperatures (≤ -78 °C). Ballard et al.²⁶⁴ produced *st*-PMMA ($\geq 70\%$ *rr*) with a narrow MWD (PDI = 1.09–1.28) in toluene at elevated temperatures (0–40 °C) using a combination of ^tBuLi with an excess of ^tBu₂Al(BHT). The ^tBuLi/3Al(ⁿOct)₃ system led to highly syndiotactic (96% *rr*) PMMA at -93 °C,²⁶⁵ while the ^tBuLi/5RAl(2,6-^tBu₂C₆H₃O)₂ system at -78 °C afforded *ht*-PMMA (67.8% *mr*)²⁶⁶ and poly(ethyl methacrylate) (87.2% *mr*)²⁶⁷ when R = Me, or *st*-PMMA, with syndiotacticity *rr* = 89.1% and 83.8% when R = Et and ^tBu, respectively.²⁶⁸ The ^tBuLi/5EtAl(2,6-^tBu₂C₆H₃O)₂ system promoted living polymerization of

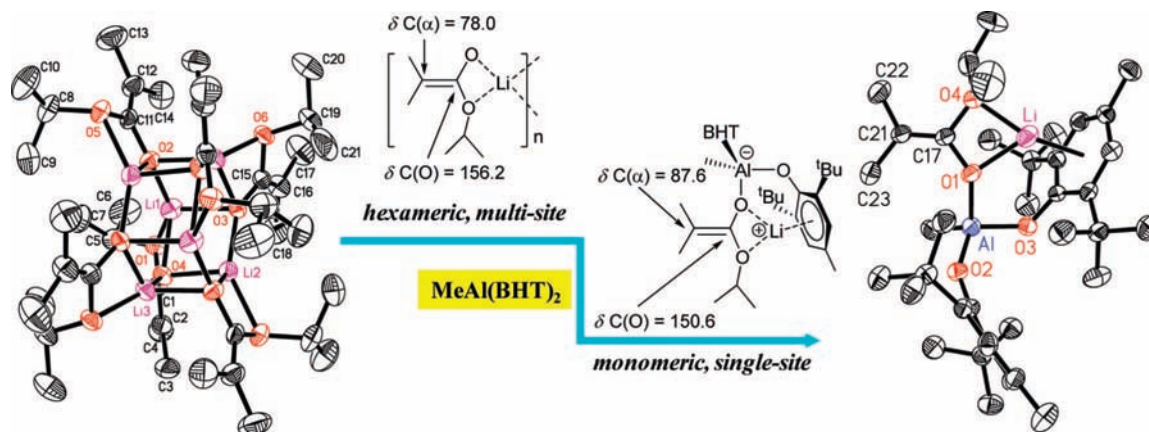
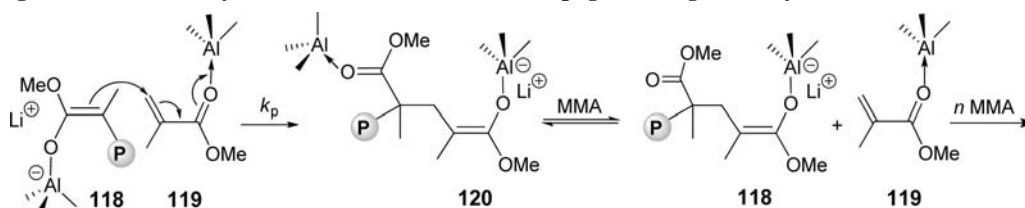


Figure 17. Generation of single-site enolaluminate active propagating species via deaggregation of lithium enolate aggregates with, and subsequent stabilization by, $\text{MeAl}(\text{BHT})_2$. Reprinted with permission from ref 286. Copyright 2005 American Chemical Society.

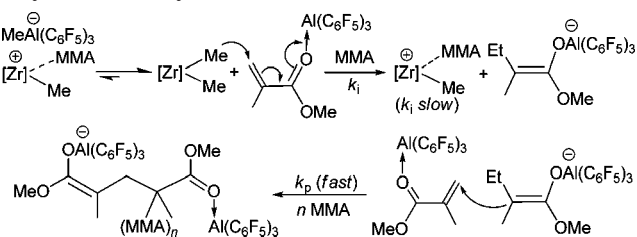
Scheme 19. Single-Site Anionic Polymerization via Bimolecular Propagation Regulated by Aluminum Lewis Acids



primary alkyl acrylates as well as block copolymerization of n BA with MMA at $-60\text{ }^\circ\text{C}$,²⁶⁹ while the combination with the methyl aluminum derivative $\text{MeAl}(2,6\text{-}^t\text{Bu}_2\text{C}_6\text{H}_3\text{O})_2$ gave polymers with a broad MWD in low yields.²⁷⁰ Schlaad and Müller²⁷¹ reported that the steric bulk and Lewis acidity of the added alkyl aluminum compounds strongly influence the tacticity and MWD of the PMMA produced by $^t\text{BuLi}$ in toluene at $-78\text{ }^\circ\text{C}$; depending on the aluminum compound used, the MWD was in the range $1.2 < M_w/M_n < 7$, and the tacticity of the PMMA can change from being highly syndiotactic to atactic, heterotactic, or highly isotactic. These above results highlight the importance of the Al/Li ratio employed and the structure of the Al Lewis acid in such systems, as the Al complex can bind to the growing active anionic chain end, the growing chain, and the monomer.

Lithium ester enolates should be, in principle, ideal initiators for the polymerization of alkyl (meth)acrylates because the propagating centers for the anionic polymerization of methacrylates initiated by organolithium compounds are the lithium ester enolates. However, the lithium ester enolate propagator tends to stabilize through aggregation ($n = 2\text{--}6$), and the existence of various aggregated ester enolates creates significant problems in controlling the polymerization rate and the polymer MWD.²⁷² Additionally, lithium ester enolates are unstable, even in the solid state, and subject to decomposition to ketenes and lithium alkoxides and β -keto ester enolates.²⁷³ Lithium ester enolates have a strong tendency to aggregate in both crystalline²⁷⁴ and solution^{275–280} states, which affects their reactivity as initiators and the resulting polymer MWD. Schlaad and Müller^{281,282} proposed, on the basis of the ^{13}C NMR spectroscopic evidence, that the bimetallic “ate” complex $\text{Li}^+[\text{Me}_2\text{C}=\text{C}(\text{OEt})\text{OAlR}_3]^-$ is an adequate model of the active center for the MMA polymerization by ethyl α -lithioisobutyrate (EiBLi) in the presence of aluminum alkyls. The calculated structures for the complex of methyl α -lithioisobutyrate (MiBLi) with AlEt_3 , however, reveal different degrees of association, $(\text{MiBLi}\cdot\text{AlEt}_3)_n$ ($n = 1, 2, 4$), and different

Scheme 20. Generation of Enolaluminates in MMA Polymerization by Zirconium Aluminates



stoichiometries, $\text{MiBLi}\cdot x\text{AlEt}_3$ ($x = 1, 2$).²⁸³ Holmes et al.^{284,285} investigated the ligand effects of organoaluminum amides $^t\text{Bu}_x\text{Al}(\text{NRR}')_{3-x}$ ($x = 1, 2$) and organoaluminum alkoxides $^t\text{Bu}_x\text{Al}(\text{OR})_{3-x}$ ($x = 1\text{--}3$) in the MMA polymerization initiated by EiBLi on polymer tacticity and MWD.

Rodríguez and Chen found that certain bulky aluminum alkyl compounds such as $\text{MeAl}(\text{BHT})_2$, when added to the anionic polymerization system initiated by lithium ester enolates, serve as both catalyst for monomer activation and deaggregator for converting the oligomeric, multisite active species to discrete, monomeric active species (i.e., ester enolaluminate anions, Figure 17).²⁸⁶ The end result is *single-site anionic polymerization* that propagates in a controlled, bimetallic fashion, producing *st*-PMMA (71% *rr*) with a narrow MWD (1.12 PDI) at $23\text{ }^\circ\text{C}$. Specifically, the bimolecular chain propagation for the MMA polymerization by the lithium ester enolaluminate and organoaluminum catalyst combination involves Michael addition of monomeric enolaluminate active species **118** to Al-activated monomer **119**, followed by the release of the coordinated aluminum catalyst to the ester group of the polymer chain in intermediate **120** by MMA to regenerate **118** and **119**. Repeated Michael additions of **118** to **119** produce the syndiotactic polymer in a living fashion (Scheme 19).²⁸⁶

It should be noted that lithium ester enolaluminates are less reactive than the parent lithium ester enolates but more selective with preferential addition to the activated monomer

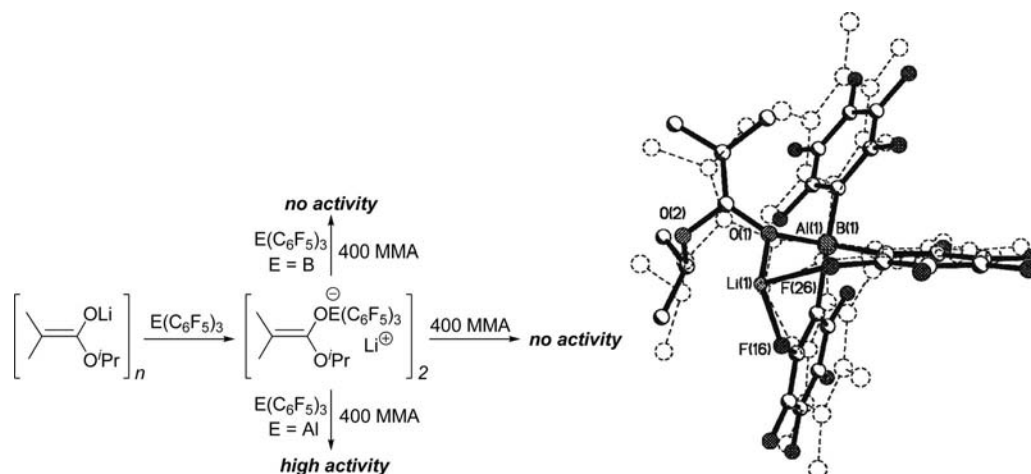


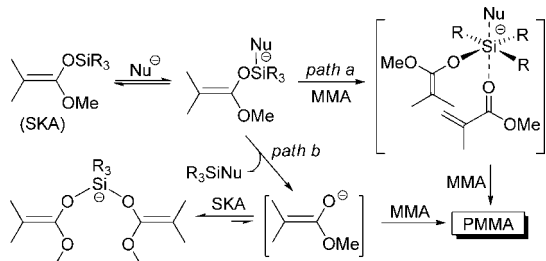
Figure 18. Remarkable Lewis acids effects on the MMA polymerization with lithium ester enolates and structural overlay of enolaluminumate and enolborate anions. Reprinted with permission from ref 287. Copyright 2007 Elsevier.

in a syndioselective fashion. Therefore, to achieve the syndiotacticity of polymer and a high degree of polymerization control, the organoaluminum compounds added to the polymerization initiated by lithium ester enolates are required to have structures capable of forming both *discrete ester enolaluminates and activated-monomer complexes*.^{286,284} Among a series of bulky aluminum Lewis acid catalysts examined, including $\text{MeAl}(\text{BHT})_2$, ${}^i\text{BuAl}(\text{BHT})_2$, ${}^i\text{Bu}_2\text{Al}(\text{BHT})$, $\text{Al}{}^i\text{Bu}_3$, $\text{Al}(\text{C}_6\text{F}_5)_3$, and $\text{Al}(\text{BHT})_3$, the alane $\text{Al}(\text{C}_6\text{F}_5)_3$ not only generates the most active system (having the highest degree of activation toward monomer) but also gives the system the highest degree of control over polymerization.²⁸⁶

While investigating the potential effects of the anion on the stereospecificity of MMA polymerization by C_2 -ligated *ansa*-zirconocene cations, Bolig and Chen found that chiral *ansa*-zirconocenium methyl aluminate complexes, unlike analogous methyl borate complexes which yield highly isotactic PMMA, produce, unexpectedly, syndiotactic PMMA.¹⁸⁵ Scheme 20 outlines the proposed mechanism for the MMA polymerization by the zirconocenium aluminates, which explains the formation of the syndiotactic PMMA, the observed spectroscopic changes while monitoring the polymerization reaction, as well as the observed nearly constant polymer syndiotacticity upon varying the cation symmetry. Owing to the Lewis acidity and oxophilicity of $\text{Al}(\text{C}_6\text{F}_5)_3$ toward MMA exceeding those of the zirconocenium cation, a MMA-separated ion-pair, formed spontaneously upon mixing a zirconocenium aluminate and MMA, is converted to the neutral zirconocene dimethyl and the $\text{MMA}\cdot\text{Al}(\text{C}_6\text{F}_5)_3$ complex. Initiation involves methyl transfer to the monomer complex forming the enolaluminumate that participates in rapid propagation via intermolecular Michael addition to the activated monomer producing *st*-PMMA. Hence, this polymerization is bimetallic and chain-end controlled through *enolaluminumate intermediates*, typically leading to syndio-rich PMMA. Using group 4 metallocenes containing an ester enolate initiating group, such as $\text{Cp}_2\text{ZrMe}[\text{OC}(\text{O}^i\text{Pr})=\text{CMe}_2]$, in combination with 2 equiv of $\text{Al}(\text{C}_6\text{F}_5)_3$, is much more effective.⁵³ For example, in a ratio of $[\text{MMA}]_0/[\text{Al}(\text{C}_6\text{F}_5)_3]_0/[\text{Zr}]_0 = 200:2:1$, a quantitative monomer conversion was achieved in 5 min at 25 °C for a high TOF of 2400 h^{-1} , producing PMMA with a syndiotacticity of 69% *rr*, M_n of 2.39×10^4 ($I^* = 84\%$), and PDI of 1.05.

The above polymerization is uniquely regulated by the anion, and the zirconocene species participates only in the initiation step, a hypothesis further supported by the observed constant PMMA syndiotacticity upon varying the metallocene cation symmetry and by the experiments with the zirconocene being replaced with anionic initiators such as ${}^i\text{BuLi}$ and $\text{Me}_2\text{C}=\text{C}(\text{OMe})\text{OLi}$.¹⁸⁵ For example, MMA polymerizations initiated by ${}^i\text{BuLi}$ or $\text{Me}_2\text{C}=\text{C}(\text{OMe})\text{OLi}$ in toluene have low activity and produce *isotactic* polymer with broad MWDs ($M_w/M_n = 14\text{--}22$), whereas the addition of 2 equiv of $\text{Al}(\text{C}_6\text{F}_5)_3$ to MMA before introducing either anionic initiator to start the polymerization (one equiv for generating enolaluminates and the second for activating monomer) brings about much faster and more controlled polymerizations, producing *syndiotactic* PMMA with tacticity ranging from moderate 76% *rr* to high 95% *rr*, T_g from moderate 127 to high 140 °C, and PDI from moderate 1.35 to low 1.08, depending on polymerization temperature.¹⁸⁵ In the case of the polymerization initiated by ${}^i\text{BuLi} + \text{Al}(\text{C}_6\text{F}_5)_3$, if ${}^i\text{BuLi}$ and $\text{Al}(\text{C}_6\text{F}_5)_3$ are premixed for 10 min before addition of MMA to start the polymerization, then the actual initiator becomes a hydride-bridged aluminate dimer $[(\text{C}_6\text{F}_5)_3\text{Al}-\text{H}-\text{Al}(\text{C}_6\text{F}_5)_3]^-$, which is formed via hydride abstraction with concomitant elimination of isobutylene.⁵³ Interestingly, in sharp contrast to the (TPP)AlMe polymerization system, which can be substantially accelerated by boranes such as BPh_3 and $\text{B}(\text{C}_6\text{F}_5)_3$,²⁶⁰ addition of $\text{B}(\text{C}_6\text{F}_5)_3$ to the anionic polymerization initiated by ${}^i\text{BuLi}$ or $\text{Me}_2\text{C}=\text{C}(\text{OMe})\text{OLi}$ completely halted MMA polymerization. This observation implies different propagation mechanisms between these systems assisted by monomer activation with organo Lewis acids.

MMA polymerization using stable alkyl lithioisobutyrate (e.g., $\text{Me}_2\text{C}=\text{C}(\text{O}^i\text{Pr})\text{OLi}$) + $\text{Al}(\text{C}_6\text{F}_5)_3$ is more controlled at RT than that using $\text{Me}_2\text{C}=\text{C}(\text{OMe})\text{OLi}$, producing PMMA with a syndiotacticity of 80% *rr* and a narrow MWD of PDI = 1.04. Polymerization of *n*BMA using this initiator system is likewise syndiospecific and well controlled. Thus, at a polymerization temperature of 23 °C, syndiotactic PBMA (79% *rr*) with a narrow MWD (1.07 PDI) was produced in 96% yield within 30 min. Lowering the polymerization temperature to 0 °C achieved higher syndiotacticity (84% *rr*) with a narrow MWD of 1.05.⁵³ There are dramatic effects of Lewis acids $\text{E}(\text{C}_6\text{F}_5)_3$ ($\text{E} = \text{Al}, \text{B}$) on polymerization of MMA mediated by $\text{Me}_2\text{C}=\text{C}(\text{O}^i\text{Pr})\text{OLi}$. While the $\text{Me}_2\text{C}=\text{C}=\text{C}(\text{O}^i\text{Pr})\text{OLi}$

Scheme 21. Associative (a) and Dissociative (b) Pathways in GTP


$C(O^iPr)OLi/2Al(C_6F_5)_3$ system is *highly active* for MMA polymerization, the seemingly analogous $Me_2C=C(O^iPr)OLi/2B(C_6F_5)_3$ system is *inactive*.²⁸⁷ Structural analyses of the resulting lithium enolate and borate adducts, $Li^+[Me_2C=C(O^iPr)OE(C_6F_5)_3]^-$ (Figure 18), coupled with polymerization studies, show that the remarkable differences observed for Al vs B are due to the inability of the lithium enolate/borate pair to effect the bimolecular, activated-monomer anionic polymerization, as does the lithium enolate/alane pair (*cf.* Schemes 19 and 20).

2.4.3. Group 14 Catalysts

Controlled polymerization of acrylic monomers by a silyl ketene acetal (SKA) and a nucleophilic or Lewis acid catalyst was discovered by DuPont scientists and termed group transfer polymerization (GTP).^{288,289} This was named such based on the initially postulated *associative* propagation mechanism in which the silyl group remains attached to the same polymer chain and is simply transferred intramolecularly to the incoming monomer through hypervalent anionic silicon species (path *a*, Scheme 21).²⁸⁸ However, it has been recently concluded²⁹⁰ that several lines of key experimental evidence now are more consistent with a *dissociative* mechanism,^{291–293} which involves ester enolate anions as propagating species and a rapid, reversible complexation (termination) of small concentrations of enolate anions with SKA or its polymer homologue (path *b*, Scheme 21). GTP can readily produce PMMA with M_n of $\leq 20,000$ in a controlled fashion at $T_p \geq$ ambient temperatures (50–80 °C range), but its synthesis of PMMA in the 60,000 range is difficult.²⁹⁰

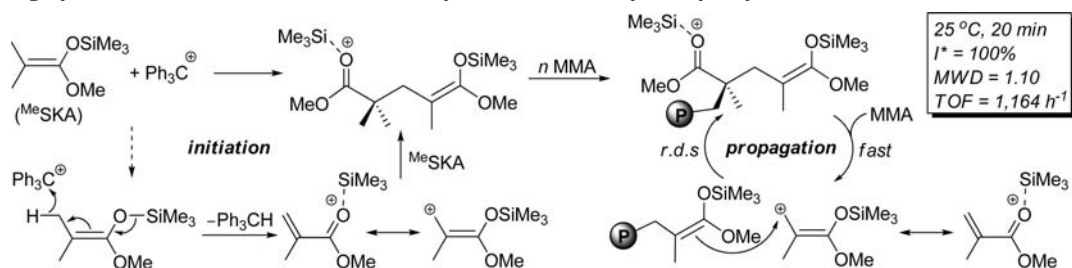
Nucleophilic catalysts are needed only in low concentrations (0.1–1.0 mol % of initiator); in fact, the polymerization is halted if too much of such catalysts is used. Among various nucleophilic anions, fluoride and bifluoride (e.g., $(Me_2N)_3S^+HF_2^-$) are the most active catalysts, typically in THF.²⁸⁸ Two recent reports also employed *N*-heterocyclic carbenes as nucleophilic catalysts for GTP at RT.^{294,295} When polymerizations are carried out at above ambient temperatures, carboxylates and bicarboxylates are preferred.²⁹⁶ Lewis acid catalysts such as zinc halides, on the other hand, are required in a large amount (10–20 mol % of monomer) and preferred for acrylate polymerization in aromatic solvents, as nucleophilic catalysts produce polyacrylates with broader MWDs.²⁹⁷ Dialkyl aluminum halides can work at lower levels (10–20 mol % of initiator), but HgI_2-Me_3SiI is by far the best Lewis acid-mediated GTP system that promotes controlled acrylate polymerization at low catalyst levels.²⁹⁸ Combination of R_3SiOTf with $B(C_6F_5)_3$ has also been found to catalyze GTP of acrylates initiated by SKA.²⁹⁹

Activation of the inactive SKA or monomer is the critical first step in the mechanisms shown in Scheme 21. It can be

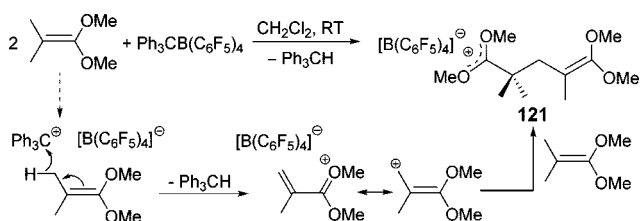
viewed that paths *a* and *b* involve *reductive activation* of SKA in terms of converting an inactive neutral Si species to an active, anionic Si species. Recently, Zhang and Chen established *oxidative activation* of SKA with a catalytic amount of $[Ph_3C][B(C_6F_5)_4]$, which led to a novel, highly active and efficient, as well as living/controlled (meth)acrylate polymerization system catalyzed by the silylium ion R_3Si^+ .³⁰⁰ The intriguing, “*monomer-less*” initiation involves oxidative activation of Me^cSKA (methyl trimethylsilyl dimethylketene acetal) by $[Ph_3C][B(C_6F_5)_4]$, leading to the Me_3Si^+ -activated MMA derived from vinylogous *hydride abstraction* of Me^cSKA with Ph_3C^+ (i.e., the monomer is generated from the initiator!); subsequent Michael addition of Me^cSKA to the activated MMA (or silylated MMA) affords the highly active, *ambiphilic* propagating species containing both nucleophilic SKA and electrophilic silylium ion (or silyl cation) sites (see the initiation manifold, Scheme 22). It is noteworthy to mention that no noticeable reactions are observed for $Et^cSKA + B(C_6F_5)_3$ (RT for 5 h) or $Me_3SiOTf + B(C_6F_5)_3$ (RT for 24 h or 70 °C for 12 h), highlighting the necessity of the use of $[Ph_3C][B(C_6F_5)_4]$ for this chemistry to occur. A propagation “catalysis” cycle consists of a fast step of recapturing the silylium catalyst from the ester group of the growing polymer chain by the incoming MMA, followed by a *r.d.s.* of the C–C bond formation via intermolecular Michael addition of the polymeric SKA to the silylated MMA (see the propagation manifold; Scheme 22).

Based on the results obtained from polymerization kinetics and mechanism studies, this polymerization can be characterized as a bimolecular *polymer-transfer polymerization* (as the growing polymer chain is transferred back and forth between the two conjugate active sites), which is different than the classic GTP in both the SKA activation method and the propagation mechanism. The methacrylate polymerization by SKA/ $[Ph_3C][B(C_6F_5)_4]$ is also living/controlled at ambient temperature, efficiently producing PMMA of low to high M_n ($>10^5$) with narrow MWDs of 1.04–1.12, with a trityl activator loading as low as 0.025 mol % relative to monomer.³⁰⁰ For example, addition of 1 equiv of $[Ph_3C][B(C_6F_5)_4]$ to a CH_2Cl_2 solution containing 400 equiv of MMA and 2 equiv of Me^cSKA achieved 97% MMA conversion in 20 min at 25 °C (TOF = 1164 h⁻¹), affording PMMA with $M_n = 3.87 \times 10^4$, PDI = 1.10, $[rr] = 69\%$, and $I^* = 100\%$. Under the same conditions, quantitative *n*BMA conversion was achieved in 60 min, yielding PBMA of $M_n = 5.44 \times 10^4$, PDI = 1.06, $[rr] = 80\%$, and again a quantitative initiator efficiency. High M_n (1.86×10^5) PMMA was readily obtained using a $[MMA]/[initiator]$ ratio of 1600.

Zhang and Chen also investigated structure–property relationships of this polymerization system catalyzed by R_3Si^+ .³⁰¹ The authors showed remarkable selectivity of the silyl group structure of the acetal initiator (and thus the derived silylium ion catalyst R_3Si^+) for monomer structure: initiators having small silyl groups, such as Me^cSKA , promote highly active and efficient polymerization of methacrylates, but they are poor initiators for polymerization of less sterically hindered, active α -H bearing acrylate monomers. On the other hand, initiators incorporating bulky silyl groups, such as the triisobutylsilyl derivative (i^tBuSKA), exhibit lower activity toward methacrylate polymerization but *exceptionally high activity for acrylate polymerization* at 25 °C (section 3.3).³⁰¹ Other group 14-based ketene acetals such as dimethylketene dimethyl acetal (DKDA) are readily activated

Scheme 22. Highly Efficient and Controlled MMA Polymerization Catalyzed by Silylium Ion R₃Si⁺

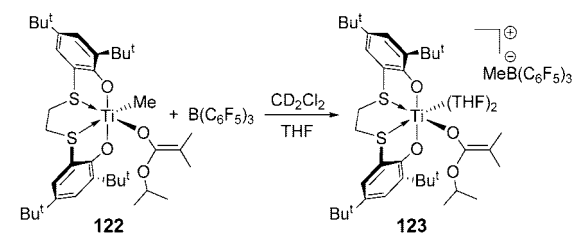
Scheme 23. Oxidative Activation of Group 14-Based Ketene Acetals



with $[\text{Ph}_3\text{C}][\text{B}(\text{C}_6\text{F}_5)_4]$ in the same fashion as the silyl acetal MeSKA . Specifically, the 2:1 ratio reaction of DKDA with $[\text{Ph}_3\text{C}][\text{B}(\text{C}_6\text{F}_5)_4]$ at RT produces cleanly the anticipated C–C bond coupling product $[(\text{MeO})_2\text{C}=\text{CMeCH}_2\text{-CMe}_2\text{C}(\text{OMe})_2]^+[\text{B}(\text{C}_6\text{F}_5)_4]^-$ (**121**), which has been structurally characterized by X-ray diffraction. Formation of **121** can be explained by conjugate addition of DKDA to the Me^+ -activated MMA (methylated MMA) generated by vinylogous hydride abstraction of DKDA with Ph_3C^+ (Scheme 23).

2.4.4. Transition-Metal Catalysts

Neutral alkyl titanium ester enolate complex **122** supported by a tetradentate bis(phenoxy)sulfur-donor $[\text{O}^-, \text{S}, \text{S}, \text{O}^-]$ -type ligand can be readily activated to the corresponding cationic ester enolate complex **123** upon methide abstraction by $\text{B}(\text{C}_6\text{F}_5)_3$ (Figure 19).³⁰² Unlike the analogous methyl cation, the ester enolate cation **123** is active for MMA polymerization, despite low activity (4.3 h^{-1} TOF) as well as the broadly distributed (2.63 PDI) and syndio-rich (55% *rr*) PMMA it produces. On the other hand, combination of **122** with 1 or 2 equiv of $\text{Al}(\text{C}_6\text{F}_5)_3$ affords PMMA with a much



	123	122/Al(C₆F₅)₃	122 + 123
<i>T_p</i> (°C)	20	20	20
TOF (h ⁻¹)	4.3	5.4	2,400
<i>M_n</i> (kD)	16	20.6	22.2
PDI	2.63	1.09	1.08
<i>I</i> [*] (%)	65	63	90
<i>rr</i> (%)	55	71	67

Figure 19. Structures of Ti Complexes Bearing the Tetradentate Bis(phenoxy)sulfur-Donor Ligand and Their MMA Polymerization Characteristics

narrower MWD (1.09 PDI) and higher syndiotacticity (71% *rr*). Lastly, combining the neutral complex **122** and the cationic complex **123** generates a highly active system with a TOF of 2400 h^{-1} and an *I*^{*} of 90%, and the PMMA produced exhibits a narrow MWD of PDI = 1.08 and a syndiotacticity of 67% *rr*, a typical syndiotacticity seen for the PMMA produced by a bimetallic propagation mechanism with the parent $[\text{Cp}_2\text{Zr}]$ system.¹⁶⁶

Titanium ester enolate complex $\text{Me}_2\text{C}=\text{C}(\text{OMe})\text{OTi}(\text{O}^i\text{Pr})_3$ gave no polymer product in its MMA polymerization carried out at 0 °C; however, at -20 °C or at -30 °C with low MMA to initiator ratios of 16 to 31, the polymerization by the same complex produced low MW polymer.³⁰³ The related “ate” complex $\text{Li}^+[\text{Me}_2\text{C}=\text{C}(\text{OMe})\text{OTi}(\text{O}^i\text{Pr})_4]^-$ afforded PMMA in higher yields of >90% (*t_p* = 1 h), as compared to 38% to 68% yield by the neutral enolate. Niobium tribenzyl imido complex $[\text{NbBz}_3(=\text{N}^i\text{Bu})]$ and tantalum aryloxo dibenzyl imido complex $[\text{Nb}(\text{OAr})\text{Bz}_2(=\text{N}^i\text{Bu})]$ (Ar = 2,6-*i*Pr₂C₆H₃), upon activation with 2 equiv of $\text{Al}(\text{C}_6\text{F}_5)_3$, showed modest activity (TOF up to 17 h^{-1} at 25 °C in toluene), producing *st*-PMMA (70% *rr*) by the Nb complex at this temperature.³⁰⁴

A large number of divalent metal complexes of groups 8 (Fe), 9 (Co), 10 (Ni, Pd), and 11 (Cu) have been reported to polymerize (meth)acrylates (MMA unless indicated otherwise) when combined with a large excess of methylaluminoxane (MAO) as activator, including the following: iron and cobalt dichloride complexes supported by pyridyl bis(imine) $[\text{N}, \text{N}, \text{N}]$ ligands³⁰⁵ (also for methyl acrylate polymerization³⁰⁶), nickel dibromide complexes bearing α -diimine $[\text{N}, \text{N}]$ ligands,³⁰⁵ nickel and palladium dihalide bimetallic complexes carrying linked iminopyridyl $[\text{N}, \text{N}]$ -linker- $[\text{N}, \text{N}]$ ligands,³⁰⁷ dinuclear nickel-acac $[\text{O}_2^-]$ complexes bridged by 2,5-diamino-1,4-benzoquinonediimine $[\text{N}_2^-]$ ligands, $[\text{Ni}(\text{acac})\{\mu\text{-C}_6\text{H}_2(=\text{NAr}_4)\}\text{Ni}(\text{acac})]$,³⁰⁸ bis(indanone-iminato) $[\text{O}^-, \text{N}]$ nickel complexes,³⁰⁹ nickel phenyl complexes supported by β -ketoiminato $[(\text{O}, \text{N})^-]$ ligands,³¹⁰ bis(β -ketoamino) $[(\text{O}, \text{N})^-]$ nickel complexes,³¹¹ nickel complexes bearing bis(8-hydroxynitroquinoline) $[\text{O}^-, \text{N}]$ ligands,³¹² bis(3,5-dinitro-salicylaldimine) $[\text{O}^-, \text{N}]$ nickel complexes,³¹³ mono(salicylaldimine) $[\text{O}^-, \text{N}]$ nickel (COD) complexes (also for copolymerization of ethylene with MMA³¹⁴),³¹⁵ bis(α -nitroacetophenone) $[\text{O}_2^-]$ and bis(salicylaldimine) $[\text{O}^-, \text{N}]$ nickel complexes (also for copolymerization of ethylene with MMA³¹⁴),³¹⁶ bis(phenoxyimine) $[\text{O}^-, \text{N}]$ nickel complexes (excess alkylaluminum),³¹⁷ $\text{Ni}(\text{acac})_2$,^{318,319} [also $\text{V}(\text{acac})_3$, $\text{Mn}(\text{acac})_2$, $\text{Cr}(\text{acac})_3$],³²⁰ $\text{Ni}(\text{acac})_2$ (for *t*Bu methacrylate),³²¹ nickelocene Cp_2Ni ,³²² substituted nickelocenes, half-sandwich nickel chloride complexes, $\text{Ni}[1,3\text{-(CF}_3)_2\text{-acac}]_2$ and $\text{Ni}(\text{R})(\text{acac})(\text{PPh}_3)$,³²³ half-sandwich palladium allyl complexes,³²⁴ β -ketoiminato $[(\text{O}, \text{N})^-]$ palladium methyl complexes,³²⁵ bis(salicylaldimine) $[\text{O}^-, \text{N}]$ copper complexes,³²⁶ as well as copper dichlorides supported by

R	TOF (s ⁻¹)	M _n (kD)	PDI	I* (%)	
Sm	Me	3.6	48	1.04	89
	Et	130	55	1.04	86
	ⁿ Bu	134	70	1.05	91
	^t Bu	4 (h ⁻¹)	16	1.03	79
Y	Me	3.0	50	1.07	86
	Et	76	53	1.05	91
	ⁿ Bu	87	72	1.04	88
	^t Bu	4 (h ⁻¹)	17	1.03	75

Figure 20. Acrylate polymerization characteristics by Cp*₂LnMe(THF).

bis(benzimidazole) [N,N] ligands (for ^tBu acrylate and its copolymerization with ethylene³²⁷ and for methacrylates, acrylates, and their copolymerization with ethylene³²⁸).

The PMMAs produced by these systems typically exhibit broad MWDs (>2) and are syndio-rich, and the mechanism of polymerization of acrylic monomers mediated by such late metal complexes, vis-a-vis coordination–insertion vs free-radical polymerization, was often not clearly demonstrated. Novak and co-workers showed that even the discrete neutral palladium(II) methyl (but not the enolate) complexes bearing pyrrole–imine [N⁻,N] ligands polymerize MA and copolymerize it with olefins by a radical mechanism.³²⁹ Sen et al. cautioned that a common practice of using the primary evidence that radical traps such as galvinoxyl, DPPH, and TEMPO fail to halt or substantially suppress the polymerization by the system employing MAO to argue against an alternative radical mechanism can lead to a wrong conclusion because excess MAO can deactivate the radical trap and thus give false-negative results.³³⁰ The polymerization results, especially derived from those systems with only modest activities, were also complicated by the activity of the activator itself, such as isobutylaluminum toward MMA polymerization, albeit low activity.³³¹ Therefore, several additional lines of evidence, such as reactivity ratios, copolymer compositions, and microstructures, besides radical trap experiments, should be presented before drawing a nonradical mechanism conclusion for acrylic polymerizations using such systems.^{329,330}

Transition-metal halides were found to significantly modulate anionic polymerization of MMA by conventional organolithium reagents. For example, ternary initiating systems consisting of R₂NLi/ⁿBuLi/metal halides (WCl₆, MoCl₅, and NbCl₅) produced highly stereoregular PMMA (1.7–7.0 PDI) with isotacticity up to 98% *mm* at –78 °C in toluene.³³² The role of the metal halides was proposed to form “ate” complexes with the organolithium reagents, which were subsequently converted to the transition-metal-centered enolate as active propagating species. On the other hand, lithium alkylnickelate and alkylpalladate bimetallic “ate” complexes, derived from the reaction of MCl₂(PPh₃)₂ (M = Ni, Pd) with 2–4 equiv of ⁿBuLi at –78 °C in THF, promote controlled MMA polymerization (PDI = 1.26–1.52, I* < 20%) at –78 °C in THF, leading to *st*-PMMA (73–75% *rr*).³³³ Other transition-metal halides in combination with different anionic initiators have also been investigated, including Ph₂NLi with divalent metal halides (FeBr₂, MnCl₂, CoCl₂, NiBr₂),³³⁴ ⁿBuLi or PhLi with ^tBu₃Al, and late metal halides (FeCl₂, FeCl₃,

cat	T _p (°C)	TOF (h ⁻¹)	M _n (kD)	PDI	I* (%)	mr (%)
124	–30	4.3	30	1.97	33	50
124	25	40	25	1.56	41	50
125	25	6.6	13	1.69	20	46

Figure 21. Acrylate Polymerization Characteristics by (CGC)Y Alkyl and Hydrido Complexes

MnCl₂, CoCl₂, NiBr₂),³³⁵ as well as ⁿBuLi with ^tBuOK and MnCl₂.³³⁶ Naturally, the degree of the polymerization control and the resulting polymer tacticity using such multicomponent systems are sensitive to the reagents of mixing and their relative ratios.

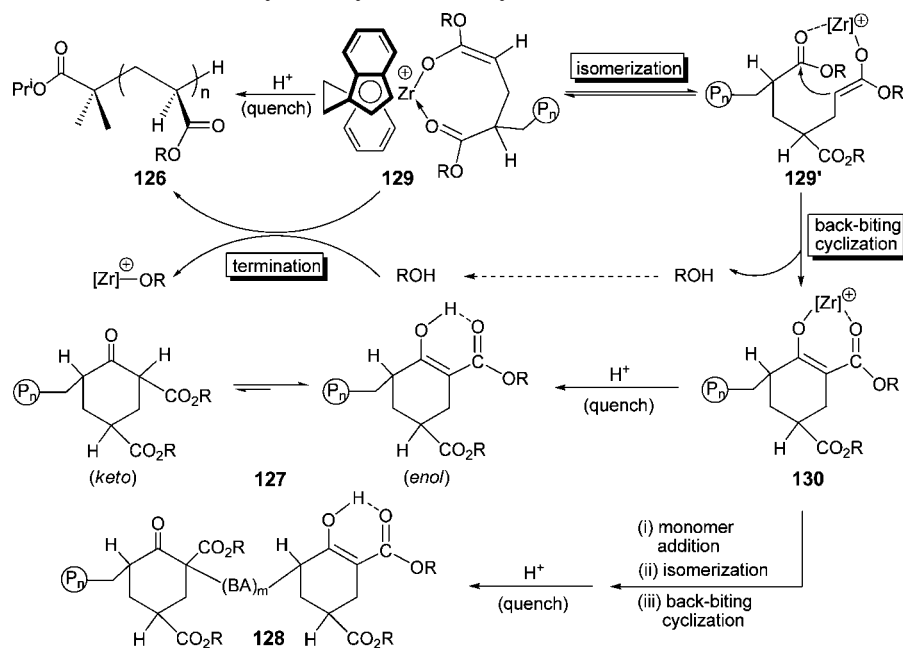
3. Acrylate Polymerization

3.1. Lanthanocenes

Controlled polymerization of acrylates, due to their active α-protons, is challenging with anionic initiators, especially at relatively high temperatures or without additives and/or mediators. Yasuda and co-workers³³⁷ discovered that trivalent lanthanocenes Cp*₂LnMe(THF) (Ln = Sm, Y) remarkably catalyze the extremely rapid and also living polymerization of alkyl acrylates CH₂=CHCOOR [R = Me (MA), Et (EA), ⁿBu (ⁿBA), and ^tBu (^tBA)] at 0 °C in toluene to high MW, essentially atactic polymers with narrow MWDs (Figure 20).³³⁸ The initiation and propagation mechanism for the acrylate polymerization was thought to proceed in the same fashion as described for the methacrylate polymerization catalyzed by trivalent lanthanocenes (*cf.* Scheme 3). The nearly identical MA polymerization behavior observed for alkyl complex Cp*₂YMe(THF) and enolate complex^{339,340} Cp*₂Y(OCH=CH₂)(THF) or [(Me₃SiC₅H₄)₂Y(OCH=CH₂)₂] provides strong evidence for the metal–O–enolate being the active propagating species.³³⁸

The acrylate polymerization catalyzed by lanthanocenes is considerably faster than the methacrylate polymerization by the same catalysts (*cf.* section 2.1.1), achieving high monomer conversions and high I* values (>80%, except for ^tBA) in seconds (for ethyl and *n*-butyl acrylates with 0.2 mol % catalyst). Using a low concentration of the Sm initiator, the synthesis of high MW poly(acrylate)s with narrow MWDs (e.g., M_n = 7.75 × 10⁵, PDI = 1.15 for PEA) was achieved.³³⁸ The apparent rate of acrylate polymerization increases with an increase in the steric bulk of the acrylate R group in the order ⁿBu > Et > Me, presumably due to the electronic effect of the alkyl group, whereas the reactivity order of the monomer is *reversed* in the case of methacrylates (i.e., ⁿBu < Et < Me).^{36,87} However, this reactivity trend cannot be extended to ^tBA, as it exhibits drastically lower activity than other alkyl acrylates (Figure 20). The resulting high MW (M_n > 2.0 × 10⁵), monodispersed (PDI < 1.07) linear P(ⁿBA) can be irradiated with an electron beam to produce cross-linked P(ⁿBA) with improved viscoelastic and adhesive properties useful for high-temperature applications.³⁴¹

Ziegler et al.³⁴² studied, through DFT calculations, the polymerization of MA with Cp₂SmMe, along with its isoelectronic group 4 catalyst Cp₂ZrMe⁺, and they found that

Scheme 24. Side Reactions Identified in Acrylate Polymerization by Zirconocenium Ester Enolate **86**

the C–C coupling (conjugate addition within the enolate catalyst–monomer complex) step is strongly exothermic and that the monomer-assisted ring-opening of the metallacycle resting intermediate is *rate-limiting* and also responsible for the tacticity of the polymer. The authors further developed a kinetic model for predicting the syndiotacticity of the polymer produced by the chain-end control mechanism.

Yttrium alkyl (**124**) and hydrido (**125**) complexes of CGC type (Figure 21) polymerize ^tBA to median MW, atactic (~50% *mr*) polymers.³⁴³ Quantitative monomer conversion was achieved only at low [monomer]/[Y] ratios (<100). The polymerization activity of the alkyl complex **124** (4.3 h⁻¹ TOF) is low at -30 °C and is increased to 40 h⁻¹ TOF at 25 °C. The hydrido complex **125** is far less active than the alkyl complex at the same *T_p*.³⁴⁴

3.2. Group 4 Metallocenes

While the polymerization of alkyl methacrylates by group 4 metallocene complexes has been extensively investigated and achieved considerable successes, reports on the polymerization of alkyl acrylates by such complexes are scarce and only limited success has been achieved. Soga and Deng³⁴⁵ employed a three-component system consisting of *rac*-(EBI)ZrMe₂/[Ph₃C][B(C₆F₅)₄]/MeAl(BHT)₂ for the polymerization of the sterically hindered ^tBA, affording iso-rich poly(^tBA) (75.9% *mm* in toluene) with moderate to broad MWDs (PDI = 1.23–2.20) in low to moderate polymer yields (6–60%) with extended reaction times (17–24 h). Collins and co-workers¹⁶¹ investigated the polymerization of the unhindered ^tBA by a two-component bimetallic system consisting of the catalyst [Cp₂ZrMe(THF)]⁺[BPh₄]⁻ and the initiator Cp₂ZrMe[OC(O^tBu)=CMe₂]; a monomer conversion of 55% and a polymer MWD of 2.02 were observed for the polymerization at 0 °C in a [^tBA]/[initiator] ratio of ~100, with higher conversions and lower polymer MWDs being achieved only at lower *T_p*. This process is not controlled, and analysis of the low-MW poly(^tBA) by MALDI–TOF MS led to two proposed modes of chain termination processes, the predominate of which involves the backbiting cyclization of the growing polymer chain. A third report on

the polymerization of acrylates (^tBA and ⁿBA) by Hadjichristidis et al.³⁴⁶ employed Soga's three-component systems, including Cp₂ZrMe₂/B(C₆F₅)₃/ZnEt₂, *rac*-(EBI)ZrMe₂/B(C₆F₅)₃/ZnEt₂, and *rac*-(EBI)ZrMe₂/[HNMe₂Ph][B(C₆F₅)₄]/ZnEt₂. The polymer yields obtained from these polymerizations of ⁿBA and ^tBA for 24 h did not exceed 30 and 32%, respectively in any case, regardless of the catalyst system or polymerization conditions employed. The results from the above three reports clearly indicate the presence of considerable chain termination processes in the polymerization of α-proton-containing acrylates using cationic group 4 metallocene complexes. This observation is in sharp contrast to the isoelectronic, neutral organolanthanide complexes such as Cp*₂SmMe(THF) which mediate the high-speed, living polymerization of alkyl acrylates (vide supra).³³⁸

Using the well-defined single-component, chiral mono-metallic propagating zirconocenium ester enolate system **86**, Chen et al.³⁴⁷ revealed mechanisms of chain transfer and termination in the polymerization of ⁿBA by **86**. This polymerization also proceeds in an uncontrolled fashion at ambient temperature to only moderate monomer conversions (47% with a 1.0 mol % catalyst loading) due to the presence of substantial chain termination processes, producing poly(ⁿBA) with one major linear structure **126** as well as two minor cyclic β-ketoester-terminated poly(ⁿBA) structures **127** and **128** (Scheme 24). The combined polymerization, chain structure, and model reaction studies have yielded an overall three-step mechanism. First, isomerization of the eight-membered-ring zirconocenium ester enolate propagating species **129** (resting state) to its ten-membered-ring homologue **129'**, followed by intramolecular backbiting cyclization involving the antepenultimate ester group of the growing polymer chain, generates the much less active six-membered-ring zirconocenium β-ketoester enolate species **130** [which leads to cyclic β-ketoester-terminated **127** upon acidic workup] and ⁿBuOH. Second, the *in situ* eliminated ⁿBuOH deactivates propagating species **129** to yield the inactive zirconocenium alkoxide species and linear chain **126**. Third, further addition of monomer to **130** followed by a second backbiting cyclization gives doubly cyclic β-ketoester-

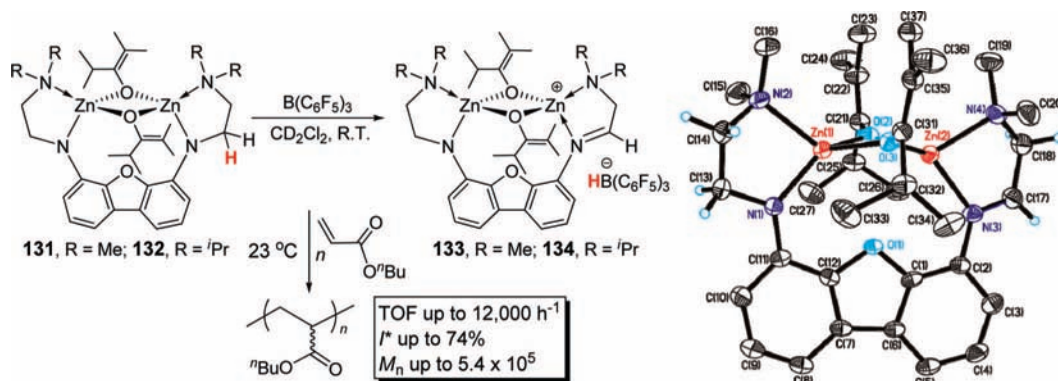


Figure 22. Generation of cationic zinc enolate catalysts for highly active polymerization of n BA at RT. Reprinted with permission from ref 351. Copyright 2006 American Chemical Society.

terminated **128** (upon acidic workup), accompanied by additional catalyst deactivation and chain termination as shown above. Overall, the *lack of steric protection* at the unhindered α -C of the ester enolate moiety in the propagating species facilitates the backbiting cyclization, whereas the active (*readily enolizable*) α -proton provides access for elimination of n BuOH that subsequently terminates the chain. Model reactions and polymerization studies show that possible chain transfer reactions involving acidic α -protons are insignificant as compared with backbiting cyclizations in the current monometallic catalyst system.

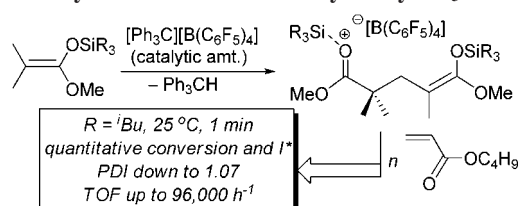
Ziegler and co-workers also examined side reactions involved in the acrylate polymerization with group 4 metallocene catalysts by DFT calculations.³⁴⁸ Through this study, the authors concluded that no competitive side reactions are possible from the eight-membered metallacycle resting state; however, isomerization to its ten-membered homologue is possible and slightly exothermic, and this process becomes more competitive as the concentration of the monomer decreases. The ten-membered species readily undergoes the backbiting reaction, and overall, this theoretical study provides support for the side reaction pathways outlined in Scheme 24.

On the other hand, Carpentier et al. found that the robust (CGC)TiMe₂/B(C₆F₅)₃ system (which generates (CGC)-TiMe⁺MeB(C₆F₅)₃⁻ *in situ*) effectively catalyzes polymerization of n BA.³⁴⁹ Nearly quantitative monomer conversions (98% yield) using a [n BA]/[Ti] ratio of 200 were achieved at T_p ranging from -20 to 20 °C, producing P(n BA) with unimodal MWD (PDI = 1.49–1.81) and a syndiotacticity of 76% *rr*. In a high [n BA]/[Ti] ratio of 800, the polymerization reached a high TOF of 5920 h⁻¹ at 70% n BA conversion or a TOF of 664 h⁻¹ and an I^* of 52% at 83% n BA conversion.

3.3. Nonmetallocenes

A dichlorozirconium complex supported by the dianionic 2,6-bis(2-benzimidazolyl)pyridine [N⁻,N,N⁻] ligand, when combined with a large excess MAO (50–1000 equiv), was reported to polymerize MA from 30 to 90 °C in 1,1,2,2-tetrachloroethane to give PMA with broad MWDs (PDI = 2.11–6.17).³⁵⁰ Chen, Hagadorn, and co-workers³⁵¹ found that binuclear zinc enolate cations supported by the dibenzofuran bis(amidoamine) ligand are highly active catalysts for the production of high MW polyacrylates at ambient temperature (Figure 22). The cationic catalysts were generated from the reaction of neutral zinc enolates **131** and **132** with B(C₆F₅)₃ that abstracts a hydride from the lower CH₂ group in the

Scheme 25. Highly Active, Efficient, and Controlled Acrylate Polymerization at RT Catalyzed by i Bu₃Si⁺



C₂H₄ side arm linker. The neutral zinc enolate complexes (**131** and **132**) or the activator B(C₆F₅)₃ are inactive for polymerization of n BA, but mixing of **131** with 1 equiv of B(C₆F₅)₃ (which spontaneously generates the corresponding cationic enolate **133**) yielded a highly active polymerization system that achieved quantitative monomer conversions within 10 min for [n BA]/[**131**] ratios ranging from 200 to 800. The polymerization was in fact complete within 5 min even for the 1000:1 ratio run, giving a TOF of 12,000 h⁻¹. All polyacrylates produced exhibit unimodal MWDs but with typical PDI values being in the range from 2.2 to 2.9, indicative of a nonliving process. Remarkably, the polymerization with a low catalyst loading of only 0.02 mol % produces high MW polymer with $M_n = 5.40 \times 10^5$ g/mol and PDI = 2.15.³⁵¹ Both isolated cationic enolates **133** and

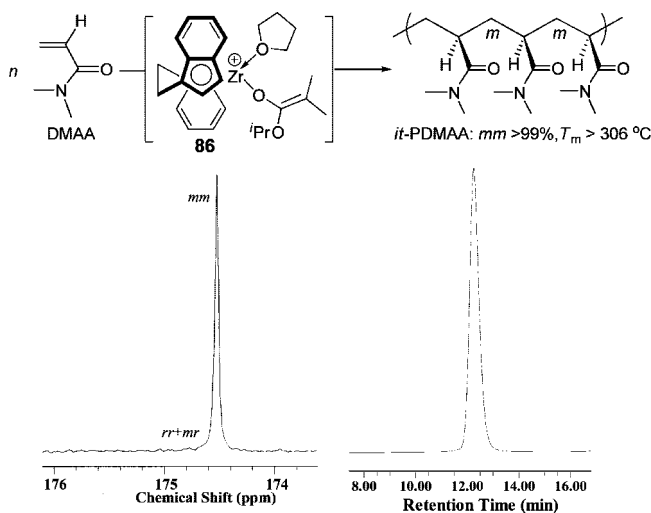


Figure 23. Highly isotactic acrylamide DMAA polymer produced by **86** as well as its ¹³C NMR spectrum (D₂O, 80 °C) of highly isotactic PDMAA showing the carbonyl triad [*mm*] >99% (bottom left) and the GPC trace of the same PDMAA showing PDI = 1.07 (bottom right). Reprinted with permission from ref 352. Copyright 2004 American Chemical Society.

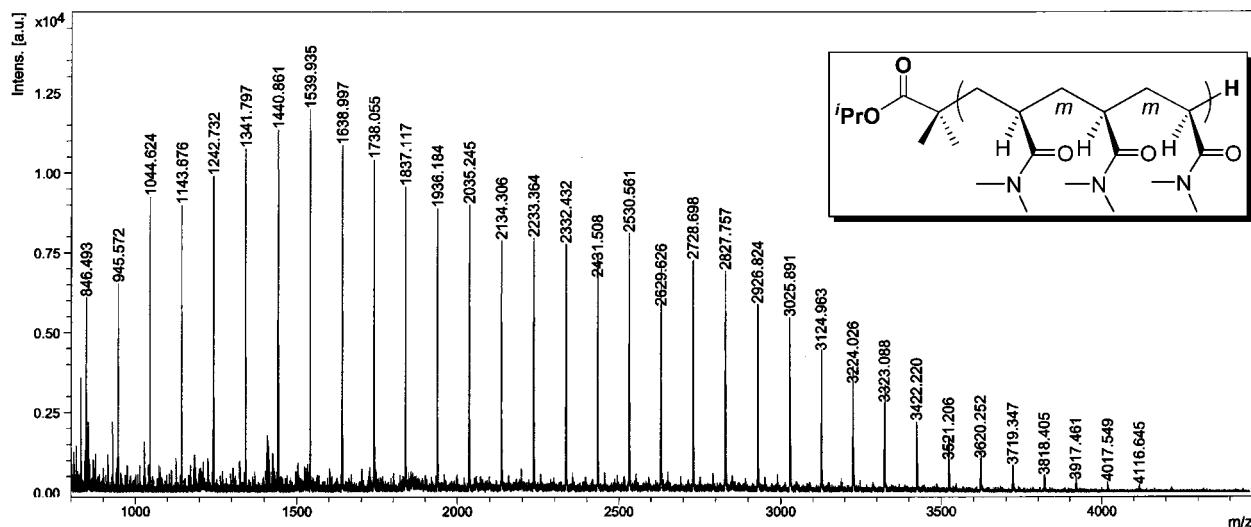


Figure 24. MALDI-TOF mass spectrum of the low-MW PDMAA produced by **86**. Reprinted with permission from ref 353. Copyright 2005 American Chemical Society.

134 showed the same high activities as the *in situ* generated catalysts. Regarding the polymerization mechanism, it was suggested that monomer additions occur at the active, cationic site of the zinc enolate in which the datively bound, “axial like” amino *N* is displaced by monomer in the initiation step, embarking a coordination–addition polymerization as in the methacrylate polymerization by the cationic metallocene enolates.

Perhaps the system that exhibits both the *highest activity and degree of control* for acrylate polymerization carried out at ambient temperature is the one catalyzed by ${}^t\text{Bu}_3\text{Si}^+$ (Scheme 25), reported by Zhang and Chen.³⁰¹ With a trityl activator loading of 0.05 mol % relative to monomer, the ${}^n\text{BA}$ polymerization at 25 °C in polar noncoordinating (CH_2Cl_2) or nonpolar hydrocarbon (toluene or cyclohexane) solvents using ${}^i\text{BuSKA}$ exhibits exceptionally high activity (completed reaction in <1 min, giving TOF up to 96,000 h^{-1}), efficiency (achieved quantitative I^*), and degree of control (regulated low to high M_n (> 10^5 Da) with narrow MWDs down to 1.07).³⁰¹

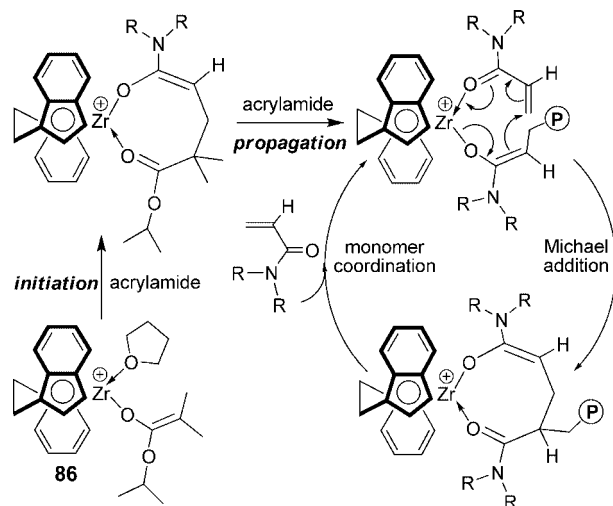
4. Acrylamide and Methacrylamide Polymerization

4.1. Acrylamides

Mariott and Chen reported highly isospecific and controlled polymerization of *N,N*-dimethyl acrylamide (DMAA) using the racemic zirconocenium ester enolate cation **86** under ambient conditions.³⁵² The PDMAA produced has a quantitative isotacticity of *mm* of >99%, a controlled M_n , a narrow MWD of 1.07, and a high T_m of >306 °C (Figure 23). This polymerization is also rapid (0.25 mol % catalyst, 25 min, 96% conversion, TOF = 922 h^{-1}) and proceeds in a living fashion, enabling the synthesis of the well-defined isotactic PMMA-*b*-PDMAA stereodiblock copolymer.³⁵³

Analysis of the MALDI-TOF mass spectrum (Figure 24) of the low-MW PDMAA sample produced by **86** confirms that the polymer has a structural formula of ${}^i\text{PrOC}(=\text{O})\text{-C}(\text{Me}_2)\text{-}(\text{DMAA})_n\text{-H}$, where the initiation chain end [${}^i\text{PrOC}(=\text{O})\text{C}(\text{Me}_2)\text{-}$] is derived from the initiating isopropyl isobutyrate group in complex **86** and the termination chain end (H) from the HCl-acidified methanol during the workup procedure.³⁵³ The kinetic and mechanistic studies show that, as in the methacrylate polymerization with this catalyst, the

Scheme 26. Initiation and Propagation Mechanism for the Coordination–Addition Polymerization of Acrylamides Using Zirconocenium Ester Enolate Cation **86**



propagation is first order in both concentrations of the monomer and the active species and proceeds via a mono-metallic, coordination–addition mechanism through cyclic amide enolate intermediates. The resting state during a propagation “catalysis” cycle is the cyclic amide enolate and associative displacement of the coordinated penultimate amide group by incoming acrylamide monomer to regenerate the active species is the rate-determining step (Scheme 26).³⁵³ This mechanism was further supported by polymerization results using an independently synthesized zirconocenium amide enolate complex that simulates the propagating species.

ansa-Zirconocenium ester enolate catalyst **86** also catalyzes rapid polymerization of bulky *N,N*-diaryl acrylamides under ambient conditions, leading to rigid-rod-like, helical poly(*N,N*-diaryl acrylamide)s.³⁵⁴ However, such catalysts are inactive toward polymerization of *N*-alkyl acrylamides such as *N*-isopropylacrylamide (IPAA), which also cannot be polymerized using common anionic initiators. The problems associated with the polymerization of IPAA by common anionic initiators seem more straightforward because of the acidic amide NH hydrogen present in IPAA. However, in the case of the metallocene catalyst, stoichiometric reaction

monomer	T_p (°C)	TOF (h ⁻¹)	I^* (%)	M_w	PDI	<i>mm</i> (%)
AMAz	25	>6,000	87	1.31×10^4	1.02	
MMAz	25	162	92	2.23×10^4	<1.01	>99
MTMAz	25	94	65	2.51×10^4	1.02	

Figure 25. Methacrylamide Monomers Investigated by DFT and Polymerization Studies³⁶⁰

of **86** with IPAA gives the single IPAA addition product that is stable in CD₂Cl₂ at ambient temperature. Although this single IPAA addition product does not effect further IPAA additions, it rapidly polymerizes DMAA to the corresponding highly isotactic PDMAA.³⁵³

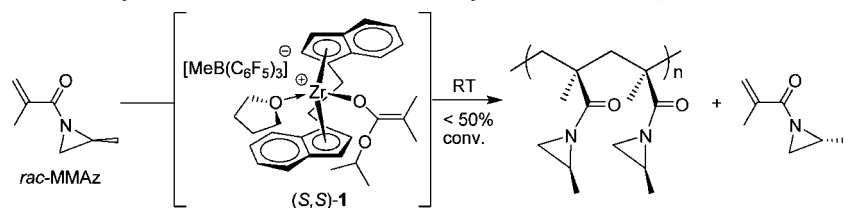
4.2. Methacrylamides

As described above, metallocene catalyst can readily polymerize *acrylamides* such as DMAA in a rapid, stereospecific, and living fashion.^{352–354} An interesting exception here is their inability to polymerize *N,N*-dialkyl *methacrylamides* such as *N,N*-dimethyl methacrylamide (DMMA).³⁵³ The nonpolymerizability of DMMA was previously noted in anionic polymerizations using organolithium initiators,³⁵⁵ which was attributed to a twisted, nonconjugated monomer conformation between the vinyl and carbonyl double bonds, a result of steric repulsions between the α -methyl group or the vinyl proton and the *N*-methyl group of DMMA. As compared to other polymerizable conjugated monomers such as DMAA, this twisted DMMA monomer conformation results in a less effective π overlap between these two functional groups and thus leads to unstable amide enolate intermediates upon nucleophilic attack by the initiator. ¹H and ¹³C NMR studies show that the NMR features (chemical shifts and peak separations) for the vinyl protons and carbonyl carbons of the nonpolymerizable *N,N*-dialkyl methacrylamides more closely resemble those of nonconjugated vinyl monomers than those of polymerizable, conjugated monomers.³⁵⁶ Interestingly, introduction of the highly strained, three-membered aziridine ring into the monomer structure provided a clever solution to the nonpolymerizability of *N,N*-dialkyl methacrylamides. For example, Okamoto and Yuki³⁵⁷ reported in 1981 successful anionic and radical polymerizations of *N*-methacryloylaziridine with ⁿBuLi or PhMgBr at –78 °C and with AIBN, and most recently Ishizone and co-workers^{358,359} reported living anionic polymerization of *N*-methacryloyl-2-methylaziridine (MMAz) with 1,1-diphenyl-3-methylpentyl lithium or diphenylmethyl potassium in the presence of LiCl or Et₂Zn at low temperatures (–78 to –40 °C).

DFT calculations were performed on a series of the monomer structures listed in Figure 25 as part of efforts to systematically rationalize the reactivity of the different methacrylamides.³⁶⁰ To characterize the assumed geometry, the torsional angle θ is defined as the C=C–C=O torsional angle, and the torsional angle ω is defined as the O=C–N–X_C torsional angle, where X_C is the middle point between the two C atoms bonded to the N atom (Figure 25). According to this definition, if the C=C bond and the N atom are conjugated to the C=O bond, then the θ and ω dihedral angles should be close to 0° and 90°, respectively.

According to the DFT calculations, DMAA, MMAz, AMAz, MTMAz, and MMPy assume a substantially planar geometry based on their small θ values (3.4–12.9°), whereas DMMA and MCBz assume a considerably nonplanar geometry, as indicated by their θ values of 131.0° and 137.7°, respectively.³⁶⁰ Moving to the ω angle, it was found that with the exception of MCBz, which presents an ω angle close to 0° for complete absence of conjugation between the N atom and the C=O bond, all the monomers present ω angles deviating considerably from 90°, indicating somewhat limited conjugation of the N lone pair to the C=O bond. Moreover, in AMAz, MMAz, and MTMAz, the *geometric constraint of the three-membered aziridine ring forces an almost sp³ hybridization at the N atom*, which results in remarkably reduced ring strain but imposes a pyramidal geometry at the N atom. Consequently, the lone pair of the N atom is in a sp³ atomic orbital that geometrically cannot overlap properly with π orbitals of the C=O bond in AMAz, MMAz, and MTMAz. However, in terms of monomer geometry, the presence of the aziridine ring pulls the N substituents away from the methacrylic methyl group, *allowing for the monomers to assume a planar geometry* around the θ angle. Hence, the nonpolymerizability of nonplanar DMMA and MCBz via the conjugate-addition mechanism, observed experimentally, is due to poor overlap between the π orbitals of the vinyl C=C and carbonyl C=O bonds. The rest of the monomers exhibit planar, conjugated conformations and are therefore polymerizable. The only exception here is MMPy, which was found not polymerized by catalyst **86** but can be explained by destabilization of the amide–enolate intermediate involved in the chain propagation by having the C=C bond moved into the six-membered ring, which introduces higher ring strain.³⁶⁰

A control run with the acrylamide AMAz (Figure 25) using **86** in CH₂Cl₂ at RT (which was designed to examine whether the reactive aziridine ring incorporated in the predictably polymerizable MMAz would remain intact under the current metallocene polymerization conditions or not) revealed that this polymerization is extremely rapid, achieving quantitative monomer conversion in <1 min with a TOF > 6000 h⁻¹; it also proceeds exclusively via C–C bond formation while leaving the aziridine ring intact.³⁶⁰ The polymer obtained has a M_w of 13.1 kg/mol by LS (light scattering) detector with a narrow MWD of 1.02, giving an I^* of 87%. Hence, the polymerization of AMAz is fast, efficient, and controlled, and it involves no ring-opening of the aziridine ring under the current conditions. Likewise, the polymerization of the methacrylamide MMAz by **86** is effective and controlled (Figure 25), although it is considerably slower than the AMAz polymerization. The polymer produced is highly isotactic (>99% *mm* by ¹³C NMR) and well-defined, with

Scheme 27. Kinetic Resolution Polymerization of Racemic MMAz by Enantiomeric (*S,S*)-**86**

the aziridine ring remaining intact. MTMAz is also readily polymerized by **86** at RT, producing the corresponding polymer with a narrow MWD of 1.02. Kinetic studies of the MMAz polymerization by **86** revealed that this polymerization follows first-order kinetics in both concentrations of monomer and catalyst, thus consistent with a monometallic propagation mechanism involving the fast step of intramolecular conjugate addition within the catalyst–monomer coordination complex leading to the eight-membered-ring resting intermediate (*cf.* Scheme 26). The polymerization of MMAz using *C_s*-ligated titanium alkyl complex (CGC)-TiMe⁺MeB(C₆F₅)₃[−] (**106**) is much slower and less controlled.³⁶⁰

As a racemic monomer, MMAz has been tested for kinetic resolution polymerization using enantiomeric catalyst (*S,S*)-**86**.³⁶⁰ Scheme 27 outlines the strategy using this chiral catalyst to preferentially polymerize one enantiomer from the racemic MMAz feed under ≤50% conversion, potentially leading to the enantiomeric monomer with hopefully appreciable % *ee* and the optically active polymer which predominately incorporates the other enantiomer from the racemic monomer feed. Experimentally, (*S,S*)-**86** showed its limited ability to kinetically resolve MMAz to some extent with a low stereoselectivity factor, or *s* value,³⁶¹ of 1.8,³⁶⁰ presumably due to a rather small methyl group at the remote γ position (with respect to the C=C bond) of the monomer.

DFT calculations explained why the kinetic resolution of MMAz is ineffective although the enantioselectivity of the polymerization was high ($\Delta E^{\ddagger}_{\text{Stereo}}$ of ~3.2 kcal/mol) for the production of highly isotactic polymer.³⁶⁰ Among four possible transition states corresponding to different combinations of the stereoconfiguration on the growing chain and on the monomer, their relative energies indicate that whatever is the configuration of the stereogenic C atom of the aziridine

ring in the growing chain, there is no substantial selectivity in the selection between the two enantiomers of MMAz. In fact, in the case of an *S*-chain, addition of *S*-MMAz is favored by only 0.2 kcal/mol with respect to addition of *R*-MMAz, while, in the case of an *R*-chain, addition of *S*-MMAz is favored by only 0.4 kcal/mol with respect to addition of *R*-MMAz. Although the most stable transition state corresponds to addition of *S*-MMAz to an *S*-chain, it is clear that the small energy differences obtained by DFT calculations are in qualitative agreement with the low kinetic resolution obtained experimentally. The structures of the four transition states, depicted in Figure 26, clearly show that in all cases the methyl group on the aziridine ring can be placed quite far away from the EBI ligand as well as from other atoms of the chain and of the monomer, explaining the low efficiency of the kinetic resolution of MMAz. A potential strategy to substantially enhance the stereoselectivity factor of this kinetic resolution polymerization is to introduce a *trans* alkyl or aryl group on the aziridine ring.

4.3. Asymmetric Polymerization

Enantiomerically pure or enriched stereoregular vinyl polymers³⁶² derived from 1-substituted or nonsymmetric 1,2-disubstituted vinyl monomers (i.e., technologically most important polymers) with configurational main chain chirality and no chiral side groups cannot be optically active because the entire polymer chain—by the infinite chain model—contains a mirror plane (for isotactic polymers) or a glide mirror plane and translational mirror planes perpendicular to the chain axis (for syndiotactic polymers),^{363–370} and thus, they are *cryptochiral*.³⁷¹ Without depending on transitional symmetry operations, assignment of polymer chirality can also be achieved with chemical applications of the $S_{2\infty}$ and C_{∞} point groups to infinite cyclic polymers.³⁷² On the other hand, low MW isotactic oligomers of propylene,³⁷³ 1-butene,³⁷⁴ and other α -olefins³⁷⁵ produced by optically active *ansa*-zirconocene catalysts showed measurable optical activity, but high MW isotactic polypropylene (*it*-PP) produced by the enantiomeric chiral catalyst did not show detectable optical activity in solution or in the melt.³⁷⁶ As a polymer chain becomes long enough, its chain-end groups impose negligible effects on the chiroptical properties of the polymer. Thus, an enantiomerically pure or enriched polymer of low enough MW and containing nonequivalent chain-end groups can be optically active, as shown by the above oligomeric α -olefin examples.

An important strategy that does not rely on chain-end groups or chiral auxiliaries to eliminate reflection elements of symmetry of stereoregular functionalized vinyl polymers is asymmetric anionic polymerization of the vinyl monomers containing bulky side groups (e.g., triarylmethyl methacrylates^{377,378} and *N,N*-diaryl acrylamides^{379–381}) with chiral organolithium initiators, typically carried out at low temperatures (−78 °C or lower), affording optically active polymers with rigid one-

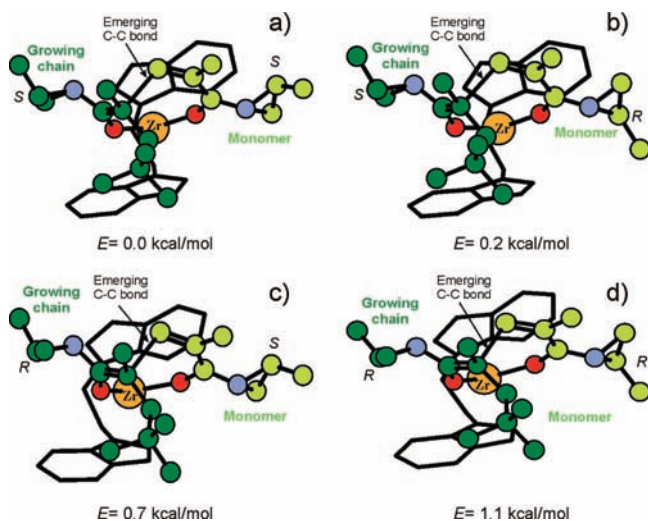


Figure 26. Calculated transition states for the kinetic resolution of MMAz by (*S,S*)-**86**. Reprinted with permission from ref 360. Copyright 2009 American Chemical Society.

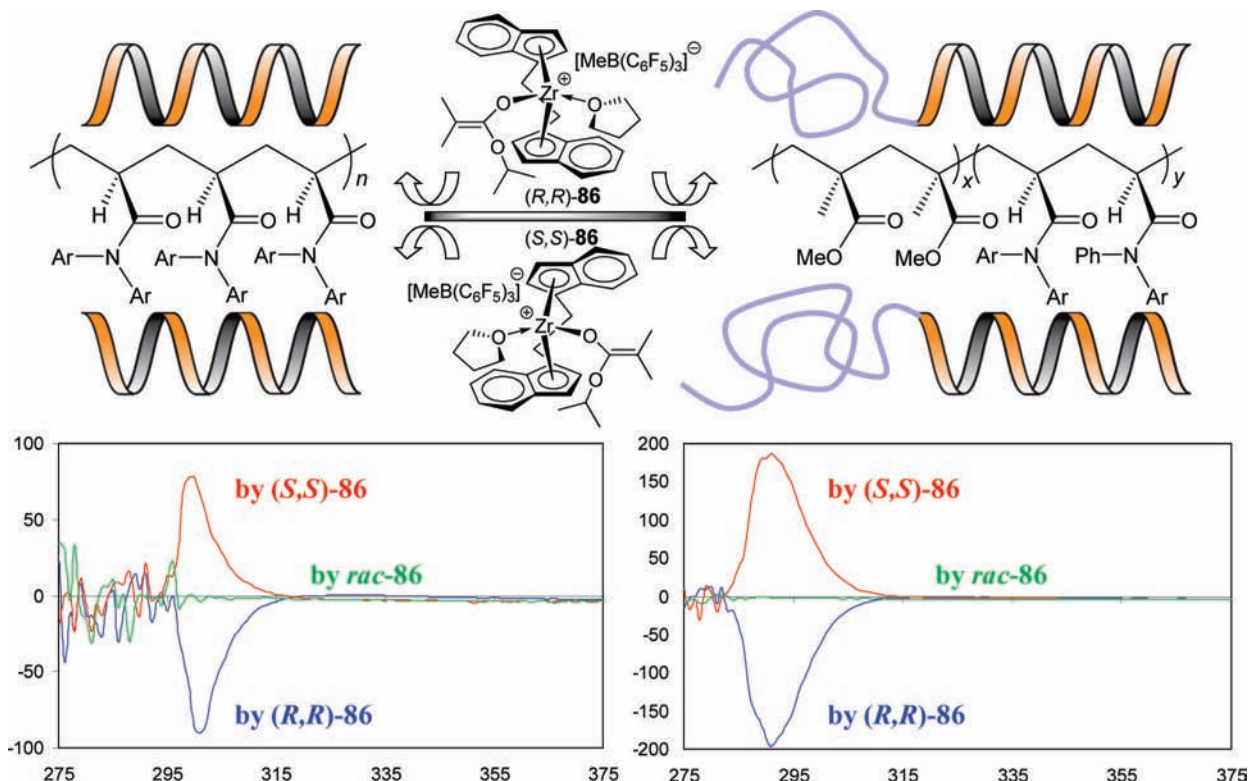


Figure 27. Asymmetric polymerization by enantiomeric catalysts **86** for the synthesis of chiroptical isotactic polar vinyl polymers. Shown on the bottom are the CD spectra of homo- and block copolymers by (*S,S*)-**86** (red), *rac*-**86** (green), and (*R,R*)-**86** (blue). Reprinted with permission from ref 354. Copyright 2007 American Chemical Society.

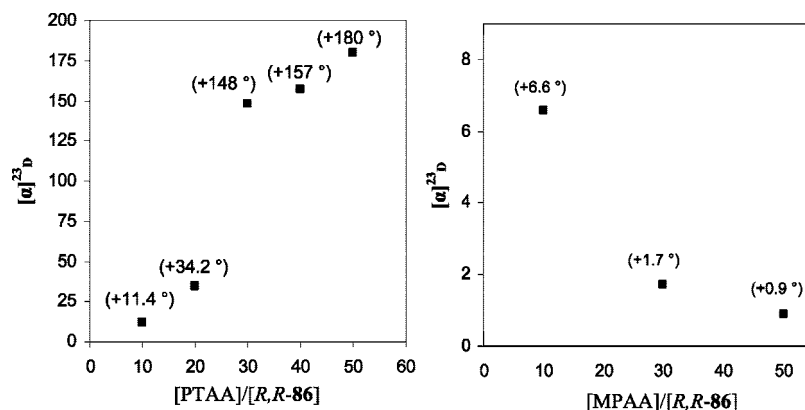


Figure 28. Plots of specific rotation $[\alpha]_D^{23}$ values of rigid-rod-like helical poly(*N*-phenyl-*N*-(4-tolyl) acrylamide) (PPTAA) and random coil poly(*N*-methyl-*N*-phenyl acrylamide) (PMPAA) as a function of monomer-to-catalyst ratios (i.e., the calculated degree of polymerization). Reprinted with permission from ref 395. Copyright 2008 American Chemical Society.

Examination of the *polymerization scope* shows that the formation of optically active poly(acrylamide)s due to solution-stable helical conformations with an excess of one-handed helicity is dictated by the sterics and rigidity of the monomer repeat units; while diaryl acrylamides can readily achieve such conformations, asymmetrically substituted diaryl acrylamides give the chiral polymers with much higher optical activity than the symmetrically substituted ones. Introduction of the long-chain alkyl group to one of the phenyl rings (i.e., *N*-(4-hexylphenyl)-*N*-phenyl acrylamide) not only accomplishes the unsymmetrical substitution but also solves the solubility issue associated with rigid helical homopolymers, enabling direct MW analysis of such polymers by LS/GPC. It is also possible for *N,N*-dialkyl acrylamides to lead to optically active, chiral helical polymers. One such example was identified, with the aid of MM2 modeling, as acryloyl piperidine (APP), a *N,N*-cyclic (CH₂)_n acrylamide (*n* = 5).³⁹⁵

Extensive asymmetric block copolymerization studies of acrylamides with MMA and other methacrylates have also been carried out to produce optically active, flexible random coil–rigid helical stereoblock copolymers.³⁹⁵ It was found that all the high MW acrylamide-*b*-methacrylate stereoblock copolymers produced by the enantiomeric catalysts **86** are optically active, even when the MW of both blocks far exceeds their cryptochiral MW and regardless of whether the acrylamide comonomer employed can render a solution-stable helical conformation or not. On the other hand, all the methacrylate-*b*-methacrylate well-defined stereodiblock or triblock copolymers produced by the enantiomeric catalysts **86** are optically inactive, which is attributable to the similar structures of the methacrylate repeat units placing the first nonequivalent atom between the different methacrylate units too far away from the asymmetric carbon center.

5. Acrylonitrile and Vinyl Ketone Polymerization

5.1. Acrylonitrile

In sharp contrast to trivalent lanthanocenes such as $\text{Cp}^*_2\text{SmMe}(\text{THF})$ and $[\text{Cp}^*_2\text{SmH}]_2$, which are completely inert toward the polymerization of $\text{CH}_2=\text{CHCN}$, divalent nonlanthanocenes $[(\text{Me}_3\text{Si})_3\text{C}]_2\text{Ln}$ ($\text{Ln} = \text{Sm}, \text{Yb}$) exhibit modest activity for AN polymerization.¹³³ Between these two lanthanide complexes, the Sm complex is much more active and reaches 27.5 h^{-1} TOF at $-78 \text{ }^\circ\text{C}$; elevating T_p from -78 to $25 \text{ }^\circ\text{C}$ reduces the polymerization activity, accompanied by a slight drop in M_n (from 2.9×10^4 to 2.6×10^4) and broadened MWD (from 1.38 to 1.68). Lanthanocene alkyl $[(\text{BuC}_5\text{H}_4)_2\text{NdMe}]_2$,³⁹⁶ divalent lanthanide bis(aryloxy) complexes $(\text{BHT})_2\text{Ln}(\text{THF})_n$ ($\text{Ln} = \text{Sm}, \text{Yb}, \text{Eu}$), and divalent samarium complex $(\text{BuCp})_2\text{Sm}(\text{THF})_2$ were also utilized to polymerize AN, yielding atactic PAN.³⁹⁷ Yttrium tris(aryloxy) complex $\text{Y}(\text{BHT})_3$ was also found to exhibit modest activity (TOF = 66 h^{-1}) toward AN polymerization in an *n*-hexane/THF mixture at $50 \text{ }^\circ\text{C}$, producing again colorless atactic polymer (46.6% *mr*).³⁹⁸ However, when polymerization was carried out in DMF, the resulting yellow polymer was syndio-rich (52% *rr*), but no MWD data were given. Half-lanthanocene $\text{Cp}^*\text{La}[\text{CH}(\text{SiMe}_3)_2]_2(\text{THF})$ (**34**) polymerizes AN to atactic PAN (40% *mr*) from -20 to $40 \text{ }^\circ\text{C}$ with modest activity (up to 31 h^{-1} TOF at $40 \text{ }^\circ\text{C}$).¹²⁷ The highest viscosity MW (M_v) was 6.03×10^4 , and MWD was not reported. Yttrocenes $[(\text{Me}_3\text{SiC}_5\text{H}_4)_2\text{YMe}]_2$ and $\text{Cp}^*_2\text{YMe}(\text{THF})$ also give atactic PAN with considerably lower activity (up to only 6 h^{-1} TOF at $40 \text{ }^\circ\text{C}$).¹²⁷ Atactic PAN with a broad MWD (5.4–27) was also prepared by CGC-type yttrium alkyl (**124**) and hydrido (**125**) complexes (up to only 5 h^{-1} TOF at $25 \text{ }^\circ\text{C}$).³⁴⁴

Lanthanoid(III) thiolate complexes, such as $\text{Ln}(\text{SPh})_3$ [$(\text{Me}_2\text{N})_3\text{P}$] ($\text{Ln} = \text{Sm}, \text{Eu}, \text{Yb}$) and $\text{Ln}(\text{SAr})_3(\text{py})_3$ ($\text{Ln} = \text{Sm}, \text{Yb}$; $\text{Ar} = 2,4,6\text{-}i\text{-Pr}_2\text{C}_6\text{H}_2$), were employed for polymerization of AN at $-78 \text{ }^\circ\text{C}$ in THF, producing atactic polymer (41–45% *mr*, 2.6–3.4 PDI).³⁹⁹ The most active complex in this series is $\text{Yb}(\text{SAr})_3(\text{py})_3$, with a TOF of 81 h^{-1} , but $\text{Sm}(\text{SPh})_3[(\text{Me}_2\text{N})_3\text{P}]_3$ produces the polymer with the highest M_n (2.58×10^5) with the same $[\text{AN}]/[\text{Ln}]$ ratio of 100, thus giving rise to extremely low I^* . Trivalent lanthanide bis(amido) complexes supported by a β -diketiminato $[\text{N}_2^-]$ ligand, $[(2,6\text{-Me}_2\text{C}_6\text{H}_3)\text{N}(\text{C}(\text{Me})\text{CHC}(\text{Me})\text{N}(2,6\text{-Me}_2\text{C}_6\text{H}_3))]_2\text{Ln}(\text{NPh}_2)(\text{THF})$ ($\text{Ln} = \text{Yb}, \text{Nd}$), are highly active for AN polymerization at 0 or $25 \text{ }^\circ\text{C}$, with the highest TOF reaching 510 h^{-1} at $25 \text{ }^\circ\text{C}$ in DME.⁴⁰⁰ The polymerization activity in polar solvents such as DME and THF is noticeably higher than that carried out in toluene, but the polymer tacticity remained essentially the same (i.e., atactic PAN with 41–46% *mr*); no MWD data were reported.

Besides the above lanthanide complexes, a large number of other metal complexes have been reported to be active for the polymerization of AN via nonradical or conventional anionic processes, including group 4 metal tetrakisamides $\text{M}(\text{NMe}_2)_4$ [$\text{M} = \text{Ti}, \text{Zr}, \text{Hf}$; in hydrocarbon solvent at -78 or $20.5 \text{ }^\circ\text{C}$ with activity following an order of $\text{Hf} \sim \text{Zr} > \text{Ti}$; $\text{M}(\text{NMe}_2)_4 > \text{Cp}_2\text{M}(\text{NMe}_2)_2$],⁴⁰¹ tetraaziridotitanium (which was derived from the reaction of $\text{Ti}(\text{NMe}_2)_4$ with aziridine; the polymerization was much more rapid than that by $\text{Ti}(\text{NMe}_2)_4$),⁴⁰² bis(amido)chromium(IV) dibenzyl complexes $(\text{BuN})_2\text{Cr}(\text{CH}_2\text{Ph})_2$ and $(\text{NCMe}_2\text{CH}_2\text{CH}_2\text{CMe}_2\text{N})_2\text{Cr}(\text{CH}_2\text{Ph})_2$ (which was carried out in toluene at $20 \text{ }^\circ\text{C}$ in the dark to exclude radical formation; M_n up to 4.64×10^5 , PDI =

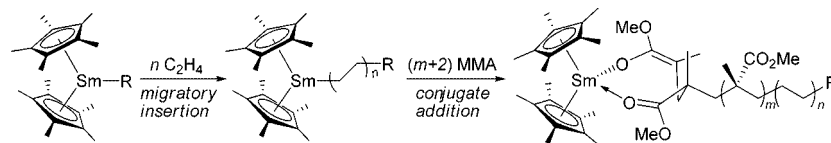
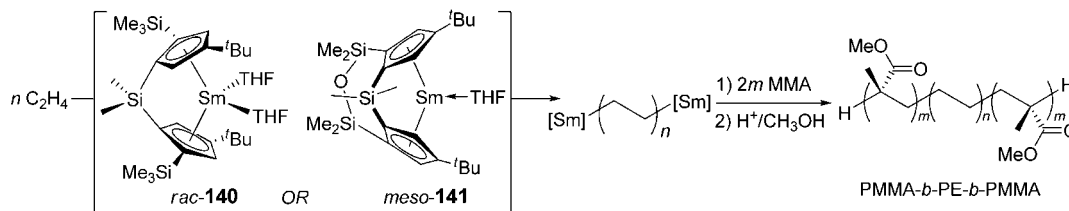
2.8; atactic PAN with 45–52% *mr*, also for copolymerization of AN and MMA),⁴⁰³ $\text{Co}(\text{acac})_2/\text{AlEt}_3$ ($50 \text{ }^\circ\text{C}$, benzene, for copolymerization of AN with styrene),⁴⁰⁴ $[\text{Co}(\text{dpa})_2(\text{CH}_3)_2]\text{I}$ ($\text{dpa} = \text{di-2-pyridylamine}$, room temperature, in neat AN; $\text{Co}(\text{dpa})_2\text{R}$ was suggested to be the actual catalytic species to proceed with a coordination insertion mechanism),⁴⁰⁵ $\text{CH}_3\text{C}(\text{CH}_2\text{PPh}_2)_3\text{Co}(\text{BH}_4)$ ($20 \text{ }^\circ\text{C}$, DMF, TOF = 21 h^{-1} , $M_n = 5.2 \times 10^5$, $I^* = 5.2\%$, 48% *mr*),⁴⁰⁶ $\text{CpCo}(\text{PPh}_3)_2\text{I}-\text{AlEt}_3$ (DMF, room temperature, TOF = 16 h^{-1} , $M_n = 5.6 \times 10^3$, PDI = 2.2, 200 equiv of AlEt_3 as activator, also active for MMA polymerization, and no activity with the Co complex alone),⁴⁰⁷ $\text{CpCu}(\text{tBuNC})$ ($0 \text{ }^\circ\text{C}$, DMF, requiring a small amount of tBuNC , PPh_3 , or $\text{P}(\text{OMe})_3$ for activation),⁴⁰⁸ and especially the systems developed by Yamamoto and co-workers^{409,410} based on the neutral metal alkyl complexes Cy_3PCuMe (**135**),^{411,412} $(\text{bipy})_2\text{FeEt}_2$ (**136**, $\text{bipy} = 2,2'\text{-bipyridine}$),^{413–416} and $(\text{bipy})_2\text{CoEt}$.⁴¹⁶ However, coordination insertion mechanisms claimed in many cases have been later questioned through recent, more detailed mechanistic studies. For example, Jordan and co-workers examined AN polymerizations by **135** and **136** and found that the major initiator in the anionic AN polymerization by **135** is actually PCy_3 liberated from the Cu complex; they also proposed a transient iron hydride complex $[\text{Fe}]-\text{H}$ formed by β -H elimination of **136** is responsible for initiating the anionic AN polymerization.⁴¹⁷ Baird and co-workers also presented evidence for radical polymerization of AN by complex **136**.⁴¹⁸

Jordan and co-workers have also investigated in detail the insertion reactions of AN with palladium(II) methyl cations supported by a series of chelating $[\text{N},\text{N}]$ ligands, “ L_2PdMe^+ ”.⁴¹⁹ The results of that study show that the *N*-bound adduct $\text{L}_2\text{PdMe}(\text{AN})^+$ undergoes 2.1-AN insertion to yield $\text{L}_2\text{Pd}\{\text{CH}(\text{CN})\text{CH}_2\text{Me}\}^+$; however, most important obstacles to insertion polymerization or copolymerization of AN using L_2PdR^+ catalysts are the tendency of $\text{L}_2\text{Pd}\{\text{CH}(\text{CN})\text{CH}_2\text{R}\}^+$ species to *aggregate*, which competes with monomer coordination, and the low insertion reactivity of $\text{L}_2\text{Pd}\{\text{CH}(\text{CN})\text{CH}_2\text{R}\}(\text{substrate})^+$ species. Similar schemes were observed for L_2PdMe^+ supported by chelating $[\text{P},\text{P}]$ diphosphine ligands, thus precluding AN polymerization or copolymerization by these systems.⁴²⁰ In a parallel study, Piers and co-workers have examined the reactions of AN with neutral and anionic Pd(II) methyl complexes of general formula $\text{LPdMe}(\text{NCCH}_3)$, where L is a bulky phenoxydiazene $[\text{O}^-,\text{N}]$ or phenoxyaldimine $[\text{O}^-,\text{N}]$ ligand.⁴²¹ Their results show that such complexes react with an excess of AN to give the products of 2.1-insertion into the Pd–Me bond, yielding dimers and/or trimers which feature bridging α -cyano groups.

5.2. Vinyl Ketones

Anionic polymerization of vinyl ketones⁴²² such as methyl vinyl ketone (MVK) by organometallic reagents (e.g., CaZnEt_4 and PhMgBr) at 0 to $-70 \text{ }^\circ\text{C}$ over one to several days afforded crystalline stereoregular polymers that have T_m about $160 \text{ }^\circ\text{C}$ and can easily form spherulites.⁴²³ The crystalline polymer was characterized to be isotactic with *m* dyads up to 90% (by Et_2Zn at $-38 \text{ }^\circ\text{C}$ for 58 days) analyzed by ^1H NMR⁴²⁴ or with 72% *m* (by Et_2Zn at $0 \text{ }^\circ\text{C}$ for 3 days) analyzed by ^{13}C NMR.⁴²⁵ Extremely rapid (reaction in seconds) polymerization of MVK was achieved using organocuprates at $-78 \text{ }^\circ\text{C}$, but the polymerization was uncontrolled, producing a low MW polymer.⁴²⁶

Scheme 29. Mechanistic Crossover in E and MMA Block Copolymerization by Lanthanocenes

Scheme 30. Synthesis of PMMA-*b*-PE-*b*-PMMA Triblock Copolymers by *ansa*-Samarocenes

Erker and co-workers reported that discrete group 4 metallocene bis(enolate)s $\text{Cp}_2\text{M}[\text{OC}(\text{Me})=\text{CH}_2]_2$ ($\text{M} = \text{Ti}, \text{Zr}, \text{Hf}$), in combination with one to many equivalents of strong Lewis acid $\text{B}(\text{C}_6\text{F}_5)_3$, is highly active for polymerization of MVK, producing atactic polymer with PDI ranging from 1.3 to 1.6.⁴²⁷ The polymerization activity increases with an increase in the borane-to-metallocene ratio, reaching a high TOF of 8160 h^{-1} at RT in CH_2Cl_2 when $\text{M} = \text{Ti}$ and the ratio = 4. This polymerization system is uncontrolled due to the presence of chain transfer and termination side reactions. The authors proposed an activated-monomer mechanism, similar to the bimetallic mechanism proposed by Collins for the MMA polymerization using the $\text{Cp}_2\text{ZrMe}[\text{OC}(\text{O}^t\text{Bu})=\text{CMe}_2]/[\text{Cp}_2\text{ZrMe}(\text{THF})]^+[\text{BPh}_4]^-$ pair:¹⁶¹ the metallocene bis(enolate) serves as initiator and the borane as catalyst (instead of the zirconocenium cation) in this MVK polymerization. A particularly interesting feature about this system is that even though $\text{B}(\text{C}_6\text{F}_5)_3$ cleanly undergoes electrophilic addition to the nucleophilic enolate α -carbon to form the corresponding mono- or bis-adducts, this adduct formation does not lead to an annihilation of the nucleophilic and electrophilic properties of these two components by means of equilibration processes, at least in the case of MVK polymerization.⁴²⁷

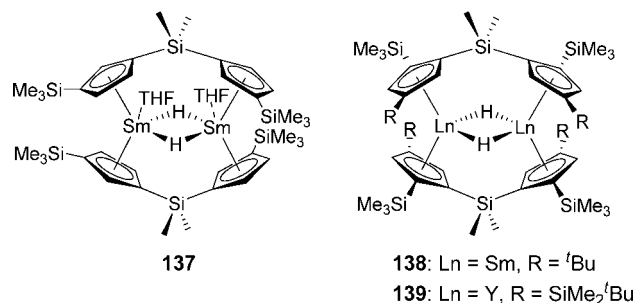
6. Copolymerization

6.1. Polar–Nonpolar Block Copolymers

Owing to the living nature of both ethylene (E) and (meth)acrylate homopolymerizations catalyzed by lanthanocenes such as $\text{Cp}^*_2\text{SmMe}(\text{THF})$ and $[\text{Cp}^*_2\text{SmH}]_2$, controlled block copolymerizations of E and (meth)acrylates were achieved using such lanthanocenes via a two-step polymerization procedure starting with E polymerization under mild conditions (20°C , 1 atm pressure, toluene) followed by addition of a polar monomer such as MMA (Scheme 29).⁴²⁸ The E to MMA molar ratio in the resulting block copolymer can be controlled on demand in the range of 100:1 to 100:103 when M_n of the initial PE was fixed to ca. 10,300, but when a higher initial M_n of the PE block exceeds 12,000, the relative ratio of the PMMA block decreases significantly due to precipitation of PE fine particles, which was assumed to encapsulate the active sites. Repeated fractionation of the copolymer product with hot THF did not alter these block ratios, arguing none to negligible amount of homopolymer PMMA formation (no homopolymer PE peak was observed either in the unimodal

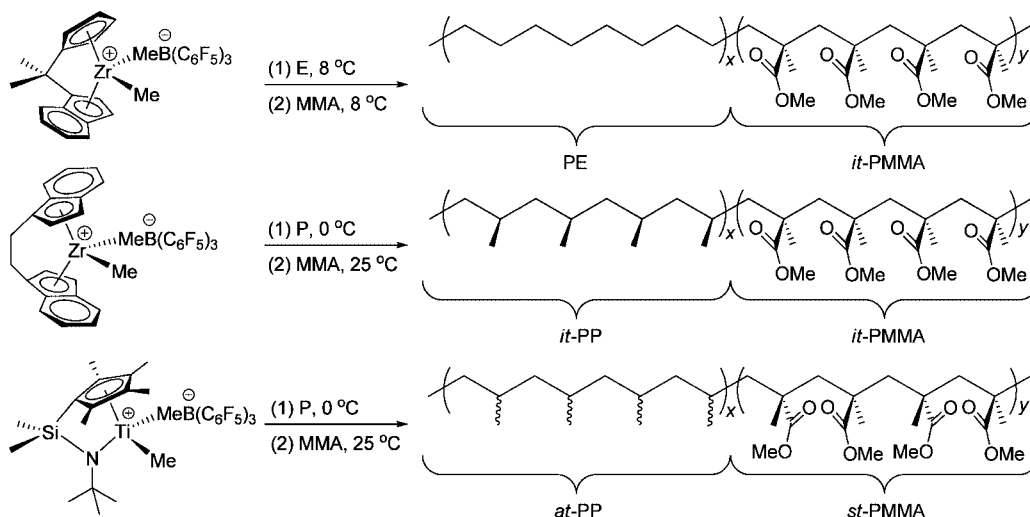
GPC trace (PDI = 1.37–1.90) of the products). This two-step block copolymerization procedure was also successfully applied to the block copolymerization of E with acrylates such as MA and EA. However, it should be pointed out that this block copolymerization is only one-directional with a mechanistic crossover from coordination insertion polymerization of E to coordination–addition polymerization of polar monomers, but it cannot be carried out in a reversed procedure because the olefin cannot insert into the $\text{Sm}-\text{O}(\text{enolate})$ bond if a polar monomer is polymerized before E.

Half-metallocene-type lanthanum complex $\text{Cp}^*\text{La}[\text{CH}(\text{SiMe}_3)_2]_2(\text{THF})$ (**34**)¹²⁷ and nondiscrete neodymium alkoxide complexes⁴²⁹ were also employed for block copolymerization of E and MMA. A binuclear samarocene hydride $[\text{Me}_2\text{Si}(\text{C}_5\text{H}_3)_2\text{SmH}(\text{THF})]_2$ (**137**) obtained from hydrogenation of the *ansa*-samarocene hydrocarbyl precursor $\text{Me}_2\text{Si}(\text{C}_5\text{H}_3)_2\text{SmCH}(\text{SiMe}_3)_2(\text{THF})$ (which was ineffective for E or P polymerization) was utilized for the synthesis of PE-*b*-PMMA ($M_n = 6-7 \times 10^4$, PDI = 1.67–1.69).⁴³⁰ The same two-step polymerization procedure was used to prepare block copolymers of higher α -olefins, $\text{CH}_2=\text{CHR}$ ($\text{R} = ^i\text{Pr}, ^i\text{Bu}$), with MMA, using binuclear hydrido samarocene (**138**) and yttrocene (**139**) complexes.⁴³¹ The yttrium catalyst is much more reactive than the samarium catalyst in the α -olefin polymerization step; the mol % of the PMMA block ranges from 48% to 64%, and the PDI of the block copolymer is between 1.41 and 2.15. Silicon surface functionalization has been achieved with PE-*b*-PMMA block copolymer brushes using the surface-bound samarocene catalyst in a two-step block copolymerization procedure.⁴³²



The synthesis of ABA-type E and MMA triblock copolymers was accomplished using divalent *ansa*-samarocene complexes *rac*-**140** or *meso*-**141** (Scheme 30), via a two-step polymerization procedure starting with polymerization of E at RT.⁴³³ The resulting triblock copolymers were treated with CHCl_3 to remove the PMMA homopolymer contaminate

Scheme 31. Olefin-MMA Diblock Copolymers Produced by Group 4 Metallocene Catalysts



and dissolved in 1,2,4-trichlorobenzene, followed by reprecipitation in a large excess of toluene; this purification procedure was repeated three times, and the purified triblock copolymers were characterized by NMR, GPC, and TEM for the block copolymer composition, MW and MWD, and morphology, respectively. The PMMA-*b*-PE-*b*-PMMA triblock copolymers produced have PDI values between 1.4 and 4.2, and the mol % of the PMMA block ranging from 5% to 35%, and the values are controlled by polymerization time. The ABA triblock copolymer shows higher break stress and tensile modulus as compared with its corresponding polymer blend.⁴³³

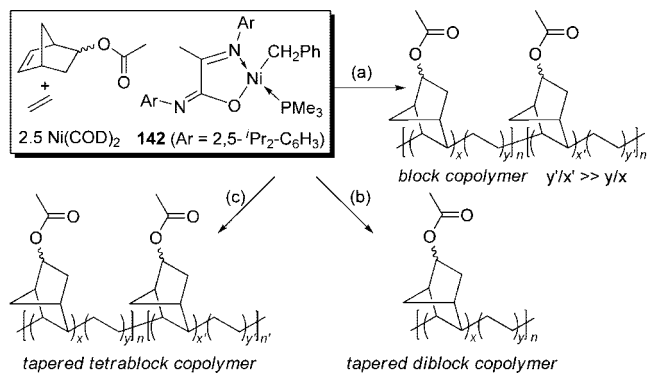
Block copolymerization of E and MMA was also achieved using a C_1 -symmetric group 4 metallocene catalyst, $\text{Me}_2(\text{Cp})(\text{Ind})\text{ZrMe}^+\text{MeB}(\text{C}_6\text{F}_5)_3^-$, by sequential addition of the monomers, starting E at 8 °C (Scheme 31).⁵⁶ The relative content of PE and PMMA in the resulting PE-*b*-PMMA block copolymer varied approximately with the length of time interval allowed for E polymerization, and the evidence obtained from characterizations using GPC (unimodality with PDI ranging between 2.4 and 2.6), NMR (existence of both PE and PMMA blocks), and solubility tests (solvent fractionation) is consistent with formation of block copolymer, rather than a polymer blend. However, this type of copolymerization is also only one directional due to mechanistic incompatibility (i.e., migratory insertion in olefin polymerization vs conjugate addition in MMA polymerization); thus, either a block copolymerization procedure by starting the MMA polymerization first or a statistical copolymerization procedure by polymerizing E and MMA simultaneously results in the formation of only the PMMA homopolymer. The block copolymer PE-*b*-PMMA ($M_w = 3.17\text{--}4.94 \times 10^4$, PDI = 2.10–2.20) has also been obtained through cascade polymerization procedures involving metallocene-catalyzed coordination copolymerization of E and allyl alcohol masked by trialkylaluminum to produce the hydroxyl-terminated PE, PE-*t*-OH,⁴³⁴ which was subsequently treated with 2-bromoisobutyryl bromide to generate a macroinitiator, PE-*t*-Br, for atom transfer radical polymerization (ATRP) of MMA.⁴³⁵ Similarly, block copolymers of E with ⁿBA and MMA were produced by initial E polymerization with a nonmetallocene catalyst incorporating the phenoxyimine ligand to afford vinyl-terminated PE (PE-*t*-CH=CH₂) of low MW ($M_n = 1.80 \times 10^3$, PDI = 1.70), which was treated with α -bromoisobutyric acid to give the corresponding macroinitiator for ATRP

of the subsequent step; with this procedure, PE-*b*-PMMA having $M_n = 1.06 \times 10^4$ and PDI = 1.59 as well as PE-*b*-P(ⁿBA) having $M_n = 2.97 \times 10^4$ and PDI = 1.35 have been synthesized.⁴³⁶ More defined block copolymers (PDI = 1.16) of E with ⁿBA and ^tBA were later obtained by coupling of degenerative transfer coordination polymerization of E with ATRP.⁴³⁷ A cationic α -diimine Pd(II) catalyst has also been used to produce branched PE, end-functionalized with 2-bromoisobutyrate, for subsequent ATRP of ⁿBA.⁴³⁸

A diblock copolymer of propylene (P) and MMA was synthesized by Doi and co-workers using a coordination catalyst system consisting of $\text{V}(\text{acac})_3/\text{AlEt}_2\text{Cl}$.⁴³⁹ Propylene was first polymerized at -78 °C in a living fashion, followed by addition of MMA; the polymerization temperature was subsequently raised to 25 °C to promote the transformation of the living PP chain end to a radical end for construction of the PMMA block. A tandem approach of metallocene-mediated polymerization of P to low MW, vinyl-terminated PP (32% *mm*), followed by subsequent conversion to a macroinitiator incorporating 2-bromoisobutyrate for ATRP of MMA, afforded well-defined diblock copolymer PP-*b*-PMMA with $M_n = 2.22 \times 10^4$ and PDI = 1.14 (after removal of the PP homopolymer by solvent extraction).⁴⁴⁰ Highly isotactic (95% *mm*) PP-*b*-PMMA block copolymer was synthesized utilizing the similar tandem approach, first polymerizing P by a C_2 -symmetric metallocene catalyst system, $\text{rac-Me}_2\text{Si}[2\text{-Me-4-Naph-Ind}]_2\text{ZrCl}_2/\text{MAO}$, to give hydroxyl-terminated isotactic PP, *it*-PP-*t*-OH (M_n up to 6.08×10^4 and PDI = 2.30), followed by its conversion to a macroinitiator bearing 2-bromoisobutyrate for ATRP of MMA.⁴⁴¹ In this context, the C_2 -symmetric metallocene catalyst system, $\text{Me}_2\text{C}(\text{Cp})(\text{Flu})\text{ZrCl}_2/\text{MAO}$, was employed to generate aluminum alkoxy-terminated syndiotactic PP, *st*-PP-*t*-OAlEt₂ (a three-step procedure involving chain transfer of *st*-PP to triethylaluminum forming *st*-PP-*t*-AlEt₂, oxidation/hydrolysis to *st*-PP-*t*-OH, and recapping with triethylaluminum), which serves as a macroinitiator for ring-opening polymerization of cyclic esters including ϵ -caprolactone and D,L-lactide, yielding the final block copolymers of *it*-PP and polyesters.⁴⁴²

Stereoblock copolymerization of P and MMA using group 4 metallocene catalysts produces PP-*b*-PMMA stereodiblock copolymers (Scheme 31).⁵⁷ Specifically, $\text{rac}(\text{EBI})\text{-ZrMe}^+\text{MeB}(\text{C}_6\text{F}_5)_3^-$ yields *it*-PP-*b*-*it*-PMMA stereodiblock copolymer, whereas $(\text{CGC})\text{TiMe}^+\text{MeB}(\text{C}_6\text{F}_5)_3^-$ affords *at*-

Scheme 32. Syntheses of Block and Tapered Block Copolymers of E and Functionalized Norbornene by Ni(II) Catalysts



PP-*b-st*-PMMA stereodiblock copolymer. In the copolymerization catalyzed by the C_2 -symmetric catalyst, a small amount of the PMMA homopolymer formed can be easily removed from the copolymer by extracting the bulk polymer product with boiling methylene chloride; however, separation of the *it*-PP homopolymer, formed possibly in various weight fractions, from the copolymer product proves very difficult due to very similar solubility between the diblock copolymer and *it*-PP in various high-boiling chlorinated solvents. On the other hand, in the copolymerization catalyzed by the C_s -symmetric catalyst, both PMMA and *at*-PP formed in small weight fractions during the copolymerization can be successfully removed from the predominant copolymer product by solvent extraction using boiling *n*-heptane. After successful removal of both homopolymers, for example, the *at*-PP-*b-st*-PMMA diblock copolymer has $M_n = 21,100$, MWD = 1.08, MMA incorporation = 33.8 mol %, and syndiotacticity (for the PMMA block) = 80% *rr*. Furthermore, the comonomer composition in the copolymer can be controlled by the P polymerization time and the MMA conversion. A pronounced activator effect was observed when the same C_s -symmetric catalyst precursor, (CGC)TiMe₂, was activated with $[\text{Ph}_3\text{C}][\text{B}(\text{C}_6\text{F}_5)_4]$, as in this case, homopolymers were formed as major products.⁵⁷

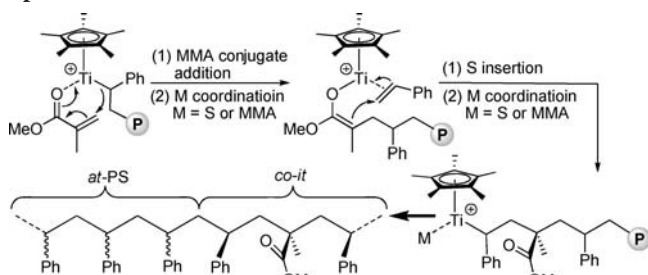
Bazan and co-workers synthesized several interesting types of block copolymers of E with a functionalized norbornene monomer, 5-norbornene-2-yl acetate (NBEA), using a Ni(II) imino-propanamide complex $[\text{N},\text{O}^-]\text{Ni}(\text{PMe}_3)\text{CH}_2\text{Ph}$ (**142**, Scheme 32), in combination with 2.5 equiv of $\text{Ni}(\text{COD})_2$. First, the E pressure (P_E)-jump technique led to the synthesis of block-type copolymers containing segments with different molar ratios of E and NBEA (i.e., an amorphous copolymer with ~25 mol % of NBEA at $P_E = 50$ psi and a semicrystalline copolymer with 1–2 mol % of NBEA at $P_E = 1100$ psi); the two blocks are sufficiently different in molecular composition to induce microphase separation (a, Scheme 32).⁴⁴³ Second, a one-pot semibatch copolymerization in which E is continuously added while NBEA is allowed to gradually deplete by its incorporation into the polymer chain afforded tapered block copolymers (b, Scheme 32); these tapered polymers form ordered microphase-separated morphologies where the phase morphology is modulated by the polymer chain length.⁴⁴⁴ Third, pseudotetrablock copolymers of E and NBEA were constructed by a two-step copolymerization sequence; the copolymerization for t_1 under a constant P_E gave the tapered block copolymer (from the amorphous, NBEA-rich domain to the semicrystalline, E-rich domain), and addition of a second feed of

NBEA at t_1 repeated the above process for t_2 , giving rise to the formation of a tapered E/NBEA copolymer containing amorphous–semicrystalline–amorphous–semicrystalline regions: a pseudotetrablock copolymer (c, Scheme 32).⁴⁴⁵ Most recently, the same group utilized this catalyst system for copolymerization of ethylene and 5-norbornene-2-yl-2'-bromo-2'-methyl propanoate to first generate PE macroinitiators carrying the 2-bromoisobutyral group attached to the norbornene units, followed by grafting MMA units through ATRP, affording the semicrystalline graft copolymer PE-*g*-PMMA.⁴⁴⁶

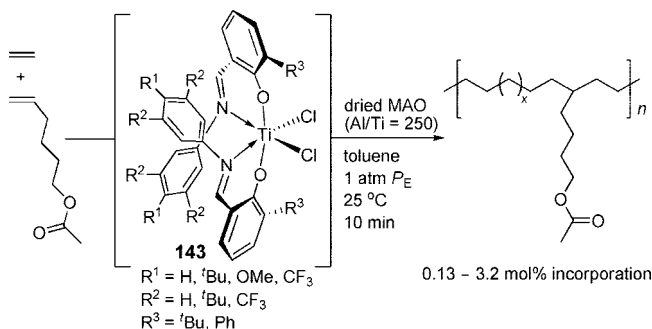
6.2. Polar–Nonpolar Random Copolymers

Reports on direct copolymerizations of olefins and (meth)acrylates by divalent metal complexes of groups 8–11 in combination with a large excess of MAO were already included in section 2.4.4 while describing homopolymerization of methacrylates by such catalyst systems. As commented there, it is likely that in most of those cases the homopolymer or copolymer products were produced by radical mechanisms or with “protected monomer” modes, but those systems have not been examined in detail from a mechanistic point of view. The role of the excess MAO present in such systems can be multifunctional, including (a) alkylation and subsequent activation of the catalyst precursor to cationic active species (the assumed main function), (b) electronic protection of functional groups of the polar monomer via complexation (the often overlooked function), (c) as scavenger for protic and oxygen impurities present in the system, (d) as catalyst for polymerization of the polar monomer (either in its original form or modified structures due to its reaction with the impurities), and (e) possible promotion of redox reactions at the metal center. In light of the above listed potential complications, rigorously classifying such processes, when a large excess of MAO or aluminum alkyls is employed as activators or scavengers, coordination–insertion polymerization or direct copolymerization using “unprotected” (or noncomplexed) polar vinyl comonomers requires presentation of several levels of collaborative evidence (see section 2.4.4). In this context, readers can find early examples of clearly demonstrated coordination–insertion olefin and polar vinyl monomer copolymerizations reviewed in 2000 by Boffa and Novak⁵⁸ and by Ittel, Johnson, and Brookhart;³¹ consequently, this section focuses on coordination–insertion copolymerization examples since those two reviews.

Regarding the *polar group protecting* strategy employed in random copolymerization, Marques and Chien utilized alkylaluminum species to passivate polar monomers, thus enabling their copolymerization with E using early⁴⁴⁷ or late^{448–450} metal-catalyzed polymerization processes. Similar strategies have been applied to copolymerization of tetradecene-1 or octane-1 with silyl-protected 10-undecene-1-ol by a C_s -symmetric hafnocene catalyst⁴⁵¹ as well as to copolymerizations of E with trialkylaluminum-protected 10-undecene-1-ol, 10-undecenoic acid, and 5-hexene-1-ol, by bis(phenoxyimino)zirconium (and titanium) dichloride,⁴⁵² α -diimine nickel complexes,⁴⁵³ both activated with MAO, and α -iminocarboxamide nickel complexes,⁴⁵⁴ activated with trimethylaluminum. Copolymerization of E with 2,7-octadienyl methyl ether by the zirconocene/MAO or (α -diimine)nickel/MAO catalyst system also requires the use of a stoichiometric amount of triisobutylaluminum (TIBA) to protect the polar comonomer.⁴⁵⁵

Scheme 33. Random Copolymerization of MMA with Styrene Catalyzed by Low-Valent, Half-Sandwich Titanium Species


As the scope of the polar vinyl monomers covered in this review is limited to those vinyl monomers bearing hard-base O, N functional groups (i.e., methacrylates, acrylates, acrylamides, methacrylamides, vinyl ketones, and acrylonitrile), olefin copolymerization with vinyl monomers functionalized with *metalloids* (e.g., Si), which are weakly interacting toward hard acid catalysts, is not reviewed in detail herein, but key recent examples of copolymerizations of E with *silylate vinyl monomers* are described as follows. Amin and Marks showed that alkenylsilanes of varying chain lengths, $\text{CH}_2=\text{CH}(\text{CH}_2)_n\text{SiH}_3$ ($n = 1, 2, 4, 6$), serve as simultaneous CTRs and comonomers in the E polymerization by *ansa*-half titanocenes such as $(\text{CGC})\text{TiMe}_2$, activated with $[\text{Ph}_3\text{C}][\text{B}(\text{C}_6\text{F}_5)_4]$, thereby producing PE with both in-chain and chain-end alkenylsilane units.^{456,457} Nomura and co-workers reported that unbridged-half titanocenes, such as $\text{Cp}'\text{TiCl}_2(\text{O}-2,6\text{-}i\text{Pr}_2\text{C}_6\text{H}_3)$ ($\text{Cp}' = \text{Cp}^*, \text{}^i\text{BuC}_5\text{H}_4$) and $\text{Cp}'\text{TiCl}_2$ ($\text{N} = \text{C}^i\text{Bu}_2$) ($\text{Cp}' = \text{Cp}^*, \text{Cp}$), upon activation with excess MAO, copolymerize E with allyltrialkylsilanes $\text{CH}_2=\text{CHCH}_2\text{SiR}_3$ ($\text{R} = \text{Me}, \text{}^i\text{Pr}$), leading to high MW copolymers ($M_n = 10^4\text{--}10^5$) with the silane incorporation up to ~ 60 mol %.⁴⁵⁸ An earlier work reported a much lower level of allylsilane incorporation (up to ~ 24 mol %) in E copolymerization using *rac*-(EBI)ZrCl₂/MAO.⁴⁵⁹ The Nomura group also demonstrated the ability of their unbridged-half titanocene catalysts to copolymerize E with vinyltrialkylsilanes $\text{CH}_2=\text{CHSiR}_3$ ($\text{R} = \text{Me}, \text{Et}$), leading to high MW copolymers with the silane incorporation up to ~ 20 mol %.⁴⁶⁰ Interestingly, the copolymerization with *tert*-butylethylene $\text{CH}_2=\text{CHCMe}_3$ gives PE with a negligible amount of comonomer incorporation. Homopolymerization of allylsilanes using C_2 -symmetric, C_s -symmetric, and enantiomeric C_2 -symmetric *ansa*-zirconocene catalysts has resulted in the formation of isotactic,⁴⁶¹ syndiotactic,⁴⁶¹ and optically active⁴⁶² poly(allylsilanes), respectively. Another class of silicon-containing vinyl monomers that can be readily copolymerized with α -olefins by metallocene catalysts is polyhedral oligomeric silsesquioxane (POSS)-based vinyl monomers, including the following: copolymerizations of E and P with POSS-vinyl monomers by *rac*-(EBI)ZrCl₂/MAO afford PE⁴⁶³ and PP⁴⁶⁴ with up to 0.62 mol % (16 wt %) and 2.6 mol % (35 wt %) POSS incorporation, respectively; an early work also investigated copolymerization of E and P with POSS-vinyl monomers by $\text{Cp}_2\text{ZrCl}_2/\text{MAO}$, *rac*-(SBI)ZrCl₂/MAO, and (CGC)TiCl₂/MAO;⁴⁶⁵ copolymerizations of E and P with a norbornylene-substituted POSS by *rac*-(EBI)ZrCl₂/MAO produces PE and *it*-PP with up to 3.4 mol % and 10.4 mol % POSS incorporation, respectively;⁴⁶⁶ terpolymerizations of E, P, and POSS-norbornenes by *rac*-(EBI)HfCl₂/MAO give E-P-POSS (up to 2.0 mol %) thermoplastic elastomers;⁴⁶⁷ copolymerization of styrene with styryl-POSS by $\text{Cp}^*\text{TiCl}_3/\text{MAO}$ ⁴⁶⁸ or

Scheme 34. Copolymerization of E with 5-Hexene-1-ylacetate by Phenoxyimine Ti Catalysts


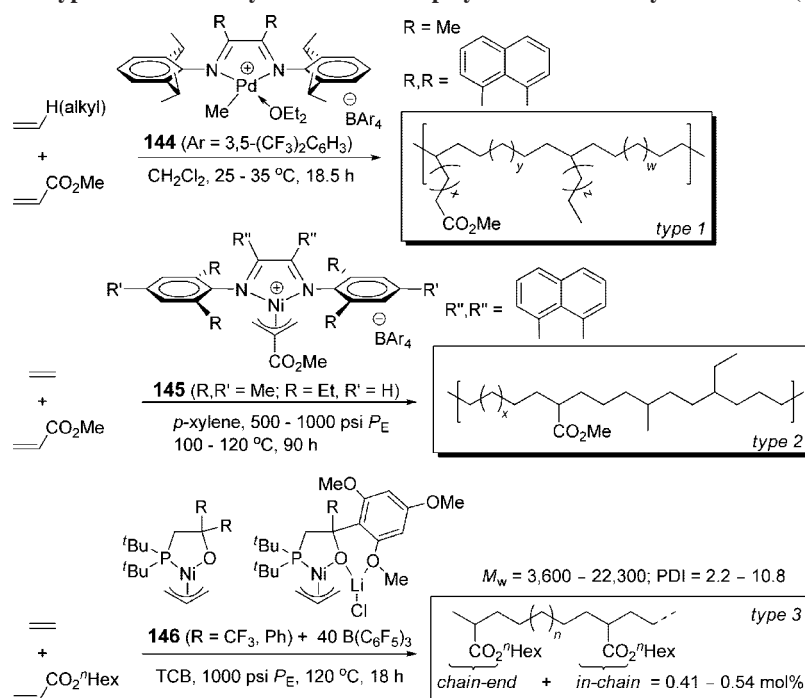
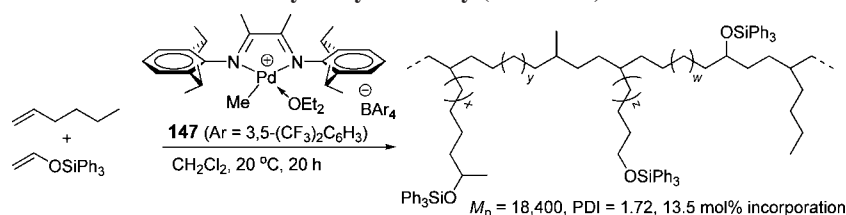
$\text{CpTiCl}_3/\text{MAO}$ ⁴⁶⁹ leads to *st*-PS with up to 4.5 mol % (45% *rr* PS by Cp^*TiCl_3) or 3.2 mol % (by CpTiCl_3) POSS incorporation; and copolymerization of E with acryloisobutyl-POSS by an (α -diimine) PdMe^+ catalyst produces hyperbranched PE tethered with POSS nanoparticles.⁴⁷⁰

In situ reduction of the $\text{Cp}^*\text{TiMe}_3 + [\text{Ph}_3\text{C}][\text{B}(\text{C}_6\text{F}_5)_4]$ reaction product by Zn generates a low-valent titanium species that polymerizes MMA to syndio-rich PMMA (66–72% *rr*) at 20 °C, but more importantly, it catalyzes random copolymerization of styrene and MMA at 50 °C to produce a copolymer with $M_w = 3.4 \times 10^4$, $M_w/M_n = 3.1$, and $\sim 4\%$ MMA incorporation.⁴⁷¹ The structure of the copolymer was characterized as containing *at*-sequences of PS with coisoselectively (ca. 80%, i.e., $\sim 80\%$ of all MMA addition events are followed immediately by styrene insertion) enchainment MMA units. Control experiments excluded noncoordination (ionic or radical) copolymerization mechanisms, and a mechanism involving sequential conjugate addition steps (Scheme 33) was suggested for the formation of this random copolymer and its stereomicrostructures. The feasibility of the second step, insertion of styrene into a Ti–O (enolate) bond to form a Ti–C bond, was argued by decreased bond energy differences between Ti–O and Ti–C bonds, which were effected by lowering the Ti oxidation state.⁴⁷¹

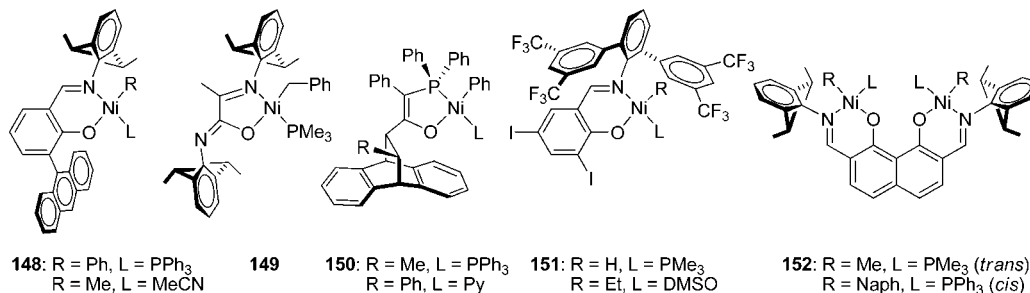
Fujita and co-workers⁴⁷² recently reported an exciting advancement in E + polar vinyl monomer copolymerization catalyzed by cationic nonmetallocene group 4 complexes. Titanium (*not zirconium*) complexes supported by bis(phenoxy-imine) ligands, $[\text{N},\text{O}^-]_2\text{TiCl}_2$ (**143**, Scheme 34), upon activation with dried MAO ($\text{Al}/\text{Ti} = 250$), copolymerize E (1 atm) with 5-hexene-1-ylacetate at 25 °C, affording PE with polar monomer incorporation up to 3.2 mol % ($M_w = 2.3 \times 10^4$, $M_w/M_n = 1.6$). The authors observed that the steric and electronic nature of the *ligand substituents significantly modulates the copolymerization activity and level of the polar monomer incorporation*. Thus, the *ortho*-phenyl substituted phenoxy ring induces higher polar monomer incorporation than the *ortho*-*t*Bu substituted one, and electron-donating groups (*t*Bu, OMe) introduced at the *para*- or *meta*-positions of the *N*-phenyl ring are more active than the *N*-phenyl one with the electron-accepting CF_3 group. Significantly, unlike the previously disclosed group 4 metal systems, no additional aluminum alkyls were added to precomplex the polar monomer, although whether the excess MAO present in the system plays a role as a protecting group (*vide supra*) or not is currently unclear.

Cationic Ni(II) and Pd(II) alkyl catalysts incorporating bulky α -diimine[N,N] ligands, developed by Brookhart and co-workers,⁴⁷³ copolymerize E and α -olefins with acrylates

Scheme 35. Three Different Types of E and Acrylate Random Copolymers Achieved by Cationic Pd(II) and Ni(II) Catalysts

Scheme 36. Copolymerization of 1-Hexene with Silyl Vinyl Ether by (α -Diimine)PdMe⁺

Scheme 37. Neutral Ni(II) Catalysts Examined for Copolymerization of E with Polar Vinyl Monomers



to produce three different types of random copolymers (Scheme 35). Type 1 copolymer afforded by Pd catalyst **144**⁴⁷⁴ is a highly branched amorphous PE with acrylate units located predominantly at *branch ends*, rather than randomly incorporated in-chain, which is made possible by a unique insertion/chain-walking mechanism (i.e., facile metal migration along the chain via β -hydride elimination/reinsertion reactions).^{475,476} type 2 copolymer produced by Ni catalyst **145**⁴⁷⁷ is a linear (or branched, depending on the catalyst and reaction conditions) PE with *in-chain* acrylate incorporation (up to 1.33 mol %). Type 3 random copolymer, produced by Ni allyl complexes **146** supported by phosphine-alkoxy [P,O⁻] (or [P,N⁻]) ligands, exhibits both in-chain and chain-end acrylate units (in \sim 1:1 ratio) incorporated into the substantially linear (none to a low degree of alkyl branching) PE backbone, rather than being located at the end of side chains (branch ends).⁴⁷⁷

The diimine backbone substituents R in catalyst **144** affect the activity (Me > An \approx H, with the Me derivative reaching a TOF of 8 h⁻¹ for MA) and also the copolymer MW (Me > An > H) but not the percentage of acrylate incorporation. On the other hand, reduction of the steric bulk of the 2,6-substituents of the aryl moieties results in an increase of the relative MA incorporation (e.g., 4.0 mol % with the 2,6-*i*Pr₂ substitution vs 14.2 mol % with the 2,6-Me₂ substitution under otherwise the same conditions), but at the expense of the MW of the copolymer. The E-polar copolymers with various branching topologies, controllable by P_E and comonomer concentration, have been realized by copolymerization of E with ω -ether or ester α -olefins using the chain-walking catalyst **144** (R = Me); for example, the copolymer becomes more dendritic with decreasing P_E and comonomer concentration.⁴⁷⁸ The copolymerization of E and acrylates (e.g., hexyl acrylate) by the Ni allyl complexes **146** requires

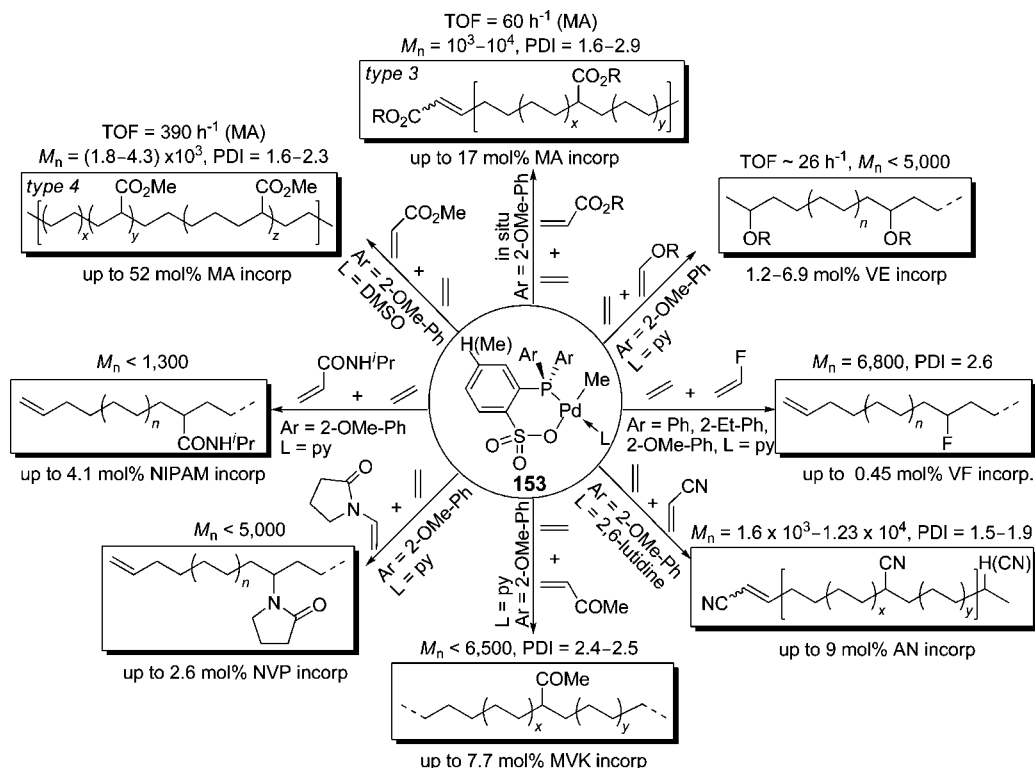


Figure 29. Coordination–insertion copolymerization of ethylene with polar vinyl monomers by neutral Pd(II) catalyst supported by the phosphine-sulfonate[P,O⁻] ligands.

addition of activators such as $B(C_6F_5)_3$ (40 equiv); the LiCl-coordinated complexes are more active than the ones without LiCl, which was attributed to a more electrophilic metal center rendered by LiCl coordination.⁴⁷⁷ Based on this hypothesis, $LiB(C_6F_5)_4$ (20 equiv) was also added to enhance the copolymerization productivity. The Ni-catalyzed copolymerizations by **145** are typically carried out under high temperatures (>80 °C) and pressures (>500 psi P_E), and addition of Lewis acids such as $B(C_6F_5)_3$ often improves the productivity.⁴⁷⁷ On the other hand, the Pd-catalyzed copolymerizations are typically carried out under ambient conditions (1–2 atm P_E and 25–35 °C), while higher pressures and temperatures result in reduced acrylate incorporation and catalyst decomposition, respectively.^{474,475} In significant extension of Brookhart's catalyst system, Guan and co-workers recently developed rigid cyclophane-based (α -diimine)M–R⁺ catalysts for enhanced thermal stability and activity for E polymerization by the Ni catalyst, thereby allowing for the production of high MW, branched PE at high temperatures (e.g., $M_n = 4.62 \times 10^5$, PDI = 1.64, $T_p = 90$ °C)⁴⁷⁹ and for enhanced acrylate incorporation by the Pd catalyst.⁴⁸⁰

Luo and Jordan reported insertion copolymerization of silyl vinyl ether (VE) $CH_2=CHOSiPh_3$ with 1-hexene (and other olefins ranging from E to 1-octadecene) by (α -diimine)PdMe⁺ catalyst **147** to produce highly branched copolymers (90–100 branches/1000 C: 60% C₁, 20% C₄ > C_n > C₂ > C₃) with the polar comonomer units located mostly (91%) at branch ends (Scheme 36).⁴⁸¹ The TOF for VE is low (<1 h⁻¹), and the copolymer example depicted in Scheme 36 has a M_n of 1.84×10^4 and a PDI of 1.72, with 13.5 mol % of VE incorporation. A typical insertion/chain-walking mechanism³¹ was implicated for the formation of such a copolymer structure, and several lines of evidence were presented to argue against a possible cationic mechanism and to confirm the formation of real copolymers. On the other hand,

copolymerization of olefins with vinyl ethers $CH_2=CHOR$ (R = ^tBu, Ph) using this catalyst system failed due to either fast cationic homopolymerization of the vinyl ether and associated decomposition of the catalyst to Pd⁰ (R = alkyl) or fast β -OAr elimination of (α -diimine)PdCH₂CHR(OAr)⁺ (R = aryl). A subsequent study showed that this catalyst system can undergo up to three sequential insertions of $CH_2=CHOSiPh_3$, ultimately forming Pd allyl products.⁴⁸² The formation of the inert cationic Pd allyl species was also recognized as the dominant catalyst deactivation pathway for the copolymerization of E with acrolein dimethyl acetal by the (α -diimine)PdMe⁺ catalyst; however, this copolymerization successfully produces a branched PE with up to 2.0 mol % polar comonomer incorporation and the catalyst deactivation occurs via alcohol elimination.⁴⁸³

Grubbs and co-workers reported neutral Ni(II) aryl and methyl complexes supported by bulky salicylaldimine ligands (Scheme 37), $[N,O^-]Ni(L)R$ (**148**: R = Ph, L = PPh₃; R = Me, L = MeCN), as single-component catalysts (without any cocatalyst) for copolymerization of E with 5-norbornen-2-yl acetate or 5-norbornen-2-ol, affording relatively linear, low-branched PE (9 branches/1000 carbon) with the functionalized norbornene incorporation up to 22 wt %.⁴⁸⁴ Subsequently, Grubbs et al. demonstrated that this single-component catalyst system can also copolymerize E with α -olefins carrying the ester, alcohol, or dioxolane functionality, albeit with reduced catalyst activity and lifetime as well as with much lower degree of polar monomer incorporation.⁴⁸⁵ For example, copolymerization of E (120 psig) with ethyl undecyleneoate at 40 °C afforded linear PE with 3.8 mol % comonomer incorporation. Bazan and co-workers also achieved copolymerization of E with functionalized norbornene monomers (incorporating 5-norbornen-2-yl acetate up to 17 mol % and 5-norbornen-2-ol up to 19 mol %) using a Ni(II) imino-propanamide complex $[N,O^-]Ni(PMe_3)CH_2Ph$ (**149**) in combination with Ni(COD)₂.⁴⁸⁶ Interestingly, co-

polymerization of E and MMA simultaneously by neutral nickel(II) catalysts (**150**) supported by bulky phosphine-enolate[P,O⁻] ligands produces MMA-end functionalized PE, CH₃CH₂(CH₂CH₂)_{n-1}CH=C(Me)CO₂Me (*n* = 40–60).⁴⁸⁷ A thorough mechanistic investigation based on well-defined model salicylaldimine Ni(II) hydride and alkyl complexes **151** by Mecking and co-workers⁴⁸⁸ revealed that MA effectively competes with E for coordination and insertion into the Ni–H bond, but the resulting 2,1-MA insertion product exhibits no ability for further E or MA insertion and, in the presence of unreacted Ni(II) hydride species, undergoes rapid bimolecular elimination of methyl propanoate even at –40 °C. Similarly, contacting the Ni(II) ethyl complex to the MA + E mixture results in immediate catalyst decomposition to give ultimately methyl pentanoate. The hydride complex reacts with vinyl acetate to give a kinetic 1,2-insertion product which rearranges into a thermodynamically favored 2,1-insertion product and decomposes via β-acetate elimination to afford ethylene and Ni(II) acetate species.⁴⁸⁸ Most recently, Marks et al. showed that bimetallic versions of salicylaldimine-ligated (phenoxyiminato) Ni(II) complexes [N,O⁻]Ni(L)R (**152**: R = Me, L = PMe₃; R = Naph, L = PPh₃), in which the two metal centers are bound in close spatial proximity with the rigid ligation supported by the 1,8-naphthalenediolato backbone, exhibit a 4-fold increase in polar comonomer incorporation (up to 10 mol %) in the copolymerization of E with functionalized norbornenes, when activated with Ni(COD)₂ and compared to the monometallic analogues.⁴⁸⁹ Remarkably, the bimetallic catalysts produce branched PE copolymers incorporating up to 11% (MA) or 9% (MMA) acrylic comonomer in copolymerization of E with MA or MMA, while the corresponding mononuclear catalysts exhibit negligible activity in the presence of such comonomers.

Neutral Pd(II) catalysts **153** (Figure 29) supported by chelating phosphine-sulfonate[P,O⁻] ligands and developed by Drent, Pugh, and co-workers effect coordination–insertion copolymerization of E with alkyl acrylates to produce linear PE, with isolated acrylate units being incorporated in-chain.⁴⁹⁰ The catalyst was generated by in situ mixing of Pd(OAc)₂ or Pd(dba)₂ (dba = dibenzylideneacetone) with the phosphine-sulfonate[P,O⁻] ligand, 2-[bis(2-methoxyphenyl)phosphino]benzenesulfonic acid. The copolymerizations were carried out at 60–80 °C in ethanol, toluene, or diglyme, under 30 atm *P*_E, producing linear copolymers with *M*_n up to 2.1 × 10⁴ (for BA), acrylate incorporation up to 17 mol % (for MA), and TOF up to 60 h⁻¹ (for MA). This high level of acrylate incorporation and TOF values can be related to the chelating phosphine-sulfonate[P,O⁻] ligand in which the sulfonate group is a rather poor electron donor to give the Pd center high electrophilicity relative to other types of neutral Pd(II) catalysts and at the same time unusual heteroatom-functionality tolerance. Owing to relatively slow insertion of E after insertion of acrylate, the rate of the copolymerization is lower than E homopolymerization and also decreases with increasing acrylate incorporation. Inspection of end groups indicates that acrylate insertion proceeds in a 2,1-mode, and chain transfer via β-hydride elimination to start a new chain occurs preferentially after the acrylate insertion.⁴⁹⁰ The formation of the linear copolymer by this neutral Pd catalyst suggests that chain-walking is slow relative to chain growth. DFT calculations by Ziegler and co-workers indeed show that the barrier to β-hydride elimination is higher for the [P,O⁻]Pd(R) species than for

(α-diimine)Pd(R)⁺.⁴⁹¹ On the other hand, a study by Mecking et al. showed that the reaction medium controls E polymerization by analogous Ni(II) catalysts [P,O⁻]Ni(L)Me (L = Py, TMEDA) so that materials ranging from low MW branched PE to high MW, strictly linear PE can be produced by variations of solvents.⁴⁹²

This significant initial discovery by Drent, Pugh et al.⁴⁹⁰ brought about subsequently intense studies of the [P,O⁻]Pd(R)(L) catalyst system by several groups. Nozaki and co-workers synthesized and structurally characterized the anionic version of catalyst **153** for copolymerization of E with MA, with or without additives such as NaB[3,5-(CF₃)₂C₆H₃]₄.⁴⁹³ The MA incorporation is similarly high (up to 16 mol %). Goodall, Claverie, and co-workers reported structural characterization of the preformed catalyst **153** (Ar = 2-[2,6-(MeO)₂C₆H₃]₂C₆H₄, L = Py, TMEDA) and employed such discrete catalysts for copolymerization of E with acrylates.⁴⁹⁴ They found that the catalyst with Ar = 2-[2,6-(MeO)₂C₆H₃] yields copolymers with higher MW, but the catalyst with Ar = 2-MeO-C₆H₄ affords copolymers with higher (>2 fold) acrylate incorporation. The catalytic copolymerization of E with MA can also be carried out in aqueous emulsion to produce colloiddally stable E/MA copolymer latexes.⁴⁹⁵

Most remarkably, Mecking and co-workers discovered that simply replacing the L ligand, the commonly employed *N*-donor donor such as pyridine, by the more labile DMSO, results in catalyst **153**, which exhibits unprecedentedly high levels of MA incorporation (9.4–52 mol %) and high acrylate TOF (up to 390 h⁻¹) in copolymerizations of E and MA under typical conditions of 5–15 atm *P*_E, 0.6–7.5 M [MA], 90 °C in toluene for 1 h.⁴⁹⁶ The resulting copolymer composition is also unique; the linear copolymers with >30 mol % MA incorporation contain, in addition to isolated acrylate units, “alternating” E/MA sequences and consecutive acrylate units in the polymer backbone (type 4 ethylene/acrylate copolymer, *y* = 1 to *n*, Figure 29). Evidence was presented to show that DMSO does not compete substantially with E binding, and the rate limiting step of the copolymerization is monomer insertion into the Pd–alkyl bond carrying α-ester group (derived from 2,1-insertion of MA), not the commonly believed opening of four-membered chelates formed by κ-*O* coordination of the last inserted acrylate unit; this means that *the last inserted MA unit significantly retards the rate of subsequent monomer insertion*. Homoinsertion polymerization of MA (2 g, 80 μmol catalyst) at 90 °C for 4 h yielded PMA with an average of DP of ~5.⁴⁹⁶ The above results are significant because they nicely filled the “35% gap” of polar vinyl monomer composition unattainable by metal catalysis⁵⁹ until now.

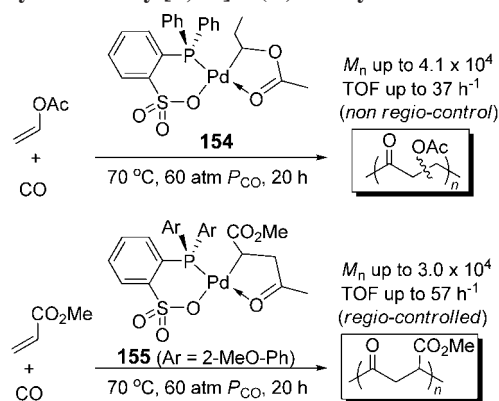
The coordination–insertion copolymerization examples summarized in Figure 29 demonstrate that the [P,O⁻]-PdMe(L) catalyst system exhibits some tantalizing versatility in its ability to incorporate *a wide range of polar vinyl monomers besides acrylates*. For example, Claverie and co-workers employed catalyst **153** (Ar = 2-MeO-Ph, L = py) to successfully copolymerize E with *N*-isopropylacrylamide (NIPAM) and *N*-vinyl-2-pyrrolidone (NVP), achieving low MW linear copolymers (*M*_n < 1300 and <5000), with NIPAM and NVP incorporating up to 4.1 mol % and 2.6 mol % (1–3 polar groups per chain), respectively.⁴⁹⁷ It was observed that chain transfer by β-H elimination occurs only after an E insertion, and no terminal NIPAM or NVP units were located, which is contrary to the copolymerization E with

acrylates. Not surprisingly, incorporation of any level of these polar vinyl monomers decreases the polymer MW and sharply reduces polymerization activity. Sen and co-workers extended applications of catalyst **153** by combining it with the BPh₃ additive for copolymerization of E with MVK, achieving linear PE with a relatively low M_n of <6500 (PDI = 2.4–2.5) and with MVK incorporation up to 7.7 mol %.⁴⁹⁸ The [P,O⁻]PdR(L) catalysts generated by in situ mixing of Pd(dba)₂ with [P,O⁻] ligands, 2-[bis(2-methoxyphenyl)phosphino]benzenesulfonic acid and 2-[bis(2,6-dimethoxyphenyl)phosphino]benzenesulfonic acid, also copolymerize E with norbornene derivatives functionalized with ester or alcohol moieties to produce copolymers with high functionalized norbornene contents (up to 44 mol %).⁴⁹⁹

Insertion copolymerization of E and alkyl vinyl ethers CH₂=CHOR (R = Et, ^tBu, ⁿBu) was also realized by Jordan et al. using neutral Pd(II) methyl catalyst **153** supported by a chelating phosphine-sulfonate [P,O⁻] ligand (Figure 29).⁵⁰⁰ The copolymerization exhibits a modest TOF of ~26 h⁻¹ (for VE), and the linear copolymer produced has a low M_n of <5000 (PDI = 1.8–2.0) under varied conditions (P_E , T_p , comonomer feed) and contains both in-chain and chain-end vinyl ether units, totaling 1.2 (R = ^tBu) to 6.9 (R = ⁿBu) mol % polar monomer incorporation. The in-chain to chain-end ratio is approximately 2 for R = Et and ⁿBu, but for R = ^tBu, this ratio is 0.2. The in-chain units can be produced by 1,2- or 2,1-insertion of CH₂=CHOR into active [Pd]–PE species, followed by E insertion, while there are several possible pathways to produce the chain-end units: initial insertion of CH₂=CHOR into [Pd]–Me, 1,2-insertion of CH₂=CHOR followed by chain walking and growth, and chain transfer from [Pd]–PE to CH₂=CHOR followed by E insertion. Addition of CH₂=CHOR lowers the polymerization rate and the polymer MW. Several lines of strong evidence were presented to argue against radical and cationic mechanisms for the copolymer formation.⁵⁰⁰ As a neutral catalyst, **153** disfavors competing cationic polymerization of vinyl ethers; furthermore, its high barrier to chain walking⁴⁹¹ leads to formation of linear polymers.

It has been a challenging goal to develop metal catalysts that can copolymerize vinyl halides CH₂CH=CHX (X = F, Cl, Br) with olefins through a coordination–insertion mechanism, as several early⁵⁰¹ or late^{502,503} metal catalyst systems have been found unsuccessful at performing this task, largely due to the following: (a) rapid β -X elimination of [M]CH₂CHXR species formed by 1,2-insertion of a vinyl halide into a M–R bond,^{501–507} the process of which affords inactive M–X species and thus terminates the polymerization, (b) low insertion activity of [M]CHXCH₂R species formed by 2,1-insertion of a vinyl halide,⁵⁰⁸ and (c) competing radical pathways by catalyst-derived radicals.^{501,503} As compared with other vinyl halides, vinyl fluoride (VF) is less susceptible to free radical polymerization and β -F elimination may be less favorable due to the high C–F bond strength. Indeed, using the catalyst system **153**, Jordan and co-workers disclosed successful copolymerization of E and VF in toluene at 80 °C to produce fluorinated, linear high-density PE (T_m ~ 130 °C) with low levels of VF (up to 0.45 mol %) incorporation (Figure 29).⁵⁰⁹ The 2-Et-Ph catalyst is more active and produces higher MW copolymer than the Ph and 2-OMe-Ph catalysts, but all three catalysts incorporate similarly low levels of VF. Increasing VF in the feed brings about a higher level of VF incorporation at the expense of polymer yield and MW.

Scheme 38. Alternating Copolymerization of CO with MA and Vinyl Acetate by [P,O⁻]Pd(II) Catalysts



Catalytic coordination–insertion copolymerization of E and AN has also been accomplished using catalyst **153** by Nozaki and co-workers, who produced moderate MW linear PE with up to 9 mol % AN incorporation (Figure 29).⁵¹⁰ Owing to the slow rate of this reaction, the copolymerization was typically carried out in toluene at 100 °C under 30 atm P_E for 120 h using 0.01 mmol of the Pd catalyst; the copolymerization follows the same trend as the copolymerizations using other polar vinyl monomers: increasing the comonomer (AN) feed boosts the polar monomer incorporation at the expense of polymerization activity and MW. The incorporated AN units are distributed within the polymer backbone and at the chain (initiating and terminating) ends in roughly equal amounts. Chain initiation was proposed to proceed via insertion of E into a Pd–Me bond or 2,1-AN into a Pd–H bond, while chain transfer occurs preferentially after the AN insertion.

6.3. Polar–Polar Copolymers

Following the initial report by Drent, Pugh, and co-workers that in situ generated neutral Pd(II) catalysts incorporating the chelating phosphine-sulfonate[P,O⁻] ligands copolymerize E and CO to give high MW, nonalternating E/CO copolymers,⁵¹¹ Nozaki and co-workers found that this fantastic catalyst system, either prepared in situ by mixing the phosphine–sulfonic acid ligand with Pd(dba)₂, or pre-formed catalyst **154** (Scheme 38), also copolymerizes vinyl acetate (VA) and CO to give alternating copolymers with M_n reaching 41,000 (PDI = 1.7).⁵¹² This copolymer is not head-to-tail regiocontrolled, but copolymerization of MA with CO using catalyst **155** affords regiocontrolled alternating copolymers (Scheme 38).⁵¹³ Evidence was provided to support the nonradical, coordination–insertion copolymerization processes for both VA/CO and MA/CO copolymerizations.

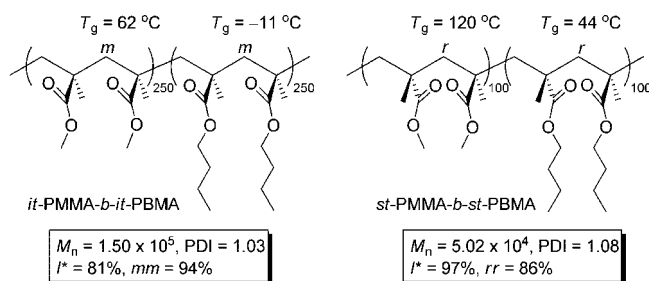


Figure 30. Stereodblock methacrylate copolymers synthesized by chiral group 4 metallocene catalysts.

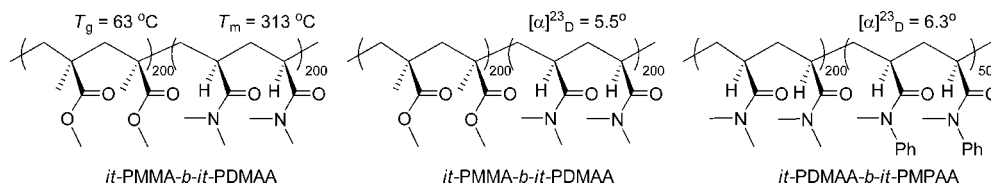


Figure 31. Amphiphilic stereodiblock copolymer PMMA-*b*-PDMAA produced by racemic **86** in CH₂Cl₂ at 23 °C as well as optically active stereodiblock copolymers of MMA and acrylamides produced by enantiomeric **86**.

Samarocene [Cp*₂SmH]₂ is a highly active and efficient catalyst for the synthesis of well-defined diblock copolymers (PDI = 1.04) of MMA with ethyl, isopropyl, and *tert*-butyl methacrylates at 0 °C.⁸⁷ Owing to the livingness of the lanthanocene-catalyzed polymerizations of both methacrylates and acrylates, Yasuda and co-workers utilized Cp*₂SmMe(THF) for the successful synthesis of well-defined MMA-*n*BA diblock copolymer (PDI = 1.05) as well as MMA (hard)-*n*BA (soft)-MMA (hard) triblock copolymers (PDI = 1.09), one of which, (MMA)₈-(*n*BA)₇₂-(MMA)₂₀, was shown to exhibit good elastic properties with an ultimate elongation of 163% and compression set of 58%.³³⁷ An ABC triblock, (MMA)₂₆-(ethyl acrylate)₄₈-(ethyl methacrylate)₂₆, showed a tensile modulus of 119 MPa and an elongation of 276%. The ABA triblock copolymer can be synthesized by either a three-step monomer addition sequence at 0 °C starting with the first feed of MMA, followed by *n*BA and the last feed of MMA, or a two-step sequence starting again with the first feed of MMA, but followed by a mixed feed of *n*BA and MMA, thanks to much higher reactivity of this system toward *n*BA than MMA.³³⁸ The synthesis of the well-defined ABA triblock copolymers containing both methacrylate and acrylate segments has also been accomplished in a two-step block copolymerization procedure using the divalent samarocene initiator Cp*₂Sm or Cp*₂Sm(THF)₂; the polymerization begins with the polymerization of monomer B to construct the middle block of the triblock, followed by polymerization of monomer A to grow simultaneously the two outer A blocks from the macromonomeric diinitiators derived from the first polymerization.⁵¹⁴

Well-defined (PDI = 1.03), highly isotactic (94% *mm*) stereodiblock methacrylate copolymer *it*-PMMA-*b*-*it*-PBMA (Figure 30) was synthesized in an efficient (*I** = 81%) and convenient (RT) manner, using catalyst **86**.¹⁸⁸ Investigations of statistical copolymerization of MMA and BMA with the same catalyst yielded monomer reactivity ratios of *r*_{MMA} = 0.62 and *r*_{BMA} = 0.72 (the Kelen–Tüdös method), indicating that the copolymer formed instantaneously, has a somewhat alternating character (*r*_{MMA} × *r*_{BMA} = 0.45).¹⁸⁸ Syndiotactic stereodiblock copolymer *st*-PMMA-*b*-*st*-PBMA (PDI = 1.08) was synthesized in a highly efficient fashion (*I** = 97%) using the C_s-ligated cationic catalyst (CGC)TiMe⁺MeB-(C₆F₅)₃⁻ (**106**).²¹⁰ Syndio-rich atactic, high MW block copolymers of MMA with other alkyl methacrylates were also synthesized by the three-component system, Cp₂ZrMe₂/B(C₆F₅)₃/Et₂Zn (excess), but MWD was broader (PDI = 1.39).¹⁷⁶ Using this three-component system, graft copolymers with the PMMA backbone and polystyrene, polyisoprene, or poly(dimethylsiloxane) branches were synthesized by copolymerizing MMA with methacryloyl macromonomers separately prepared by anionic polymerization.⁵¹⁵ The synthesis was further extended to other complex macromolecular architectures⁵¹⁶ and statistical copolymers of MMA with other alkyl methacrylates^{517,518} utilizing this metallocene-based catalyst system.

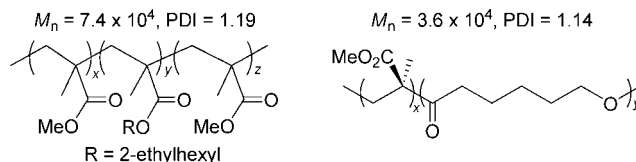
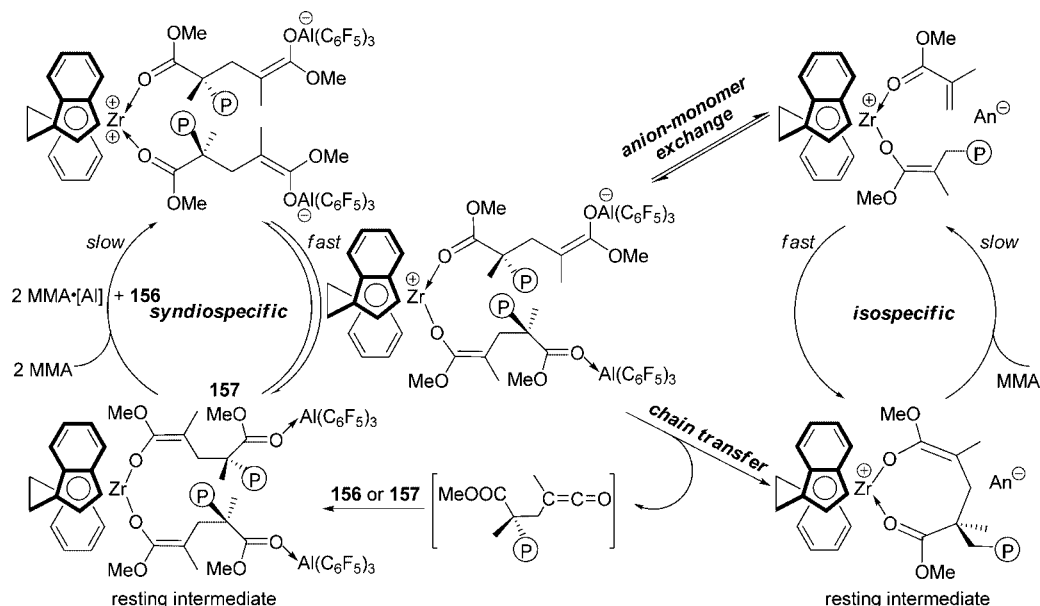


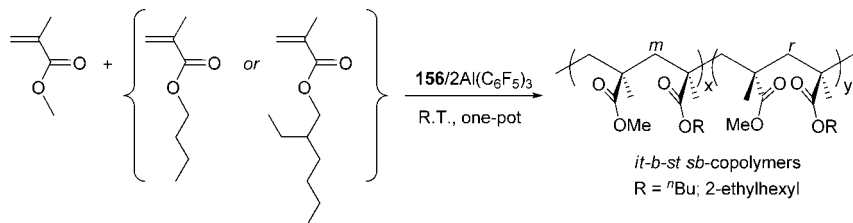
Figure 32. Triblock methacrylate copolymer and MMA-*b*-lactone diblock copolymer synthesized by group 4 metallocene and lanthanocene catalysts.

Methacrylate–acrylate diblock copolymer PMMA-*b*-P(*n*BA) has been synthesized using the (CGC)TiMe₂/B(C₆F₅)₃ catalyst system at *T*_p = 20 and 80 °C.³⁴⁹ The block copolymer features a syndiotacticity of 80% *rr* for the PMMA block and 75% *rr* for the P(*n*BA) block. The studies indicate that an initial PMMA block of a minimal length of 50 MMA units is needed for achieving high conversion of the *n*BA block due to the nonliving nature of the acrylate polymerization by this catalyst system. The polymerization system consisting of Me₂C=C(OMe)OSi⁺Bu₃[Ph₃C][B(C₆F₅)₄] (0.09 equiv) carried out at 25 °C in CH₂Cl₂ or toluene produced well-defined methacrylate–acrylate diblock copolymer PMMA-*b*-P(*n*BA) with a quantitative *I** and a low PDI value of 1.09.³⁰¹ The diblock copolymer PMMA-*b*-P(*n*BA) with a PDI value of 1.18 was prepared by catalyst **86** at 23 °C.³⁴⁷ Block copolymers of MMA with *n*BA and *t*BA were also prepared by the three-component system consisting of *rac*-(EBI)-ZrMe₂/[HNMe₂Ph][B(C₆F₅)₄]/ZnEt₂ at 0 °C.³⁴⁶

The living and isospecific nature of catalyst **86** toward polymerization of both methacrylates and acrylamides enabled the synthesis of the well-defined isotactic PMMA-*b*-PDMAA stereodiblock copolymer (Figure 31).³⁵³ This amphiphilic block copolymer, prepared from starting the polymerization of MMA followed by the DMAA polymerization, exhibits a *T*_g characteristic of the *it*-PMMA component segment (*T*_g = 63 °C) and a *T*_m characteristic of the *it*-PDMAA component segment (*T*_m = 313 °C). Owing to the high crystallinity of the highly isotactic PDMAA block, there is no apparent *T*_g, but a distinct *T*_m, for this component segment. Interestingly, the sequential block copolymerization starting from polymerization of DMAA followed by polymerization of MMA, or the statistical copolymerization using a 1:1 DMAA/MMA monomer feed, afforded only homopolymer PDMAA. Detailed studies indicate that the observed copolymerization behavior was attributed to the inability of MMA to displace the coordinated, more basic amide oxygen of the cyclic amide enolate intermediate, thus failing to enter the coordination site of the Zr center.³⁵³ Optically active, stereodiblock acrylamide-*b*-methacrylate and unsymmetric acrylamide-*b*-acrylamide copolymers (Figure 31) have also been synthesized using the enantiomeric catalyst **86**.³⁹⁵ It is worth noting here again that enantiomeric, high MW, nonhelical homopolymers of methacrylates and acrylamides as well as diblock or triblock copolymers of methacrylates, produced by the enantiomeric catalysts **86**, are optically inactive due to their cryptochirality (*cf.* section 4.3).

Scheme 40. Proposed Overall Mechanism of DIPP by the 156/2Al(C₆F₅)₃ Catalyst System¹⁸⁹

Scheme 41. Stereomultiblock Copolymerization of MMA with Other Methacrylates Using DIPP



polymer chains must undergo infrequent exchange between the cationic and anionic sites. When two sites are diastereospecific, the IPP system becomes a DIPP system.

The switching of a growing polymer chain from the isospecific, cationic zirconocenium site to the syndiospecific, anionic aluminate site was demonstrated by the synthesis of highly stereoregular *it-b-st sb*-PMMA (Figure 34).⁵²² In this sequential polymerization, the first MMA feed was polymerized with *rac*-(EBI)ZrMe⁺MeB(C₆F₅)₃⁻ at RT to an isotactic block via the living, isospecific cationic zirconocenium enolate propagating species. Next, the methyl zirconocenium aluminate complex *rac*-(EBI)ZrMe⁺MeAl(C₆F₅)₃⁻ was added to convert the cationic enolate to the neutral methyl zirconocenium enolate. After cooling to -78 °C, a second feed of MMA was then added, and the polymerization was reinitiated via Michael addition of the isotactic polymeric enolate ligand at Zr to the activated MMA at Al, starting the construction of a syndiotactic block via the syndiospecific enolaluminate propagating species. The resulting polymer is both highly isotactic and syndiotactic, as evidenced by the methyl triad distributions of $[mm]/[rr]/[mr] = 46.4/45.7/7.9$ derived from the ¹H NMR of the methyl triad region and by a pentad distribution of $[mmmm] = 42.8$ and $[rrrr] = 39.6$ derived from the ¹³C NMR spectrum of the C=O pentad region (Figure 34). The molecular weight of the stereodiblock PMMA is approximately double that of the two PMMA homopolymers.⁵²²

The greater challenge was to switch the growing polymer chains back and forth between diastereospecific cation M⁺ and anion An⁻ centers in a one-pot polymerization of DIPP. This has been achieved by employing a catalyst mixture containing chiral zirconocenium methyl cations paired with

both methyl borate and methyl aluminate anions, e.g., *rac*-(EBI)ZrMe⁺[MeB(C₆F₅)₃⁻]_{0.5}[MeAl(C₆F₅)₃⁻]_{0.5}, which is generated by activating *rac*-(EBI)ZrMe₂ with a 1:1 ratio of Lewis acids E(C₆F₅)₃ (E = B, Al).⁵²¹ The MMA polymerization by such a system was proposed to proceed in a diastereospecific ion-pairing fashion, in which the Zr⁺/B⁻ ion pair produces the *it*-block via the zirconium ester enolate cation and the Zr⁺/Al⁻ ion pair affords the *st*-block via the enolaluminate anion, whereas the exchange of growing diastereomeric polymer chains occurs via a neutral zirconocenium bis(ester enolate) intermediate to yield *it-b-st* stereomultiblock PMMA, *sb*-PMMA. Scheme 39 illustrates how the diastereomeric polymer chains can be switched back and forth between the cationic and the anionic sites. In this proposed reaction sequence, the chiral zirconocenium cation renders *it*-blocks via a unimetallic propagation, whereas the enolaluminate anion furnishes *st*-blocks via a bimetallic propagation. The polymer chain exchange occurs via intermolecular Michael addition of the *st*-enolate chain in the anionic enolaluminate propagating species to the Zr-activated MMA in the cationic zirconocenium enolate species. Subsequently, the *it*-polymeric enolate ligand in the resulting neutral bis-enolate zirconocenium intermediate immediately attacks the MMA-alane adduct to form back to the same ion-pairing propagating species, but each propagating species is now carrying a diastereomeric block (denoted as P_{it(st)} or P_{st(it)}). If the propagation rates at both sites are compatible and the chain exchange rate is comparable with the propagation rates, *sb*-PMMA is formed. Noteworthy here is that no such *sb*-PMMA is produced using either cationic diastereospecific metallocene pairs or cationic diastereomeric *ansa*-

metallocene mixtures, indicating growing polymer chains did not undergo exchange between such diastereospecific cationic sites.¹⁶⁹

The slow initiation steps in this first-generation DIPP system involved transfers of methyl groups to the activated monomers by the Zr cation and by the Al Lewis acid to generate cationic zirconocenium ester enolate and anionic ester enolaluminate diastereospecific propagating species, respectively, for DIPP; these slow steps hampered mechanistic studies and also resulted in the formation of ill-defined polymer products. On the basis of the hypothesis presented in Scheme 39, Ning and Chen developed the second-generation DIPP system that directly employs zirconocene bis(ester enolate) complex *rac*-(EBI)Zr[OC(OⁱPr)=CMe₂]₂ (**156**), in combination with 2 equiv of Al(C₆F₅)₃, for higher efficiency and enhanced control over the polymerization.¹⁸⁹ Detailed investigations (polymerization characteristics, kinetics, elementary reactions, characterization, and behavior of the isolated key intermediates, as well as temperature and Lewis acid effects) have yielded a mechanism for the DIPP of MMA by the **156**/2Al(C₆F₅)₃ system (**156** denotes the starting bis-ester enolate **156** and its derived homologues in Scheme 40). This mechanism consists of four manifolds—an isospecific cycle by the metallocenium cation, a syndiospecific cycle by the enolaluminate anion, anion–monomer exchange, and then chain transfer, with the latter two serving to interconvert diastereospecific propagating manifolds.¹⁸⁹

The proposed overall mechanism is consistent with the evidence collected and explains the formation of the various polymer stereomicrostructures formed under given conditions. This unique polymerization technique has also been applied to stereoblock polymerization of other methacrylates and stereoblock copolymerization of MMA with methacrylates having longer alkyl chains, leading to functionalized polymeric materials with tunable properties controlled by their stereomicrostructures and the nature of the comonomer (Scheme 41).¹⁸⁹ This IPP system has also been extended to other catalysts such as Cp₂Zr[OC(OⁱPr)=CMe₂]₂/2[Al(C₆F₅)₃], which has been utilized for the synthesis of well-defined homopolymers as well as diblock and triblock copolymers of methacrylates.²⁸⁷

8. Summary and Outlook

The major promise for ever growing interest in the metal-catalyzed coordination polymerization of polar or nonpolar vinyl monomers can be attributed to (1) its precision in catalyst-based stereochemical and architectural control and (2) its ability to produce new classes of polymeric materials—features unattainable by other means of polymerization, such as ionic or radical polymerization. To this end, remarkable successes have been accomplished by each of the two types of metal-catalyzed coordination polymerization of polar vinyl monomers described in this review. Specifically, *coordination–addition* polymerization of polar vinyl monomers by single-site early metal and lanthanide catalysts shows a *dazzling display of a variety of stereomicrostructures* it can generate, in addition to its high activity and high degree of control over polymer characteristics. On the other hand, *coordination–insertion* copolymerization of α -olefins with polar vinyl monomers by late metal catalysts demonstrates some *tantalizing versatilities incorporating a wide range of polar vinyl monomers at controllable levels* into polyolefins with diverse topologies (e.g., linear, branched,

dendritic), thereby producing new classes of copolymers (e.g., filling the composition gap) unattainable by other means.

As can be readily realized, no single type of polymerization or catalyst system can meet all demanding needs and challenges. In the opinion of this author, future research in the area of metal-catalyzed coordination polymerization of polar vinyl monomers will be largely directed toward addressing the following *five major unmet challenges*: (1) direct random copolymerization of polar–nonpolar vinyl monomers by early or lanthanide catalysts (which will take advantage of their remarkable activity, control, and versatility already demonstrated for both respective homopolymerizations); (2) catalytic production of the stereochemically controlled polar vinyl polymers by early or lanthanide catalysts (which will render its economical production of stereoregular, crystalline polar vinyl polymers); (3) stereospecific polymerization of polar vinyl monomers and copolymerization with olefins by late metal catalysts (which has been limited to early metal catalysts); (4) high MW polar vinyl polymers and polar/nonpolar copolymers by late metal catalysts (through the development of high-speed insertion polymerization overcoming low insertion rates of polar vinyl monomers into a metal–olefin bond or olefins into a metal–polar monomer (chelating) bond); and (5) polymerization or incorporation of biorenewable polar vinyl monomers (for the synthesis of environmentally sustainable polymers).

9. Acknowledgments

The author's own work described herein was supported by the U.S. National Science Foundation, an Alfred P. Sloan research fellowship, and the donors of the Petroleum Research Fund, administered by the American Chemical Society. The author is indebted to his students and co-workers whose names appear in the cited references, for their invaluable contributions to the author's portion of the research included in this review. The author is also appreciative of the work by other groups or individuals cited herein which made writing of this review possible and enjoyable.

10. References

- (1) Guan, Z., Vol. Ed.; *Top. Organomet. Chem.* 2009, **26**, 3. and contributions therein (volume on "*Metal Catalysts in Olefin Polymerization*").
- (2) *Stereoselective Polymerization with Single-Site Catalysts*; Baugh, L. S., Canich, J. A. M., Eds.; CRC Press/Taylor & Francis Group: Boca Raton, FL, 2008.
- (3) Marks, T. J., Ed. *Proc. Natl. Acad. Sci. U.S.A.* 2006, **103**, 15288. and contributions therein (issue on "*Polymerization Special Feature*").
- (4) Alt, H. G., Ed. *Coord. Chem. Rev.* 2006, **250**, 1. and contributions therein (issue on "*Metallocene Complexes as Catalysts for Olefin Polymerization*").
- (5) Janiak, C. *Metallocene Catalysts*. In *Kirt-Othmer Encyclopedia of Chemical Technology*; Seidel, A., Ed.; John Wiley & Sons, Inc.: Hoboken, NJ, 2006; Vol. 16, p 79.
- (6) *Late Transition Metal Polymerization Catalysis*; Rieger, B., Baugh, L. S., Kacker, S., Striegler, S., Eds.; Wiley-VCH: Weinheim, 2003.
- (7) Gladysz, J. A., Ed. *Chem. Rev.* 2000, **100**, 1167. and contributions therein (issue on *Frontiers in Metal-Catalyzed Polymerization*).
- (8) Marks, T. J.; Stevens, J. C. *Top. Catal.* **1999**, **7**, 1. and contributions therein (issue on *Advances in Polymerization Catalysis. Catalysts and Processes*).
- (9) *Metalorganic Catalysts for Synthesis and Polymerization: Recent Results by Ziegler–Natta and Metallocene Investigations*; Kaminsky, W., Ed. Springer-Verlag: Berlin, 1999.
- (10) Jordan, R. F., Ed. *J. Mol. Catal., A: Chem.* 1998, **128**, 1. and contributions therein (issue on *Metallocene and Single-Site Olefin Catalysts*).

- (11) *Ziegler Catalysts*; Mülhaupt, R., Brintzinger, H.-H., Eds.; Springer-Verlag: Berlin, 1995.
- (12) Soga, K.; Terano, M. *Stud. Surf. Sci. Catal.* **1994**, *89*, 1. and contributions therein (issue on *Catalyst Design for Tailor-Made Polyolefins*).
- (13) *Metallocenes: Synthesis—Reactivity—Applications*; Togni, A., Halterman, R. L., Eds.; Wiley-VCH: Weinheim: 1998.
- (14) Resconi, L.; Chadwick, J. C.; Cavallo, L. In *Comprehensive Organometallic Chemistry III*; Bochmann, M., Vol. Ed.; Mingos, M. P., Crabtree, R. H., Chief Eds.; Elsevier: Oxford, 2007; Vol. 4, p 1005.
- (15) Chen, E. Y.-X.; Rodríguez-Delgado, A. In *Comprehensive Organometallic Chemistry III*; Bochmann, M., Vol. Ed.; Mingos, M. P.; Crabtree, R. H., Chief Eds.; Elsevier: Oxford, 2007; Vol. 4, p 759.
- (16) Cuenca, T. In *Comprehensive Organometallic Chemistry III*; Bochmann, M., Vol. Ed.; Mingos, M. P., Crabtree, R. H., Chief Eds.; Elsevier: Oxford, 2007; Vol. 4, p 323.
- (17) Yoshida, Y.; Matsui, S.; Fujita, T. *J. Organomet. Chem.* **2005**, *690*, 4382.
- (18) Bochmann, M. *J. Organomet. Chem.* **2004**, *689*, 3982.
- (19) Suzuki, N. *Top. Organomet. Chem.* **2004**, *8*, 177.
- (20) Coates, G. W. *Chem. Rev.* **2000**, *100*, 1223.
- (21) Resconi, L.; Cavallo, L.; Fait, A.; Piemontesi, F. *Chem. Rev.* **2000**, *100*, 1253.
- (22) Alt, H. G.; Köppl, A. *Chem. Rev.* **2000**, *100*, 1205.
- (23) Brintzinger, H. H.; Fischer, D.; Mülhaupt, R.; Rieger, B.; Waymouth, R. M. *Angew. Chem., Int. Ed.* **1995**, *34*, 1143.
- (24) Bochmann, M. *J. Chem. Soc., Dalton Trans.* **1996**, 255.
- (25) McKnight, A. L.; Waymouth, R. M. *Chem. Rev.* **1998**, *98*, 2587.
- (26) Kaminsky, W.; Arndt, M. *Adv. Polym. Sci.* **1997**, *127*, 143.
- (27) Chum, P. S.; Kruper, W. J.; Guest, M. J. *Adv. Mater.* **2000**, *12*, 1759.
- (28) Kawai, K.; Fujita, T. *Top. Organomet. Chem.* **2009**, *26*, 3.
- (29) Gibson, V. C.; Spitzmesser, S. K. *Chem. Rev.* **2003**, *103*, 283.
- (30) Britovsek, G. J. P.; Gibson, V. C.; Wass, D. F. *Angew. Chem., Int. Ed.* **1999**, *38*, 429.
- (31) Ittel, S. D.; Johnson, L. K.; Brookhart, M. *Chem. Rev.* **2000**, *100*, 1169.
- (32) Mecking, S. *Angew. Chem., Int. Ed. Engl.* **2001**, *40*, 534.
- (33) Hou, Z.; Wakatsuki, Y. *Coord. Chem. Rev.* **2002**, *231*, 1.
- (34) Yasuda, H.; Ihara, E. *Adv. Polym. Sci.* **1997**, *133*, 53.
- (35) Nakayama, Y.; Yasuda, H. *J. Organomet. Chem.* **2004**, *689*, 4489.
- (36) Yasuda, H.; Tamai, H. *Prog. Polym. Sci.* **1993**, *18*, 1097.
- (37) Sita, L. R. *Angew. Chem., Int. Ed.* **2009**, *48*, 2464.
- (38) Lamberti, M.; Mazzeo, M.; Pappalardo, D.; Pellicchia, C. *Coord. Chem. Rev.* **2009**, *253*, 2082.
- (39) Schellenberg, J. *Prog. Polym. Sci.* **2009**, *34*, 688.
- (40) Rodrigues, A.-S.; Kirillov, E.; Carpentier, J.-F. *Coord. Chem. Rev.* **2008**, *252*, 2115.
- (41) Chen, E. Y.-X.; Marks, T. J. *Chem. Rev.* **2000**, *100*, 1391.
- (42) Pédeutour, J.-N.; Radhakrishnan, K.; Cramail, H.; Deffieux, A. *Macromol. Rapid Commun.* **2001**, *22*, 1095.
- (43) Piers, W. E. *Adv. Organomet. Chem.* **2005**, *52*, 1.
- (44) Domski, G. J.; Rose, J. M.; Coates, G. W.; Bolig, A. D.; Brookhart, M. *Prog. Polym. Sci.* **2007**, *32*, 30.
- (45) Coates, G. W.; Hustad, P. D.; Reinartz, S. *Angew. Chem., Int. Ed. Engl.* **2002**, *41*, 2236.
- (46) Yasuda, H. *Prog. Polym. Sci.* **2000**, *25*, 573.
- (47) Yasuda, H.; Ihara, E. *Bull. Chem. Soc. Jpn.* **1997**, *70*, 1745.
- (48) Amin, S. B.; Marks, T. J. *Angew. Chem., Int. Ed. Engl.* **2008**, *47*, 2006.
- (49) Bochmann, M. In *Stereoselective Polymerization with Single-Site Catalysts*; Baugh, L. S., Canich, J. A. M., Eds.; CRC Press/Taylor & Francis Group: Boca Raton, FL, 2008; p 297.
- (50) Dong, J.-Y.; Hu, Y. *Coord. Chem. Rev.* **2006**, *250*, 47.
- (51) Chung, T. C. *Prog. Polym. Sci.* **2002**, *27*, 39.
- (52) Yasuda, H. *J. Organomet. Chem.* **2002**, *647*, 128.
- (53) Chen, E. Y.-X. *J. Polym. Sci., Part A: Polym. Chem.* **2004**, *42*, 3395.
- (54) Marshall, E. L.; Gibson, V. C. In *Stereoselective Polymerization with Single-Site Catalysts*; Baugh, L. S., Canich, J. A. M., Eds.; CRC Press/Taylor & Francis Group: Boca Raton, FL, 2008; p 593.
- (55) Yasuda, H. *J. Polym. Sci., Part A: Polym. Chem.* **2001**, *39*, 1955.
- (56) Frauenrath, H.; Balk, S.; Keul, H.; Höcker, H. *Macromol. Rapid Commun.* **2001**, *22*, 1147.
- (57) Jin, J.; Chen, E. Y.-X. *Macromol. Chem. Phys.* **2002**, *203*, 2329.
- (58) Boffa, L. S.; Novak, B. M. *Chem. Rev.* **2000**, *100*, 1479.
- (59) Goodall, B. L. *Top. Organomet. Chem.* **2009**, *26*, 159.
- (60) Sen, A.; Borkar, S. *J. Organomet. Chem.* **2007**, *692*, 3291.
- (61) Berkefeld, A.; Mecking, S. *Angew. Chem., Int. Ed.* **2008**, *47*, 2538.
- (62) Chen, E. Y.-X. *Comments Inorg. Chem.* **2009**, *30*, 7.
- (63) Abe, H.; Imai, K.; Matsumoto, M. *J. Polym. Sci., Part C* **1968**, *23*, 469.
- (64) Abe, H.; Imai, K.; Matsumoto, M. *J. Polym. Sci., Part B* **1965**, *3*, 1053.
- (65) Simionescu, Cr.; Asandei, N.; Benedek, A. I.; Ungureanu, C. *Eur. Polym. J.* **1969**, *5*, 449.
- (66) Ballard, D. G. H.; van Lienden, P. W. *Makromol. Chem.* **1972**, *154*, 177.
- (67) Farnham, W. B.; Hertler, W. U.S. Patent 4,728,706, 1988.
- (68) Yasuda, H.; Yamamoto, H.; Yokota, K.; Miyake, S.; Nakamura, A. *J. Am. Chem. Soc.* **1992**, *114*, 4908.
- (69) Collins, S.; Ward, S. G. *J. Am. Chem. Soc.* **1992**, *114*, 5460.
- (70) Hatada, K.; Kitayama, T.; Ute, K. *Prog. Polym. Sci.* **1988**, *13*, 189.
- (71) Ewen, J. A. *J. Am. Chem. Soc.* **1984**, *106*, 6355.
- (72) Quirk, R. P.; Lee, B. *Polym. Int.* **1992**, *27*, 359.
- (73) IUPAC Compendium of Chemical Terminology, electronic version, <http://goldbook.iupac.org/S05995.html>.
- (74) IUPAC Compendium of Chemical Terminology, electronic version, <http://goldbook.iupac.org/S05989.html>.
- (75) Odian, G. *Principles of Polymerization*, 4th ed.; John Wiley & Sons: Hoboken, NJ, 2004; p 624.
- (76) Caporaso, L.; Gracia-Budria, J.; Cavallo, L. *J. Am. Chem. Soc.* **2006**, *128*, 16649.
- (77) Caporaso, L.; Cavallo, L. *Macromolecules* **2008**, *41*, 3439.
- (78) Davis, T. P.; Haddleton, D. M.; Richards, S. N. *J. Macromol. Sci. Rev. Macromol. Chem. Phys.* **1994**, *C34*, 243–324.
- (79) Ouchi, M.; Terashima, T.; Sawamoto, M. *Acc. Chem. Res.* **2008**, *41*, 1120.
- (80) Kamigaito, M.; Ando, T.; Sawamoto, M. *Chem. Rev.* **2001**, *101*, 3689.
- (81) Braunecker, W. A.; Matyjaszewski, K. *Prog. Polym. Sci.* **2007**, *32*, 93.
- (82) Baskaran, D.; Müller, A. H. E. *Prog. Polym. Sci.* **2007**, *32*, 173.
- (83) Baskaran, D. *Prog. Polym. Sci.* **2003**, *28*, 521.
- (84) Vlček, P.; Lochmann, L. *Prog. Polym. Sci.* **1999**, *24*, 793.
- (85) Hatada, K.; Kitayama, T.; Ute, K. *Prog. Polym. Sci.* **1988**, *13*, 189.
- (86) Beylen, M. V.; Bywater, S.; Smets, G.; Szwarc, M.; Worsfold, D. J. *Adv. Polym. Sci.* **1988**, *86*, 87.
- (87) Yasuda, H.; Yamamoto, H.; Yamashita, M.; Yokota, K.; Nakamura, A.; Miyake, S.; Kai, Y.; Kanehisa, N. *Macromolecules* **1993**, *26*, 7134.
- (88) Ni, X. F.; Shen, Z. Q.; Yasuda, H. *Chin. Chem. Lett.* **2001**, *12*, 821.
- (89) Yasuda, H.; Nakayama, Y.; Satoh, Y.; Shen, Z.; Ni, X.; Inoue, M.; Namba, S. *Polym. Int.* **2004**, *53*, 1682.
- (90) Barros, N.; Schappacher, M.; Dessuge, P.; Maron, L.; Guillaume, S. *Chem.—Eur. J.* **2008**, *14*, 1881.
- (91) Odian, G. *Principles of Polymerization*, 4th ed.; John Wiley & Sons, Inc.: Hoboken, NJ, 2004; pp 640 and 699.
- (92) Satoh, Y.; Ikitake, N.; Nakayama, Y.; Okuno, S.; Yasuda, H. *J. Organomet. Chem.* **2003**, *667*, 42.
- (93) Mao, L.; Shen, Q.; Sun, J. *J. Organomet. Chem.* **1998**, *566*, 9.
- (94) Mal, L.; Shen, Q. *J. Polym. Chem., Part A: Polym. Chem.* **1998**, *36*, 1593.
- (95) Shen, Q.; Wang, Y.; Zhang, K.; Yao, Y. *J. Polym. Chem., Part A: Polym. Chem.* **2002**, *40*, 612.
- (96) Wang, Y.; Shen, Q.; Xue, F.; Yu, K. *J. Organomet. Chem.* **2000**, *598*, 359.
- (97) Qian, Y.; Bala, M. D.; Yousaf, M.; Zhang, H.; Huang, J.; Sun, J.; Liang, C. *J. Organomet. Chem.* **2002**, *188*, 1.
- (98) Jiang, G. J.; Hwu, J. M. *J. Polym. Sci., A: Polym. Chem.* **2000**, *38*, 1184.
- (99) Xie, X.; Huang, J. *Appl. Organomet. Chem.* **2004**, *18*, 282.
- (100) Xie, X.; Huang, J. *Appl. Organomet. Chem.* **2009**, *23*, 1.
- (101) Zhou, L.; Yao, Y.; Li, C.; Zhang, Y.; Shen, Q. *Organometallics* **2006**, *25*, 2880.
- (102) Zhou, L.; Sheng, H.; Yao, Y.; Zhang, Y.; Shen, Q. *J. Organomet. Chem.* **2007**, *692*, 2990.
- (103) Gridnev, A. A.; Ittel, S. D. *Chem. Rev.* **2001**, *101*, 3611.
- (104) Nodono, M.; Tokimitsu, T.; Tone, S.; Makino, T.; Yanagase, A. *Macromol. Chem. Phys.* **2000**, *201*, 2282.
- (105) Yamamoto, H.; Yasuda, H.; Yokota, K.; Nakamura, A.; Kai, Y.; Kasai, N. *Chem. Lett.* **1988**, 1963.
- (106) Boffa, L. S.; Novak, B. M. *Macromolecules* **1994**, *27*, 6993.
- (107) Boffa, L. S.; Novak, B. M. *J. Mol. Catal., A: Chem.* **1998**, *133*, 123.
- (108) Boffa, L. S.; Novak, B. M. *Macromolecules* **1997**, *30*, 3494.
- (109) Barbier-Baudry, D.; Bouyer, F.; Bruno, A. S. M.; Visseaux, M. *Appl. Organomet. Chem.* **2006**, *20*, 24.
- (110) Knjazhanski, S. Y.; Elizalde, L.; Gadenas, G.; Bulychiev, B. M. *J. Polym. Chem., Part A: Polym. Chem.* **1998**, *36*, 1599.
- (111) Knjazhanski, S. Y.; Elizalde, L.; Gadenas, G.; Bulychiev, B. M. *J. Organomet. Chem.* **1998**, *568*, 33.
- (112) Sheng, E.; Zhou, S.; Wang, S.; Yang, G.; Wu, Y.; Feng, Y.; Mao, L.; Huang, Z. *Eur. J. Inorg. Chem.* **2004**, 2923.
- (113) Wang, S.; Feng, Y.; Mao, L.; Sheng, E.; Yang, G.; Xie, M.; Wang, S.; Wei, Y.; Huang, Z. *J. Organomet. Chem.* **2006**, *691*, 1265.
- (114) Wang, S.; Tang, X.; Vega, A.; Saillard, J.-Y.; Zhou, S.; Yang, G.; Yao, W.; Wei, Y. *Organometallics* **2007**, *26*, 1512.

- (115) Wei, Y.; Yu, Z.; Wang, S.; Zhou, S.; Yang, G.; Zhang, L.; Chen, G.; Qian, H.; Fan, J. *J. Organomet. Chem.* **2008**, *693*, 2263.
- (116) Kirillov, E.; Lehmann, C. W.; Razavi, A.; Carpentier, J.-F. *Organometallics* **2004**, *23*, 2768.
- (117) Qian, C.; Nie, W.; Chen, Y.; Sun, J. *J. Organomet. Chem.* **2002**, *645*, 82.
- (118) Lee, M. H.; Hwang, J.-W.; Kim, Y.; Kim, J.; Han, Y.; Do, Y. *Organometallics* **1999**, *18*, 5124.
- (119) Nie, W.; Qian, C.; Chen, Y.; Sun, J. *J. Organomet. Chem.* **2002**, *647*, 114.
- (120) Qian, C.; Nie, W.; Sun, J. *Organometallics* **2000**, *19*, 4134.
- (121) Yasuda, H.; Ihara, E. *Macromol. Chem. Phys.* **1995**, *196*, 2417.
- (122) Qian, C.; Zou, G.; Chen, Y.; Sun, J. *Organometallics* **2001**, *20*, 3106.
- (123) Qian, C.; Zou, G.; Jiang, W.; Chen, Y.; Sun, J.; Li, N. *Organometallics* **2004**, *23*, 4980.
- (124) Sun, J.; Pan, Z.; Yang, S. *J. Appl. Polym. Sci.* **2001**, *79*, 2245.
- (125) Sun, J.; Pan, Z.; Yu, Z.; Hu, W.; Yang, S. *Eur. Polym. J.* **2000**, *36*, 2375.
- (126) Giardello, M. A.; Yamamoto, Y.; Brard, L.; Marks, T. J. *J. Am. Chem. Soc.* **1995**, *117*, 3276.
- (127) Tanaka, K.; Furo, M.; Ihara, E.; Yasuda, H. *J. Polym. Sci., Part A: Polym. Chem.* **2001**, *39*, 1382.
- (128) Okuda, J. *Dalton Trans.* **2003**, 2367.
- (129) Kirillov, E.; Toupet, L.; Lehmann, C. W.; Razavi, A.; Carpentier, J.-F. *Organometallics* **2003**, *22*, 4467.
- (130) Zi, G.; Li, H.-W.; Xie, Z. *Organometallics* **2002**, *21*, 1136.
- (131) Yao, Y.; Zhang, Y.; Zhang, Z.; Shen, Q.; Yu, K. *Organometallics* **2003**, *22*, 2876.
- (132) Fabri, F.; Mutterle, R. B.; de Oliveira, W.; Schuchardt, U. *Polymer* **2006**, *47*, 4544.
- (133) Qi, G.; Nitto, Y.; Saiki, A.; Tomohiro, T.; Nakayama, Y.; Yasuda, H. *Tetrahedron* **2003**, *59*, 10409.
- (134) Gauvin, R.; Mortreux, A. *Chem. Commun.* **2005**, 1146.
- (135) Zhou, S.; Wang, S.; Yang, G.; Liu, X.; Wheng, E.; Zhang, K.; Cheng, L.; Huang, Z. *Polyhedron* **2003**, *22*, 1019.
- (136) Karl, M.; Seybert, G.; Massa, W.; Harms, K.; Agarwal, S.; Maleika, R.; Stelter, W.; Greiner, A.; Heitz, W.; Neumuller, B.; Dehnicke, K. *Z. Anorg. Allg. Chem.* **1999**, *625*, 1301.
- (137) Cui, C.; Shafir, A.; Reeder, C. L.; Arnold, J. *Organometallics* **2003**, *22*, 3357.
- (138) Xiang, L.; Wang, Q.; Song, H.; Zi, G. *Organometallics* **2007**, *26*, 5323.
- (139) Wang, Q.; Xiang, L.; Zi, G. *J. Organomet. Chem.* **2008**, *693*, 68.
- (140) Ahmed, S. A.; Hill, M. S.; Hitchcock, P. B.; Mansell, S. M.; St. John, O. *Organometallics* **2007**, *26*, 538.
- (141) Eppinger, J.; Nikolaidis, K. R.; Zhang-Presse, M.; Riederer, F. A.; Rabe, G. W.; Rheingold, A. L. *Organometallics* **2008**, *27*, 736.
- (142) Fang, X.; Deng, Y.; Xie, Q.; Moingeon, F. *Organometallics* **2008**, *27*, 2892.
- (143) Yao, Y.; Luo, Y.; Chen, J.; Zhang, Z.; Zhang, Y.; Shen, Q. *J. Organomet. Chem.* **2003**, *679*, 229.
- (144) Yuan, F.; Zhu, Y.; Xiong, L. *J. Organomet. Chem.* **2006**, *691*, 3377.
- (145) Skvortsov, G. G.; Yakovenko, M. V.; Fukin, G. K.; Cherkasov, A. V.; Trifonov, A. A. *Russ. Chem. Bull. Int. Ed.* **2007**, *56*, 1742.
- (146) Yao, Y.; Zhang, Z.; Peng, H.; Zhang, Y.; Shen, Q.; Lin, J. *Inorg. Chem.* **2006**, *45*, 2175.
- (147) Gamer, M. T.; Rastätter, M.; Roesky, P. W.; Steffens, A.; Glanz, M. *Chem.—Eur. J.* **2005**, *11*, 3165.
- (148) Bonnet, F.; Hillier, A.; Collins, A.; Dubberley, S. R.; Mountford, P. *Dalton Trans.* **2005**, 421.
- (149) Luo, Y.; Yao, Y.; Li, W.; Chen, J.; Zhang, Z.; Zhang, Y.; Shen, Q. *J. Organomet. Chem.* **2003**, *679*, 125.
- (150) Nakayama, Y.; Shibahara, T.; Fukumoto, H.; Nakamura, A.; Mashima, K. *Macromolecules* **1996**, *29*, 8014.
- (151) Estler, F.; Eickering, G.; Herdtweck, E.; Anwander, R. *Organometallics* **2003**, *22*, 1212.
- (152) Ihara, E.; Koyama, K.; Yasuda, H.; Kanehisa, N.; Kai, Y. *J. Organomet. Chem.* **1999**, *574*, 40.
- (153) Cui, P.; Chen, Y.; Zeng, X.; Sun, J.; Li, G.; Xia, W. *Organometallics* **2007**, *26*, 6519.
- (154) Goshō, A.; Nomura, R.; Tomita, I.; Endo, T. *Macromol. Chem. Phys.* **2001**, *202*, 1614.
- (155) Hu, J.; Qi, G.; Shen, Q. *Yingyong Huaxue* **1995**, *12*, 94.
- (156) Nodono, M.; Tokimitsu, T.; Makino, T. *Macromol. Chem. Phys.* **2003**, *204*, 877.
- (157) Woodman, T. J.; Schormann, M.; Hughes, D. L.; Bochmann, M. *Organometallics* **2003**, *22*, 3028.
- (158) Woodman, T. J.; Schormann, M.; Bochmann, M. *Organometallics* **2003**, *22*, 2938.
- (159) Woodman, T. J.; Schormann, M.; Hughes, D. L.; Bochmann, M. *Organometallics* **2004**, *23*, 2972.
- (160) Simpson, C. K.; White, R. F.; Carlson, C. N.; Wroblewski, D. A.; Kuehl, C. J.; Croce, T. A.; Steele, I. M.; Scott, B. L.; Young, V. G., Jr.; Hanusa, T. P.; Sattelberger, A. P.; John, K. D. *Organometallics* **2005**, *24*, 3685.
- (161) Li, Y.; Ward, D. G.; Reddy, S. S.; Collins, S. *Macromolecules* **1997**, *30*, 1875.
- (162) Sustmann, R.; Sicking, W.; Bandermann, F.; Ferenz, M. *Macromolecules* **1999**, *32*, 4204.
- (163) Bandermann, F.; Ferenz, M.; Sustmann, R.; Sicking, W. *Macromol. Symp.* **2000**, *161*, 127.
- (164) Bandermann, F.; Ferenz, M.; Sustmann, R.; Sicking, W. *Macromol. Symp.* **2001**, *174*, 247.
- (165) Ferenz, M.; Bandermann, F.; Sustmann, R.; Sicking, W. *Macromol. Chem. Phys.* **2004**, *205*, 1196.
- (166) Stojcevic, G.; Kim, H.; Taylor, N. J.; Marder, T. B.; Collins, S. *Angew. Chem., Int. Ed.* **2004**, *43*, 5523.
- (167) Lian, B.; Toupet, L.; Carpentier, J.-F. *Chem.—Eur. J.* **2004**, *10*, 4301.
- (168) Lian, B.; Lehmann, C. W.; Navarro, C.; Carpentier, J.-F. *Organometallics* **2005**, *24*, 2466.
- (169) Ning, Y.; Cooney, M. J.; Chen, E. Y.-X. *J. Organomet. Chem.* **2005**, *690*, 6263.
- (170) Shiono, T.; Saito, T.; Saegusa, N.; Hagihara, H.; Ikeda, T.; Deng, H.; Soga, K. *Macromol. Chem. Phys.* **1998**, *199*, 1573.
- (171) Chen, Y.-X.; Metz, M. V.; Li, L.; Stern, C. L.; Marks, T. J. *J. Am. Chem. Soc.* **1998**, *120*, 6287.
- (172) Wang, C.; Luo, H.-K.; van Meurs, M.; Stubbs, L. P.; Wong, P.-K. *Organometallics* **2008**, *27*, 2908.
- (173) Soga, K.; Deng, H.; Yano, T.; Shiono, T. *Macromolecules* **1994**, *27*, 7938.
- (174) Deng, H.; Shiono, T.; Soga, K. *Macromol. Chem. Phys.* **1995**, *196*, 1971.
- (175) Patra, B. N.; Bhattacharjee, M. *J. Polym. Sci., Part A: Polym. Chem.* **2005**, *43*, 3797.
- (176) Karanikolopoulos, G.; Batis, C.; Pitsikalis, M.; Hadjichristidis, N. *Macromolecules* **2001**, *34*, 4697.
- (177) Karanikolopoulos, G.; Batis, C.; Pitsikalis, M.; Hadjichristidis, N. *Macromol. Chem. Phys.* **2003**, *204*, 831.
- (178) Cameron, P. A.; Gibson, V.; Graham, A. J. *Macromolecules* **2000**, *33*, 4329.
- (179) Saegusa, N.; Shiono, T.; Ikeda, T.; Mikami, K. *Jpn. Patent JP 10330391 A2*, 1998.
- (180) Sun, J.; Pan, Z.; Yu, Z.; Hu, W.; Yang, S. *Eur. Polym. J.* **2002**, *38*, 545.
- (181) Frauenrath, H.; Keul, H.; Höcker, H. *Macromolecules* **2001**, *34*, 14.
- (182) Hölscher, M.; Keul, H.; Höcker, H. *Macromolecules* **2002**, *35*, 8194.
- (183) Strauch, J. W.; Fauré, J.-L.; Bredeau, S.; Wang, C.; Kehr, G.; Fröhlich, R.; Luftmann, H.; Erker, G. *J. Am. Chem. Soc.* **2004**, *126*, 2089.
- (184) Deng, H.; Shiono, T.; Soga, K. *Macromolecules* **1995**, *28*, 3067.
- (185) Bolig, A. D.; Chen, E. Y.-X. *J. Am. Chem. Soc.* **2001**, *123*, 7943.
- (186) Collins, S.; Ward, D. G.; Suddaby, K. H. *Macromolecules* **1994**, *27*, 7222.
- (187) Bolig, A. D.; Chen, E. Y.-X. *J. Am. Chem. Soc.* **2004**, *126*, 4897.
- (188) Rodriguez-Delgado, A.; Chen, E. Y.-X. *Macromolecules* **2005**, *38*, 2587.
- (189) Ning, Y.; Chen, E. Y.-X. *Macromolecules* **2006**, *39*, 7204.
- (190) Rodriguez-Delgado, A.; Mariott, W. R.; Chen, E. Y.-X. *J. Organomet. Chem.* **2006**, *691*, 3490.
- (191) Hong, E.; Kim, Y.; Do, Y. *Organometallics* **1998**, *17*, 2933.
- (192) Stuhldreier, T.; Keul, H.; Höcker, H. *Macromol. Rapid Commun.* **2000**, *21*, 1093.
- (193) Hölscher, M.; Keul, H.; Höcker, H. *Chem.—Eur. J.* **2001**, *7*, 6419.
- (194) Jin, J.; Chen, E. Y.-X. *Organometallics* **2002**, *21*, 13.
- (195) Jin, J.; Mariott, W. R.; Chen, E. Y.-X. *J. Polym. Chem., Part A: Polym. Chem.* **2003**, *41*, 3132.
- (196) Razavi, A.; Thewalt, U. *J. Organomet. Chem.* **1993**, *445*, 111.
- (197) Razavi, A.; Ferrara, J. *J. Organomet. Chem.* **1992**, *435*, 299.
- (198) Ewen, J. A.; Jones, R. L.; Razavi, A.; Ferrara, J. D. *J. Am. Chem. Soc.* **1988**, *110*, 6255.
- (199) Ning, Y.; Chen, E. Y.-X. *J. Am. Chem. Soc.* **2008**, *130*, 2463.
- (200) Shapiro, P. J.; Cotter, W. D.; Schaefer, W. P.; Labinger, J. A.; Bercaw, J. E. *J. Am. Chem. Soc.* **1994**, *116*, 4623.
- (201) Okuda, J. *Comments Inorg. Chem.* **1994**, *16*, 185.
- (202) Okuda, J. *Chem. Ber.* **1990**, *123*, 1649.
- (203) Shapiro, P. J.; Bunel, E.; Schaefer, W. P.; Bercaw, J. E. *Organometallics* **1990**, *9*, 867.
- (204) Piers, W. E.; Shapiro, P. J.; Bunel, E.; Bercaw, J. E. *Synlett* **1990**, *2*, 74.
- (205) Brauschweig, H.; Breiting, F. M. *Coord. Chem. Rev.* **2006**, *250*, 2691.
- (206) Chum, P. S.; Kruper, W. J.; Guest, M. J. *Adv. Mater.* **2000**, *12*, 1759.
- (207) McKnight, A. L.; Waymouth, R. M. *Chem. Rev.* **1998**, *98*, 2587.
- (208) Stevens, J. C. *Stud. Surf. Sci. Catal.* **1996**, *101*, 11–20; **1994**, *89*, 277.
- (209) Nguyen, H.; Jarvis, A. P.; Lesley, M. J. G.; Kelly, W. M.; Reddy, S. S.; Taylor, N. J.; Collins, S. *Macromolecules* **2000**, *33*, 1508.

- (210) Rodriguez-Delgado, A.; Mariott, W. R.; Chen, E. Y.-X. *Macromolecules* **2004**, *37*, 3092.
- (211) Jin, J.; Wilson, D. R.; Chen, E. Y.-X. *Chem. Commun.* **2002**, 708.
- (212) Lian, B.; Thomas, C. M.; Navarro, C.; Carpentier, J.-F. *Organometallics* **2007**, *26*, 187.
- (213) Ning, Y.; Caporaso, L.; Correa, A.; Gustafson, L. O.; Cavallo, L.; Chen, E. Y.-X. *Macromolecules* **2008**, *41*, 6910.
- (214) Severn, J. R.; Chadwick, J. C.; Duchateau, R.; Friederichs, N. *Chem. Rev.* **2005**, *105*, 4073.
- (215) Mariott, W. R.; Chen, E. Y.-X. *J. Am. Chem. Soc.* **2003**, *125*, 15726.
- (216) Mariott, W. R.; Escudé, N. C.; Chen, E. Y.-X. *J. Polym. Sci., Part A: Polym. Chem.* **2007**, *45*, 2581.
- (217) Kumaki, J.; Kawauchi, T.; Okoshi, K.; Kusanagi, H.; Yashima, E. *Angew. Chem., Int. Ed.* **2007**, *46*, 5348.
- (218) Serizawa, T.; Hamada, K.-I.; Akashi, M. *Nature* **2004**, *429*, 52.
- (219) Slager, J.; Domb, A. J. *Adv. Drug Delivery Rev.* **2003**, *55*, 549.
- (220) Serizawa, T.; Hamada, K.; Kitayama, T.; Fujimoto, N.; Hatada, K.; Akashi, M. *J. Am. Chem. Soc.* **2000**, *122*, 1891.
- (221) Hatada, K.; Kitayama, T.; Ute, K.; Nishiura, T. *Macromol. Symp.* **1998**, *132*, 221.
- (222) te Nijenhuis, K. *Adv. Polym. Sci.* **1997**, *130*, 67–81; 244.
- (223) Spevacek, J.; Schneider, B. *Adv. Colloid Interface Sci.* **1987**, *27*, 81.
- (224) Allen, K. A.; Gowenlock, B. G.; Lindsell, W. E. *J. Polym. Sci., Polym. Chem.* **1974**, *12*, 1131.
- (225) Li, Y.; Deng, H.; Brittain, W.; Chisholm, M. S. *Polym. Bull.* **1999**, *42*, 635.
- (226) Steffens, A.; Schumann, H. *Macromol. Symp.* **2006**, *236*, 203.
- (227) Mashima, K.; Matsuo, Y.; Tani, K. *Proc. Jpn. Acad.* **1998**, *74B*, 217.
- (228) Mashima, K. *Macromol. Symp.* **2000**, *159*, 69.
- (229) Matsuo, Y.; Mashima, K.; Tani, K. *Angew. Chem., Int. Ed. Engl.* **2001**, *40*, 960.
- (230) Feng, S.; Roof, G. R.; Chen, E. Y.-X. *Organometallics* **2002**, *21*, 832.
- (231) Mariott, W. R.; Gustafson, L. O.; Chen, E. Y.-X. *Organometallics* **2006**, *25*, 3765.
- (232) Mariott, W. R.; Hayden, L. M.; Chen, E. Y.-X. *ACS Symp. Ser.* **2003**, *857*, 101.
- (233) Sánchez-Nieves, J.; Royo, P. *Organometallics* **2007**, *26*, 2880.
- (234) Chakraborty, D.; Chen, E. Y.-X. *Organometallics* **2003**, *22*, 769.
- (235) Baskaran, D. *Prog. Polym. Sci.* **2003**, *28*, 521.
- (236) Vlček, P.; Lochmann, L. *Prog. Polym. Sci.* **1999**, *24*, 793.
- (237) Fayt, R.; Forte, R.; Jacobs, C.; Jérôme, R.; Ouhadi, T.; Teyssié, Ph.; Varshney, S. K. *Macromolecules* **1987**, *20*, 1442.
- (238) Varshney, S. K.; Hautekeer, J. P.; Fayt, R.; Jérôme, R.; Teyssié, Ph. *Macromolecules* **1990**, *23*, 2618.
- (239) Baskaran, D.; Sivaram, S. *Macromolecules* **1997**, *30*, 1550.
- (240) Vlček, P.; Otoupalová, J.; Janata, M.; Polická, P.; Masař, B.; Toman, L. *Polymer* **2002**, *43*, 7179.
- (241) Dvořánek, L.; Vlček, P. *Macromolecules* **1994**, *27*, 4881.
- (242) Vlček, P.; Otoupalová, J.; Janata, M.; Látalová, P.; Kurková, D.; Toman, L.; Masař, B. *Macromolecules* **2004**, *37*, 344.
- (243) Zundel, T.; Teyssié, Ph.; Jérôme, R. *Macromolecules* **1998**, *31*, 2433.
- (244) Zune, C.; Zundel, T.; DuBois, P.; Teyssié, Ph.; Jérôme, R. *J. Polym. Sci., Part A: Polym. Chem.* **1999**, *37*, 2525.
- (245) Kitaura, T.; Kitayama, T. *Macromol. Rapid Commun.* **2007**, *28*, 1889.
- (246) Honeyman, G. W.; Kennedy, A. R.; Mulvey, R. E.; Sherrington, D. C. *Organometallics* **2004**, *23*, 1197.
- (247) Hatada, K.; Ute, K.; Tanaka, K. *Polym. J.* **1986**, *18*, 1037.
- (248) Hatada, K.; Ute, K.; Tanaka, K. *Polym. J.* **1985**, *17*, 977.
- (249) Hatada, K.; Nakanishi, H.; Ute, K. *Polym. J.* **1986**, *18*, 581.
- (250) Dove, A. P.; Gibson, V. C.; Marshall, E. L.; White, A. J. P.; Williams, D. J. *Chem. Commun.* **2002**, 1208.
- (251) Zheng, Z.; Elm-kaddem, M. K.; Fischmeister, C.; Roisnel, T.; Thomas, C. M.; Carpentier, J.-F.; Renaud, J.-L. *New J. Chem.* **2008**, *32*, 2150.
- (252) Hsueh, M.-L.; Ko, B.-T.; Athar, T.; Lin, C.-C.; Wu, T.-M.; Hsu, S.-F. *Organometallics* **2006**, *25*, 4144.
- (253) Kuroki, M.; Aida, T.; Inoue, S. *J. Am. Chem. Soc.* **1987**, *109*, 4737.
- (254) Aida, T.; Inoue, S. *Acc. Chem. Res.* **1996**, *29*, 39.
- (255) Arai, T.; Sato, Y.; Inoue, S. *Chem. Lett.* **1990**, 1167.
- (256) Sugimoto, H.; Inoue, S. *Adv. Polym. Sci.* **1999**, *146*, 39.
- (257) Adachi, T.; Sugimoto, H.; Aida, T.; Inoue, S. *Macromolecules* **1993**, *26*, 1238.
- (258) Kuroki, M.; Watanabe, T.; Aida, T.; Inoue, S. *J. Am. Chem. Soc.* **1991**, *113*, 5903.
- (259) Sugimoto, H.; Kuroki, M.; Watanabe, T.; Kawamura, C.; Aida, T.; Inoue, S. *Macromolecules* **1993**, *26*, 3403.
- (260) Sugimoto, H.; Aida, T.; Inoue, S. *Macromolecules* **1993**, *26*, 4751.
- (261) Cameron, P. A.; Gibson, V. C.; Irvine, D. *Angew. Chem., Int. Ed.* **2000**, *39*, 2141.
- (262) Litvinenko, G.; Müller, A. H. E. *Macromolecules* **1997**, *30*, 1253.
- (263) Kitayama, T.; Shinozaki, T.; Sakamoto, T.; Yamamoto, M.; Hatada, K. *Makromol. Chem. Suppl.* **1989**, *15*, 167.
- (264) Ballard, D. G. H.; Bowles, R. J.; Haddleton, D. M.; Richards, S. N.; Sellens, R.; Twose, D. L. *Macromolecules* **1992**, *25*, 5907.
- (265) Kitayama, T.; Shinozaki, T.; Masuda, E.; Yamamoto, M.; Hatada, K. *Polym. Bull.* **1988**, *20*, 505.
- (266) Kitayama, T.; Hirano, T.; Zhang, Y.; Hatada, K. *Macromol. Symp.* **1996**, *107*, 297.
- (267) Kitayama, T.; Hirano, T.; Hatada, K. *Polym. J.* **1996**, *28*, 1110.
- (268) Kitayama, T.; Hirano, T.; Hatada, K. *Tetrahedron* **1997**, *53*, 15263.
- (269) Kitayama, T.; Tabuchi, M.; Kawauchi, T.; Hatada, K. *Polym. J.* **2002**, *43*, 7185.
- (270) Tabuchi, M.; Kawauchi, T.; Kitayama, T.; Hatada, K. *Polymer* **2002**, *34*, 370.
- (271) Schlaad, H.; Müller, A. H. E. *Macromol. Symp.* **1996**, *107*, 163.
- (272) Kunkel, D.; Müller, A. H. E.; Janata, M.; Lochmann, L. *Macromol. Symp.* **1992**, *60*, 315.
- (273) Seebach, D. *Angew. Chem., Int. Engl.* **1988**, *27*, 1624.
- (274) Seebach, D.; Amstutz, R.; Laube, T.; Schweizer, W. B.; Dunitz, J. D. *J. Am. Chem. Soc.* **1985**, *107*, 5403.
- (275) Yakimansky, A. V.; Müller, A. H. E. *J. Am. Chem. Soc.* **2001**, *123*, 4932.
- (276) Yakimansky, A. V.; Müller, A. H. E. *Macromolecules* **1999**, *32*, 1731.
- (277) Weiss, H.; Yakimansky, A. V.; Müller, A. H. E. *J. Am. Chem. Soc.* **1996**, *118*, 8897.
- (278) Kříž, J.; Dybal, J.; Vlček, P.; Janata, M. *Macromol. Chem. Phys.* **1994**, *195*, 3039.
- (279) Wang, J. S.; Jérôme, R.; Warin, R.; Teyssié, Ph. *Macromolecules* **1993**, *26*, 1402.
- (280) Halaska, V.; Lochmann, L. *Collect. Czech. Chem. Commun.* **1973**, *38*, 1780.
- (281) Schlaad, H.; Müller, A. H. E. *Macromol. Rapid Commun.* **1994**, *15*, 517.
- (282) Schlaad, H.; Müller, A. H. E. *Macromol. Symp.* **1995**, *95*, 13.
- (283) Schmitt, B.; Schlaad, H.; Müller, A. H. E.; Mathiasch, B.; Steiger, S.; Weiss, H. *Macromolecules* **1999**, *32*, 8340.
- (284) Peace, R. J.; Horton, M. J.; Péron, G. L. N.; Holmes, A. B. *Macromolecules* **2001**, *34*, 8409.
- (285) Péron, G. L. N.; Peace, R. J.; Holmes, A. B. *J. Mater. Chem.* **2001**, *11*, 2915.
- (286) Rodriguez-Delgado, A.; Chen, E. Y.-X. *J. Am. Chem. Soc.* **2005**, *127*, 961.
- (287) Ning, Y.; Zhu, H.; Chen, E. Y.-X. *J. Organomet. Chem.* **2007**, *692*, 4535.
- (288) Webster, O. W.; Hertler, W. R.; Sogah, D. Y.; Farnham, W. B.; RajanBabu, T. V. *J. Am. Chem. Soc.* **1983**, *105*, 5706.
- (289) Sogah, D. Y.; Hertler, W. R.; Webster, O. W.; Cohen, G. M. *Macromolecules* **1987**, *20*, 1473.
- (290) Webster, O. W. *Adv. Polym. Sci.* **2004**, *167*, 1.
- (291) Quirk, R. P.; Bidinger, G. P. *Polym. Bull.* **1989**, *22*, 63.
- (292) Quirk, R. P.; Kim, J.-S. *J. Phys. Org. Chem.* **1995**, *8*, 242.
- (293) Müller, A. H. E.; Litvinenko, G.; Yan, D. *Macromolecules* **1996**, *29*, 2346.
- (294) Scholten, M. D.; Hedrick, J. L.; Waymouth, R. M. *Macromolecules* **2008**, *41*, 7399.
- (295) Raynaud, J.; Ciolino, A.; Baceiredo, A.; Destarac, M.; Bonnette, F.; Kato, T.; Gnanou, Y.; Taton, D. *Angew. Chem., Int. Ed.* **2008**, *47*, 5390.
- (296) Dicker, I. B.; Cohen, G. M.; Farnham, W. B.; Hertler, W. R.; Laganis, E. D.; Sogah, D. Y. *Macromolecules* **1990**, *23*, 4034.
- (297) Hertler, W. R.; Sogah, D. Y.; Webster, O. W.; Trost, B. M. *Macromolecules* **1984**, *17*, 1415.
- (298) Zhuang, R.; Müller, A. H. E. *Macromolecules* **1995**, *28*, 8043.
- (299) Ute, K.; Ohnuma, H.; Kitayama, T. *Polym. J.* **2000**, *32*, 1060.
- (300) Zhang, Y.; Chen, E. Y.-X. *Macromolecules* **2008**, *41*, 36.
- (301) Zhang, Y.; Chen, E. Y.-X. *Macromolecules* **2008**, *41*, 6353.
- (302) Lian, B.; Spanio, T. P.; Okuda, J. *Organometallics* **2007**, *26*, 6653.
- (303) Yong, T.-M.; Holmes, A. B.; Taylor, P. L.; Robinson, J.; Segal, J. A. *Chem. Commun.* **1996**, 863.
- (304) Arteaga-Müller, R.; Sánchez-Nieves, J.; Ramos, J.; Royo, P.; Mosquera, M. E. G. *Organometallics* **2008**, *27*, 1417.
- (305) Kim, I.; Hwang, J.-M.; Lee, J. K.; Ha, C. S.; Woo, S. I. *Macromol. Rapid Commun.* **2003**, *24*, 508.
- (306) Fullana, M. J.; Miri, M. J.; Vadhavkar, S. S.; Kolhatkar, N.; Delis, A. C. *J. Polym. Sci., Part A: Polym. Chem.* **2008**, *46*, 5542.
- (307) Bahuleyan, B. K.; Kim, J. H.; Seo, H. S.; Oh, J. M.; Ahn, I. Y.; Ha, C.-S.; Park, D.-W.; Kim, I. *Catal. Lett.* **2008**, *126*, 371.
- (308) Huang, Y.-B.; Tang, G.-R.; Jin, G.-Y.; Jin, G.-X. *Organometallics* **2008**, *27*, 259.
- (309) Tang, G.-R.; Jin, G.-X. *Dalton Trans.* **2007**, 3840.
- (310) Li, X.-F.; Li, Y.-G.; Li, Y.-S.; Chen, Y.-X.; Hu, N.-H. *Organometallics* **2005**, *24*, 2502.
- (311) He, X.; Yao, Y.; Luo, X.; Zhang, J.; Liu, Y.; Zhang, L.; Wu, Q. *Organometallics* **2003**, *22*, 4952.

- (312) Carlini, C.; de Luise, V.; Martinelli, M.; Galletti, A. M. R.; Sbrana, G. *J. Polym. Sci., Part A: Polym. Chem.* **2006**, *44*, 620.
- (313) Carlini, C.; Martinelli, M.; Galletti, A. M. R.; Sbrana, G. *J. Polym. Sci., Part A: Polym. Chem.* **2003**, *41*, 2117.
- (314) Carlini, C.; Martinelli, M.; Galletti, A. M. R.; Sbrana, G. *Macromol. Chem. Phys.* **2002**, *203*, 1606.
- (315) Carlini, C.; Martinelli, M.; Galletti, A. M. R.; Sbrana, G. *J. Polym. Sci., Part A: Polym. Chem.* **2003**, *41*, 1716.
- (316) Carlini, C.; Martinelli, M.; Passaglia, E.; Galletti, A. M. R.; Sbrana, G. *Macromol. Rapid Commun.* **2001**, *22*, 664.
- (317) Hu, Y.-J.; Zou, H. H.; Zeng, M.-H.; Weng, N. S. *J. Organomet. Chem.* **2009**, *694*, 366.
- (318) Endo, K.; Inukai, A. *Polym. Int.* **2000**, *49*, 110.
- (319) Coutinho, F. M. B.; Costa, M. A. S.; Monteiro, L. F.; de Santa Maria, L. C. *Polym. Bull.* **1997**, *38*, 303.
- (320) Endo, K.; Inukai, A.; Otsu, T. *Macromol. Rapid Commun.* **1994**, *15*, 893.
- (321) Endo, K. *Macromol. Chem. Phys.* **1999**, *200*, 1722.
- (322) Endo, K.; Yamanaka, Y. *Macromol. Rapid Commun.* **2000**, *21*, 785.
- (323) Ihara, E.; Fujimura, T.; Yasuda, H.; Maruo, T.; Kanehisa, N. *J. Polym. Sci., Part A: Polym. Chem.* **2000**, *38*, 4764.
- (324) Ihara, E.; Maeno, Y.; Yasuda, H. *Macromol. Chem. Phys.* **2001**, *202*, 1518.
- (325) Wang, L.; Cao, D.; Wu, Q. *Eur. Polym. J.* **2009**, *45*, 1820.
- (326) Galletti, A. M. R.; Carlini, C.; Giaiacopi, S.; Martinelli, M.; Sbrana, G. *J. Polym. Sci., Part A: Polym. Chem.* **2007**, *45*, 1134.
- (327) Stibrany, R. T.; Schulz, D. N.; Kacker, S.; Patil, A. O.; Baugh, L. S.; Rucker, S. P.; Zushma, S.; Berluche, E.; Sissano, J. A. *Macromolecules* **2003**, *36*, 8584.
- (328) Baugh, L. S.; Sissano, J. A.; Kacker, S.; Berluche, E.; Stibrany, R. T.; Schulz, D. N.; Rucker, S. P. *J. Polym. Sci., Part A: Polym. Chem.* **2006**, *44*, 1817.
- (329) Tian, G.; Boone, H. W.; Novak, B. M. *Macromolecules* **2001**, *34*, 7656.
- (330) Nagel, M.; Paxton, W. F.; Sen, A.; Zakharov, L.; Rheingold, A. L. *Macromolecules* **2004**, *37*, 9305.
- (331) Wu, B.; Lenz, R. W.; Hazer, B. *Macromolecules* **1999**, *32*, 6856.
- (332) Ihara, E.; Omura, N.; Tanaka, S.; Itoh, T.; Inoue, K. *J. Polym. Sci., Part A: Polym. Chem.* **2005**, *43*, 4405.
- (333) Mardare, D.; Matyjaszewski, K. *Macromol. Chem. Phys.* **1995**, *196*, 399.
- (334) Ihara, E.; Todaka, T.; Inoue, K. *J. Polym. Sci., Part A: Polym. Chem.* **2004**, *42*, 31.
- (335) Ihara, E.; Todaka, T.; Inoue, K. *J. Polym. Sci., Part A: Polym. Chem.* **2003**, *41*, 1962.
- (336) Ihara, E.; Todaka, T.; Inoue, K. *Macromol. Rapid Commun.* **2002**, *23*, 64.
- (337) Ihara, E.; Morimoto, M.; Yasuda, H. *Proc. Jpn. Acad.* **1995**, *71* (B), 126.
- (338) Ihara, E.; Morimoto, M.; Yasuda, H. *Macromolecules* **1995**, *28*, 7886.
- (339) Evans, W. J.; Dominguez, R.; Hanusa, T. P. *Organometallics* **1986**, *5*, 1291.
- (340) Heeres, H. J.; Maters, M.; Teuben, J. H.; Helgesson, G.; Jagner, S. *Organometallics* **1992**, *11*, 350.
- (341) Kawaguchi, Y.; Yasuda, H. *J. Appl. Polym. Sci.* **2001**, *80*, 432.
- (342) Tomasi, S.; Weiss, H.; Ziegler, T. *Organometallics* **2006**, *25*, 3619.
- (343) Hultsch, K. C.; Spaniol, T. P.; Okuda, J. *Angew. Chem., Int. Ed.* **1999**, *38*, 227.
- (344) Arndt, S.; Beckerle, K.; Hultsch, K. C.; Sinnema, P.-J.; Voth, P.; Spaniol, T. P.; Okuda, J. *J. Mol. Catal.* **2002**, *190*, 215.
- (345) Deng, H.; Soga, K. *Macromolecules* **1996**, *29*, 1847.
- (346) Kostakis, K.; Mourmouris, S.; Pitsikalis, M.; Hadjichristidis, N. *J. Polym. Sci., Part A: Polym. Chem.* **2005**, *43*, 3337.
- (347) Mariott, W. R.; Rodriguez-Delgado, A.; Chen, E. Y.-X. *Macromolecules* **2006**, *39*, 1318.
- (348) Tomasi, S.; Weiss, H.; Ziegler, T. *Organometallics* **2007**, *26*, 2157.
- (349) Lian, B.; Thomas, C. M.; Navarro, C.; Carpentier, J.-F. *Macromolecules* **2007**, *40*, 2293.
- (350) Cho, H. Y.; Tarte, N. H.; Cui, L.; Hong, D. S.; Woo, S. I.; Gong, Y.-D. *Macromol. Chem. Phys.* **2006**, *207*, 1965.
- (351) Garner, L. E.; Zhu, H.; Hlavinka, M. L.; Hagadorn, J. R.; Chen, E. Y.-X. *J. Am. Chem. Soc.* **2006**, *128*, 14822.
- (352) Mariott, W. R.; Chen, E. Y.-X. *Macromolecules* **2004**, *37*, 4741.
- (353) Mariott, W. R.; Chen, E. Y.-X. *Macromolecules* **2005**, *38*, 6822.
- (354) Miyake, G. M.; Mariott, W. R.; Chen, E. Y.-X. *J. Am. Chem. Soc.* **2007**, *129*, 6724.
- (355) Xie, X.; Hogen-Esch, T. E. *Macromolecules* **1996**, *29*, 1746.
- (356) Kodaira, T.; Tanahashi, H.; Hara, K. *Polym. J.* **1990**, *22*, 649.
- (357) Okamoto, Y.; Yuki, H. *J. Polym. Sci., Polym. Chem. Ed.* **1981**, *19*, 2647.
- (358) Suzuki, T.; Kusakabe, J.; Ishizone, T. *Macromolecules* **2008**, *41*, 1929.
- (359) Suzuki, T.; Kusakabe, J.; Ishizone, T. *Macromol. Symp.* **2007**, *249*–250, 412.
- (360) Miyake, G. M.; Caporaso, L.; Cavallo, L.; Chen, E. Y.-X. *Macromolecules* **2009**, *42*, 1462.
- (361) Eliel, A. L.; Wilen, S. H.; Mander, L. N. *Stereochemistry of Organic Compounds*; John Wiley & Sons Inc.: New York, 1994; p 266.
- (362) Farina, M. *Top. Stereochem.* **1987**, *17*, 1.
- (363) Yashima, E.; Maeda, K. *Macromolecules* **2008**, *41*, 3.
- (364) Yamamoto, C.; Okamoto, Y. *Bull. Chem. Soc. Jpn.* **2004**, *77*, 227.
- (365) Nakano, T.; Okamoto, Y. *Chem. Rev.* **2001**, *101*, 4013.
- (366) Cornelissen, J. J. L. M.; Rowan, A. E.; Nolte, R. J. M.; Sommerdijk, N. A. J. M. *Chem. Rev.* **2001**, *101*, 4029.
- (367) Okamoto, Y.; Nakano, T. *Chem. Rev.* **1994**, *94*, 349.
- (368) Okamoto, Y.; Yashima, E. *Prog. Polym. Sci.* **1990**, *15*, 263.
- (369) Wulff, G. *Angew. Chem. Int. Engl.* **1989**, *28*, 21.
- (370) Pino, P. *Adv. Polym. Sci.* **1965**, *4*, 393.
- (371) Wulff, G.; Zweering, U. *Chem.-Eur. J.* **1999**, *5*, 1898.
- (372) Miller, S. A. *Chem. Commun.* **2006**, 862.
- (373) Pino, P.; Cioni, P.; Wei, J. *J. Am. Chem. Soc.* **1987**, *109*, 6189.
- (374) Kaminsky, W.; Ahlers, A.; Möller-Lindenhof, N. *Angew. Chem., Int. Ed.* **1989**, *28*, 1216.
- (375) Pino, P.; Galimberti, M.; Prada, P.; Consiglio, G. *Makromol. Chem.* **1990**, *191*, 1677.
- (376) Kaminsky, W. *Angew. Makromol. Chem.* **1986**, *145/146*, 149.
- (377) Nakano, T.; Okamoto, Y.; Hatada, K. *J. Am. Chem. Soc.* **1992**, *114*, 1318.
- (378) Okamoto, Y.; Suzuki, K.; Ohta, K.; Hatada, K.; Yuki, H. *J. Am. Chem. Soc.* **1979**, *101*, 4763.
- (379) Shiohara, K.; Habaue, S.; Okamoto, Y. *Polym. J.* **1998**, *30*, 249.
- (380) Okamoto, Y.; Hayashida, H.; Hatada, K. *Polym. J.* **1989**, *21*, 543.
- (381) Okamoto, Y.; Adachi, M.; Shohi, H.; Yuki, H. *Polym. J.* **1981**, *13*, 175.
- (382) Yashima, E.; Maeda, K.; Furusho, Y. *Acc. Chem. Res.* **2008**, *41*, 1166.
- (383) Tang, H.-Z.; Garland, E. R.; Novak, B. M.; He, J.; Polavarapu, P. L.; Sun, F. C.; Sheiko, S. S. *Macromolecules* **2007**, *40*, 3575.
- (384) Tsuji, M.; Azam, A. K. M. F.; Kamigaito, M.; Okamoto, Y. *Macromolecules* **2007**, *40*, 3518.
- (385) Kajitani, T.; Okoshi, K.; Sakurai, S.-I.; Kumaki, J.; Yashima, E. *J. Am. Chem. Soc.* **2006**, *128*, 708.
- (386) Tang, H.-Z.; Boyle, P. D.; Novak, B. M. *J. Am. Chem. Soc.* **2005**, *127*, 2136.
- (387) Tian, G.; Lu, Y.; Novak, B. M. *J. Am. Chem. Soc.* **2004**, *126*, 4082.
- (388) Aoki, T.; Kaneko, T.; Maruyama, N.; Sumi, A.; Takahashi, M.; Sato, T.; Teraguchi, M. *J. Am. Chem. Soc.* **2003**, *125*, 6346.
- (389) Azam, A. K. M. F.; Kamigaito, M.; Okamoto, Y. *J. Polym. Sci., Part A: Polym. Chem.* **2007**, *45*, 1304.
- (390) Hoshikawa, N.; Hotta, Y.; Okamoto, Y. *J. Am. Chem. Soc.* **2003**, *125*, 12380.
- (391) Nakano, T.; Okamoto, Y. *Macromolecules* **1999**, *32*, 2391.
- (392) Nanano, T.; Shikisai, Y.; Okamoto, Y. *Polym. J.* **1996**, *28*, 51.
- (393) Wulff, G.; Petzoldt, J. *Angew. Chem., Int. Ed. Engl.* **1991**, *30*, 849.
- (394) LoCoco, M. D.; Jordan, R. F. *J. Am. Chem. Soc.* **2004**, *126*, 13918.
- (395) Miyake, G. M.; Chen, E. Y.-X. *Macromolecules* **2008**, *41*, 3405.
- (396) Ren, J.; Hu, J.; Shen, Q. *Chin. J. Appl. Chem.* **1995**, *12*, 105.
- (397) Yao, Y.; Sen, Q.; Zhang, L. *Chin. Sci. Bull.* **2001**, *46*, 1443.
- (398) Zheng, H.; Zhang, Y.; Shen, Q. *Polym. Int.* **2002**, *51*, 622.
- (399) Nakayama, Y.; Fukumoto, H.; Shibahara, T.; Nakamura, A.; Mashima, K. *Polym. Int.* **1999**, *48*, 502.
- (400) Xue, M.; Yao, Y.; Shen, Q.; Zhang, Y. *J. Organomet. Chem.* **2005**, *690*, 4685.
- (401) Jenkins, A. D.; Lappert, M. F.; Srivastava, R. C. *J. Polym. Sci., Part B: Polym. Lett.* **1968**, *6*, 865.
- (402) Billingham, N. C.; Lees, P. D. *Makromol. Chem.* **1993**, *194*, 1445.
- (403) Siemeling, U.; Kölling, L.; Stammer, A.; Stammer, H.-G.; Kaminski, E.; Fink, G. *Chem. Commun.* **2000**, 1177.
- (404) Gandhi, V. G.; Sivaram, S.; Bhardwaj, I. S. *J. Macromol. Sci.* **1983**, *A19*, 147.
- (405) Suh, M. P.; Oh, Y.-H.; Kwak, C.-H. *Organometallics* **1987**, *6*, 411.
- (406) Tsuchihara, K.; Suzuki, Y.; Asai, M.; Soga, K. *Chem. Lett.* **1999**, 891.
- (407) Tsuchihara, K.; Suzuki, Y.; Asai, M.; Soga, K. *Polym. J.* **2000**, *32*, 700.
- (408) Saegusa, T.; Horiguchi, S.; Tsuda, T. *Macromolecules* **1975**, *8*, 112.
- (409) Yamamoto, A. *J. Chem. Soc., Dalton Trans.* **1999**, 1027.
- (410) Yamamoto, A.; Yamamoto, T. *J. Polym. Sci., Macromol. Rev.* **1978**, *13*, 161.
- (411) Ikariya, T.; Yamamoto, A. *J. Organomet. Chem.* **1974**, *72*, 145.
- (412) Miyashita, A.; Yamamoto, T.; Yamamoto, A. *Bull. Chem. Soc. Jpn.* **1977**, *50*, 1109.
- (413) Yamamoto, T.; Yamamoto, A.; Ikeda, S. *Bull. Chem. Soc. Jpn.* **1972**, *45*, 1111.

- (414) Yamamoto, T.; Yamamoto, A.; Ikeda, S. *Bull. Chem. Soc. Jpn.* **1972**, *45*, 1104.
- (415) Yamamoto, T.; Yamamoto, A.; Ikeda, S. *J. Polym. Sci., Part B: Polym. Lett.* **1971**, *9*, 281.
- (416) Yamamoto, A.; Shimizu, T.; Ikeda, S. *Makromol. Chem.* **1970**, *136*, 297.
- (417) Schaper, F.; Foley, S. R.; Jordan, R. F. *J. Am. Chem. Soc.* **2004**, *126*, 2114.
- (418) Yang, P.; Chan, B. C. K.; Baird, M. C. *Organometallics* **2004**, *23*, 2752.
- (419) Wu, F.; Foley, S. R.; Burns, C. T.; Jordan, R. F. *J. Am. Chem. Soc.* **2005**, *127*, 1841.
- (420) Wu, F.; Jordan, R. F. *Organometallics* **2006**, *25*, 5631.
- (421) Groux, L. F.; Weiss, T.; Reddy, D. N.; Chase, P. A.; Piers, W. E.; Ziegler, T.; Parvez, M.; Benet-Buchholz, J. *J. Am. Chem. Soc.* **2005**, *127*, 1854.
- (422) Tsuruta, T.; Fujio, R.; Furukawa, J. *Makromol. Chem.* **1964**, *80*, 172.
- (423) Fujio, R.; Tsuruta, T.; Furukawa, J. *Makromol. Chem.* **1962**, *52*, 233.
- (424) Merle-Aubry, L.; Merle, Y.; Selegny, E. *Makromol. Chem.* **1975**, *176*, 709.
- (425) Matsuzaki, K.; Kanai, T.; Aoki, Y. *Makromol. Chem.* **1981**, *182*, 1027.
- (426) Day, P.; Eastmond, G. C.; Gilchrist, T. L.; Page, P. C. B. *J. Macromol. Sci., Part A: Pure Appl. Chem.* **1992**, *A29*, 545.
- (427) Spaether, W.; Kläß, K.; Erker, G.; Zippel, F.; Fröhlich, R. *Chem.—Eur. J.* **1998**, *4*, 1411.
- (428) Yasuda, H.; Furo, M.; Yamamoto, H.; Nakamura, A.; Miyake, S.; Kibino, N. *Macromolecules* **1992**, *25*, 5115.
- (429) Gromada, J.; Chenal, T.; Mortreux, A.; Leising, F.; Carpentier, J.-F. *J. Mol. Catal. A: Chem.* **2002**, *182/183*, 523.
- (430) Desurmont, G.; Li, Y.; Yasuda, H. *Organometallics* **2000**, *19*, 1811.
- (431) Desurmont, G.; Tokimitsu, T.; Yasuda, H. *Macromolecules* **2000**, *33*, 7679.
- (432) Ingall, M. D. K.; Joray, S. J.; Duffy, D. J.; Long, D. P.; Bianconi, P. A. *J. Am. Chem. Soc.* **2000**, *122*, 7845.
- (433) Desurmont, G.; Tanaka, M.; Li, Y.; Yasuda, H.; Tokimitsu, T. *J. Polym. Sci., Part A: Polym. Chem.* **2000**, *38*, 4095.
- (434) Imuta, J.-I.; Kashiwa, N.; Toda, Y. *J. Am. Chem. Soc.* **2002**, *124*, 1176.
- (435) Matsugi, T.; Kojoh, S.-I.; Kawahara, N.; Matsuo, S.; Kaneko, H.; Kashiwa, N. *J. Polym. Sci., Part A: Polym. Chem.* **2003**, *41*, 3965.
- (436) Inoue, Y.; Matyjaszewski, K. *J. Polym. Sci., Part A: Polym. Chem.* **2004**, *42*, 496.
- (437) Kaneyoshi, H.; Inoue, Y.; Matyjaszewski, K. *Macromolecules* **2005**, *38*, 5425.
- (438) Zhang, K.; Ye, Z.; Subramanian, R. *Macromolecules* **2008**, *41*, 640.
- (439) Doi, Y.; Koyama, T.; Soga, K. *Makromol. Chem.* **1985**, *186*, 11.
- (440) Matyjaszewski, K.; Saget, J.; Pyun, J.; Schlogl, M.; Rieger, B. *J. Macromol. Sci., Pure Appl. Chem.* **2002**, *A39*, 901.
- (441) Yi, Q.; Fan, G.; Wen, X.; Dong, J.-Y.; Han, C. C. *Macromol. React. Eng.* **2009**, *3*, 91.
- (442) Tzeng, F.-Y.; Ling, M.-C.; Wu, J.-Y.; Kuo, J.-C.; Tasi, J.-C.; Hsiao, M.-S.; Chen, H.-L.; Cheng, S. Z. D. *Macromolecules* **2009**, *42*, 3073.
- (443) Diamanti, S. J.; Khanna, V.; Hotta, A.; Yamakawa, D.; Shimizu, F.; Kramer, E. J.; Fredrickson, G. H.; Bazan, G. C. *J. Am. Chem. Soc.* **2004**, *126*, 10528.
- (444) Diamanti, S. J.; Khanna, V.; Hotta, A.; Coffin, R. C.; Yamakawa, D.; Kramer, E. J.; Fredrickson, G. H.; Bazan, G. C. *Macromolecules* **2006**, *39*, 3270.
- (445) Coffin, R. C.; Diamanti, S. J.; Hotta, A.; Khanna, V.; Kramer, E. J.; Fredrickson, G. H.; Bazan, G. C. *Chem. Commun.* **2007**, 3550.
- (446) Schneider, Y.; Azoulay, J. D.; Coffin, R. C.; Bazan, G. C. *J. Am. Chem. Soc.* **2008**, *130*, 10464.
- (447) Marques, M. M.; Correia, S. G.; Ascenso, J. R.; Ribeiro, A. F. G.; Gomes, P. T.; Dias, A. R.; Foster, P.; Rausch, M. D.; Chien, J. C. W. *J. Polym. Sci., Part A: Polym. Chem.* **1999**, *37*, 2457.
- (448) Correia, S. G.; Marques, M. M.; Ascenso, J. R.; Ribeiro, A. F. G.; Gomes, P. T.; Dias, A. R.; Blais, M.; Rausch, M. D.; Chien, J. C. W. *J. Polym. Sci., Part A: Polym. Chem.* **1999**, *37*, 2471.
- (449) Marques, M. M.; Fernandes, S.; Correia, S. G.; Ascenso, J. R.; Carço, S.; Gomes, P. T.; Mano, J.; Pereira, S.; Nunes, T.; Dias, A. R.; Rausch, M. D.; Chien, J. C. W. *Macromol. Chem. Phys.* **2001**, *201*, 2464.
- (450) Fernandes, S.; Marques, M. M.; Correia, S. G.; Mano, J.; Chien, J. C. W. *Macromol. Chem. Phys.* **2001**, *201*, 2566.
- (451) Kotzabasakis, V.; Petzetakis, N.; Pitsikalis, M.; Hadjichristidis, N.; Lohse, D. J. *J. Polym. Sci., Part A: Polym. Chem.* **2009**, *47*, 876.
- (452) Zhang, X.; Chen, S.; Li, H.; Zhang, Z.; Lu, Y. *J. Polym. Sci., Part A: Polym. Chem.* **2007**, *45*, 59.
- (453) Carone, C. L. P.; Crossetti, G. L.; Basso, N. R. S.; Moraes, A. G. O.; Dos Santos, J. H. Z.; Bisatto, R.; Galland, G. B. *J. Polym. Sci., Part A: Polym. Chem.* **2007**, *45*, 5199.
- (454) Carone, C. L. P.; Bisatto, R.; Galland, G. B.; Rojas, R.; Bazan, G. J. *Polym. Sci., Part A: Polym. Chem.* **2008**, *46*, 54.
- (455) Fernandes, M.; Kaminsky, W. *Macromol. Chem. Phys.* **2009**, *210*, 585.
- (456) Amin, S. A.; Marks, T. J. *J. Am. Chem. Soc.* **2006**, *128*, 4506.
- (457) Amin, S. A.; Marks, T. J. *J. Am. Chem. Soc.* **2007**, *129*, 2938.
- (458) Liu, J.; Nomura, K. *Macromolecules* **2008**, *41*, 1070.
- (459) Byun, D.-J.; Shin, S.-M.; Han, C. J.; Kim, S. Y. *Polym. Bull.* **1999**, *43*, 333.
- (460) Nomura, K.; Kakinuki, K.; Fujiki, M.; Itagaki, K. *Macromolecules* **2008**, *41*, 8974.
- (461) Zeigler, R.; Resconi, L.; Balbontin, G.; Guerra, G.; Venditto, V.; De Rosa, C. *Polymer* **1994**, *35*, 4648.
- (462) Habaue, S.; Baraki, H.; Okamoto, Y. *Macromol. Chem. Phys.* **1998**, *199*, 2211.
- (463) Zhang, H.-X.; Jung, M.-S.; Shin, Y.-J.; Yoon, K.-B.; Lee, D.-H. *J. Appl. Polym. Sci.* **2009**, *111*, 2697.
- (464) Zhang, H.-X.; Shin, Y.-J.; Yoon, K.-B.; Lee, D.-H. *Eur. Polym. J.* **2009**, *45*, 40.
- (465) Tsuchida, A.; Bolln, C.; Sernetz, F. G.; Frey, H.; Mühlaupt, R. *Macromolecules* **1997**, *30*, 2818.
- (466) Zheng, L.; Farris, R. J.; Coughlin, E. B. *Macromolecules* **2001**, *34*, 8034.
- (467) Seurer, B.; Coughlin, E. B. *Macromol. Chem. Phys.* **2008**, *209*, 1198.
- (468) Zhang, H.-X.; Lee, H.-Y.; Shin, Y.-J.; Yoon, K.-B.; Noh, S.-K.; Lee, D.-H. *Polym. Int.* **2008**, *57*, 1351.
- (469) Zheng, L.; Kasi, R. M.; Farris, R. J.; Coughlin, E. B. *J. Polym. Sci., Part A: Polym. Chem.* **2002**, *40*, 885.
- (470) Wang, J.; Ye, Z.; Joly, H. *Macromolecules* **2007**, *40*, 6150.
- (471) Jensen, T. R.; Yoon, S. C.; Dash, A. K.; Luo, L.; Marks, T. J. *J. Am. Chem. Soc.* **2003**, *125*, 14482.
- (472) Terao, H.; Ishii, S.; Mitani, M.; Tanaka, H.; Fujita, T. *J. Am. Chem. Soc.* **2008**, *130*, 17636.
- (473) Johnson, L. K.; Killian, C. M.; Brookhart, M. *J. Am. Chem. Soc.* **1995**, *117*, 6414.
- (474) Johnson, L. K.; Mecking, S.; Brookhart, M. *J. Am. Chem. Soc.* **1996**, *118*, 267.
- (475) Mecking, S.; Johnson, L. K.; Wang, L.; Brookhart, M. *J. Am. Chem. Soc.* **1998**, *120*, 888.
- (476) Tempel, D. J.; Johnson, L. K.; Huff, R. L.; White, P. S.; Brookhart, M. *J. Am. Chem. Soc.* **2000**, *122*, 6686.
- (477) Johnson, L.; Wang, L.; McLain, S.; Bennett, A.; Dobbs, K.; Hauptman, E.; Ionkin, A.; Itel, S.; Kunitzky, K.; Marshall, W.; McCord, E.; Radzewich, C.; Rinehart, A.; Sweetman, K. J.; Wang, Y.; Yin, Z.; Brookhart, M. *ACS Symp. Ser.* **2003**, *857*, 131.
- (478) Chen, G.; Ma, X. S.; Guan, Z. *J. Am. Chem. Soc.* **2003**, *125*, 6697.
- (479) Camacho, D. H.; Salo, E. V.; Ziller, J. W.; Guan, Z. *J. Angew. Chem., Int. Ed.* **2004**, *43*, 1821.
- (480) (a) Popeney, C. S.; Guan, Z. *J. Am. Chem. Soc.* **2009**, *131*, 12384.
(b) Popeney, C. S.; Camacho, D. H.; Guan, Z. *J. Am. Chem. Soc.* **2007**, *129*, 10062.
- (481) Luo, S.; Jordan, R. F. *J. Am. Chem. Soc.* **2006**, *128*, 12072.
- (482) Chen, C.; Luo, S.; Jordan, R. F. *J. Am. Chem. Soc.* **2008**, *130*, 12892.
- (483) Li, W.; Zhang, X.; Meetsma, A.; Hessen, B. *J. Am. Chem. Soc.* **2004**, *126*, 12246.
- (484) Younkin, T. R.; Connor, E. F.; Henderson, J. I.; Friedrich, S. K.; Grubbs, R. H.; Bansleben, D. A. *Science* **2000**, *287*, 460.
- (485) Connor, E. F.; Younkin, T. R.; Henderson, J. I.; Hwang, S.; Grubbs, R. H.; Roberts, W. P.; Litza, J. J. *J. Polym. Sci., Part A: Polym. Chem.* **2002**, *40*, 2842.
- (486) Diamanti, S. J.; Ghosh, P.; Shimizu, F.; Bazan, G. C. *Macromolecules* **2003**, *36*, 9731.
- (487) Gibson, V. C.; Tomov, A. *Chem. Commun.* **2001**, 1964.
- (488) Berkefeld, A.; Drexler, M.; Möller, H.; Mecking, S. *J. Am. Chem. Soc.* **2009**, *131*, 10.1021/ja901360b.
- (489) Rodriguez, B. A.; Delferro, M.; Marks, T. J. *J. Am. Chem. Soc.* **2009**, *131*, 5902.
- (490) Drent, E.; van Dijk, R.; van Ginkel, R.; van Oort, B.; Pugh, R. I. *Chem. Commun.* **2002**, 744.
- (491) Haras, A.; Anderson, G. D. W.; Michalak, A.; Rieger, B.; Ziegler, T. *Organometallics* **2006**, *25*, 4491.
- (492) Guironnet, D.; Rünzi, T.; Göttker-Schnetmann, I.; Mecking, S. *Chem. Commun.* **2008**, 4965.
- (493) Kochi, T.; Noda, S.; Yoshimura, K.; Nozaki, K. *J. Am. Chem. Soc.* **2007**, *129*, 8948.
- (494) Skupov, K. M.; Marella, P. R.; Simard, M.; Yap, G. P. A.; Allen, N.; Conner, D.; Goodall, B. L.; Claverie, J. P. *Macromol. Rapid Commun.* **2007**, *28*, 2033.
- (495) Claverie, J. P.; Goodall, B. L.; Skupov, K. M.; Marella, P. R.; Hobbs, J. *Polym. Prepr. (Am. Chem. Soc., Div. Polym. Chem.)* **2007**, *48*, 191.
- (496) Guironnet, D.; Rünzi, T.; Göttker-Schnetmann, I.; Mecking, S. *J. Am. Chem. Soc.* **2009**, *131*, 422.

- (497) Skupov, K. M.; Piche, L.; Claverie, J. P. *Macromolecules* **2008**, *41*, 2309.
- (498) Borkar, S.; Newsham, D. K.; Sen, A. *Organometallics* **2008**, *27*, 3331.
- (499) Liu, S.; Borkar, S.; Newsham, D. K.; Yennawar, H.; Sen, A. *Organometallics* **2007**, *26*, 210.
- (500) Luo, S.; Vela, J.; Lief, G. R.; Jordan, R. F. *J. Am. Chem. Soc.* **2007**, *129*, 8946.
- (501) Stockland, R. A., Jr.; Foley, S. R.; Jordan, R. F. *J. Am. Chem. Soc.* **2003**, *125*, 796.
- (502) Foley, S. R.; Stockland, R. A., Jr.; Shen, H.; Jordan, R. F. *J. Am. Chem. Soc.* **2003**, *125*, 4350.
- (503) Boone, H. W.; Athey, P. S.; Mullins, M. J.; Philipp, D.; Muller, R.; Goddard, W. A. *J. Am. Chem. Soc.* **2002**, *124*, 8790.
- (504) Strazisar, S. A.; Wolczanski, P. T. *J. Am. Chem. Soc.* **2001**, *123*, 4728.
- (505) Kang, M.; Sen, A.; Zakharov, L.; Rheingold, A. L. *J. Am. Chem. Soc.* **2002**, *124*, 12080.
- (506) Watson, L. A.; Yandulov, D. V.; Caulton, K. G. *J. Am. Chem. Soc.* **2001**, *123*, 603.
- (507) Gaynor, S. G. *Macromolecules* **2003**, *36*, 4692.
- (508) Foley, S. R.; Shen, H.; Qadeer, U. A.; Jordan, R. F. *Organometallics* **2004**, *23*, 600.
- (509) Weng, W.; Shen, Z.; Jordan, R. F. *J. Am. Chem. Soc.* **2007**, *129*, 15450.
- (510) Kochi, T.; Noda, S.; Yoshimura, K.; Nozaki, K. *J. Am. Chem. Soc.* **2007**, *129*, 8948.
- (511) Drent, E.; van Dijk, R.; van Ginkel, R.; van Oort, B.; Pugh, R. I. *Chem. Commun.* **2002**, 964.
- (512) Kochi, T.; Nakamura, A.; Ida, H.; Nozaki, K. *J. Am. Chem. Soc.* **2007**, *129*, 7770.
- (513) Nakamura, A.; Munakata, K.; Kochi, T.; Nozaki, K. *J. Am. Chem. Soc.* **2008**, *130*, 8128.
- (514) Boffa, L. S.; Novak, B. M. *Tetrahedron* **1997**, *53*, 15367.
- (515) Batis, C.; Karanikolopoulos, G.; Pitsikalis, M.; Hadjichristidis, N. *Macromolecules* **2000**, *33*, 8925.
- (516) Batis, C.; Karanikolopoulos, G.; Pitsikalis, M.; Hadjichristidis, N. *Macromolecules* **2003**, *36*, 9763.
- (517) Karanikolopoulos, G.; Batis, C.; Pitsikalis, M.; Hadjichristidis, N. *J. Polym. Sci., Part A: Polym. Chem.* **2004**, *42*, 3761.
- (518) Kostakis, K.; Mourmouris, S.; Kotakis, K.; Nikogeorgos, N.; Pitsikalis, M.; Hadjichristidis, N. *J. Polym. Sci., Part A: Polym. Chem.* **2005**, *43*, 3305.
- (519) Yamashita, M.; Takemoto, Y.; Ihara, E.; Yasuda, H. *Macromolecules* **1996**, *29*, 1798.
- (520) Kostakis, K.; Mourmouris, S.; Karanikolopoulos, G.; Pitsikalis, M.; Hadjichristidis, N. *J. Polym. Sci., Part A: Polym. Chem.* **2007**, *45*, 3524.
- (521) Chen, E. Y.-X.; Cooney, M. J. *J. Am. Chem. Soc.* **2003**, *125*, 7150.
- (522) Bolig, A. D.; Chen, E. Y.-X. *J. Am. Chem. Soc.* **2002**, *124*, 5612.

CR9000258